REPORT DOCUMENTATION PAGE

Form Approved
OMB No. 0704-0188

1. Agency Use Only (Leave blank).	2. Report Date. September 1998	3. Report Type and Dates Covered. Final

4. Title and Subtitle.

Coastal Benthic Boundary Layer (CBBL) Research Program: A review of the fourth year

5. Funding Numbers.

*Program Element No.*0601153N

Project No. R3103

Task No. 000

*Accession No.*DN252025

Work Unit No. 74-5258-08

6. Author(s)

Michael D. Richardson

7. Performing Organization Name(s) and Address(es).

Naval Research Laboratory
Marine Geosciences Division
Stennis Space Center, MS 39529-5004

8. Performing Organization Report Number

NRL/MR/743--98-8214

9. Sponsoring/Monitoring Agency Name(s) and Address(es).

Office of Naval Research
Dr. Fred Saalfeld
Code 01
Ballston Centre Tower One
800 North Quincy Street
Arlington, VA 22217-5660

10. Sponsoring/Monitoring Agency Report Number.

11. Supplementary Notes.

12a. Distribution/Availability Statement.

Approved for public release; distribution unlimited

12b. Distribution Code.

13. Abstract (Maximum 200 words).

The Coastal Benthic Boundary Layer (CBBL) Special Research program is a 5-year Office of Naval Research study that addressed the physical characterization and modeling of benthic boundary layer processes and the impact these processes have on seafloor structure, properties and behavior. The report is a summary of the results compiled and published during the fourth year of the program. Quantitative physical models of the benthic boundary layer are being tested in a series of experiments at coastal locations where differing environmental processes determine sediment structure. The sites were Eckernförde Bay, Baltic Sea; the West Florida Sand Sheet off Panama City, Florida; the lower Florida Keys; and the shallow continental shelf off Northern California. Predictive models developed through this program should enhance MCM technological capabilities in several important areas including acoustic and magnetic detection, classification, and neutralization of proud and buried mines; shock wave propagation; prediction of mine burial; and sediment classification. This report includes an introduction to the program, a list of publications that have resulted from CBBL research to date, and fourth year final reports from 21 groups supported by the CBBL.

14. Subject Terms.

Sediments, acoustics, mines

15. Number of Pages. 170

16. Price Code.

17. Security Classification of Report	18. Security Classification of This Page.	19. Security Classification of Abstract.	20. Limitation of Abstract.
UNCLASSIFIED	UNCLASSIFIED	UNCLASSIFIED	

COASTAL BENTHIC BOUNDARY LAYER: A REVIEW OF THE FOURTH YEAR

NRL MEMORANDUM REPORT
1 September 1998

Michael D. Richardson
Chief Scientist, CBBL
Marine Geosciences Division
Naval Research Laboratory

ABSTRACT

The Coastal Benthic Boundary Layer (CBBL) Special Research program is a 5-year Office of Naval Research study that addressed the physical characterization and modeling of benthic boundary layer processes and the impact these processes have on seafloor structure, properties and behavior. This report is a summary of the results compiled and published during the fourth year of the program. Quantitative physical models of the benthic layer are being tested in a series of experiments at coastal locations where differing environmental processes determine sediment structure. The sites were Eckernförde Bay, Baltic Sea; the West Florida Sand Sheet off Panama City, Florida; the lower Florida Keys; and the shallow continental shelf off Northern California. Predictive models developed through this program should enhance MCM technological capabilities in several important areas including acoustic and magnetic detection, classification, and neutralization of proud and buried mines; shock wave propagation; prediction of mine burial; and sediment classification. This report includes an introduction to the program, a list of publications that have resulted from CBBL research to date, and fourth year final reports from 21 groups supported by the CBBL.

1.0 Introduction

The Coastal Benthic Boundary Layer (CBBL) program is a five-year program (FY92-97) funded by the Office of Naval Research (ONR) and managed by the Naval Research Laboratory (NRL). The objectives of the program are to characterize and model benthic boundary layer processes and the impact these processes have on seafloor structure, properties and behavior (Richardson, 1994; Richardson and Bryant, 1996, Lavoie et al., 1997). The central hypothesis of the program is that sediment structure is affected by biological, biochemical, geochemical, hydrodynamic, and geological processes, which in turn, affect sediment bulk properties; acoustic, electromagnetic and rheological behavior; and can be sensed remotely by acoustic, electrical and magnetic techniques. During the course of the CBBL program, investigators tested quantitative physical models in several coastal sites where different environmental processes dominate the benthic environment. The sites are Eckernförde Bay, Baltic Sea, the West Florida Sand Sheet off Panama City, Florida, and the Lower Florida Keys. The Baltic Sea site is located in gas-rich soft mud, where biogeochemical processes form subsurface methane bubbles that significantly effect sediment acoustic behavior. The West Florida Sand Sheet is made up of a mixture of clastic sands and shells that are reworked by wave-current action. Hydrodynamic processes (major storms and hurricanes) control long term changes in sediment type but short term changes in bottom characteristics result from mixing sediments by larger megafauna. The Lower Florida Keys sites consist of carbonate sediments derived from the breakdown of coralline algae and other reef inhabitants. Hydrodynamic, biochemical and biological processes all play significant roles in determining sediment structure and properties in these carbonate sediments. The following reports represent progress made during the fourth year of the CBBL program and include significant results from all three aforementioned experiments.

Richardson, M.D. (1994) Investigating the coastal benthic boundary layer. EOS 75:201-206.

Richardson, M.D. and W.R. Bryant (1996) Benthic boundary layer processes in coastal environments: an introduction. Geo-Marine Letters 16:133-203.

Lavoie, D.L., M.D. Richardson and C. Holmes (1997) Benthic boundary layer processes in the Florida Lower Keys. Geo-Marine Letters 17:232-236.

ACKNOWLEDGMENTS: The primary financial support for the Coastal Benthic Boundary Layer (CBBL) Special Research Program was provided by the Office of Naval Research (ONR) with contributing support from the Naval Research Laboratory (NRL) and by Forschungsantalt der Bundeswehr Für Wasserschall- und Geophysik (FWG). Dr. Fred E. Saalfeld, Technical Director of ONR, provided the original program direction. All CBBL scientists thank Dr. Saalfeld for his unwavering support of their research during the 6-year existence of the program. Professor Peter Wille (Technical Director, FWG) and Dr. Timothy Coffey (Director of Research, NRL) were both strong supporters of the CBBL contributing both encouragement as well as program financial support. Operational support for the many experiments was provided by Forschungsantalt der Bundeswehr Für Wasserschall- und Geophysik (FWG), Wehrtechnische Dienstelle-71, University of Kiel, Naval Air Station (NAS) Key West, US Park Service, Florida Keys National Marine Sanctuary, and US Coast Guard. CBBL program research team included M.D. Richardson (chief scientist) and the following principal investigators, technicians, and graduate students: D.B. Albert, R. Anandrajah, A.L. Anderson, A. Ag, R.J. Baerwald, E.O. Bautista, S.J. Bentley, R.H. Bennett, H.G. Brandes, K.B. Briggs, D.R. Brogen, G.R. Brooks, C.A. Brunner, W.A. Bryant, P.J. Burkett, W.-A. Chiou, N.P. Chotiros, J.C. Cranford, N.I. Craig, A.F. D'Andra, A.M. Davis, K.S. Davis, M.E. Duncan, J. Dvorkin, R.W. Faas, K.M. Fischer, P. Fleischer, R.C. Flint, N.L. Frazer, C.T. Friedrichs, G.V. Frisk, S.S. Fu, Y. Furukawa, R. Gammish, S. Gibson, K.E. Gilbert, R.R. Goodman, T. Gorgas, S.R. Griffin, T. Hebert, R. Haynes, J.A. Hawkins, C.A. Holmes, R.J. Holyer, M.H. Hulbert, D.G. Huws, D.R. Jackson, P.D. Jackson, J.J. Kolle, D.N. Lambert, Dawn Lavoie, Dennis Lavoie, L.R. LeBlanc, G.R. Lopez, A.P. Lyons, C.S. Martens, A.C. Mueller, M. M. Myer, E.C. Mozely, C.A. Nittrouer, T.H. Orsi, J. Pyrah, H.A. Pittenger, R.I. Ray, M.H. Sadd, J.C. Sandidge, W.A. Sawyer, S.G. Schock, A.M. Schiller, A.J. Silva, N.C. Slowey, S. Stanic, T.K. Stanton, K.P. Stephens, R.D. Stoll, G. Sykora, D.J. Tang, K. Thornton, G.E. Veyera, D.J. Walter, K.L. Williams, R.H. Wilkens, W.A. Wood, L.D. Wright, D.C. Young, D.K. Young, and L. Zhang. Numerous other technicians, ship crew, and graduate students also contributed to the CBBL experiments. Other contributors include I.H Stender, T.F. Wever, G. Fechner, and H.M. Fiedler of FWG; R. Grotrian of WTD-71; F. Abegg, D. Milkert, F. Theilen, and F. Werner of the University of Kiel; and M. Schlüter, I Bussman, and E Suess of GEOMAR. Workshops were hosted by R. H. Bennett, C.S. Clay, W.A. Dunlap, G.D. Gilbert, D.R. Jackson, P.A. Jumars, H.J. Lee, and T.G. Muir. The NRL contribution number is NRL/MR/7430--98-8214.

2.0 PROJECT REPORTS FOR FY95

The following 19 reports summarize results for projects supported by the CBBL:

2.1 Discrete Element Simulation of the Microstructure of Marine Cohesive Sediments (Principal Investigator: A. Anandarajah)

A. ANANDARAJAH

Professor of Civil Engineering
Department of Civil Engineering
The Johns Hopkins University
Baltimore, Maryland 21218, U.S.A.

INTRODUCTION

The objective of this project is to investigate, for the Baltic Sea sediments, the relationship between microstructure and macroscopic properties including compressibility, shear strength, and shear and compressional wave propagation characteristics. The goal is to be achieved using a numerical simulation technique known as the discrete element method (DEM), which is similar to the molecular dynamic approach, but applied at the particle level rather than at the molecular level. The primary soil type in Eckernförde Bay where most of the CBBL experiments were conducted is clay and the DEM analysis to be used in the study accounts for the special characteristics of clayey sediments. The currently available DEM program needs to be modified to include the other microstructural features found in Eckernförde Bay, namely organic contents, ovoid pellets and methane gas bubbles.

The project began in April 1996 and the primary task to be accomplished in the first project period is parallelization of the existing DEM scalar computer code so as to analyze an assembly of large number of particles (say, 10,000) in one of the existing parallel supercomputers (e.g., T3D at Pittsburgh Supercomputing Center or the DOD's T3E supercomputer). The work is coordinated with the NRL research personnel, with Dawn Lavoie acting as the coordinator. The proposed simulation studies are to be conducted during the second project period and this phase will be a collaborative effort between Johns Hopkins and NRL.

DESCRIPTION OF ANALYSIS METHOD

The most systematic and comprehensive analysis method for determining the behavior of an assembly of soil in terms of its fabric and compositional properties is perhaps the discrete element method (DEM) of Cundall and Strack (1979). The method was originally developed for a granular assembly, and it has thus far been applied only to such material assemblies. The first successful application of DEM to an assembly of clay particles was presented by Anandarajah (1994).

The DEM analysis of an assembly of clay particles requires (1) a method of quantifying the double-layer repulsive force between two arbitrarily oriented clay particles, (2) a method of quantifying the van der Waals attractive force between two arbitrarily oriented clay particles, (3) a suitable method simulating the mechanical interaction between two clay particles, including slip and separation, and (4) a method of simulating the bending of individual clay platelets.

A study was initiated several years ago to systematically address these aspects, which has yielded reasonable solutions to each of the four aspects listed. A method is now available for computing the double-layer repulsive force between two platy particles immersed in a fluid as shown in Fig. 1. (Anandarajah and Lu, 1991a; Anandarajah and Chen, 1994). An approximate method was proposed by Anandarajah (1994) in utilizing the theory developed for the system shown in Fig. 1 to compute the force between two randomly oriented particles; the method is still used in the current version of the DEM computer program.

A similar method has been developed for computing the second most significant physico-chemical force between two clay particles: the van der Waals attractive force. In this case, a closed-form solution has been developed for the plate-fluid-wall system shown in Fig. 2. While a plate-fluid-plate system is what is needed to model a soil system, the plate-fluid-wall system provides a good approximation, except for small edge effects. The details of these theories may be found in Anandarajah and Chen (1995, 1996a) and Chen and Anandarajah (1996).

The bending of clay platelets are simulated by dividing each clay particle into a number of smaller discrete elements and using the elastic beam bending stiffness to simulate the behavior of contacts between the discrete elements ("intra-element'" contacts); refer to Anandarajah and Lu (1991b) for further details. The inter-element contact interactions are simulated by recognizing edge-to-face, face-to-face and edge-to-edge associations, and using a modified Mohr-Coulomb criterion to simulate slip, and employing zero tensile normal stiffness to simulate separation at these contacts; further details may be found in Anandarajah (1994). The interparticle contact behavior needs further work in simulating the wave propagation characteristics to be studied in the present project.

AN EXAMPLE OF PREVIOUSLY CONDUCTED DEM ANALYSIS OF ONE-DIMENSIONAL COMPRESSION

A preliminary study was reported in Anandarajah (1994), and is briefly described here to show the potential of the method in achieving the objective of the present project. In this preliminary study, where the objective was largely to demonstrate the feasibility of performing a DEM analysis on an assembly of platy cohesive particles, the double-layer repulsive force was simulated, along with the contact mechanical forces and the bending of clay particles, but the van der Waals force was ignored. It was shown that numerical results on one-dimensional compression behavior resembled that of dispersive clays such as montmorillonite, where the repulsive force is the dominant component, owing to large particle's specific surface. The analysis allows the evolution of fabric anisotropy to be computed. Recent experimental studies (Anandarajah et al., 1995, 1996b; Kuganenthira et al., 1996) are in good agreement with the discrete element studies.

In the study, an assembly of 174 particles was first formed using computer random numbers for orientation, coordinates, length, etc. This was done purely based on kinematic considerations (particles should fit in a box, they should not cross each other, etc.). The repulsive forces were then turned on. At static equilibrium, the assembly looks like the one shown in Fig. 3a. Note that in the figure, the lines represent the centroidal axes of the clay platelets. This assembly may be considered to represent a soil slurry with random particle arrangements. The assembly was then subjected to a one-dimensional compression loading by moving the two horizontal walls of the box in a strain-controlled mode. The assembly shown in Fig. 3b corresponds to an intermediate loading stage.

The results available may be processed in any desired manner. Macroscopic (stresses on the walls, strains of the assembly, void ratio, etc.), and microscopic (interparticle forces, contact normal and particle distributions, etc.) are available for further analysis. For example, the plots shown in Fig. 4 is an example of quantities that can be calculated. The first two plots in Fig. 4 shows the compressibility relation (i.e., vertical pressure versus void ratio) obtained from the numerical analysis.

Similarly, other average quantities such as the variation of the number of mechanical contacts, coefficient of fabric anisotropy, K_o (earth pressure at rest or the ratio between horizontal and vertical normal stress) have been computed and plotted in Fig. 4. The results are reasonable, and the study proved the feasibility of performing such a numerical simulation on cohesive particles, just as it has been done on granular particles for now almost two decades.

PRELIMINARY SIMULATION OF COMPRESSIONAL WAVE PROPAGATION

The presence of water in soils complicates numerical simulation of the compression wave propagation. Water is almost an incompressible fluid, where as a skeleton of clay particle network is compressible. The DEM program that we have at present can not simultaneously simulate the combined effect; it can only simulate the wave propagation through a skeleton, with all interparticle forces existing in a saturated skeleton, however, properly simulated. As such, mixture theories need to be used in computing the compressional wave velocity. Another feature that needs special attention in simulating wave propagation is accurate modeling of the interparticle interactions. Our past research has yielded accurate methods of quantifying the physico-chemical interactions, but the mechanical contact interactions need further work. In particular, normal and tangential stiffness at interparticle mechanical contacts must be modeled accurately. Work is currently in progress to address these issues. No specific numerical calculations are attempted in the example presented below.

An assembly of 194 clay particles (316 discrete elements), consolidated one-dimensionally under a strain-controlled mode, is shown in Fig. 5. The assembly is in static equilibrium at this stage.

The top horizontal wall is then subjected to a step velocity loading of short duration, and the propagation of the wave is monitored by computing the force on the bottom horizontal wall, and plotting the assembly at suitable time intervals. Fig. 6 shows the variation of the force at the bottom wall with time step number. For comparison, another analysis is conducted with the walls held stationary, and the force on bottom horizontal wall is superimposed in the figure. It may be

seen that the wave that originated at the top horizontal wall reaches the bottom horizontal wall and changes the forces on it between 2,210,000 and 2,260,000 cycles.

The propagation of the wave is seen in Figs. 7a-7c, where the particles shown by solid lines represent assembly with walls held stationary and those shown by dotted lines represent assembly with a step velocity loading applied at the top horizontal wall.

While the power of the DEM analysis method in capturing the wave propagation characteristics is evident from the results, it is clear that the number of particles in the assembly are too few for the numerical results to be representative of real behavior of cohesive sediments. Larger assemblies can not be analyzed in workstations, where the analysis shown in Figs. 6 and 7 was performed.

PROGRESS IN CODE PARALLELIZATION

The results described in the preceding section clearly point out the need for using an assembly with large number of clay particles in simulating wave propagation characteristics, and the difficulty of using workstation type computers for the purpose. One solution is to use a parallel supercomputer. With a starter grant from the Pittsburgh Supercomputing Center on the T3D parallel computer, the DEM code has been parallelized and debugged; the details are summarized here.

The PSC's T3D computer currently has 512 ALPHA processors (referred to hereafter as processing elements or simply PEs).

The code has been parallelized using the method of domain decomposition and the standard MPI commands. The assembly to be analyzed is partitioned into a number of rectangular regions. For example, an assembly used during the debugging phase is shown in Fig. 8a, which consists of 32 single discrete element particles. With the intention of using 16 PEs (PE, PE1, PE2 ... PE15, the domain is divided into 16 regions. Each region is then augmented with an interfacial region around the boundaries to properly simulate the interparticle interactions. Every expanded region is assigned to a given PE, with data of elements whose centroids fall within these expanded regions transferred to the respective PE. Thus, elements in the interfacial regions will exist not only in their own PE, but also in adjacent PE (or PEs at corner regions).

At the start of the analysis, coordinates of elements and connectivity information are read from an external data file into one of the PEs (this will be referred to as the “host PE” and normally PE0 is used for this purpose), processed and transferred to the appropriate PE. The elements in the interfacial regions are further transferred between PEs.

During every time step, analysis is performed independently in individual PEs. At the end, the data associated with interfacial regions are communicated to the adjacent PEs, thus updating their new coordinates and inter-element forces.

At any stage of the analysis, assembly-based quantities (e.g., wall stresses) may be required. This is achieved by bringing appropriate quantities to the host PE (PE0), processed and printed.

The major steps are: (1) Read element data and transfer them to appropriate PEs, (2) perform analysis independently in each PE, (3) compute assembly-based quantities, if and when required, (4) repeat the process as many time steps as specified.

It turned out that significant modifications had to be made to our scalar code in performing the aforementioned tasks; most of which had to do with inter-PE communication. We are confident that the code has been carefully modified at this stage, and we are ready to formulate and proceed with some realistic runs. No major runs have yet been made; analysis performed to date involve only a few cycles and two examples are described here.

The 32-particle assembly shown in Fig. 8a was used during most part of the development work, where the particles were manually arranged to invoke certain key aspects. The results after every single task were checked by comparing with those obtained with the scalar code.

Two smaller rectangular regions are zoomed and presented in Figs. 8b and 8c. Assemblies at the start and after performing 10 time steps of loading are superposed in these figures. Loading applied consists only of internal loading; i.e., interparticle repulsive, attractive and mechanical forces are turned on, which results in unbalanced static forces, leading to movement of particles until the forces do balance.

Some elements were placed very near each other so that the interparticle forces would be large enough to cause noticeable movement within a few cycles (10 in this case). Some were placed within the interfacial regions and some right near the walls.

The corner zoom area (Fig. 8b) shows elements in and around PE0. It is seen that there is only one particle whose centroid falls within PE0, and this element is placed very close to the corner of two of the four walls. Another is placed at the interface between PE_0 and PE_1, another at the interfaces between PE_0 and PE_1, PE_4 and PE_5, and a third one at the interface between PE_0 and PE_4.

The central zoom area (Fig. 8c) shows four PE regions, with a pair of elements placed at the interface between PE_4 and PE_9. One of this pair has its centroid in PE_4 and the other in PE_9, and thus, unless the inter-PE communications are properly achieved, their behavior will not be accurately captured.

It may be observed that (1) the element placed very close to the wall (Fig. 8b) experiences noticeable movement as expected, and this has been correctly computed within PE0 and results printed out properly by the assembly-based communication algorithm, (2) the element that is placed at the interface between PE_5 and PE_9 experiences noticeable movement, where the calculations would be performed in both PE_4 and PE_9, and (2) the remaining elements that are at the interfaces seen in Figs. 8b and 8c are far away from other elements, and their movement during the 10 steps of loading is absent as expected.

In addition, the assembly was analyzed under identical conditions using 4 PEs, and the computed assembly-based quantities were found to be identical (e.g., stresses on the walls at the end of 10 time steps of internal loading).

Having thus verified the validity of algorithm employed, we tried larger assemblies, with the largest analyzed so far shown in Fig. 9a. The assembly consists of 10,000 discrete elements, which is close to what we intended using in the present Baltic Sea project. As in the earlier cases, Fig. 9b and 9c present a corner and a central zoom areas respectively. 64 PEs were used in this particular analysis.

The assembly was generated with the coordinates, length, and orientation of each particles selected randomly; our scalar program was used for this purpose. The data was written out to a file, transferred and read into the supercomputer. 1000 time steps of internal loading was performed, but the movements of the elements are not noticeable because the elements are not close enough to each other for the inter-particle forces to be large enough to cause noticeable movements within 1000 time steps of loading. All other aspects have been properly analyzed and computed as in the earlier 32-element assembly.

RESEARCH PLAN FOR THE SECOND PROJECT YEAR

Now, we have the tools necessary to at least analyze an assembly of cohesive particles. The number of discrete elements that could be analyzed increases from about 500 on a workstation to over 10,000 on a supercomputer. We have not only developed and verified a code that can run on a T3D computer, but developed a feel for CPU time, clock time, and computer storage requirements. As the message passing commands that we have employed in the code are standard MPI commands, we are confident that our code is portable. We have exhausted the service units (SUs) granted to us as part of the PSC starter grant, and currently preparing a production grant proposal. In the mean time, we have applied for CPU time on one of the DOD supercomputers and are awaiting approval.

Our plan during the second year is to perform several small scale runs (with 500 particles) on our workstations, develop experience and formulate a few selected problems to be analyzed on a supercomputer. The computer runs to be made during the second year would be on Baltic Sea sediments, employing real microstructural properties and seeking macroscopic properties which have been experimentally measured in the field during the Eckernförde campaign and in the lab by other CBBL researchers.

We plan to define the problems to be analyzed and compile the microscopic data necessary in collaboration with the NRL personnel, with Dawn Lavoie coordinating the effort from the NRL side. I have already paid a visit to NRL, and arrangements are currently underway for a Hopkins' doctoral student to spend the summer at NRL.

Several research initiatives have already been set in motion in preparation for the second year's research work. For example, we have begun developing methods of obtaining particle coordinate and length information from electron micrograph images; P. J. Burkett and Dawn Lavoie have sent us a sample of micrographs for use in this preliminary work. Several other preparations are

also being made. Soon, we will begin work that will seek to develop a more accurate method of evaluating mechanical contact stiffness properties, which, as pointed out earlier, will have a significant impact on the calculated shear and compressional wave velocities.

During the second half of the second project year, our focus would be to develop methods of considering pellets and methane gas bubbles in the analysis.

PUBLICATIONS RESULTING FROM THE RESEARCH

Anandarajah, A. and Yao, M. (1997), "Parallel Algorithm for the Discrete Element Analysis of Clays," Proc. Sym. Mech. of. Granular. Materials, Joint ASCE/ASME Summer meeting, Northwestern University, June 29-July 2.

Anandarajah, A. and Yao, M. (1997), "Discrete Element Analysis of Clays on a Parallel Computer," Proc. ASCE Fourth Congress on Computing in Civil Engineering, Philadelphia, June 16-18.

Anandarajah, A. (1997), "Discrete Element Modeling of Wave Propagation Through Clays," Proc. 9th. Intl. Conf. on Computer Methods and Advances in Geomechanics, The Chinese Academy of Sciences, Wuhan, China, Nov. 2-7.

REFERENCES CITED IN THE TEXT

Anandarajah, A. (1994), "Discrete Element Method for Simulating Behavior of Cohesive Soils," J. Geotech. Eng. Div., ASCE **120**, 1593-1615.

Anandarajah, A. and Chen, J. (1995), "Single Correction Function for Retarded van der Waals Attraction," J. Coll. Inter. Sci. **176**, 293-300.

Anandarajah, A. and Chen, J. (1996a), "Van der Waals Attractive Force Between Clay Particles in Water and Contaminant," Soils and Foundations, JSSMFE (in press).

Anandarajah, A., Kuganenthira, N. and Zhao, D. (1996b), "Variation of Fabric Anisotropy of Kaolinite in Triaxial Loading," J. Geo. Engr. Div., ASCE, Vol. 122, No. 8, Aug., pp. 633-640.

Anandarajah, A. and Chen, J. (1994), "Double-Layer Repulsive Force Between Two Inclined Platy Particles According to Gouy-Chapman Theory," J. Coll. Inter. Sci. **168**, 111-117.

\item Anandarajah, A. and Lu, N. (1991a), "Numerical Study of the Electrical Double-Layer Repulsion between Non-Parallel Clay Particles of Finite Length," Int. J. Numer. Analy. Meth. Geomech. **15**, 683-702.

Anandarajah, A. and Lu, N. (1991b), "Structural Analysis by the Distinct Element Method," J. Engr. Mech. Div., ASCE **117**, 2156-2159.

Anandarajah, A. and Kuganenthira, N. (1995), “Some Aspects of Fabric Anisotropy of Soils,” Geotechnique, 45, 69-81.

Chen, J. and Anandarajah, A. (1996), “Van der Waals Attractive Force Between Spherical Particles,” J. Colloid Interface Sci., Vol. 180, 1996, pp. 519-523.

Cundall, P. A. and Strack, O. D. L. (1979), “A Discrete Numerical Model for Granular Assemblies,” Geotechnique, **29**, 47-65.

Kuganenthira, N., Zhao, D. and Anandarajah, A. (1996), “Measurement of Fabric Anisotropy in Triaxial Shearing,” Geotechnique, Vol. 46, No. 3, 1996.

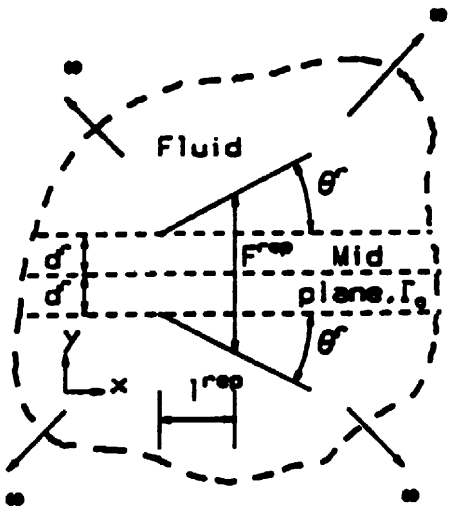

Fig. 1. A System of Two-Particles Immersed in a Fluid and Repulsive Force Between them.

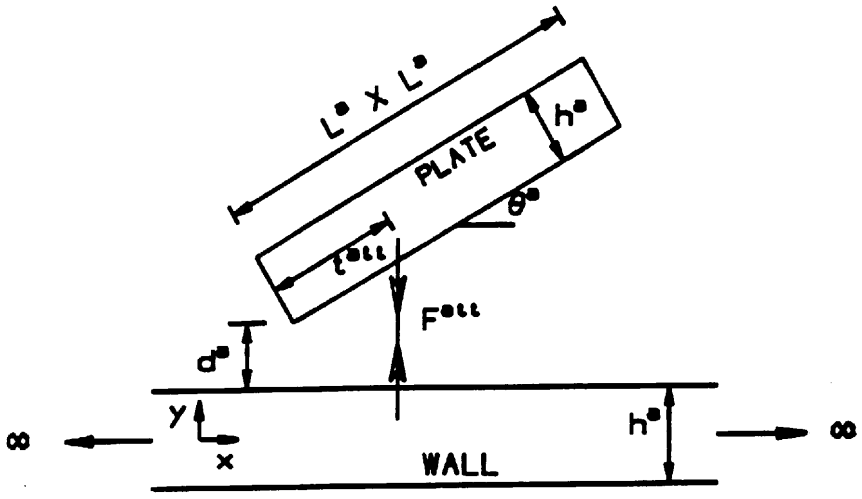

Fig. 2 A Plate-Wall System and Attractive Force Between the Plate and Wall.

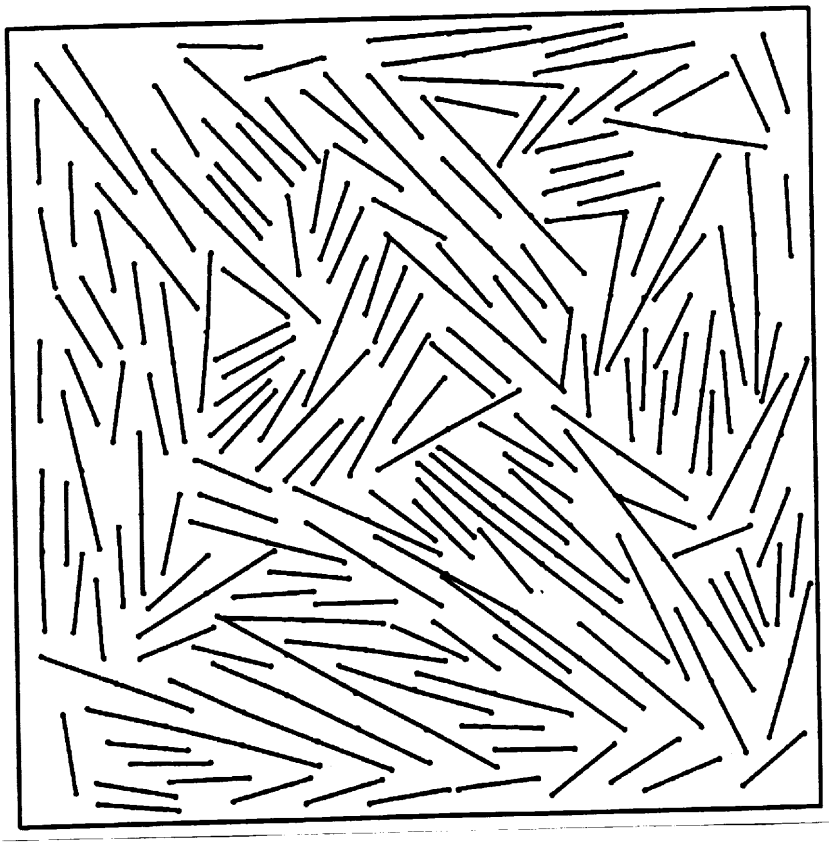

(a) Initial Assembly, e=4.0.

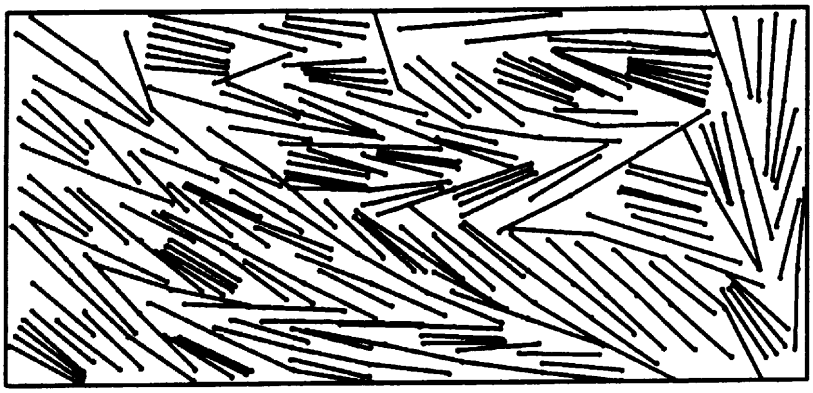

(b) Assembly at e=1.868.

Fig. 3. One-Dimensional Compression of Clays: DEM Simulation.

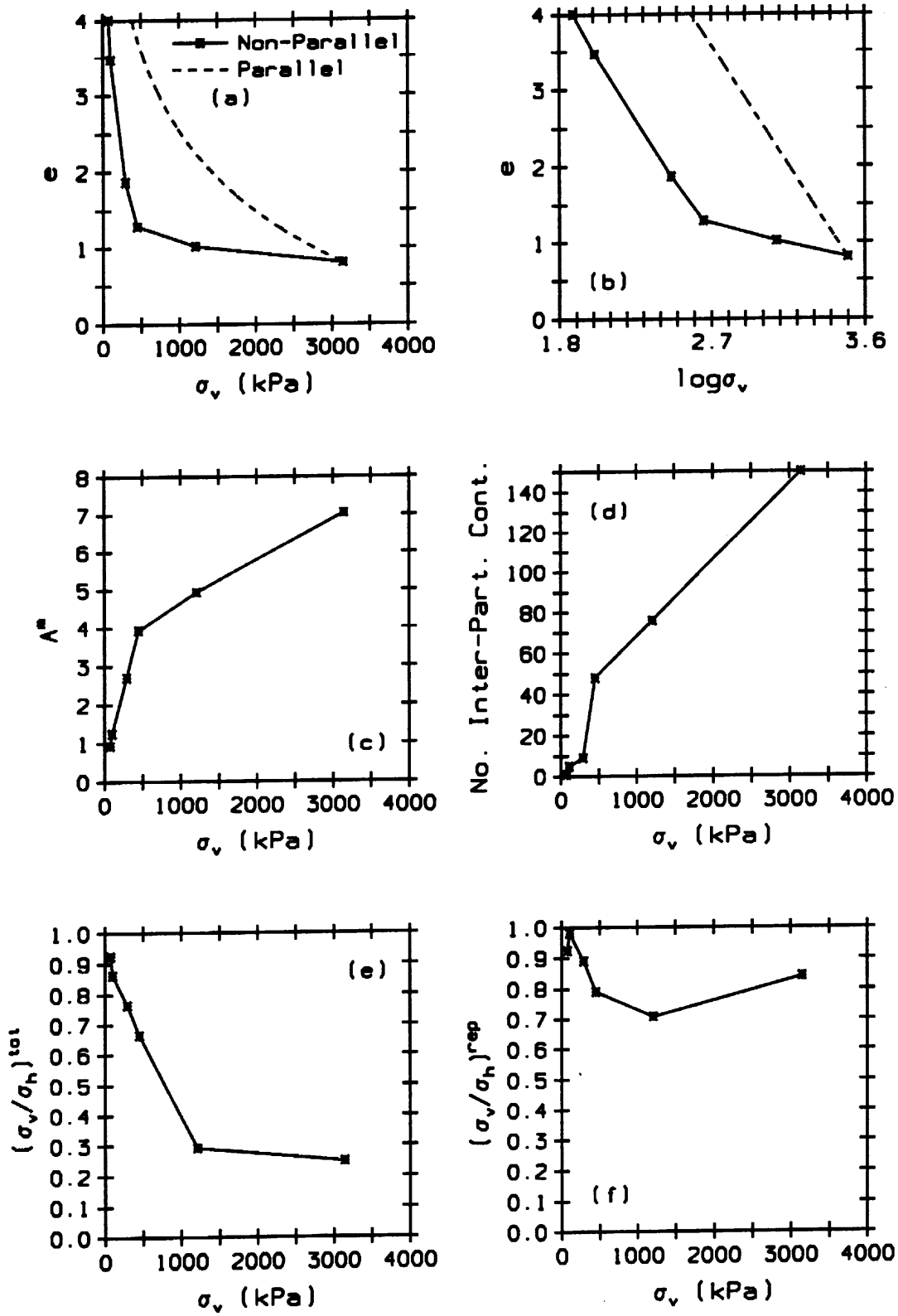

Fig. 4. Behavior of Numerical Assembly During One-Dimensional Loading.

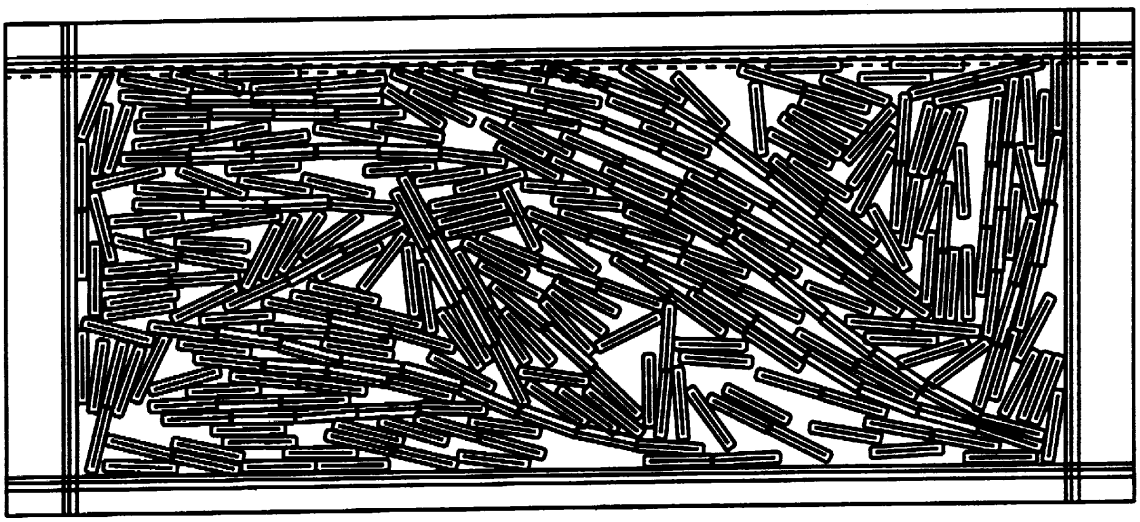

Fig. 5. Numerical Assembly of Clay Particles.

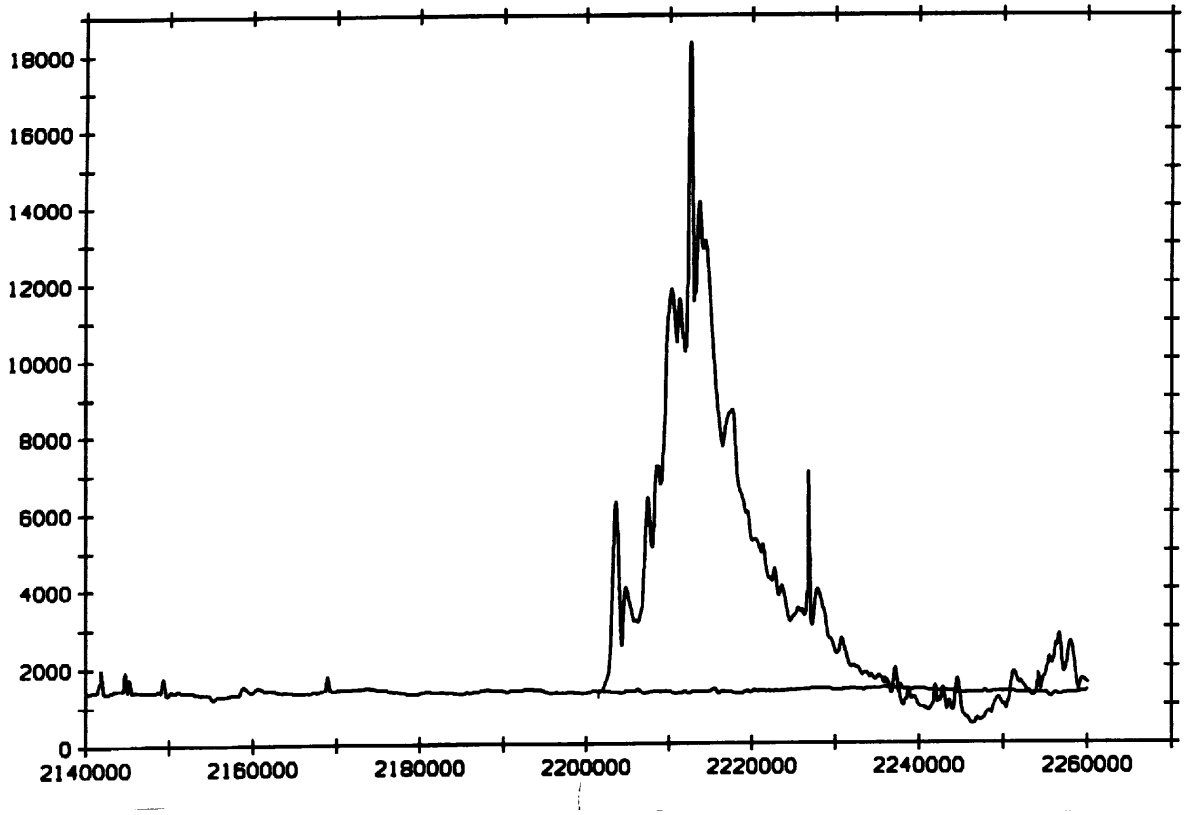

Fig. 6. Comparison of Force on Bottom Horizontal Wall with and without Loading on Top Horizontal Wall.

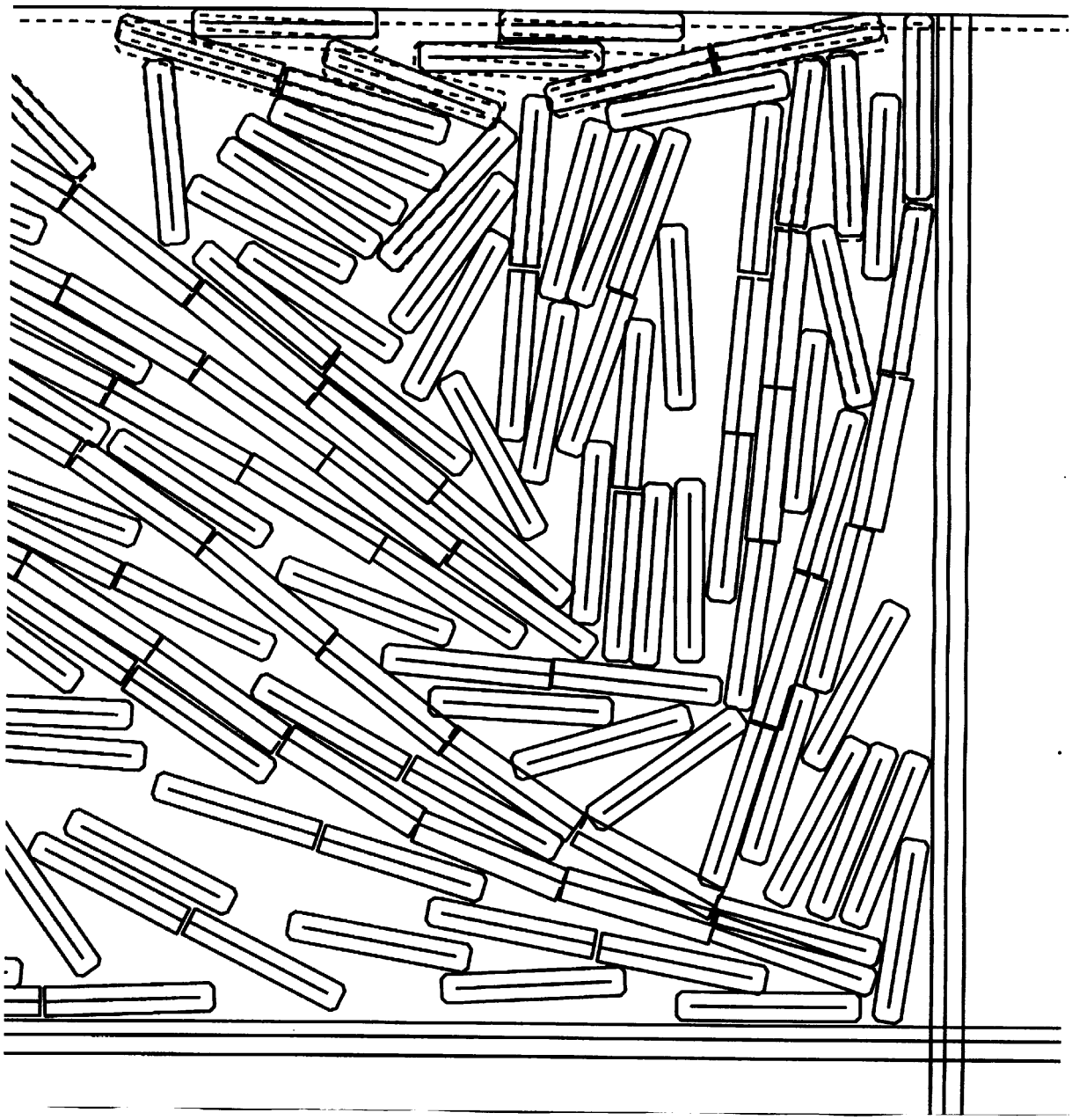

Fig. 7a. Propagation of Compressional Wave: 500 Time Steps After Loading on Top Wall.

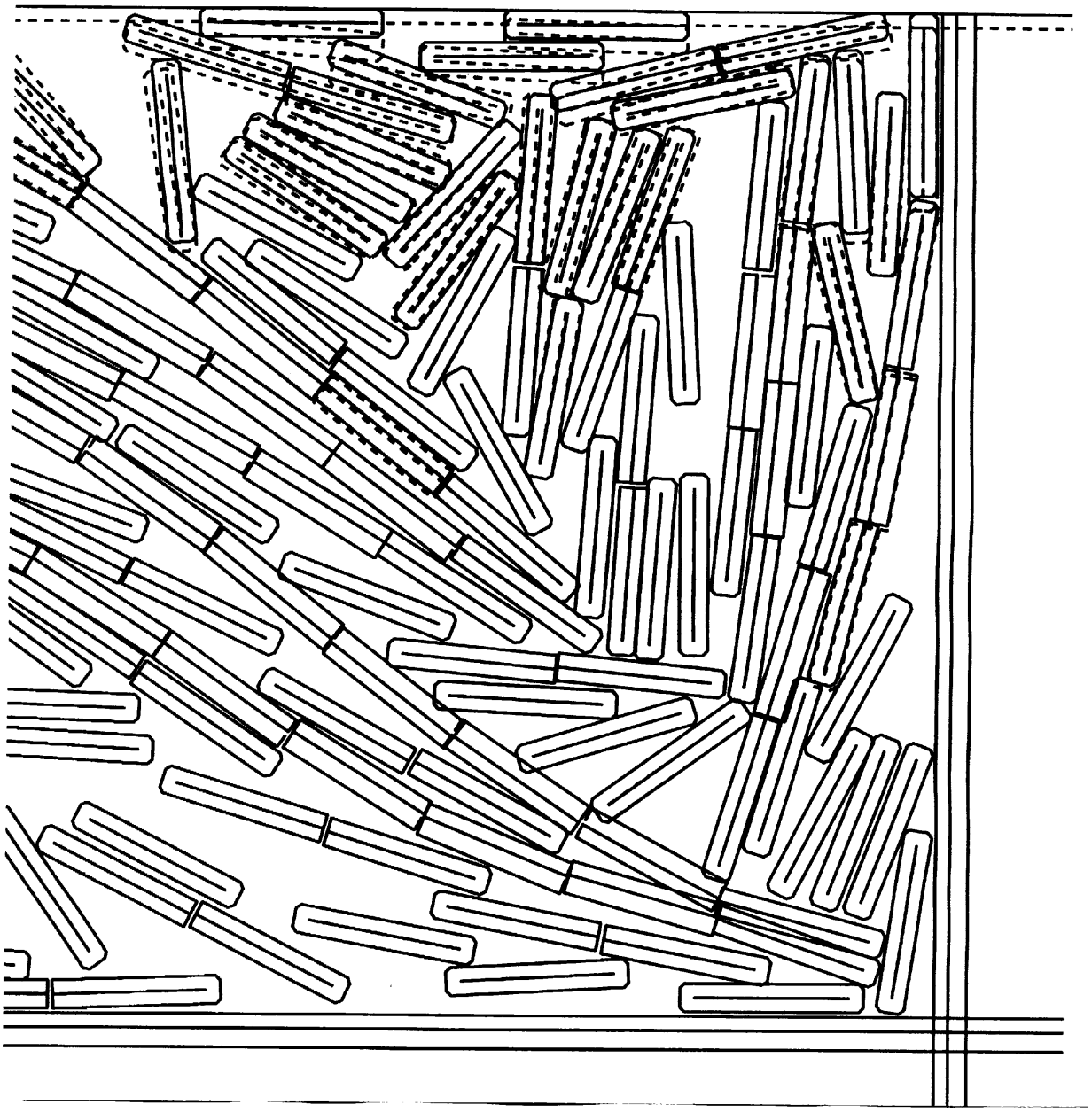

Fig. 7b. Propagation of Compressional Wave: 1000 Time Steps After Loading on Top Wall.

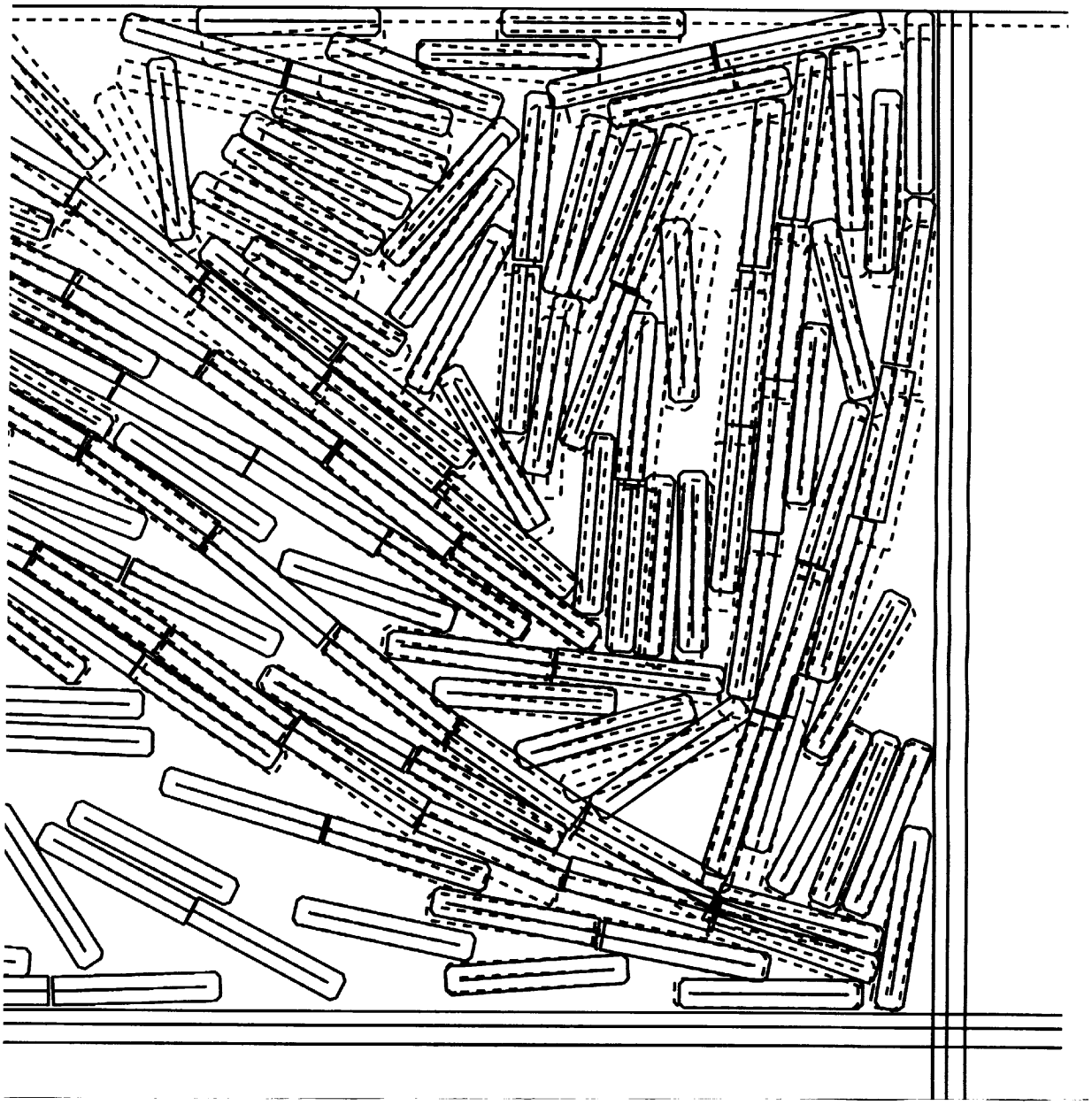

Fig. 7c. Propagation of Compressional Wave: 6000 Time Steps After Loading on Top Wall.

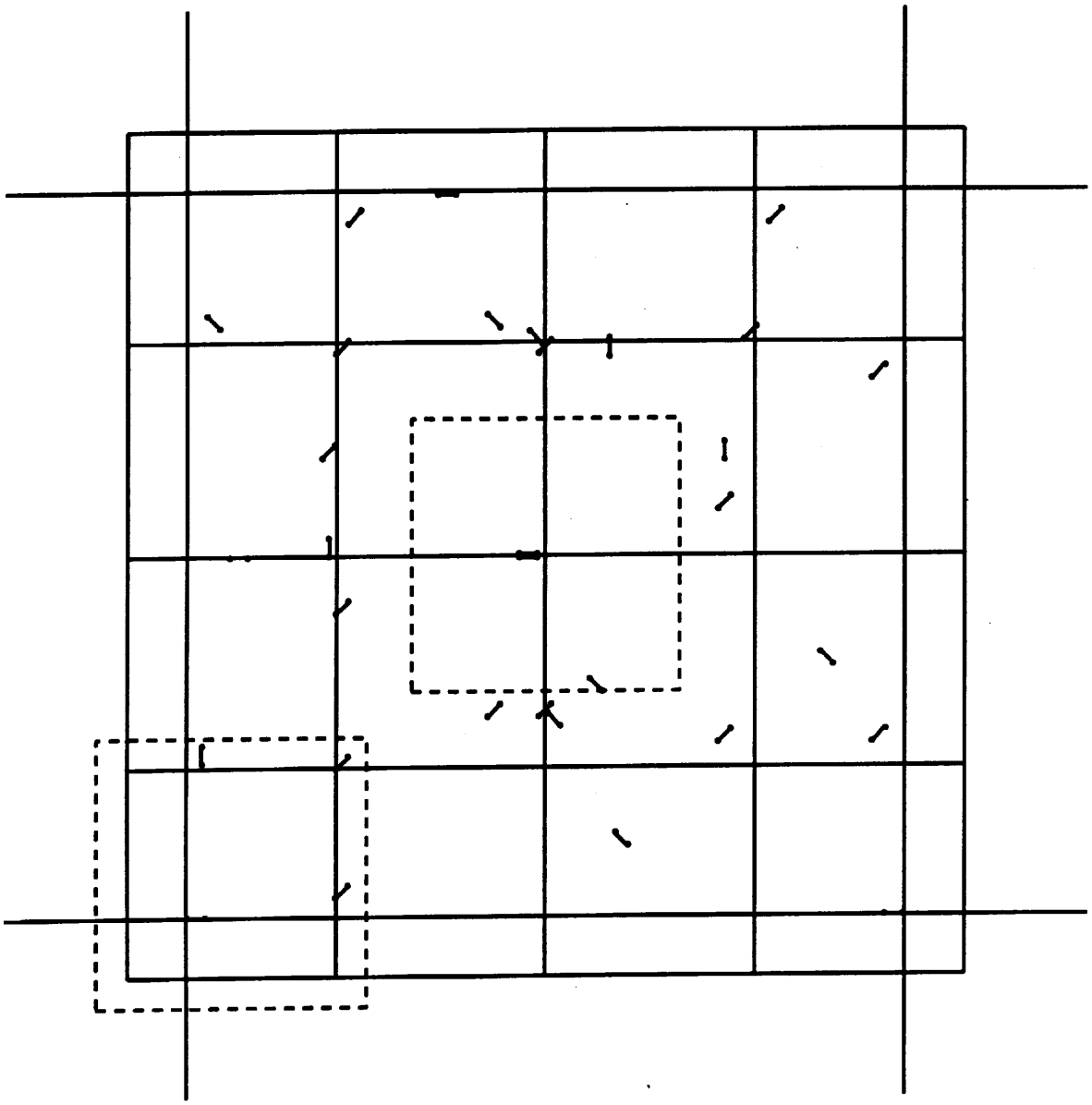

Fig. 8a. An Assembly of 32 Particles Analysed Using 16 PEs.

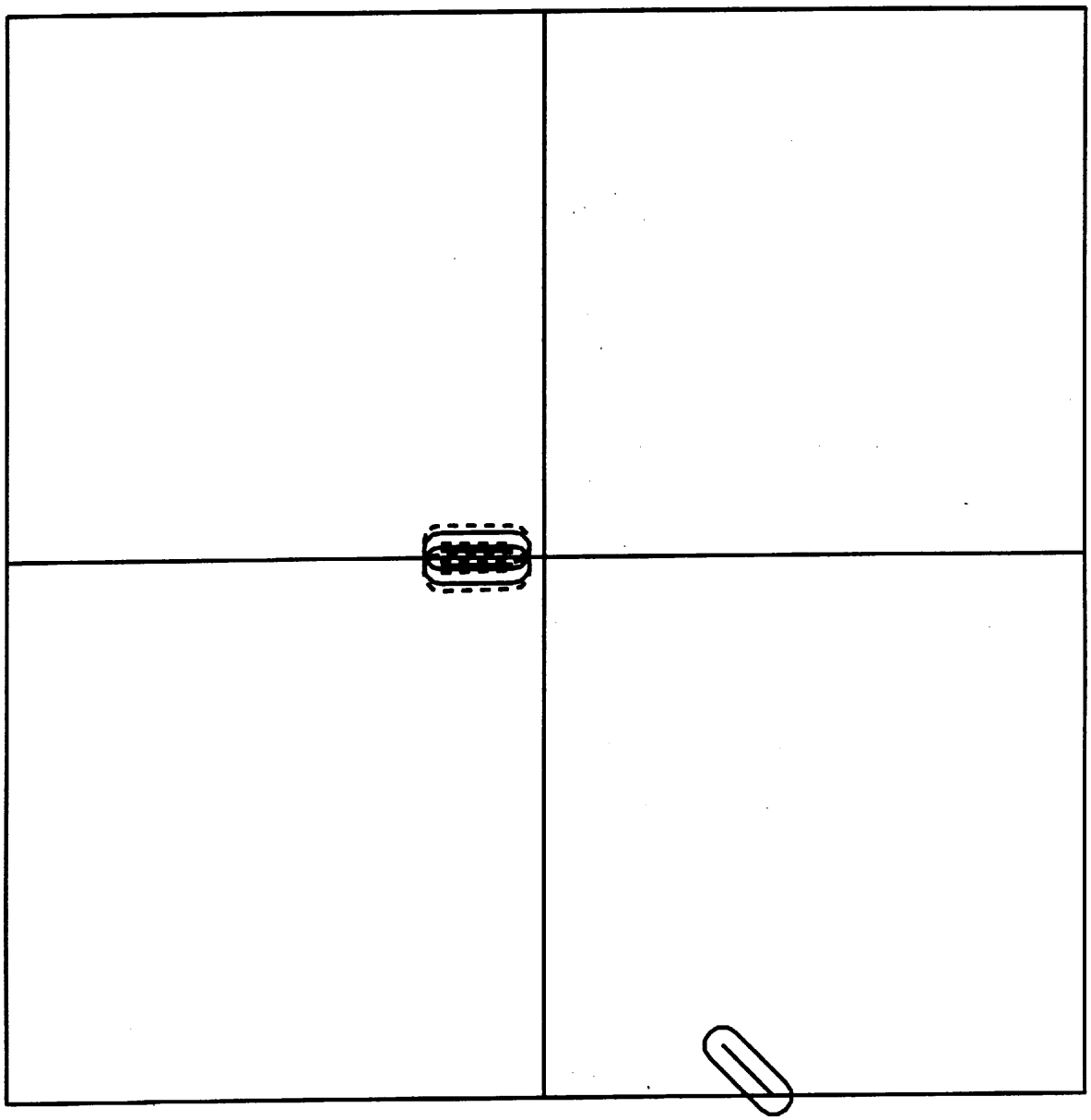

Fig. 8b. Corner Zoom Area of 32 Particle Assembly: Comparison of Initial Assembly with that After 10 Time Steps of Loading.

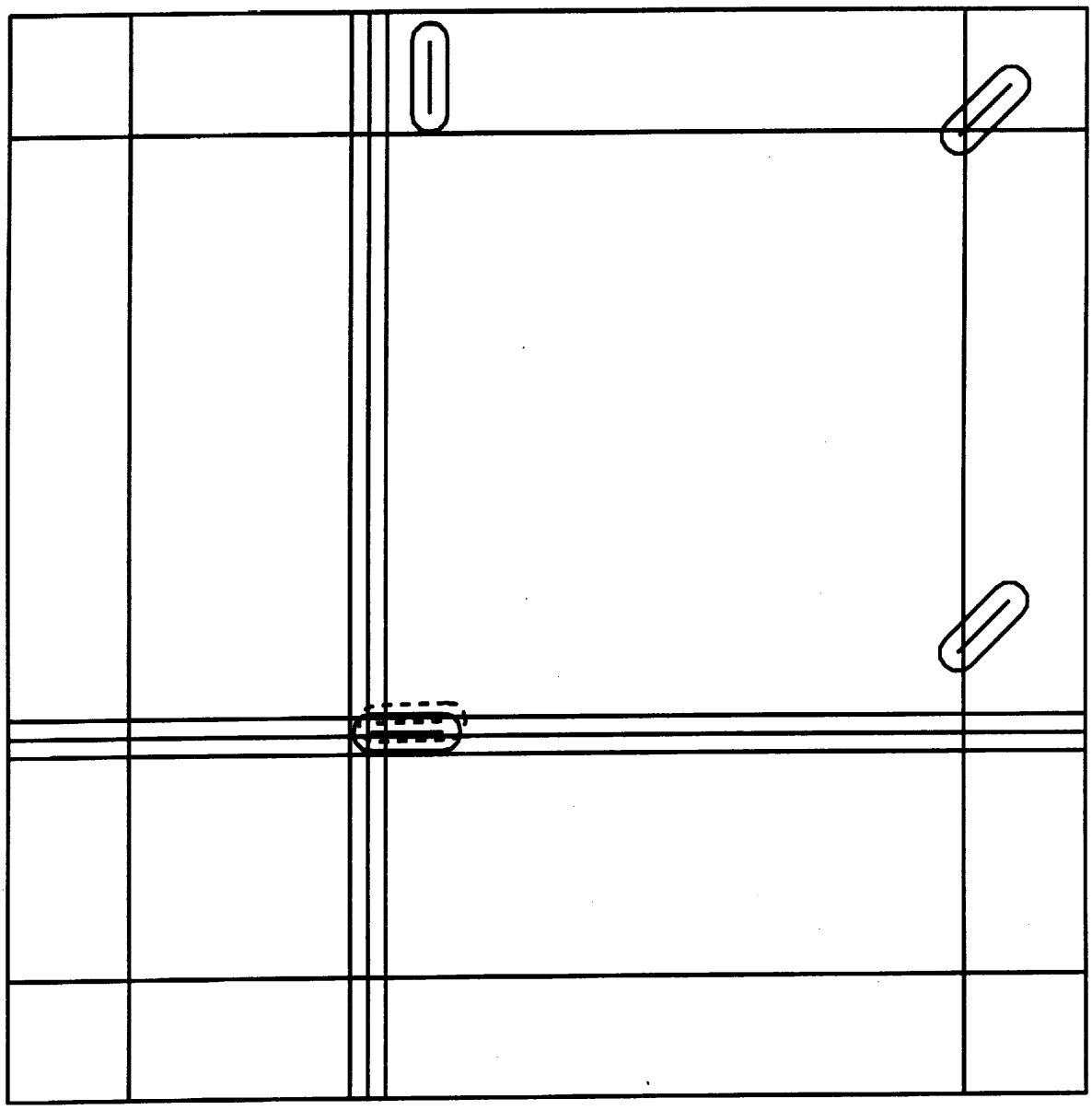

Fig. 8c. Central Zoom Area of 32 Particle Assembly: Comparison of Initial Assembly with that After 10 Time Steps of Loading.

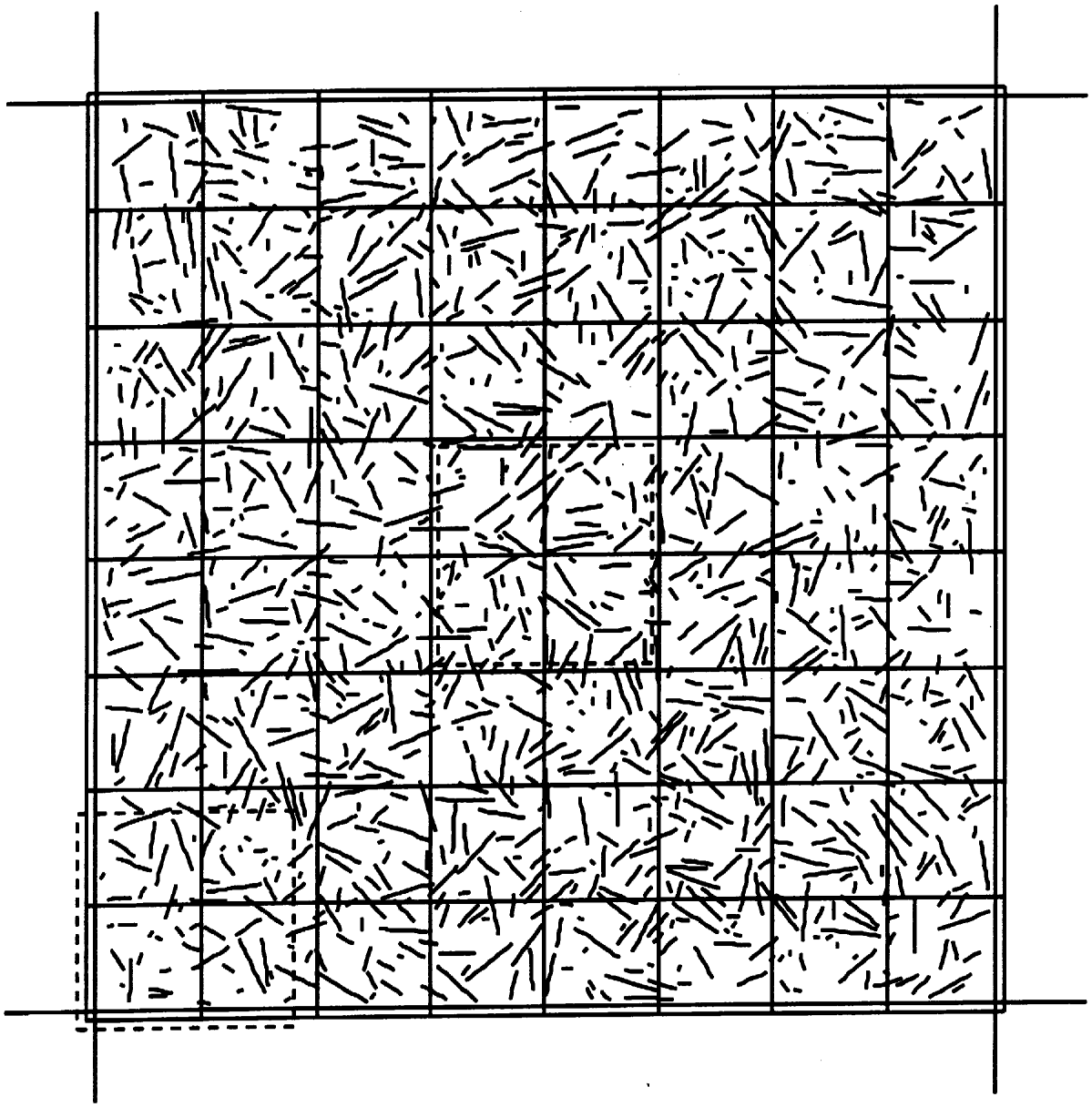

Fig. 9a. An Assembly of 10,000 Particles Analysed Using 64 PEs.

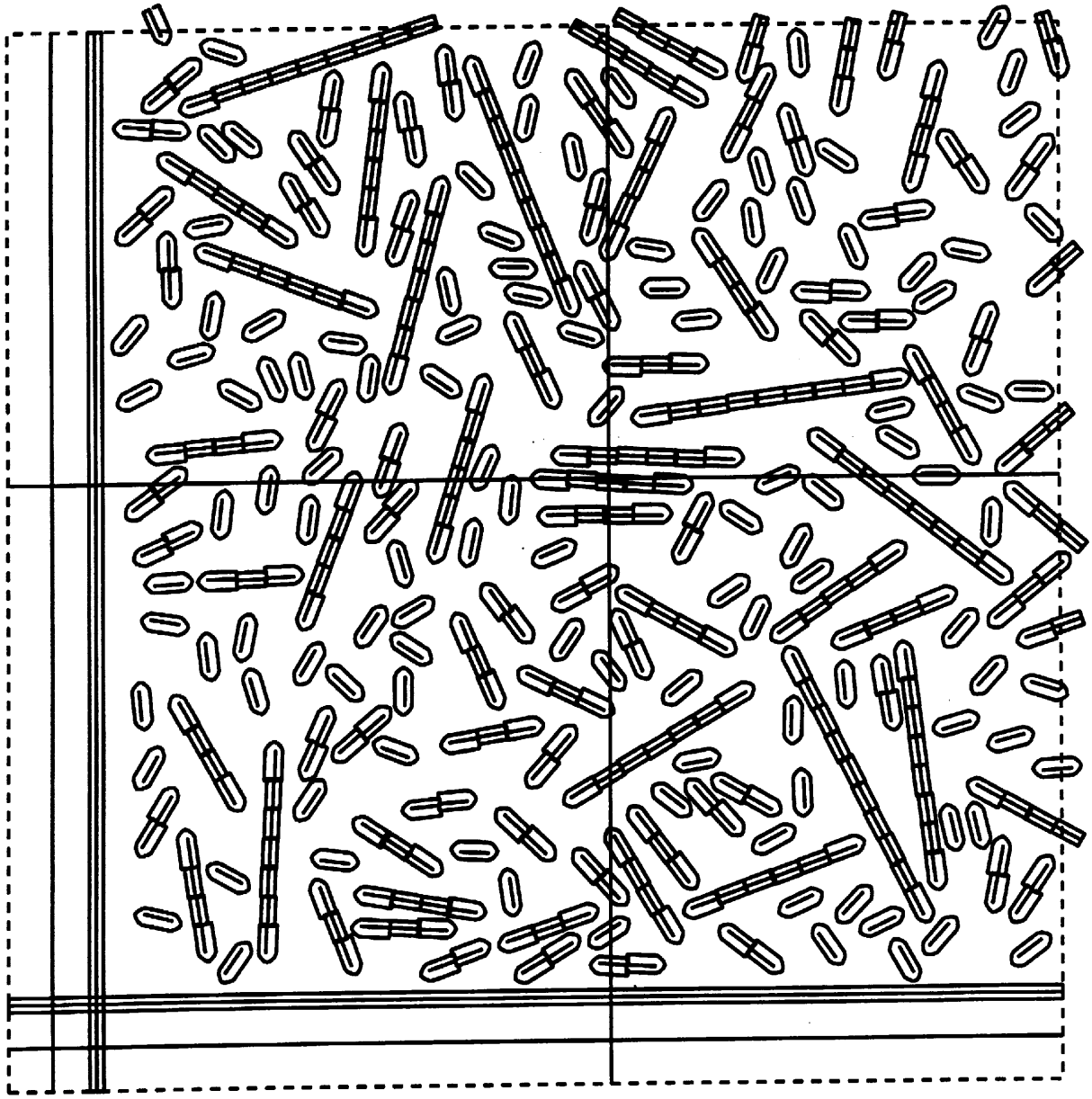

Fig. 9b. Corner Zoom Area of 10,000 Particle Assembly: Comparison of Initial Assembly with that After 1000 Time Steps of Loading.

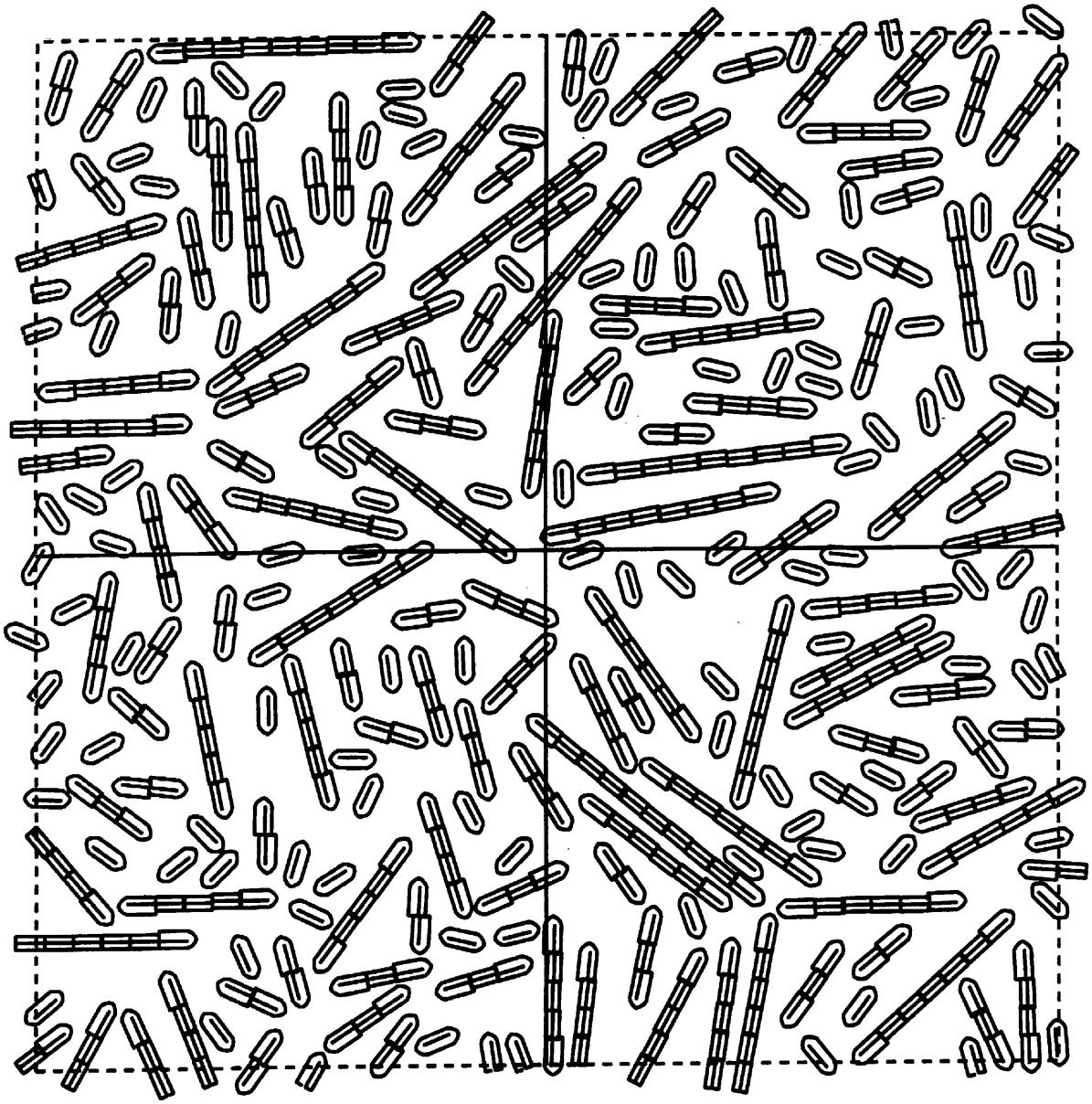

Fig. 9c. Central Zoom Area of 10,000 Particle Assembly: Comparison of Initial Assembly with that After 1000 Time Steps of Loading.

2.2 Measurement and Description of Upper Seafloor Sub-Decimeter heterogeneity for Macrostructure Geoacoustic Modeling (Principal Investigators: A.L. Anderson, James A. Hawkins, Michael E. Duncan and Richard A. Weitz)

Aubrey L. Anderson, James A. Hawkins, Michael E. Duncan, Richard A. Weitz
Department of Oceanography
Texas A&M University
College Station, Texas 77843-3146

INTRODUCTION

The interaction of acoustic energy with the seafloor can involve several physical processes. These include reflection and scattering from the water-sediment interface and from buried interfaces, volume scattering from heterogeneities within the seafloor, propagation through seafloor intervals with attendant refraction and attenuation or propagation as interface waves. Understanding acoustic data involving seafloor interaction, prediction and simulation of such interaction or application of acoustic systems to characterize the seafloor qualitatively or quantitatively all require understanding the various physical processes of seafloor acoustic interaction. Thus, many research programs have investigated such interaction. The CBBLSRP includes seafloor acoustic interaction as a portion of its investigations.

The primary goal of the project reported here is to characterize the volume heterogeneity of the seafloor at CBBL field sites on scales from about a decimeter (the nominal diameter of many seafloor samples) down to about 1 mm. A primary tool used for this characterization is the X-ray computed tomography (CT) scan. The seafloor samples measured for these studies are cylindrical samples recovered by one of three methods: gravity (or piston) cores obtained with samplers operated from a ship, diver cores, or subsamples of box cores. When the purpose of sampling is to investigate free gas within the seafloor, divers seal the samples in pressure tight aluminum pressure transfer chambers (APTC) at the seafloor.

Multiple CT scans of the seafloor cores provide, for each core, a three dimensional data base of digital values which are interpreted as bulk density. Each value represents the density of a very small volume element (voxel) of the sediment sample. Because of the small size of these voxels, a high-resolution description of the three-dimensional distribution of sediment internal density can be made. Based on this distribution, a geoacoustic characterization of the sediment internal heterogeneity is produced that is appropriate for calculation of the frequency dependent sediment acoustic internal volume scattering strength and, thus, for simulation of the backscattering of energy from the internal volume of the sediment. Both seafloor heterogeneity and sediment scattering properties are parameterized as part of this research. When bubbles of free gas are present, they often represent the dominant heterogeneity controlling sediment volume scattering as well as the internal variations of sediment bulk properties such as sound speed and attenuation. Thus, in the presence of seafloor gas, a major goal of this project is the identification and description of populations of free bubbles under in situ conditions within the

sediment. A geoacoustic characterization of the seafloor is obtained from both measurements and simulations.

PROGRESS

During fiscal year 1996, work on this project was concentrated on analysis of existing x-ray CT scanning data plus the acquisition of new cores and scans from Eckernförde Bay. During August 1996, these five new pressure-tight cores were recovered and scanned to test several new procedures and to obtain gassy sediment data with the better samples and scanning protocol. This section first describes some of the results of the analysis of previously acquired data, then presents the motivation for and preliminary results of the new (1996) sampling/scanning.

In the annual report of this project for FY94, seven cores were identified as having been taken from Eckernförde Bay, retrieved in pressure-tight aluminum pressure transfer chambers (APTC) and x-ray CT scanned during the summer of 1994. Four of these cores were obtained from the 'NRL Site' and these were designated as: 706-BS-DC (P1), 707-BS-DC (P2), 708-BS-DC (P3) and 711-BS-DC (P6). They were closely spaced along a line with the center of P1 at one end of the line, P2 about 2 m from P1, then P3 another 20 cm from P2 (1.2 m from P1) and, finally, P6 another 2 m beyond P3 - at the opposite end of the line from P1. The first three were diver cores and they were obtained over a two day sampling period while core P6 is a gravity core that was obtained one week after P1. All four cores were retrieved from the seafloor in pressure tight APTCs and each was CT scanned on the day it was taken. Depth profiles of free gas concentration, obtained from the CT scan data, are presented for these four cores in Figure 1.

In Figure 1, the depth of the top of the profile for each of the cores P1, P2 and P3 has been adjusted to align several small density horizons that appeared in each core. The exact location of the top of the sediment material in these cores was not identifiable because the tops of sediment in the cores were stabilized at the seafloor by sponges inserted into the core barrel by divers. This depth uncertainty, together with the disturbance of the upper several centimeters of the sediment material, was the motivation for one of the improvements in core collection procedures that was made prior to acquiring the August 1996 cores. The improvement is described later in this report.

Core P6 was a gravity core which was taken with a 3 m coring barrel and liner to obtain a longer sample of the sediment. Unfortunately, an even higher degree of uncertainty exists for the depth axis of this core. The gravity corer clearly overpenetrated the bottom. Sediment completely filled the topmost meter of the core liner. A gap of somewhat over 30 cm occurred in the sediment material recovered in the second meter of the core liner. Most of the small density layers used to align cores P1, P2 and P3 are not identifiable in the CT scan data for P6. Thus, the free gas concentration depth profile for P6 in Figure 1 has been somewhat arbitrarily adjusted to align the depth of the shallowest occurrence of significant gas with the rather uniform depth of this feature in the other three cores. The sediment gap for core P6 has been closed up in this presentation of the profile data.

Both similarities and differences are evident in the horizontally displaced vertical profiles of free gas concentration presented in Figure 1. One obvious feature is that the depth of initiation of significant quantities of gas (about 80 cm) is consistent over the horizontal extent sampled here (recall that the depth alignment of cores P1, P2 and P3 was made on the basis of a 'coda' depth variation of density in the cored sediment, not on the basis of features of the gas concentration profile). Although gas initial occurrence depth is the same for the profiles, few of the peak concentrations align from core to core. Some of the differences among the profiles result from the different lengths of sediment material recovered (P1 was the shortest). Recalling the discussion in last year's annual report, it is often the case that the peaks of gas concentration are produced by a very small number of moderate to large sized bubbles. The differences in concentration profile details in Figure 1 suggest that the bubbles in the seafloor sampled here do not tend to collect on depth horizons of significant lateral extent (recall that the center-to-center separation of cores P2 and P3 is only about 20 cm).

Three depth zones, each with different characteristics, are implied by the profiles in Figure 1. At the shallowest depths, down to about 80 cm, there is almost no free gas indicated by the CT scan data. Some of these cores suggest that there are small but non-zero concentrations of free gas at a few depths within this upper zone. However, in general, the indications of free gas within the topmost 80 cm are minuscule and no large bubbles or bubble concentrations are indicated. These characteristics are consistent with previous observations for the shallowest several decimeters of the gassy seafloor at this site. The gas concentration profiles for the next 80 cm or so have a very 'spikey' appearance implying that many of the indications of gas result from a relatively sparse population of bubbles and that these bubbles are somewhat widely distributed spatially. Cores P2 and P6, the only two to provide data for depths into the sediment greater than 1.5 m, suggest a deeper zone of more continuously distributed free gas - that is, the gas bubbles appear to occur more nearly continuously with depth deeper than about 1.6 m. This deeper zone would yield a higher depth averaged value of free gas concentration than would be obtained for the 80 cm to 160 cm depth interval.

Two of the 'P cores' of the summer of 1994 were obtained in the frequently visited pockmark in Eckernförde Bay (P4 and P5; i.e. 709-BS-DC and 710-BS-DC). As has been noted numerous times previously, there are considerably higher gas concentrations in the floor of the pockmark than in other, nearby gassy sediments of the bay floor. This fact is illustrated in the gas concentration profile of Figure 2. Several types of information are presented in this figure. The depth dependence of gas concentration in the first panel can be compared directly with the depth distribution of bubble sizes in the second panel. Both profiles illustrate that there is also a depth zonation of the free gas bubble population within the pockmark floor. Although the gas within the pockmark floor begins at a very shallow sub-seafloor depth, in the uppermost depth zone (down to about 20 cm), there is a comparatively small concentration of gas and most of the bubbles are of small size. There is an appearance of a 'ceiling' just below 20 cm where a large amount of gas is collected and some of this is in very large bubbles. The gas concentration here is almost 9% and is one of the largest measured to date. The entire interval from 20 to about 50 cm exhibits somewhat higher average gas concentration than does the shallower zone and many more larger bubbles occur in this interval. The interval of essentially zero gas concentration near 60 cm separates the second depth zone (20 to 50 cm) from the deepest, third depth zone wherein even higher gas concentrations are noted and there are more bubbles of all sizes.

Information about the bubble sizes and locations, such as that presented in Figure 2, has been found to be crucial to an accurate calculation of the acoustic impulse response of the seafloor. One of the next challenges to such calculations, and to simulations of acoustic profiler response, is incorporation of the horizontal bubble population variation as suggested by the gas concentration profiles of Figure 1.

The sampling, measurement and analysis techniques used in this project provide useful information about the gassy sediment bubble population and distribution. This is a somewhat undersampled 'snapshot' of the bubbly interior of the seafloor. To the extent that it is possible to do so, accounting for the undersampling (primarily in the horizontal), extrapolation of observations outside a physically sampled region and development of sampling strategies for other times or areas would be greatly enhanced by an understanding of how the bubble population/distribution 'came to be' what it is observed to be. Many of the CBBL studies of other investigators contribute, in part, to providing such understanding. In this project, we are beginning to examine additional information in our CT data base which may also contribute to this understanding (relationships of bubble population features to density horizons, zones of identifiable sediment structures such as relict burrows, and such features as shell inclusions).

Another way in which the seafloor bubble population is undersampled is the limitation on minimum bubble size resolvable by techniques presently applied to delineate the bubbles. Some aspects of the bubbly seafloor acoustic response are somewhat reduced for an individual bubble as bubble size decreases. As shown in the second year annual report for this project, theoretical predictions indicate that the scattering cross-section for a bubble decreases as bubble size decreases (and thus as resonance frequency increases). This tends to decrease the significance of an individual resonant bubble scatterer as bubble size decreases. However, it is frequently observed that, for some bubble size range, the number of bubbles in a natural population increases with decreasing size. This is commonly observed for gas bubble populations in seawater wherein a peak in noted in the number vs size distribution. As bubble size continues to decrease below this 'peak' size, the number of bubbles decreases with decreasing size (e.g. Farmer and Vagle, JASA, 86, 1897-1908, 1989). Other authors have speculated that a similar distribution would obtain for bubble populations within sediments (e.g. Boyle and Chotiros, JASA, 98, 525-530, 1995). As illustrated in the third panel of Figure 2, over the size span of bubbles observable by the presently applied x-ray CT scanning, the number of bubbles monotonically increases as bubble size decreases. Thus, the relative significance of the small bubbles in the population, and even of bubbles not resolvable by the present method, is increased in importance for acoustic volume scattering over that which would obtain for a uniform distribution of sizes in the bubble population. A very large number of small bubbles which are uniformly distributed throughout a sediment volume can also be important in reducing the sound speed through the bubbly interval for acoustic frequencies below the bubble resonance.

As shown by Figure 3, the bubble population distribution for cores P1, P2, P3 and P6 (all from the NRL site) was of similar form to that for core P5 (from the pockmark site). All of the bubble size distributions are for the bubble populations of entire cores. The detailed distributions for smaller depth intervals sometimes vary from this overall population distribution. Thus, either the

volume scattering response or acoustic bulk properties of small depth intervals can vary and will be controlled by the details of the bubble population for that zone.

Analysis of ASCS, and other profiler, data from the CBBL Eckernförde Bay measurements has provided both (1) interesting confirmations of the validity of some of the acoustic simulations based on bubble distribution data such as that described here and (2) some tantalizing ambiguities from expected behavior. Because of the spatial variability of the bubble populations, especially in the horizontal, it would not be expected that an exact match would be achieved between simulated signals and profiler data. A very encouraging degree of agreement has been achieved between simulations and ASCS data from the gassy seafloor of the NRL Site in Eckernförde Bay as reported by Lyons, et al., 1996 (see list of Publications and Presentations). The degree of agreement observed was only achieved when the full seafloor impulse response for the bubbly seafloor was calculated by (1) taking into account the frequency dependent scattering cross-section of each small depth interval, based on the bubble population observed from CT scanned, pressure-tight cores, (2) properly relating, in depth or time, this cross-section to those of other small depth intervals and (3) accounting for the reduced net acoustic response from deeper bubbly intervals that results from absorption and scattering losses in overlying bubbly intervals.

Similar simulations have been calculated for the bubble populations observed in the 'P-cores' obtained during 1994. This has been done with a variety of simulated acoustic source waveforms - especially for short duration pulses of single frequency sinusoids. As would be expected, the depth intervals of the seafloor producing the strongest returns for a given simulated acoustic pulse are strongly correlated with the depth intervals of the impulse response that indicate strong scattering strengths from bubbles resonant at the dominant frequencies of the acoustic pulse. This is relevant to Abegg and Anderson's (1997) reported observation for Eckernförde Bay that the depth within the seafloor at which total methane concentration exceeds calculated saturation values is typically several decimeters shallower than the depth of the top of the acoustic turbidity as observed by a 3.5 kHz acoustic profiler. It would be expected that bubbles initially formed when a gas species reaches supersaturation within the seafloor would be very small and that they would grow with time as additional molecules are accumulated in the bubbles - until gas pressures within and outside the bubbles equilibrate. Such initial formation of very small bubbles has been noted immediately after reducing pressure on gassy mud samples by Martens for Cape Lookout Bight samples (personal communication) and by Abegg and other people working on this project for Eckernförde Bay samples. It is likely that the depth distribution of bubble sizes, with larger (including 3.5 kHz resonant) bubbles only occurring at greater depths, is the origin of the saturation and turbidity depth differences.

As noted by Lyons, et al. (1996), as used to collect Eckernförde Bay profiling data, the ASCS system source pulse contained significant energy both at 15 kHz and 30 kHz. This fortunate circumstance allowed the wider band comparison between simulations and data reported by Lyons, et al. Further analysis of some of the ASCS pulses for this data set has led to an interesting observation. Rather than a frequency independent return of acoustic energy from the water sediment interface of Eckernförde Bay, a somewhat higher return of energy, relative to the incident energy, is observed for 30 kHz as compared with 15 kHz. This frequency dependent seafloor interaction is not consistent with a plane wave reflection model. However, the initial

pulse of energy returned from the seafloor is of essentially the same temporal duration as the ensonifying pulse. Thus, one is left to speculate about the possible origin of the observed frequency dependence. Although we have considered several possible origins for this modest frequency dependence of the seafloor interaction, including interface roughness, near surface gradients within the sediments and bulk property heterogeneity, none of these matched the combination of observables in the acoustic data. The only model that exhibited promise was a few very small bubbles, so small as to be resonant at or somewhat above 30 kHz, constrained to a sediment depth zone within a few mm of the water-sediment interface. Bubbles of this size would be just beyond the size resolution of the CT scanning method as applied through 1995. Volume scattering from such a bubble population, if present, would not produce all of the acoustic energy observed to be returned from the water-sediment interface but it could influence the frequency dependence of the return.

Other CBBL investigators have observed the topmost one or two centimeters of the sediment of the floor of Eckernförde Bay to be oxygenated, highly reworked and pelletized by intensive biological activity. The mucous coated fecal pellets within this zones could provide candidate microenvironments for formation of very small bubbles of free gas. Because of an interest in the details of the internal structure of the sediments in the very near surface (of the sediment) zone in general, and an interest in seeking information about the possibility of very near surface gas bubbles in particular, a new method was devised for stabilizing the tops of the core samples before they are capped and inserted into the APTCs at the seafloor. Fritz Abegg designed a piston which is inserted into the coring tube after a core is taken and while the core remains vertical at the seafloor. This piston is designed to free fall slowly, under gravitational forcing, until it comes to rest gently at the water-sediment interface of the core sample. Upon reorientation to the horizontal, a weight at the top of the piston causes the piston to cant to the side slightly, thus becoming lodged within the coring tube and preventing slumping or disturbance of the surficial sediment material.

Two of the major purposes of the new cores taken from Eckernförde Bay in August 1996 were (1) to obtain cores from the NRL site with the water-surface interface preserved by the above described surface-stabilizing piston and (2) to seek to increase the resolution of the x-ray CT scan data for the pressure tight Eckernförde Bay samples. Higher resolution data would provide information about smaller bubbles than those identified to date. Such information would contribute to better definition of the size distribution of the bubble population throughout a core sample in general (thus contributing to our understanding of the shape of this size distribution - and how near the peak in the distribution our present descriptions may be). Smaller bubble information should also assist in determining whether a tiny bubble population constrained near the sediment surface is contributing to the observed frequency dependence of acoustic interaction with the water-sediment interface. A different mode of operation of the ELSCINT Twin scanner in the Prüner Gang clinic was used to achieve the higher resolution. This mode involved a different scanning geometry and longer scanning time (to reduce noise that would otherwise reduce the data quality at this higher resolution). By application of this technique, the minimum radius of an equivalent-size spherical bubble that could be identified was improved to about 0.2 mm.

During August, 1996, over a period of three days, five seafloor cores were recovered in pressure-tight APTCs from near the NRL site in Eckernförde Bay. All were high quality cores with the top of the sample stabilized by one of the new pistons. All were scanned on the day taken at the Prüner Gang radiology clinic in Kiel. The cost, in time and money, for the new, very high resolution CT scanning precluded application of the method to entire cores. Instead, the topmost 4 cm of each core, and thicker depth intervals at greater depth in some cores were subjected to such high resolution scanning. The full length of the cores was also scanned using the lower resolution approach which has been applied in our previous work. After scanning, the APTC for each core section was opened and physical samples of the sediment were taken through taped, pre-drilled holes in the sidewall of the coring tube in the usual manner used by Fritz Abegg. These samples were subjected to subsequent analysis for methane content by gas chromatography.

The whole core 'normal resolution' scans of these new samples indicate that, as usual there is little or no gas in the surficial several decimeters below the seafloor with the now familiar 'spikey' gas concentration profile beginning near 1 m depth into the seafloor. There is little or no depth ambiguity for these new data because the sediment surface is preserved by the new stabilizing piston. Data for the surficial four cm of the sediment of one core (tentative identification DC194) are shown in Figure 4. The topmost panel shows a free gas concentration profile for this depth interval based on the usual resolution scanning mode as applied for previous cores from the area. The bottom panel of the figure shows such a profile based on data from the new, higher resolution scanning mode. Obviously, some gas does exist in bubbles within about the topmost centimeter of the seafloor and most of this gas is in bubbles smaller than about 0.4 mm equivalent radius. This result provides interesting support for the hypothesis of tiny bubbles, existing only within a very thin surficial zone and resonant at frequencies near or above 30 kHz, contributing to the noted frequency dependence of acoustic returns from the interface. Information about the bubbles, and sediment internal density structure, has only become available now for the surficial sediment by use of the new method for stabilizing the surface of the sediment sample.

No new sampling is planned for the final year of this project. Instead, we will concentrate on analysis of the existing base of CT scan data to provide increased knowledge about the distribution of gas in the floor of Eckernförde Bay. Additional acoustic simulations will be carried out to refine our understanding of the response to be expected in profiles of such regions from acoustic systems. Correlations of bubble occurrence with other observables in the CT scan data base will also be examined. Analysis will proceed for delineating the internal heterogeneity of scanned samples from the sandy shelf off Panama City, Florida and the carbonate seafloor off Key West, Florida.

PUBLICATIONS AND PRESENTATIONS (four years cumulative)

F. Abegg and A.L. Anderson 'The acoustic turbid layer in muddy sediments Eckernförde Bay, Western Baltic: methane concentration, saturation and bubble characteristics' scheduled for Marine Geology, vol. 137, nos. 1 & 2, February 1997.

T.H. Orsi, A.L. Anderson and A.P. Lyons 'X-ray tomographic analysis of sediment macrosctructure and physical property variability in Eckernförde Bay, Western Baltic Sea' Geo-Marine Letters, vol. 16, no. 3, August 1996, 232-239.

T.H. Orsi, F. Werner, D. Milkert, A.L. Anderson, and W.R. Bryant 'Environmental overview of Eckernförde Bay, Northern Germany' Geo-Marine Letters. vol. 16, no. 3, August 1996, 140-147.

A.P. Lyons, M.E. Duncan, A.L. Anderson and J.A. Hawkins 'Predictions of the acoustic scattering response of free-methane bubbles in muddy sediments' J. Acoust. Soc. Am., vol. 99, January 1996, 163-172.

T.H. Orsi and A.L. Anderson 'X-ray computed tomography of macroscale variability in sediment physical properties, offshore Louisiana' Gulf Coast Association of Geological Societies Transactions, Vol. 45, pp. 475-480, 1995 also presented at the GCAGS Convention, Baton Rouge, Louisiana, October 1995; abstract published in AAPG Bulletin, vol. 79, no. 10, p. 1565, 1995.

T.H. Orsi, A.L. Anderson, W.R. Bryant, K. Davis, R. Rezak, K.M. Fischer and C. Brunner 'Computed tomography of physical property heterogeneity of carbonate muds from Marquesas Keys and Dry Tortugas, South Florida' presented at the first SEPM Congress on Sedimentary Geology, St. Pete Beach, Florida, August 13-16, 1995; abstract in Congress Program and Abstracts, Vol. 1, p. 96.

A.P. Lyons 'Acoustic volume scattering from the seafloor and the small scale structure of heterogeneous sediments' unpublished Ph.D. thesis, College Station, Texas, Texas A&M University, August 1995.

A.L. Anderson 'Indications of seafloor free gas, the interaction of underwater sound and bubbly sediment' presented at the Workshop on Modelling Methane-Rich Sediments of Eckernförde Bay, Eckernförde, Germany, June 26-30, 1995.

A.L. Anderson, F. Abegg and R.A. Weitz 'Gas concentration and bubble distribution in the floor of Eckernförde Bay: ground truth from core sample measurements' presented at the Workshop on Modelling Methane-Rich Sediments of Eckernförde Bay, Eckernförde, Germany, June 26-30, 1995, extended abstract pp. 70-72 In: Wever, T.F. (ed.), Proceedings of the Workshop on Modelling Methane-Rich Sediments of Eckernförde Bay, FWG-Report 22, Keil, June 1995.

A.L. Anderson, A.P. Lyons, F. Abegg, M.E. Duncan, J.A. Hawkins and R.A. Weitz 'Modeling acoustic volume scattering by a bubbly mud seafloor with examples from Eckernförde Bay' presented at the Workshop on Modelling Methane-Rich Sediments of Eckernförde Bay, Eckernförde, Germany, June 26-30, 1995, extended abstract pp. 243-247 In: Wever, T.F. (ed.), Proceedings of the Workshop on Modelling Methane-Rich Sediments of Eckernförde Bay, FWG-Report 22, Keil, June 1995.

J.A. Hawkins, D.N. Lambert, D.J. Walter, A.P. Lyons, M.E. Duncan and A.L. Anderson 'Spectral characterization of bubbly sediments using high frequency, short duration acoustic

pulses' presented at the Workshop on Modelling Methane-Rich Sediments of Eckernförde Bay, Eckernförde, Germany, June 26-30, 1995, extended abstract pp. 65-69 In: Wever, T.F. (ed.), Proceedings of the Workshop on Modelling Methane-Rich Sediments of Eckernförde Bay, FWG-Report 22, Keil, June 1995.

A.P. Lyons, M.E. Duncan, J.A. Hawkins and A.L. Anderson 'Predictions of the acoustic response of free methane bubbles in muddy sediments' invited paper presented at the special session on High Frequency Inversions for Sediment Properties at the 128th meeting of the Acoustical Society of America in Austin, Texas, November 28, 1994, abstract published in J. Acoust. Soc. Am., V. 96, N. 2, pt 2, 3217, 1994.

M.D. Richardson, S.R. Griffin, K.B. Briggs, A.L. Anderson and A.P. Lyons 'The effects of free methane bubbles on the propagation and scattering of compressional and shear wave energy in muddy sediments' invited paper presented at the special session on High Frequency Inversions for Sediment Properties at the 128th meeting of the Acoustical Society of America in Austin, Texas, November 28, 1994, abstract published in J. Acoust. Soc. Am., V. 96, N. 2, pt 2, 3218, 1994.

T.H. Orsi and A.L. Anderson 'Bubble characteristics in gassy sediments' Gulf Coast Association of Geological Societies Convention, Austin, Texas, October 5-7, 1994.

F. Abegg and A.L. Anderson 'The acoustic turbid layer in soft mud: methane concentration, saturation and bubble characteristics. Examples from Eckernförde Bay, Germany' Proceedings, Third International Conference on Gas in Marine Sediments, Texel, The Netherlands, September 25-28, 1994.

A.P. Lyons, A.L. Anderson and T.H. Orsi 'Modeling acoustic volume backscatter from two shallow-water marine environments by side-scan sonar' IEEE-OES OCEANS 94, Brest, France, September 13-16, 1994, Proceedings Vol I:862-865.

T.H. Orsi, A.L. Anderson and A.P. Lyons 'Geoacoustic characterization of shallow-water marine sediments for high-frequency applications' IEEE-OES OCEANS 94, Brest, France, September 13-16, 1994, Proceedings Vol I:866-871.

T.H. Orsi 'Computed tomography of macrostructure and physical property variability of seafloor sediments' unpublished PhD thesis, College Station, TX, Texas A&M University, August 1994.

F. Abegg, A.L. Anderson, L. Buzi, A.P. Lyons and T.H. Orsi 'Free methane concentration and bubble characteristics in Eckernförde Bay, Germany' pp. 84-89 In: Wever, T.F. (ed.) Proceedings of the Gassy Mud Workshop held at Forschungsanstalt der Bundeswehr für Wassershall und Geophysic (FWG), Kiel, Germany, July 11-12, 1994.

A.L. Anderson, A.P. Lyons, L. Buzi, F. Abegg and T.H. Orsi 'Modeling acoustic interaction with a gassy seafloor including examples from Eckernförde Bay' pp. 90-94 In: Wever, T.F. (ed.) Proceedings of the Gassy Mud Workshop held at Forschungsanstalt der Bundeswehr für Wassershall und Geophysic (FWG), Kiel, Germany, July 11-12, 1994.

A.L. Anderson and F. Abegg 'Measurement of gas bubble concentration and distribution in the seafloor of Eckernförde Bay, Germany' 1994 AGU/ASLO Ocean Sciences Meeting, San Diego, California, February 21-25, 1994; Abstract published in EOS Supplement, Vol. 75, No. 3, p. 159, January 18, 1994.

A.P. Lyons, A.L. Anderson and T.H. Orsi 'Estimates of volume scattering cross section and related parameters due to property variability in Eckernförde Bay' 1994 AGU/ASLO Ocean Sciences Meeting, San Diego, California, February 21-25, 1994; Abstract published in EOS Supplement, Vol. 75, No. 3, p. 203, January 18, 1994.

T. H. Orsi and A.L. Anderson 'Macroscale heterogeneity of sediments from Eckernförde Bay (Western Baltic Sea): Quantitative characterization using x-ray CT' 1994 AGU/ASLO Ocean Sciences Meeting, San Diego, California, February 21-25, 1994; Abstract published in EOS Supplement, Vol. 75, No. 3, p. 220, January 18, 1994.

K. M. Fischer and T.H. Orsi 'Porosity gradients in Eckernförde Bay (Baltic Sea), Germany: carbon content' 1994 AGU/ASLO Ocean Sciences Meeting, San Diego, California, February 21-25, 1994; Abstract published in EOS Supplement, Vol. 75, No. 3, p. 220, January 18, 1994.

T.H. Orsi 'Computed tomography of macrostructure and physical property heterogeneity in surface sediments of Eckernförde Bay (Western Baltic Sea)' 6th Annual Student Symposium, College of Geosciences and Maritime Studies/Ocean Drilling Program, Texas A&M University, College Station, TX, February 19, 1994.

A.P. Lyons and T.H. Orsi 'Characterization of seafloor property variability and estimates of acoustic volume scattering cross section in Eckernförde Bay, Germany' 6th Annual Student Symposium, College of Geosciences and Maritime Studies/Ocean Drilling Program, Texas A&M University, College Station, TX, February 19, 1994.

T.H. Orsi 'A method for quantifying bubble characteristics in gassy aqeous sediments' 6th Annual Student Symposium, College of Geosciences and Maritime Studies/Ocean Drilling Program, Texas A&M University, College Station, TX, February 19, 1994.

T.H. Orsi and A.L. Anderson 'Computer tomography of biological structures in marine sediments' IEEE-OES OCEANS 93, Victoria, Canada, September, 1993.

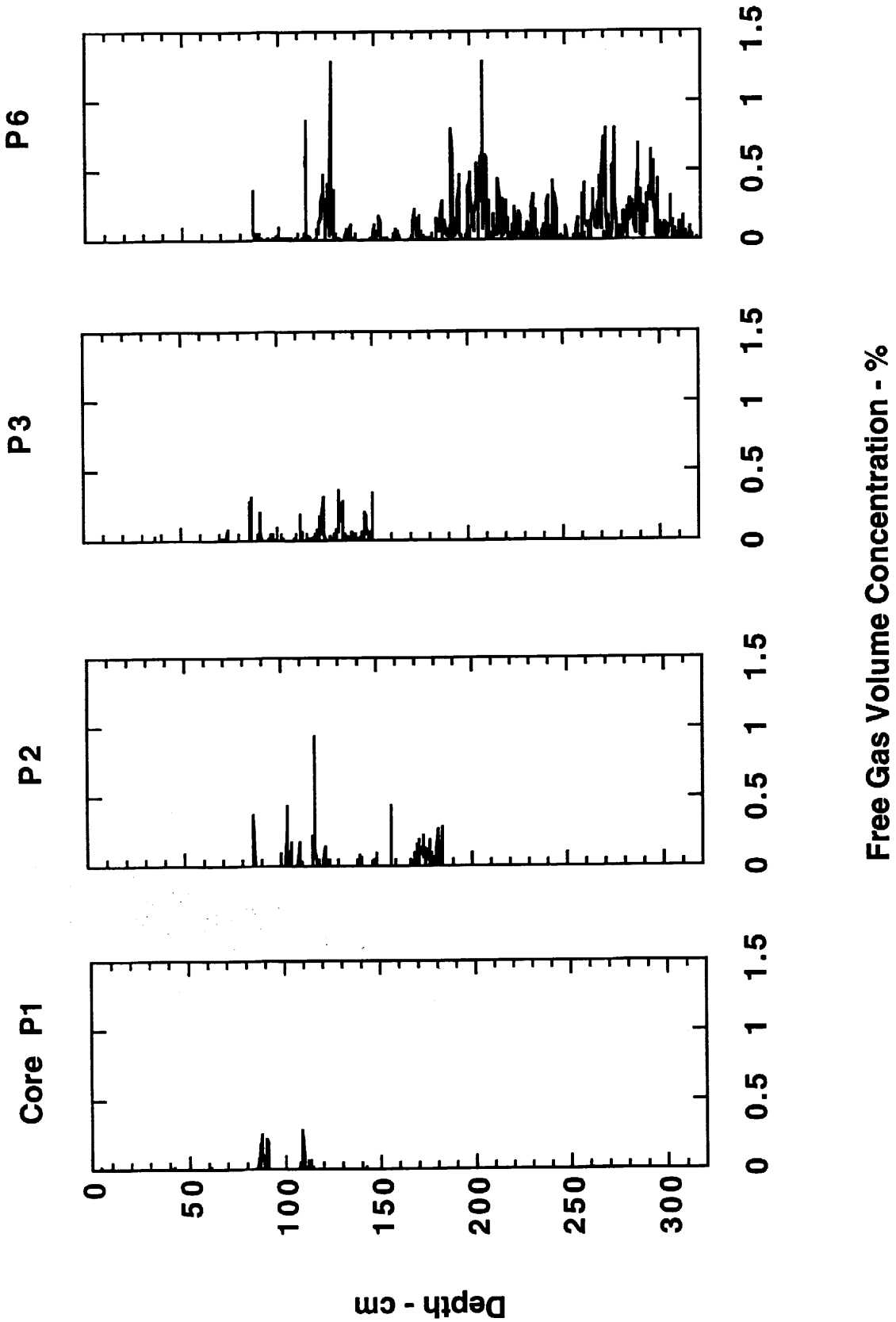
Core P1
P2
P3
P6
0
50
100
150
200
250
300
Depth - cm
0
0.5
1
1.5
Free Gas Volume Concentration - %

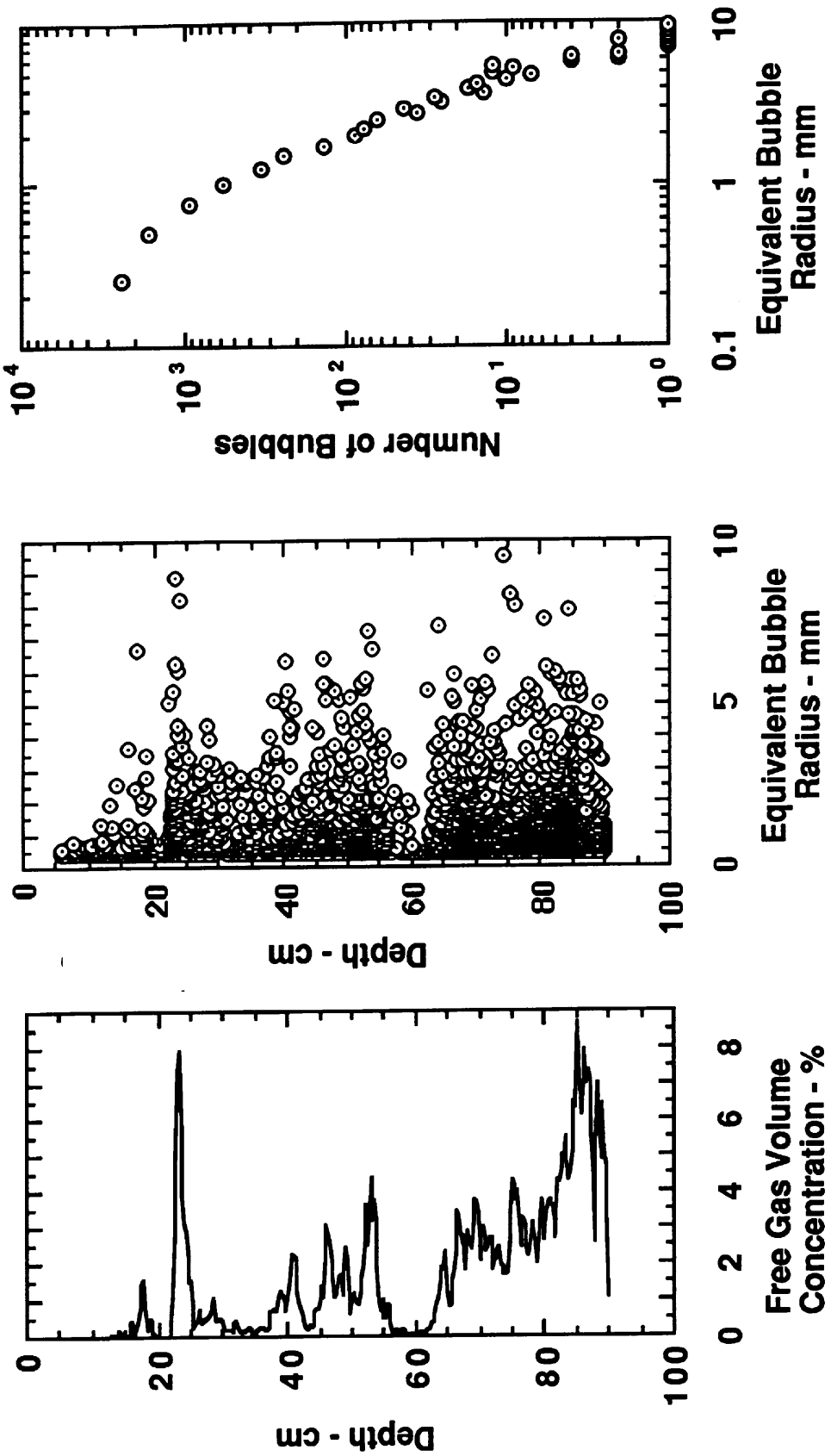
Number of Bubbles
10^4
10^3
10^2
10^1
10^0
0.1
1
10
Equivalent Bubble Radius - mm
Depth - cm
0
20
40
60
80
100
0
5
10
Equivalent Bubble Radius - mm
Depth - cm
0
20
40
60
80
100
0
2
4
6
8
Free Gas Volume Concentration - %

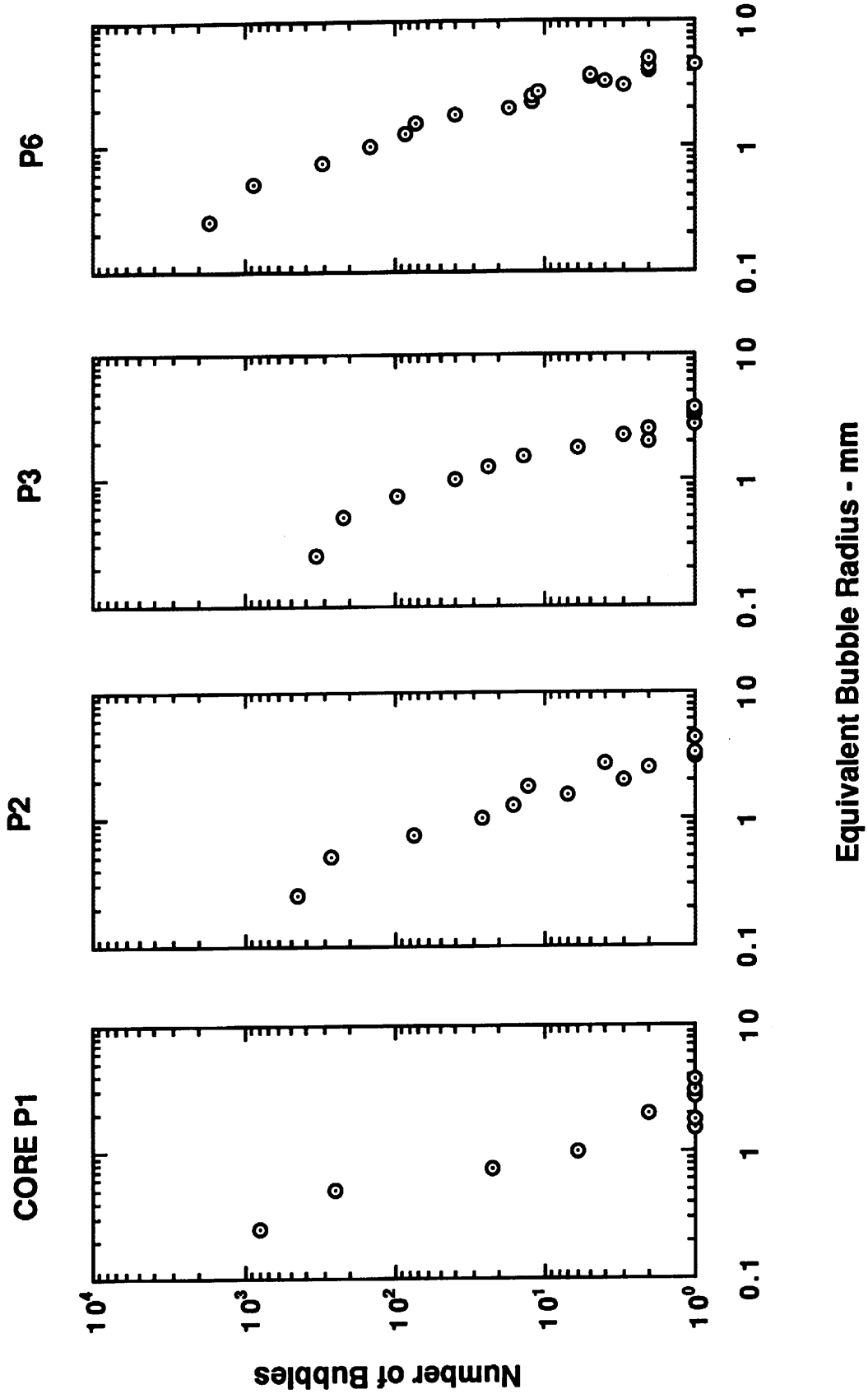
CORE P1
P2
P3
P6
Number of Bubbles
Equivalent Bubble Radius - mm
10^4
10^3
10^2
10^1
10^0
0.1
1
10

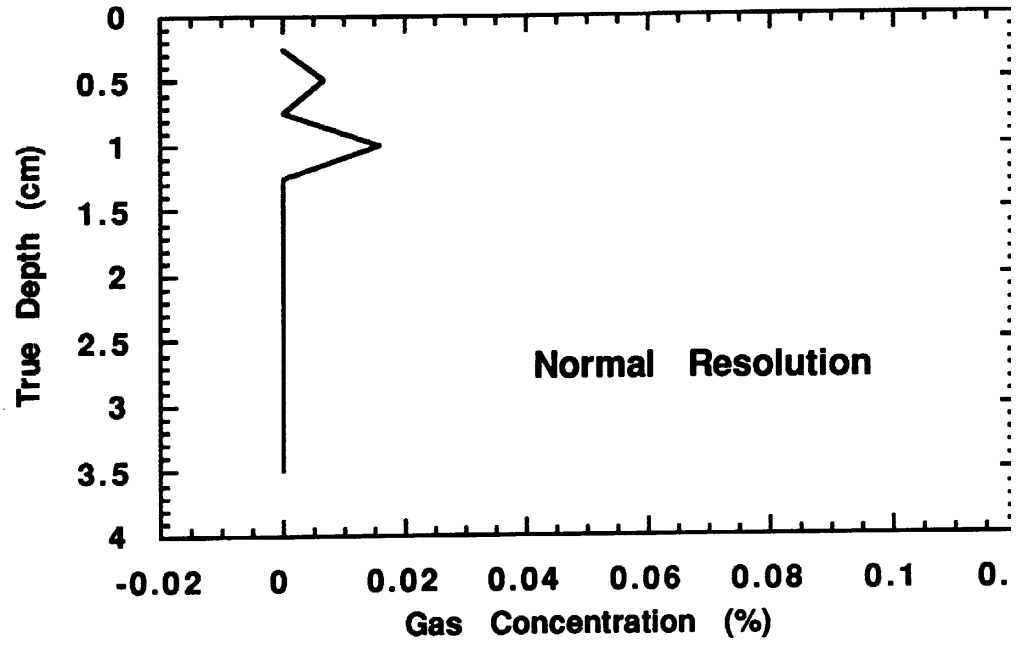
True Depth (cm)
0
0.5
1
1.5
2
2.5
3
3.5
4
-0.02
0
0.02
0.04
0.06
0.08
0.1
0.
Gas Concentration (%)
Normal Resolution

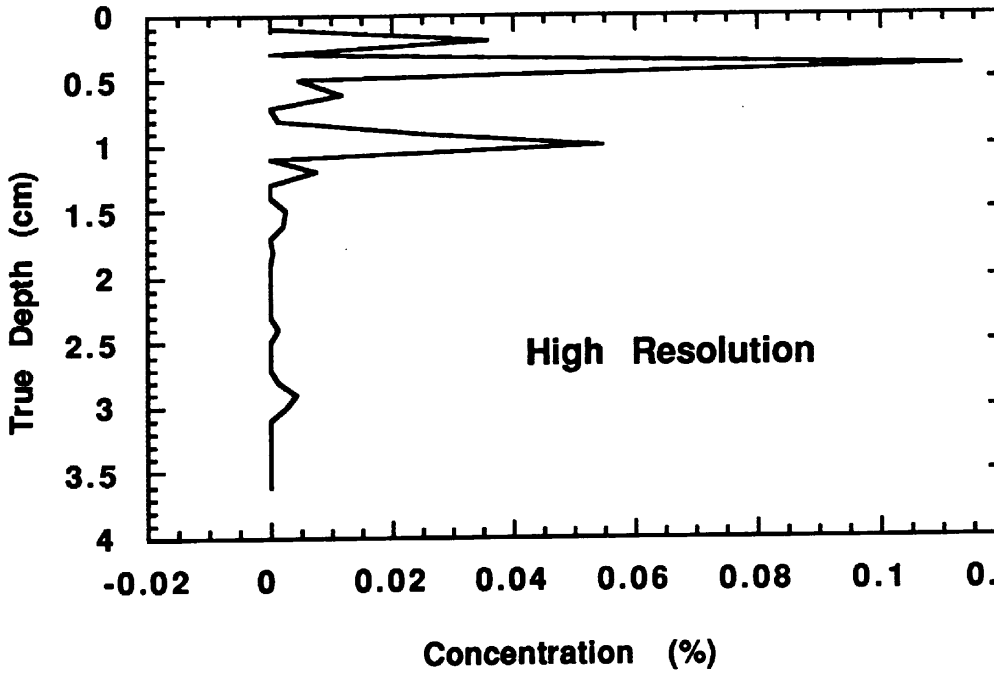
True Depth (cm)
0
0.5
1
1.5
2
2.5
3
3.5
4
-0.02
0
0.02
0.04
0.06
0.08
0.1
0.
Concentration (%)
High Resolution

2.3 High-Frequency Acoustic Scattering from Sediment Surface Roughness and Sediment Volume Inhomogeneities (Principal Investigators: K.B. Briggs and M.D. Richardson)

Kevin Briggs and Michael Richardson
NRL Code 7431, Stennis Space Center, MS 39529-5004

Introduction

The objectives in this research effort are to characterize sediment structure and understand the processes which determine sediment properties, to characterize the statistical parameters describing the microtopography of the sea floor, and to provide parameterization of the significant sediment properties which create high-frequency bottom reverberation in shallow water. Progress toward these objectives was accomplished through the analysis of data collected during the three field experiments of FY93-95. Measurements of sediment geoacoustic (compressional and shear wave velocity and attenuation) and physical (porosity, density, and grain size) properties were processed in order to ascertain the statistical variability of the properties at each site. From such statistical parameters, input values for models predicting acoustic bottom scattering, mine burial, or sediment diagenesis may be generated.

This year, investigators characterized sediment volume heterogeneity in order to better understand geoacoustic variability at the Dry Tortugas and Eckernförde Bay experiment sites. Investigators also characterized the sediment interface roughness within the ensonified areas of the FY93 Panama City experiment site over extended pathlengths and the FY95 Dry Tortugas experiment site both before and after diver manipulation. Laboratory analyses of sediment properties from the FY95 experiments were compiled in a data report. In addition, x-radiography and electrical resistivity of sediment from the Eckernförde Bay experiment site were compared as diagnostic tools for ascertaining sediment heterogeneity. As a natural follow-on to the objectives of the CBBL, a survey of the StrataForm site off the Eel River was conducted in order to extend the understanding of the type of processes occurring in shallow-water environments to an area exhibiting strong biological and hydrodynamic influences.

Accomplishments

Eckernförde

A technique combining X-ray and resistivity imaging is being developed for use on x-radiographs cores and successfully used to identify heterogeneity due to shells and storm layers. The technique offers the possibility of combining porosity and formation factor data to assess the pore morphologies associated with the two different microstructures resulting from pelletized or silt/fine sand graded bedding. Our approach involves the digitized images from X-radiograph cores 195-1 and 222-1 from the central experiment site in Eckernförde Bay. The porosity data from diver cores are averaged and applied to the X-ray density and electrical resistivity data from the two X-radiograph cores. Horizontal and vertical correlation lengths are calculated by assuming an exponential form for the autocorrelation functions. Some data indicate that horizontal correlation lengths tend to be greater than vertical correlation lengths, indicating the predominance of

continuous, horizontal layering within the sediment structure. A manuscript describing and evaluating the results of this technique is being prepared.

Panama City

Underwater stereo photogrammetry was used to generate roughness power spectral slopes and intercepts in FY93 off Panama City, Florida. The use of a stereo camera supported on large, moveable levels allowed divers to collect overlapping stereo photographic for the purpose of examining microroughness over longer pathlengths. The longer pathlengths over which roughness measurements were made in this experiment extended the roughness power spectra into lower spatial frequencies while preserving the high-resolution (<1 cm) advantage of close-range photogrammetry. The behavior of the power spectra generated from digitized transects of 50, 100, and 200-cm is being examined with respect to the "flattening" of the spectra at the lowest spatial frequencies. The data exhibit trends similar to previous experiments, appearing to support the universality of low-spatial-frequency spectrum behavior irrespective of seafloor sediment type. A presentation for publication in a symposium volume is being prepared with these data.

Key West

Sediment physical property and microroughness data were published in a NRL Memorandum Report and this data report was disseminated to CBBL colleagues. Stereo photogrammetry was used to measure interface roughness at the Dry Tortugas site. The roughness power spectra had an average slope of -2.29 and an intercept of 2.09×10^{-3} cm^3. Areas that were smoothed by divers exhibited a roughness spectra slope of -2.60 and an intercept of 7.25×10^{-4} cm^3, documenting the removal of fine-scale roughness elements by the smoothing tool. An area gouged by divers exhibited a roughness spectra slope of -2.80 and an intercept of 1.36×10^{-3} cm^3, documenting the introduction of large-scale (10's of cm) roughness elements. These data are presented, along with those from Eckernförde Bay and Panama City, in an IEEE Journal of Oceanic Engineering paper to be published in fall of 1996.

The Marquesas Keys and Dry Tortugas sites were compared to examine the significant effects of bioturbation on these carbonate sediments. Sediment at the Marquesas Keys site is characterized by fine laminations of sand-silt-clay in the upper 4 cm and a striking increase in proportion of gravel-size mollusk shells below 5 cm. The Dry Tortugas site has a sand-silt-clay with fewer gravel-size particles and surficially dominant bioturbation. Fewer shell fragments result in less variability in acoustic properties. Different fauna at the two study sites create small-scale differences in the sediment heterogeneity, manifested by either fine laminations at the Marquesas Keys site, the result of resettling of particles ejected from thalassinid shrimp burrows, or patchy, burrowed and winnowed sediment at the Dry Tortugas site. X-radiographs documenting the differences between the processes occurring at the two sites are displayed in a manuscript submitted to the journal Geo-Marine Letters.

Digital image analysis of the seven x-radiographic cores collected in the Dry Tortugas area was initiated. Patterns of sediment mixing appear to be random and extend to 15-18 cm sediment depth. Patterns of electrical resistivity also appear to be random in distribution.

Eel River

A cruise was conducted in June which consisted of a survey of geological and geoacoustic properties of the northern California shelf along two transects. One transect followed the "S-line" from 20 to 100 m water depth; the other transect followed the 70-m depth contour from the "C-line" to the "U-line". Individual deployments of the In-Situ Sediment geoAcoustic Measurement System were accompanied by collection of samples from grabs, box cores, and gravity cores. Of chief interest was the variability at station S60, where deployment of the Applied Physics Laboratory-University of Washington Benthic Acoustic Measurement System tower was planned. This site was characterized by a clayey silt (38% clay/58% silt) consisting of layers of successive flood deposits. Figure 1 shows the vertical distribution of porosity in the top 35 cm of sediment. The results of shear strength measurements (Fig. 2) followed the trend exhibited by sediment porosity, namely, that there are several discrete layers indicated by cyclic fluctuations of high-porosity, low-shear strength sediment. Vertical profiles of compressional wave velocity at 400 kHz exhibit a similar trend (Fig. 3).

Plans for FY97

The manuscript evaluating the use of X-radiographic and electrical resistivity imaging to determine the statistical characteristics of sediment inhomogeneity will be submitted to a peer-reviewed journal. The 3-dimensional electrical resistivity imaging of Dry Tortugas sediments will be processed and evaluated for another manuscript. X-radiographs from the Dry Tortugas site will be digitized and compared to sediment density structure analyzed from Eckernförde Bay.

The roughness power spectra from the extended pathlengths digitized from Panama City stereo photographs will be averaged, smoothed and compared with other long pathlength roughness measurements of the sea floor. The results of this comparison will be presented in a Shallow-Water Acoustics Conference in Beijing, China. Permeability cores from the FY93 Panama City experiment will be analyzed.

The method for determining the 1-dimensional autocorrelation functions for sediment porosity and compressional velocity fluctuations will be presented at a conference for High-Frequency Acoustics in Shallow Water held in La Spezia, Italy. The presentation will include a conceptual model for predicting hydrodynamic and biological processes from variability of sediment porosity and sound velocity fluctuations. The data presented will include results from the FY93 and FY95 experiments.

The grain size analysis for cores collected on the Eel River cruise will be completed and the results compared with the sediment porosity, shear strength, X-radiographic and sound velocity data to delineate individual layers in vertical profiles along the S-line and the 70-m contour. A manuscript reporting the results of these analyses will be submitted for possible publication in a special issue of Marine Geology.

Presentations and Publications

Briggs, K.B., M.D. Richardson and D.B. Percival. 1994. Correlation functions estimated from vertical profiles of sediment porosity and compressional wave velocity fluctuations. *EOS*, 75: 202.

Briggs, K.B. and M.D. Richardson. 1994. Geoacoustic and physical properties of near surface sediments in Eckernförde Bay. *Proceedings of the Gassy Mud Workshop held at the FWG, Kiel.* Kiel, Germany, 11-12 July, 1994, pp. 39-46.

Briggs, K.B. 1994. Correlation functions for sediment acoustic properties. *J. Acoust. Soc. Am.*, 96: 3245-3246.

Briggs, K.B., M.D. Richardson and D.R. Jackson. 1994. High-frequency bottom backscattering: volume scattering from gassy mud. *J. Acoust. Soc. Am.*, 96: 3218.

Briggs, K.B. and M.D. Richardson. 1995. Physical property variability in sediments in and proximal to Eckernförde Bay. In, Wever, T.F. (ed.), *Proceedings of the Workshop Modelling Methane-Rich Sediments of Eckernförde Bay.* Eckernförde, Germany, 26-30 June 1995, pp. 208-214.

Briggs, K.B. and M.D. Richardson. 1995. Geoacoustic and physical properties of carbonate sediments from the Key West Campaign. SEPM Congress on Sedimentary Geology, St. Petersburg, FL, 13-16 Aug. 1995, p. 33.

Briggs, K.B. and M.D, Richardson. (1996). Variability in in situ shear strength of gassy sediments. *Geo-Mar. Ltrs.*, 16: 189-195.

Briggs, K.B. and M.D. Richardson. (1996). Small-scale fluctuations in acoustic and physical properties in surficial carbonate sediments. *EOS*, 76: OS172.

Bennett, R.H., M.H. Hulbert, M. Meyer, D.M. Lavoie, **K.B. Briggs**, D.L. Lavoie, R.J. Baerwald, and W.-A. Chiou. (1996). Fundamental response of pore water pressure to microfabric and permeability characteristics: Eckernförde Bay. *Geo-Mar. Ltrs.*, 16: 182-188.

Briggs, K.B., D.L. Lavoie, K.P. Stephens, M.D. Richardson and Y. Furukawa. 1996. Physical and Geoacoustic Properties of Sediments Collected for the Key West Campaign, February 1995: A Data Report. Naval Research Laboratory, NRL/MR/7431--96-8002, 400p.

Holyer, R.J., D.K. Young, J.R. Chase and **K.B. Briggs**. 1994. Sediment density structure inferred by textural analysis of cross-sectional x-radiographs and electron microscopy images. *EOS*, 75: 202.

Holyer, R.J., D.K. Young, J.C. Sandidge, and **K.B. Briggs**. (1996). Sediment density structure derived from textural analysis of cross-sectional x-radiographs. *Geo-Mar. Ltrs.*, 16: 204-211.

Jackson, D.R., K.L. Williams, and **K.B. Briggs**. (1996). High-frequency acoustic observations of benthic spatial and temporal variability. *Geo-Mar. Ltrs.*, 16: 212-218.

Jackson, D.R., **K.B. Briggs**, K.L. Williams and M.D. Richardson. (1996). Tests of models for high-frequency sea-floor backscatter. *IEEE J. Ocean. Engin.*, 21: 458-470.

Jackson, P.D., **K.B. Briggs**, R.F. Flint, M.A. Lovell and P.K. Harvey. 1994. Evaluation of the porosity structure of coastal benthic boundary layer sediments using micro-resistivity imaging. *EOS*, 75: 201.

Jackson, P.D., **K.B. Briggs**, R.F. Flint, M.A. Lovell and P.K. Harvey. 1994. The investigation of millimeter scale heterogeneity in Coastal Benthic Boundary Layer sediments using microresistivity and x-ray imaging of "diver" cores. *J. Acoust. Soc. Am.*, 96: 3245.

Jackson, P.D. and **K.B. Briggs**. 1995. Evaluation of heterogeneity within gas-rich sediments using micro-resistivity imaging and x-radiography. In, Wever, T.F. (ed.), *Proceedings of the*

Workshop Modelling Methane-Rich Sediments at Eckernförde Bay. Eckernförde, Germany, 26-30 June 1995, pp. 215-216.

Jackson, P.D., **K.B. Briggs** and R.C. Flint. (1996). Evaluation of sediment heterogeneity using micro-resistivity imaging and X-radiography. *Geo-Mar. Ltrs.*, 16: 219-225.

Richardson, M.D., S. Griffin and **K.B. Briggs**. 1994. In-situ sediment geoacoustic properties: a comparison of soft mud and hard packed sand sediments. *EOS*, 75: 220.

Richardson, M.D. and **K.B. Briggs**. (1996). In-situ and laboratory geoacoustic measurements in soft mud and hard-packed sand sediments. *Geo-Mar. Ltrs.*, 16: 196-203.

Richardson, M.D., **K.B. Briggs** and A.M. Davis (1996). Geoacoustic properties of carbonate sediments. *EOS*, 76: OS172.

Stephens, K., D.L. Lavoie, Y. Furakawa and **K.B. Briggs**. 1995. Variability of physical properties from the Dry Tortugas and Marquesas Keys. SEPM Congress on Sedimentary Geology, St. Petersburg, FL, 13-16 Aug 1995, p. 117.

Correlation functions estimated from vertical profiles of sediment porosity and compressional wave velocity fluctuations. AGU-ASLO Ocean Sci. Meeting, 21-25 February 1994, Town and Country Hotel, San Diego, CA.

Geoacoustic and physical properties of near surface sediments in Eckernförde Bay. Gassy Mud Workshop, 11-12 July 1994, FWG, Kiel, Germany.

Correlation functions for sediment acoustic properties. ASA Meetings, 28 Nov-2 Dec 1994, Stouffer Austin Hotel, Austin, TX.

High-frequency bottom backscattering: volume scattering from gassy mud. ASA Meetings, 28 Nov-2 Dec 1994, Stouffer Austin Hotel, Austin, TX.

Physical property variability in sediments in and proximal to Eckernförde Bay. Workshop Modelling Methane-Rich Sediments of Eckernförde Bay, 26-30 June 1995, Stadthotel, Eckernförde, Germany.

Geoacoustic and physical properties of carbonate sediments from the Key West Campaign. SEPM Congress on Sedimentary Geology, 13-16 August 1995, TradeWinds Resort Convention Center, St. Petersburg, FL.

Small-scale fluctuations in acoustic and physical properties in surficial carbonate sediments. AGU-ASLO Ocean Sci. Meeting, 12-16 February 1996, Town and Country Hotel, San Diego, CA.

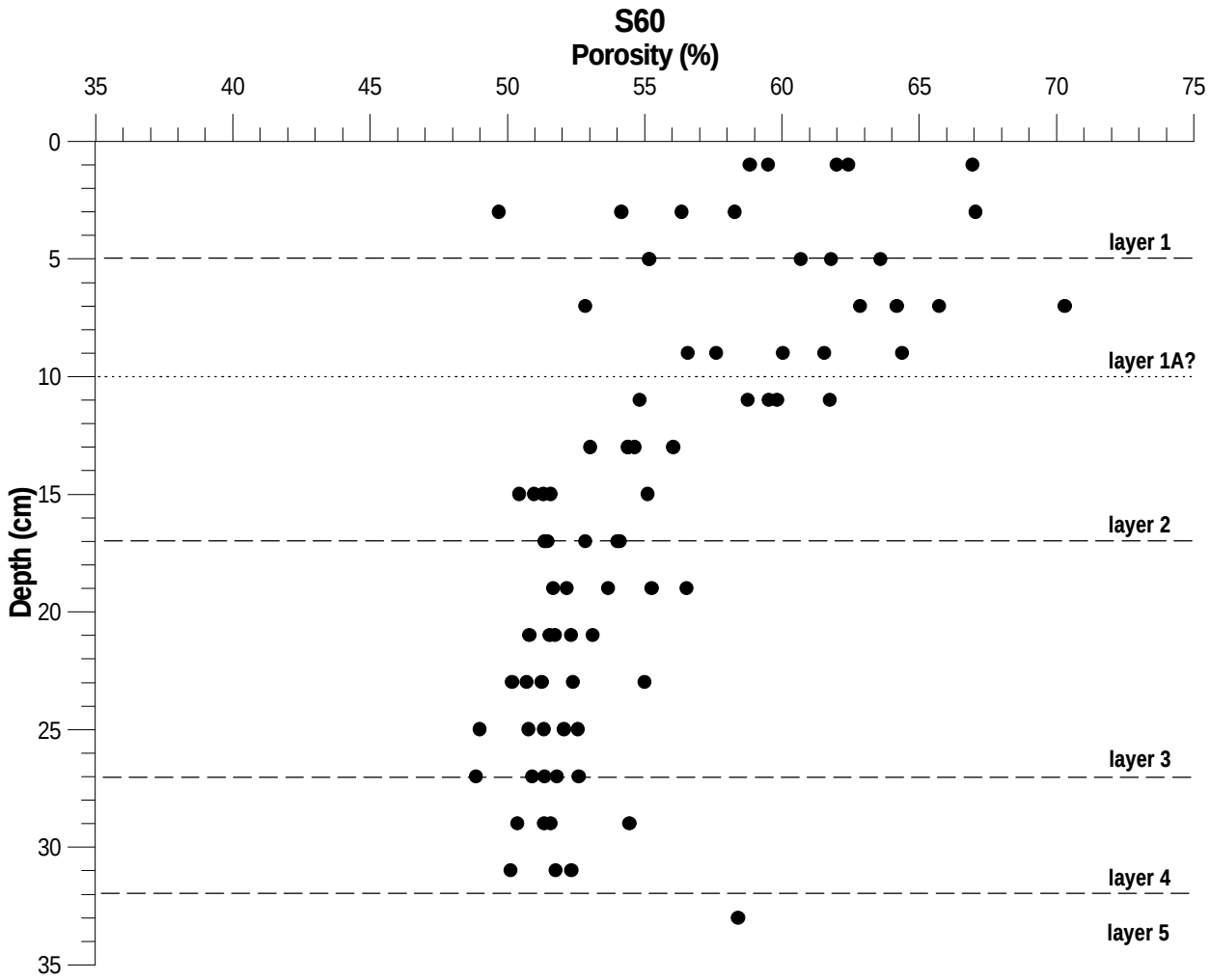

Figure 1. Vertical distribution of sediment porosity at site S60 from the Eel River survey.

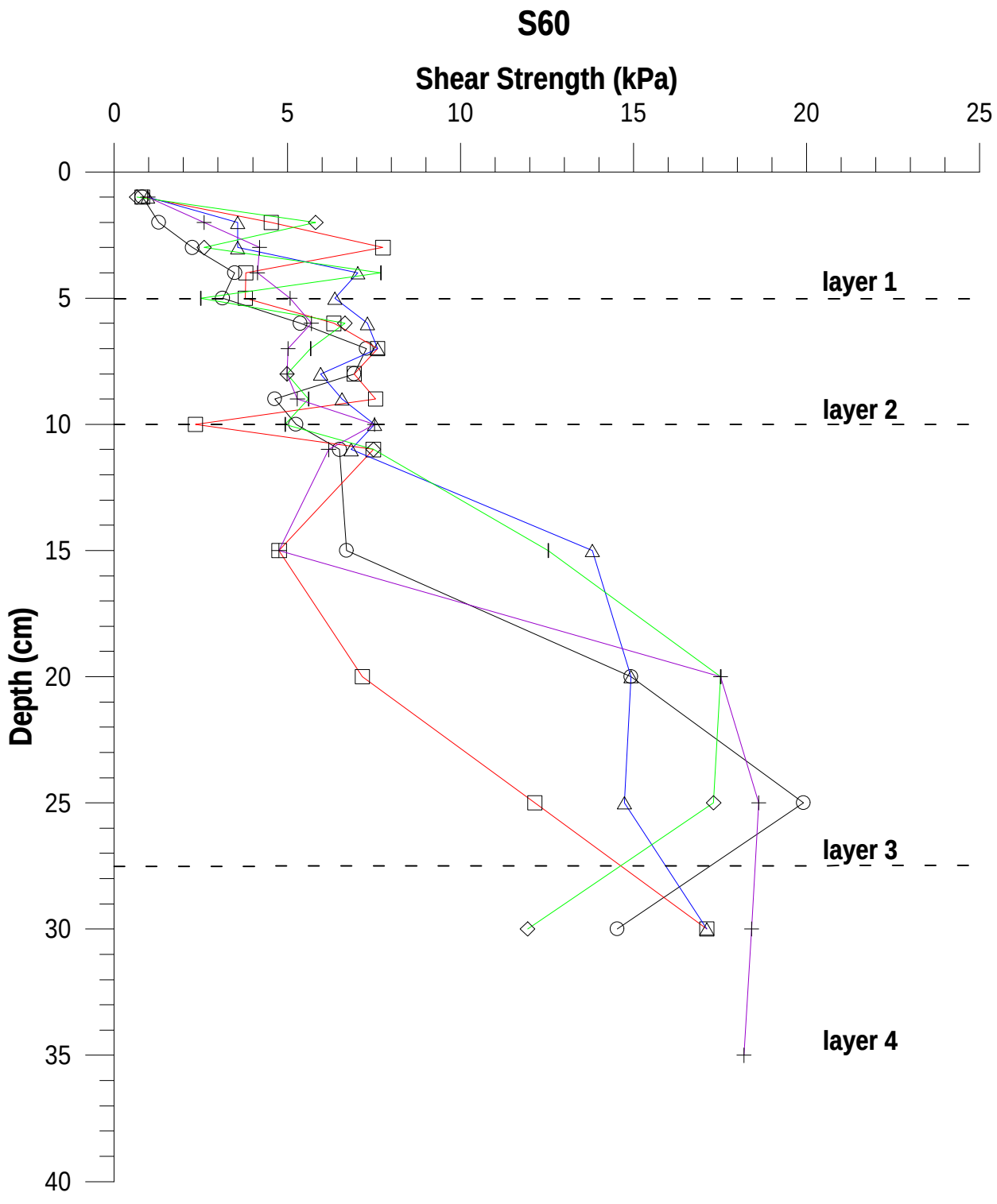

Figure 2. Vertical distribution of sediment shear strength measured at site S60.

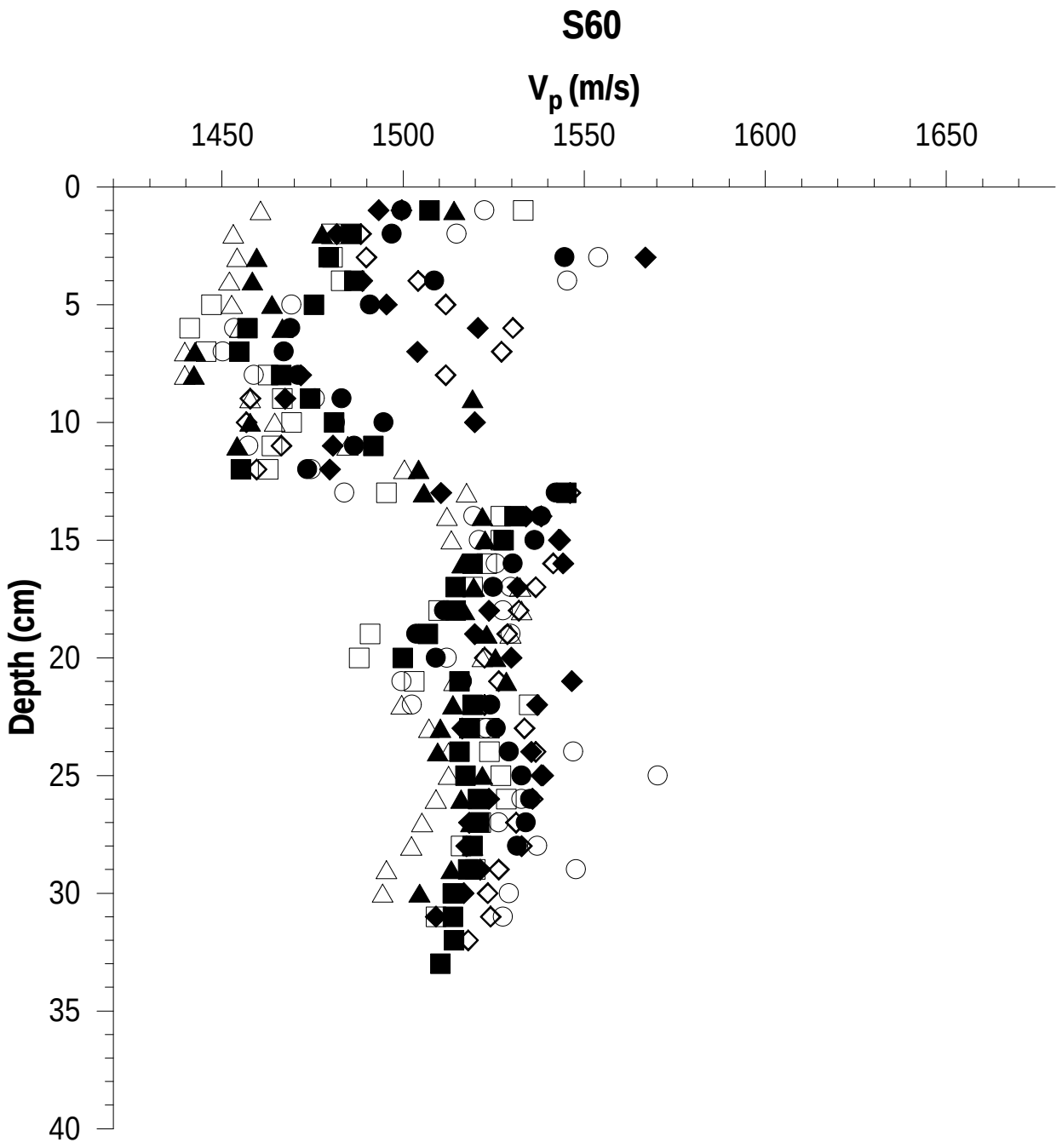

Figure 3. Vertical profile of sediment compressional wave velocity measured at 400 kHz from site S60.

2.4 Effects of Carbonate Dissolution and Precipitation on Sediment Physical Properties and Structure: Microfossils Component (Principal Investigator: C.A. Brunner)

Charlotte A. Brunner

Institute of Marine Sciences
The University of Southern Mississippi
John C. Stennis Space Center, MS 39529

PROJECT OBJECTIVES

This report describes the activities of the second fiscal year of this contract, for which funding began April 13, 1995 in the middle of the first fiscal year. The objectives of the three-year contract are to assess and quantify the effects of organic matter oxidation on the solid constituents of neritic carbonate sediment, with particular focus on foraminiferal tests as an indicator of general sediment condition. Effects include dissolution of carbonate tests, precipitation of calcium carbonate in test interiors and host sediment, and formation of pyrite, phosphorite, or manganese oxides. Results will be compared to reactions predicted from pore water chemistry done on identical core samples under a separate contract to Dr. Alan Shiller of USM.

INTRODUCTION

Oxidation of organic matter is an important process in surface sediments of the Tortugas region, based on preliminary data (Shiller et al., 1995). Early diagenesis of organic matter proceeds through a sequence of reducing reactions described by Froelich et al. (1979). The reactions include bacterial reduction of oxygen followed by manganese oxide, nitrate, iron oxides, and sulfate. Some of these reactions produce protons, which promote the dissolution of carbonate, and other reactions consume protons, which promote carbonate precipitation. The resultant dissolution and cementation could significantly affect the acoustic properties of sediment, and so study of early diagenesis is relevant to the CBBL project.

DATA COLLECTION

The principal goal during the 1996 fiscal year has been to generate data in preparation for analysis and reporting during the final fiscal year of the contract. The data will be used to address the following questions, which were discussed in detail in the 1995 year-end report. 1) *Do foraminiferal tests harbor indications of early diagenesis due to oxidation of organic matter in a pattern consistent with the pore water chemistry?* 2) *Does the reduction sequence in the sediment column occur in test interiors sooner (e.g., at a shallower depth) than in the matrix hosting the tests due to formation of chemical micro-habitats in test interiors?* 3) *Does test composition promote or retard precipitation? 4) Can the differences in frequencies of benthonic foraminiferal species be used as proxies of oxidation intensity in the geologic record.*
Box core 185 was selected to address the first three questions. The core was divided into 15

depth intervals, and selected species of high- and low-magnesian calcite benthonic foraminifers were picked from the sediment, mounted in SPURR resin, and sectioned for SEM analysis using backscattered electrons. Approximately 120 specimens of Peneroplidae and 120 specimens of *Nonionella* were examined by SEM and described in detail for evidence of dissolution, carbonate precipitation, pyrite and phosphorite formation, and other useful characteristics. The data have been compiled into a spread sheet and readied for multivariate analysis. Additionally, approximately 50 SEM photographs document the principal description categories.

The silt- and clay-size sediment of two samples from the surface and from 8-9 cm depth in box core 185 were assessed for quantity of pyrite in material external to foraminifer tests. The samples were chosen from an interval in which test interiors showed little pyrite and an interval in which test interiors contained common pyrite. Samples were imbedded in SPURR and polished. The polished plugs were divided into sectors, which were selected at random and inspected for the total area of pyrite visible by backscattered electrons. Pyrite identifications were confirmed by x-ray analysis. Mean quantities of pyrite between the samples were tested for significance.

The samples from 15 depth intervals of box core 185 were also prepared for a census of benthonic foraminifer species by picking a random sample of 300 to 600 specimens from each sample (Patterson and Fishbein, 1989). A total of about 7,500 specimens were picked, sorted, and are now ready for identification (Cushman, 1922; Bock et al., 1971; Rose and Lidz, 1977) . To address the fourth question, two gravity cores (KW-PE-GC-213 and 225) were selected for analysis. Both cores sample the four lithostratigraphic units, which were defined by Mr. Kevin Stephens (personal communication, 1996) and which lie above the Pleistocene basement limestone. Forty-seven samples were taken at 10-cm intervals throughout the cores and prepared for a census of benthonic foraminifer species by picking a random sample of 300 to 600 specimens from each sample. A total of almost 23,500 specimens were picked and sorted this year, and now stand ready for identification.

In preparation for the foraminiferal census, I visited the foraminifer collections at the U.S. National Museum of Natural History for three days in July, 1996 to verify identification of selected species by comparison to holotype and secondary type specimens from the Florida Keys and adjacent areas.

PUBLICATIONS

Shiller, A. M., Hebert, T. L., Thornton, K. R., and Brunner, C. A., 1995. Sediment chemistry and pore water fluxes in the vicinity of the Dry Tortugas, *The 1st SEPM Congress on Sedimentary Geology, Congress Program and Abstracts*, v. 1, p. 113.

Brunner, C., Reed, A., Elder, R., Falster, A., and Shiller, A., 1996. Effects of organic carbon respiration on preservation of foraminifers from the Dry Tortugas, Florida. *Journal of the Mississippi Academy of Sciences*, 41(1): 54.

REFERENCES

Bock, W. D., Hay, W. W., Jones, J. I., Lyntz, G. W., Smith, S. L., and Wright, R. C., 1971. *A Symposium of Recent South Florida Foraminifera,* Miami Geological Society Memoir 1, 245p.

Cushman, Joseph A., 1922. *Shallow-water foraminifera of the Tortugas Region,* Carnegie Institution of Washington No. 133, 97p.

Froelich, P. N., Klinkhammer, G. P., Bender, M. L., Luedtke, N. A., Heath, G. Ross, Cullen, Doug, and Dauphin, Paul, 1979. Early oxidation of organic matter in pelagic sediments of the eastern equatorial Atlantic: suboxic diagenesis. *Geochimica et Cosmochimica Acta*, 43:1075-1090.

Patterson, R. T., and Fishbein, E., 1989. Re-examiniation of the statistical methods used to determine the number of point counts needed for micropaleontological quantitative research, *J. Paleont.,* 63(2): 245-248.

Rose, P. R., and Lidz, B., 1977. *Diagnostic foraminfieral assemblages of shallow-water modern environments: South Florida and the Bahamas,* Sedimenta VI, published by The Comparative Sedimentology Laboratory Division of Marine Geology and Geophysics Rosenstiel School of Marine and Atmospheric Science, University of Miami (Miami, Florida), 55p.

Shiller, A. M., Hebert, T. L., Thornton, K. R., and Brunner, C. A., 1995. Sediment chemistry and pore water fluxes in the vicinity of the Dry Tortugas, *The 1st SEPM Congress on Sedimentary Geology, Congress Program and Abstracts,* v. 1, p. 113.

2.5 Processes of Macro Scale Volume Inhomogeneity in the Benthic Boundary Layer (Principal Investigators: W.R. Bryant and N.C. Slowey)

Co-Principal Iinvestigators
William R. Bryant and Niall C. Slowey
Department of Oceanography
Texas A & M University
College Station, Texas 77843

Introduction

The goals of this project are to understand how and why the physical and geologic properties of the benthic boundary layer vary within various shallow water environments and to relate these variations to the state of stress as a function of time and to the penetration and stability of objects on the seafloor. Specifically, we have been investigating the geotechnical stratigraphy--which includes the density, shear strength (cohesion), porosity, saturation (gas) and sediment component distribution and their three-dimensional structural arrangement--within the boundary layer in more detail than has previously been possible. We also have been investigating the relationship between the geotechnical stratigraphy of the sediments and the velocity and impedance of acoustic waves.

This report briefly describes our activities and results during the year 1995-1996. We focused our attention on (1) the summary and analysis of the geotechnical and geoacoustic data we collected from the cohesive sediments at the Eckernförde Bay study site, (2) the measurement and preliminary analysis of the geotechnical and geoacoustic properties of sediments in the large suite of cores we collected at the Dry Tortugas and Marquesas Keys area of the Florida Keys study site, and (3) dissemination of our results via presentations and publications so that they are accessible to participants of the Coastal Benthic Boundary Layer (CBBL) program and other interested people. These efforts are leading to increased understanding of the variability of the geotechnical and geoacoustic properties of sediments within the benthic boundary layer. They are also yielding predictive models from which the values of specific sediment properties can be estimated based upon our existing knowledge of other properties. Our project therefore continues to contribute to the accomplishment of the Coastal Benthic Boundary Layer program's primary objectives.

Analysis of Eckernförde Bay Data

During the first three years of the project, the geotechnical and geoacoustic properties of sediments in the upper 5 m of the seafloor of Eckernförde Bay were measured in the laboratory or calculated (based upon our laboratory measurements or in situ measurements by other CBBL participants). The properties include percent sand, silt, and clay, water content, bulk density, void ratio, porosity, effective overburden pressure, undrained shear strength, dynamic shear modulus, and compressional and shear wave velocities. Silty clays are the main sediment type

found in Eckernförde Bay and they have some unique characteristics, including high water content (up to 400%, mean ~200%), low bulk density (~1.2 g/cm^3), high void ratio (up to 10, mean ~5 to 6), high porosity (up to 90%), low shear strength (<1 kPa in upper 20 cm), and low compressional (<1500 m/s) and shear wave (<10 m/s) velocities in surficial sediments.

Tiesong Lu, a graduate student at Texas A & M, used statistical techniques such as multiple regression analysis to investigate correlations among the physical, geotechnical and geoacoustic properties of the sediments of Eckernförde Bay as the basis of his Ph.D. dissertation. This effort accomplished several objectives. First, an evaluation/comparison of vane shear and fall cone shear strength measurements was made. Using a paired *t*-test, the fall cone strengths calculated using the K_{60} values of Hansbo (1957) and Wood (1985) were found to underestimate and overestimate the vane shear strengths, respectively (Fig. 1). However, the fall cone strengths calculated with a newly derived K_{60} value did not show significant difference when compared with the vane shear strengths, so the new K_{60} value is more appropriate for calculating fall cone strength for soft marine sediments such as in Eckernförde Bay. A paper describing this work was submitted to a marine geotechnical journal and is now in press.

Empirical models that relate various sediment properties were developed and evaluated. Measured compressional wave velocity correlates with sand percent, water content, and undrained shear strength in non-gassy sediments. Unfortunately, no usable relationship between the compressional wave velocity and other properties of gassy sediments could be determined because it was difficult to accurately measure the compressional wave velocity of these sediments in the laboratory. Shear wave velocity, estimated from relationship between in situ measured shear modulus and depth, correlates with undrained shear strength, bulk density, and effective pressure. It was found that undrained shear strength increases with increasing subbottom depth and effective pressure in both non-gassy sediments (Fig. 2) and gassy sediments, with the rate of increase being slightly greater in non-gassy sediments. Depth and effective overburden pressure are the best properties from which to estimate shear strength (*y*):

$$y = 1.3182 + 0.0269x_5 \qquad R^2 = 0.77$$

$$y = 1.5896 + 1.0133x_6 \qquad R^2 = 0.74$$

where x_5 is depth (cm) and x_6 is effective overburden pressure (kPa). When other independent variables are included in a regression model, they do not significantly improve the model (the increase of R^2 is small). A draft manuscript describing this work is complete and is now being revised prior to submission to a scientific journal.

Based upon laboratory measurements of void ratio (*e*) and effective overburden pressure (*p*) of surficial sediments (the upper 2 m of the seafloor), a new empirical model was developed for estimating the shear modulus:

$$m = b_0 (p)^{b_1} \exp[-b_2 e + b_3 (\ln p)^2]$$

where b_0 = 284.89, b_1 = 0.08, b_2 = 0.0079, b_3 = 0.0227 and R^2 = 0.9571. The void ratio and effective pressure range from 2.01 to 10.03 and from 0.04 to 6.13 kPa, respectively. The results indicate that the term $\exp[b_3 (\ln p)^2]$ is needed in the model to accommodate the properties of the Eckernförde Bay surficial sediments. Shear wave velocities calculated using this model are

comparable to those measured in situ when the depth is more than 50 cm. A draft manuscript describing this work is complete and is now being revised prior to submission to a scientific journal.

Finally, we have been working together with the groups led by A. Silva of URI, D. Lambert of NRL and S. Schock of FAU on syntheses of the geotechnical and the geoacoustic results of our Eckernförde Bay efforts.

Collection and Preliminary Analysis of Florida Keys Data

Thirty-five 4-inch diameter gravity cores and nine vibracores were recovered from the Marquesas and Dry Tortugas during 1995. These cores were returned to Texas A&M for laboratory analysis.

Eddy Lee, a graduate student at Texas A & M, is examining the geotechnical and geoacoustic properties of the gravity cores as the basis of his Ph.D. dissertation research. We suspect that under the influence of hydrodynamic forces at the study site, the non-spherically shaped biogenic sediment grains may well become preferentially oriented with the sediments at the seafloor. The cores are therefore being examined for evidence of compressional wave and bulk density anisotropy that may result. Compressional wave velocities and density were measured at 30 degree intervals around the circumference of each core and in some cases at 15 degree intervals around half the circumference (the data is being analyzed now). The cores were then split, described visually and then various geotechnical and geoacoustic properties were measured at regular intervals. All measurements were completed during this past year and the data is currently being analyzed.

In a separate effort, we also tried to measure the compressional wave velocity of sandy sediments collect in un-openned vibra cores. Velocity is determined by measuring the travel time of a sound pulse directly across the core. Unfortunately, wave energy propagates quickly and efficiently around the aluminum liner of the vibracore and combines with the wave energy that propagates directly across the core, presenting a significant difficulty for this approach. Knowledge of velocity in sandy sediments is therefore limited. The approach we are trying is, essentially, to characterize the form of the wave pulse that is transmitted around the liner and to subtract it from the total received signal. Digital waveform data was collected and is currently being analyzed.

Finally, we have been working together with the groups led by D. Lambert of NRL and A. Silva of URI to synthesize and integrate the geotechnical and the geoacoustic results of our Florida Keys efforts.

Final Year Work

Our efforts during the final year of the CBBL program will be devoted to continued analysis of the Florida Keys data and to dissemination of results.

Project-related Presentations and Publications in 1995-96

Slowey, N. C., W. R. Bryant, K. S. Davis, D. N. Lambert, and D. J. Walter, 1995, Geoacoustic stratigraphy of the Marquesas Keys, SEPM Congress on Sedimentary Geology, Program and Abstracts, v. 1, p. 34.

Yeager, M. and N. C. Slowey, 1996, A new method for measuring the bulk volume of rock samples for porosity and mass accumulation determinations, *Journal of Sedimentary Research*, v. 66, p. 1036-1039.

Slowey, N. C., W. R. Bryant, and D. N. Lambert, 1996, Comparison of high-resolution seismic profiles and the geoacoustic properties of Eckernförde Bay sediments, *Geo-Marine Letters*, v. 16, p. 240-248.

Davis, K., N. Slowey, I. Stender, H. Fiedler, W. Bryant, and G. Fechner, 1996, Acoustic backscatter and sediment textural properties of inner shelf sands, northeastern Gulf of Mexico, *Geo-Marine Letters*, v. 16, p. 273-278.

Tiesong, Lu, 1996, Statistical Analysis and Correlation of Physical and Geotechnical Properties of Marine Sediments in Eckernforde Bay, Baltic Sea, Ph.D. Dissertation, Texas A &M University, 149 pp.

Tiesong, Lu, and W. Bryant, in press, Comparison of vane shear and fall cone strengths of soft marine clay, *Marine Georesources and Technology*.

Silva, A ., H. G. Brandes, and N. C. Slowey, submitted, Geotechnical properties and behavior of high-porosity, organic-rich sediments in Eckernförde Bay, *Continental Shelf Research*.

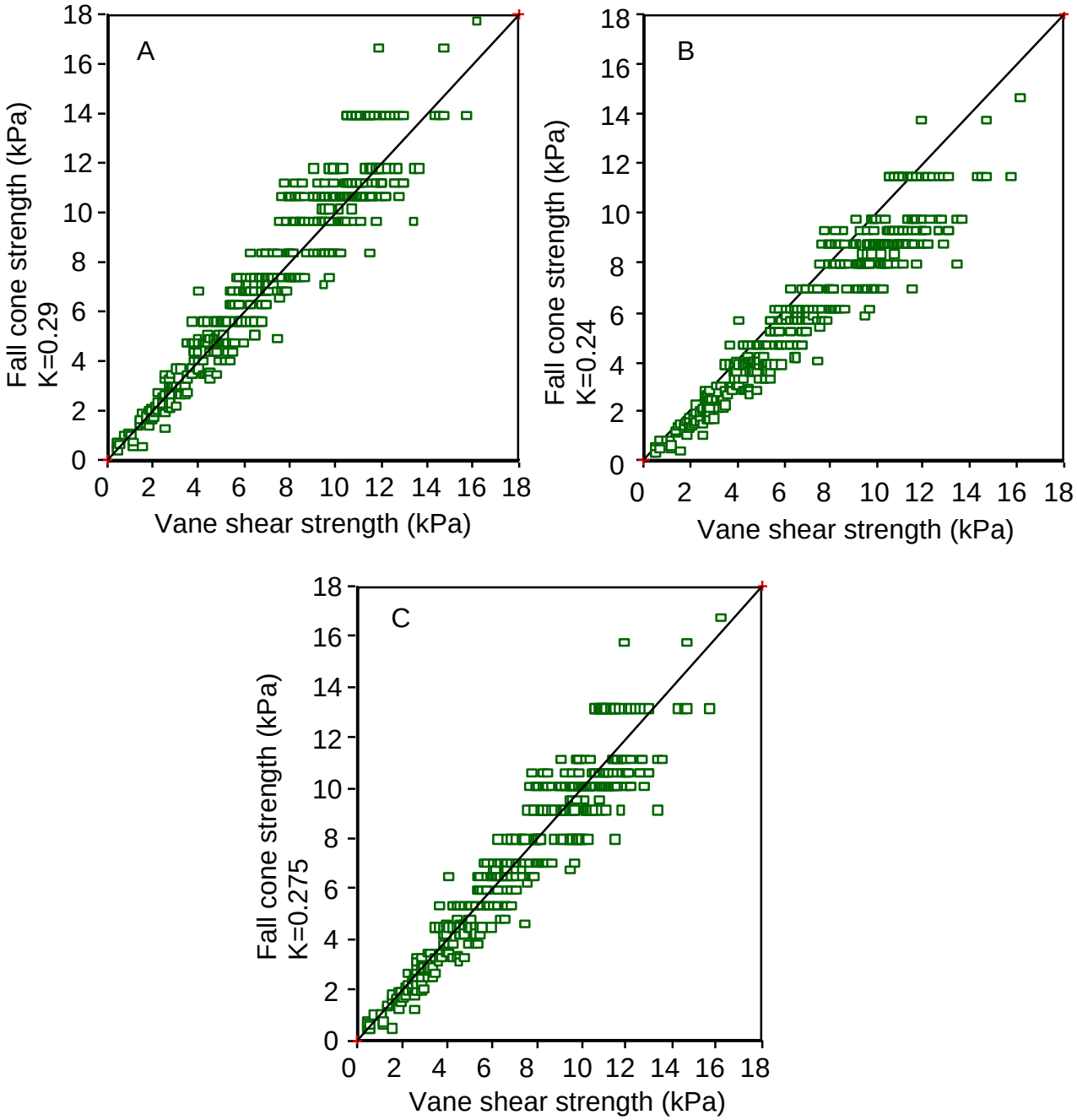

Figure 1. Comparison of fall cone and vane shear stengths of Eckernförde Bay sediments: (A) Wood's fall cone strength seems to overestimate the vane shear strength. (B) Hansbo's fall cone strength underestimates the vane shear strength. (C) Our newly derived fall cone strength estimates the vane shear strength better.

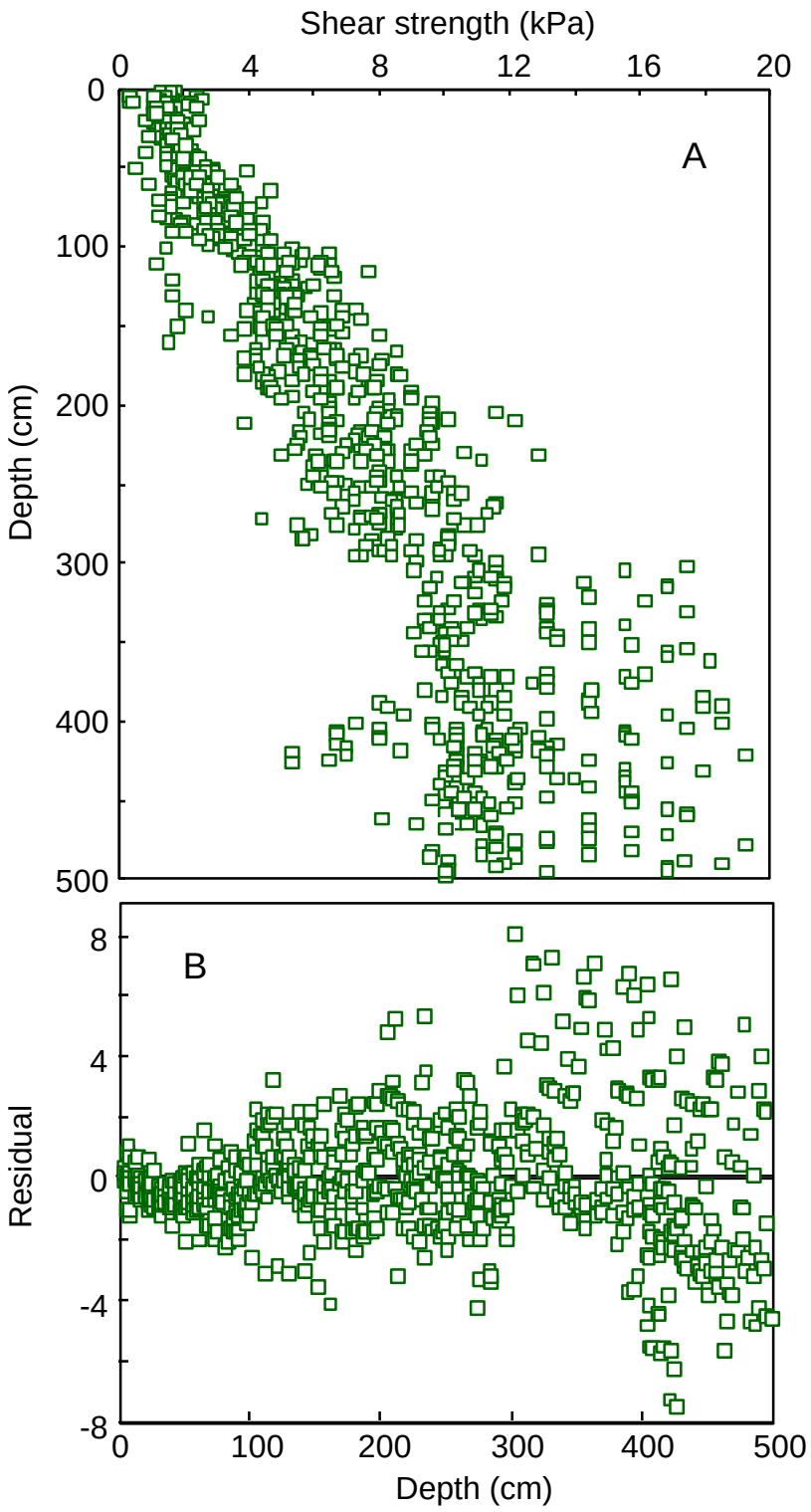

Figure 2. In non-gassy sediments from Eckernförde Bay, undrained shear strength increases with depth (A). A linear model (see text) describes this relationship well, as indicated by the lack of systematic patterns in the residual plot (B).

2.6 Bottom Backscatter Measurements of Key West, Florida (Principal Investigator: N.P. Chotiros)

Nicholas P. Chotiros

Applied Research Laboratories
University of Texas at Austin
Austin, TX 78713-8029

Bottom scattering strength measurement and analysis

Introduction

The objective is to collect high frequency reverberation data from shallow water sediments, particularly coral and mud sediments for measurement of spatial backscatter statistics, using sensors mounted on a tripod on the bottom and on a ROV, in support of high frequency sonar imaging applications and sediment classification.

Accomplishments in FY96

The data collected in FY95 were analyzed to determine the underlying physical processes. The apparent dependence of backscattering strength on sonar height above bottom (HAB) is of particular interest. A sample of the data[1] is shown in Fig. 1.

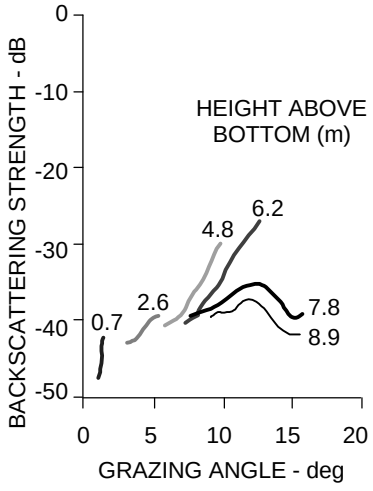

Fig. 1. Example of backscattering strength vs. grazing angle at various sonar heights above bottom at 200 kHz

Apparent dependence on HAB was observed in the Eckernförde data, because the scattering layer was not at the water-sediment interface but significantly deeper. In the Key West site, this is not expected to be the case, because high acoustic attenuation in the sediment[2] rules out the possibility of scattering from any depth greater than about 5 cm below the water-sediment interface.

Current backscattering models are based on the single scatter approximation: the scattering medium is assumed to be populated by scatterers; each scatterer is assumed to interact with the incident sound wave independently, as if it were the only scatterer in the medium; the resulting scattered signal from all scatterers are summed, but acoustic interactions involving two or more scatterers are ignored. This approach yields a simple expression that is easy to understand and manipulate, and has been successfully applied in many areas. For backscattering from a rough surface, or even a thin layer of volume scatterers just beneath the surface, a dependence on grazing angle is predicted, but not on HAB.

A scattered acoustic pulse typically generates a random signal whose envelope, on average, decays exponentially. If the decay time constant is large, it may cause an apparent dependence on HAB. Under the single scatter approximation, the decay time constant was expected to be less than 1 ms. To fit the data in Fig. 1, a 5 ms time constant was indicated. In a granular medium, such as sand, the most likely cause of a long decay time constant is multiple scattering. This involves acoustic interactions involving two or more scatterers, in which acoustic energy is scattered from one scatterer to several others in a cascading fashion. Such a process may be approximated by diffusion theory[3].

[1] Chotiros, N. P., Altenburg, R. A., and Piper, J. (1996). "Analysis of acoustic backscatter in the vicinity of the Dry Tortugas and Marquesas Keys," submitted to Geomarine Letters.

[2] Briggs, K. B. et. al. (1996). "Physical and Geoacoustic Properties of Sediments Collected for the Key West Campaign, February 1995: A Data Report," NRL/MR/7431 - 96-8002, Naval Research Laboratory, Stennis Space Center, MS 39529-5004, 10 May 1996.

[3] Chotiros, N. P., Mautner, A. M., and Laughlin, J. (1995). "Backscatter Analysis from a Smooth Sand Surface: Diffusion Approximation," Applied Research Laboratories Technical Report No. TR-95-30, Applied Research Laboratories, The University of Texas at Austin, 1 September 1995.

Plans

Due to exhaustion of funds, there are no plans for FY97.

Cumulative list of publications

Journal Articles

Chotiros, N. P. (1995). "Biot model of sound propagation in water saturated sand," J. Acoust. Soc. Am. 97(1):199.

Chotiros, N. P., Altenburg, R. A., and Piper, J. (1996). "Analysis of acoustic backscatter in the vicinity of the Dry Tortugas and Marquesas Keys," submitted to Geomarine Letters.

Chotiros, N. P., "Acoustic penetration of sandy and muddy sediments at shallow grazing angles," under preparation.

Symposium Proceedings

Boyle, F. A., and Chotiros, N. P. (1994). "A model for bistatic scattering trapped gas bubbles in sandy sediment," Proc. Inst. of Acoustics Conference on Underwater Acoustic Scattering, December 20-22, Weymouth, United Kingdom, pp 189-208.

Chotiros, N. P. (1994). "Ocean bottom acoustic interactions in MCM," Proc. IEEE-OES OCEANS94, Brest, France, September 13-16 1994, Vol. II:250-254.

Chotiros, N. P. (1994). "Inversion and sandy ocean sediments," Full Field Inversion Methods in Ocean and Seismic Acoustics, edited by Diachok, Caiti, Gerstoft, Schmidt, NATO Conference Proceedings, ISBN0-7923-3459-0, Kluwer Academic Press, 1995.

Chotiros, N. P. and Stanic, S. J. (1995). "Acoustic sediment penetration measurement with a buried hydrophone array in Eckernförde Bay," Proc. of Modeling Methane-Rich Sediments of Eckernförder Bay, edited by T. F. Wever, Eckernförder, E26-30 June, 1995, pp 89-96.

Priebe, R. D., Chotiros, N. P., Walter, D. J., and Lambert, D. N. (1995). "Gas bubble recognition by wavelet analysis and echo-sounder signals," Proc. of Modeling Methane-Rich Sediments of Eckernförder Bay, edited by T. F. Wever, Eckernförder, 26-30 June, 1995, pp 104-113.

Technical Reports

Chotiros, N. P. (1995). "Analysis of Sea Test Data I," Applied Research Laboratories Technical Report No. TR-95-11, Applied Research Laboratories, The University of Texas at Austin, 20 April 1995.

Published Abstracts

Chotiros, N. P., Altenburg, R. A., and Stanic, S. J. (1994). "High-frequency acoustic penetration of ocean sediments," J. Acoust. Soc. Am. 96(5) 3265.

Chotiros, N. P., Altenburg, R. A., and Boyle, F. A. (1994). "Reflection coefficient of sandy ocean sediments in shallow water," EOS, 75(3):181.

Altenburg, R. A. and Chotiros, N. P. (1995). "Measurements of the acoustic (200 kHz) backscatter from a carbonate sediment at low grazing angles," J. Acoust. Soc. Am. 98(5), Pt. 2, 2987

2.7 Geophysical Approaches to Determining the Geotechnical Characteristics of Sea Floor Sediments (Principal Investigators: A. Davis, D. Huws, and R. Haynes)

Angela Davis, Dei Huws & Jim Pyrah
School of Ocean Sciences
University of Wales, Bangor
Menai Bridge, UK

INTRODUCTION

As a continuation of UWB's contribution to the CBBL project, a series of *in situ* geophysical measurements were made on the Californian continental shelf in May/June 1996 during a collaborative research cruise on board the RV Wecoma (Briggs and Logan, 1996). To complement these *in situ* measurements, laboratory tests on recovered samples are now being carried in UWB's Laboratories in North Wales.

AIMS OF THE CALIFORNIAN SHELF SURVEY

The Eel River survey area has been extensively studied over recent years as part of the STRATAFORM project and, being a mixed sediment type region, provides an ideal platform for the characterisation of the relatively complex physical behaviour of such sediment. The UWB contribution aims to characterise the *in situ* deformation behaviour of the sea floor deposits under dynamic loading regimes by combining field data, acquired using the UWB 'Magic Carpet' system (Davis et al, 1989) with laboratory data, collected via a recently set-up instrumented cyclic triaxial testing apparatus.

IN SITU SHEAR WAVE MEASUREMENTS

In situ shear wave data were acquired along the 'S-line' survey track over two separate deployments, covering a bathymetric range of between 36 m and 70 m (referred to as S36 and S70 respectively). The track plot, relative to positions on the S-line proper, is shown in fig.1.

The surveyed track deviated from the intended line joining S30 to S70 because of the presence of sea floor obstructions in the form of crab pots.

INTERPRETATION OF *IN SITU* SHEAR WAVE DATA

Initial interpretation - variation of apparent velocity along the line

The shear wave data were interpreted initially on the basis of the apparent velocity measured between the source and the first sea floor geophone (at 2.55 m source-receiver range). Whilst the interpreted velocities are from an unspecified depth in all cases, this type of broad brush interpretation serves as a useful tool for ascertaining general trends in the data. Figure 2 shows

values of apparent shear wave velocity against distance along the survey line, with the main survey points (S40 to S70) shown for reference. Velocities are observed to decrease with increasing water depth, probably reflecting a change in sediment type (and associated void ratio). The largest change appears to occur between c. 42 m and 55 m water depth. Between 36 m and 42 m, velocities seem to vary somewhat - in the range 70-85 m/s - and beyond the 55 m point, values remain fairly constant until S70, being in the range 25-40 m/s.

Calculating velocity-depth data

In order to more rigorously interpret the shear wave data, the depth associated with each velocity has been calculated. This is done using delay times between the first geophone and the geophones at larger source-receiver ranges. The interpreted data are shown in fig.3. Note that the data have been split into bands each relating to a particular range of water depth.

A number of points can be raised from this plot. The trend of decreasing velocity with increasing bathymetric depth is still apparent (though, of course, water depth is not the direct causal mechanism for the velocity trend). Given the observed trend, it can be concluded that the gap in the data occurs because no data were acquired between 46 m and 53 m water depth. Within each band of data, the shear wave velocity appears to increase with depth. However, since it is suspected that the physical properties of the sediment change with bathymetric depth along the whole survey line, it cannot be concluded that the velocity-depth trend seen within one particular band reflects the velocity-depth relationship for a particular sediment type i.e. the data cannot be quantitatively interpreted in the bands shown. Finally, the data acquired with the magic carpet system would appear to agree well with the preliminary interpretation of the data collected with the NRL ISSAMS probe (data by *pers. comm.*, Richardson 1996).

Predictions from Shear Wave Velocity - Depth Data

It has been established, either quantitatively or qualitatively, that shear wave velocity (or shear modulus) varies with a whole range of physical properties and conditions for sediments (unconsolidated or otherwise) e.g. Hardin & Black, 1968; Stoll, 1989; Woods, 1991. However, it is generally accepted that the two most important parameters that can be used to simply model the variation in velocity are effective confining pressure and void ratio. The first investigators of this link were Hardin and Richart (1963) and later Hardin (1978). They performed a series of resonant column experiments on Ottowa Sand and derived empirical relationships between shear modulus, effective confining pressure and void ratio within a specific range of void ratio and pressure. Subsequently, Bryan and Stoll (1988) measured shear wave velocity whilst monitoring void ratio and effective confining pressure for 493 samples in the laboratory, with the intention of deriving as universal a relationship as possible. Whilst the confining pressure range was between 24 to 700kPa, the data shown in their paper would suggest that the empirical relationship derived should function reasonably at the smaller pressures involved in this study (approx. 2.5 kPa at 30 cms depth).

The relationship of Bryan and Stoll (1988) for sands is as follows:

$$G/p_a = 2526\ exp^{-1.5e}(\star_o/p_a)^{0.45} \quad .....(1)$$

where G = dynamic shear modulus (G = bulk density* $(Vs)^2$)
p_a = atmospheric pressure
e = void ratio
$\star_0$= overburden pressure

Similarly, Richardson et al. (1991) derived a 'working' empirical relationship relating shear wave velocity to void ratio and depth:

$$Vs = (85/e)\ z^{0.3} \quad .....(2)$$

where: z = depth below sea floor

Given that the magic carpet has provided *in situ* velocity-depth data, it would appear possible to predict void ratio either by directly applying Richardson et al.'s (1991) relationship, or indirectly applying the Bryan and Stoll formula. Plotted on fig.4 are the data of fig.3 with velocity-depth trends of the two relationships for a range of void ratio values superimposed (here plotted as porosity (porosity = e/(1+e)).

It would appear that there are quite large disparities between the two models, the differences being most accentuated at porosity values of 50% and at shallower depths.

Based upon ISSAMS data acquired over the last five years, relationship (2) would appear to be valid for a range of siliclastic sediment types over the depth ranges for which *in situ* data are available in this study (*pers. comm.*, Richardson 1996) and it is perhaps worth applying it to calculate the variation of void ratio along the line. It should be noted that implicit in the application of this formula is the assumption that void ratio does not vary with depth.

The calculated void ratio data are plotted as porosity against `distance along survey line' in figure (5) and would appear to make some intuitive sense - in that porosity ranges from between 37 - 45% in water depths of < 50m., and subsequently rises to 53 - 63% by c. 70 m. water depth. Preliminary inspection with porosity data acquired from subsampled box-core data (*pers. comm.* Briggs, 1996) would appear to show very good agreement with the predicted values shown in figure (5).

STUDIES OF BEHAVIOURAL PREDICTION

BACKGROUND

Accurate shallow-water mine burial prediction is important for most mine countermeasures operations, and recent studies have shown that sediment liquefaction may be a dominant mechanism in many sandy environments.

The field of sand liquefaction itself has been undergoing research and development since the classical works of Casagrande (1936) who first proposed the critical void ratio concept, which later developed into the steady state or critical state approach to sand liquefaction. Since then a significant research effort has been applied to studying the problem of sand liquefaction under both static and cyclic loading. Many different laboratory and field techniques have been used in a wide range of approaches attempting to predict liquefaction potential.

Possibly the most commonly used laboratory test to study sand behaviour under cyclic loading has been the undrained cyclic triaxial test. At its simplest, this apparatus subjects a sample, which has been previously saturated and either isotropically or anisotropically consolidated, to controlled sinusoidal variations in either deviator stress or axial strain. Stress controlled tests (i.e. for tests in which a deviator stress amplitude is specified), are the most commonly used type and consist of two main types: those that cycle around zero deviator stress (stress reversing tests) and those that only induce positive deviator stresses (non-stress reversing). Typically under such conditions, loose samples tend to display a rapid increase in pore pressure, strain rapidly and display a residual low shear strength. This condition may be defined as true, or flow liquefaction. Denser samples initially tend to dilate, decreasing pore pressures and 'stiffening' the sample significantly. However, if sufficient loading cycles are imposed, pore pressures may begin to increase once again, until at the peak of each loading cycle they equal the confining pressure, causing momentary condition of liquefaction in the sample (a phenomenon known as cyclic mobility) and rapid deformation of the sample.

Clearly, in an undrained scenario both situations could cause the burial of a mine. However, in the fairly high energy, shallow water areas of particular interest to this project, wave action is likely to have a significant affect on the seabed, particularly during a storm, making it unlikely to encounter the very loose sands required to achieve flow liquefaction in these areas. For this reason, the most likely process causing burial of mines would be that of cyclic mobility which will tend to reduce effective stresses to the point where a mine would sink through the surficial sediments by virtue of its own weight. However, acting against this tendency for pore pressure increase is the dissipative effect of permeability, and obviously any failure to take into account the effects of permeability in a mine burial scenario could result in very conservative predictions.

Possibly one the most significant problems remaining in this particular field is obtaining what may be regarded as an undisturbed sample. Even under 'ideal' situations, sands are notoriously hard to sample without some element of disturbance. Because of this, some more recent laboratory methods have employed seismic shear wave velocities recorded both *in situ* and in the laboratory to allow some degree of correlation between laboratory data and the field situation. The principal advantages of using shear wave velocities (Vs) for this type of approach include:

- Vs is a dynamic soil property with a clear physical meaning and well defined controlling factors (principally effective stress and void ratio),
- Vs may be measured non-destructively, and
- Vs is relatively easily measured in both the field and laboratory.

PRACTICAL DEVELOPMENTS IN LABORATORY TESTING

The laboratory work being conducted at UWB as part of the CBBL program represents a natural progression of the work of Pyrah (1996): research into the use of shear wave velocity as a predictor of liquefaction susceptibility, carried out as part of an ESPRC funded PhD program (1992-95).

To date, the major effort has been towards the development of a specialist test facility to allow simultaneous measurement of a sediment's geophysical and mechanical behaviour under varying conditions of cyclic loading. This has involved:

- Installation of, and familiarisation with a 'Tri-test 50' triaxial apparatus recently purchased from ELE International Limited;

- Development and testing of software to interface between a data logger, and the triaxial stepper motor, enabling the controlled cycling of deviator stress, allowing consolidated undrained cyclic triaxial tests to be performed;

- Fabrication of modified end platens allowing the incorporation of shear wave 'bender elements' allowing the measurement of sediment shear wave velocities;

- Fabrication of shear wave bender elements to be used with the modified end platens.

PRELIMINARY RESULTS OF LABORATORY TEST PROGRAMME

Figure 6 illustrates the void ratio, effective stress, shear wave velocity behaviour of a sample of laboratory prepared Key West carbonate sand. The sand itself was prepared using the water sedimentation technique, followed by progressive increases in back pressure, until the `B' value reached at least 0.95, thus ensuring complete saturation. These data will be combined with data from other tests to enable the relationship between velocity/void ratio and effective stress (or depth) to be elucidated. However, early analysis of the data collected so far indicates that this relationship may be approximated as:

$$V_s = \left({}^{108}/_{e}\right) \times z^{0.3}$$

which compares to Richardson relationship for a silicate sand as:

$$V_s = \left({}^{85}/_{e}\right) \times z^{0.3}$$

In addition, the sample can be anisotropically consolidated, allowing the effects of stress ratio upon velocity to be additionally quantified.

Figure 7 illustrates the behaviour of the same sample under undrained cyclic loading with no stress reversal having first been anisotropically consolidated. This type of behaviour typifies a medium dense sand under these kind of conditions. As can be seen, with each stress cycle the

sample gradually strained, with the amount of strain gradually decreasing with each cycle. The effective confining stress loop (Fig 7c) slowly moves to the left. Failure of the sample of this kind tends to occur through excess development of permanent strain rather than liquefaction. This is confirmed by the normalised mean pore pressure (normalised with respect to confining stress) response slowly increasing but never reaching the confining stress, thus never causing liquefaction. Further tests of this kind will allow the relationship between cyclic stress ratio and number of cycles to be determined, thus elucidating the cyclic liquefaction behaviour of the sample.

SUMMARY AND CONCLUSIONS

On the Eel River Survey:

- The study performed along the 'S-line' has revealed that shear wave velocity decreases in parallel with increasing water depth. This is thought to reflect the changing sediment type and resulting change in void ratio.

- The trend is still present when the velocity data are plotted against depth for each measurement point.

- *In situ* shear wave velocity is known to depend on may parameters concerning the sediment itself and the measurement techniques involved. For this case, the two most fundamental controls on shear wave velocity are effective confining pressure (depth) and void ratio. Many empirical relationships have been formulated, of which two are studied. It is apparent that the relationships differ in their predicted velocity - particularly at porosities c. 50% and at shallower depths. On the basis of recent experience, the relationship derived by Richardson et al. (1991) is taken as being the most applicable to the data acquired during this study.

- *In situ* porosity has been predicted which shows variation from c. 40% at S40 to c. 57% at S70. Preliminary inspection would suggest that this agrees well with porosity data acquired from sub-sampled box core sediment gathered along the S-line during the survey.

On combining field and laboratory findings

- If shear wave velocity can be used successfully as a means of estimating *in situ* void ratio, then it may also provide a means of attempting to extrapolate laboratory triaxial data to field conditions, providing shear wave velocity is measured during the geotechnical test procedure.

- Focus is now placed upon combining results from *in situ* shear wave velocity measurements with liquefaction prediction derived from steady state monotonic and cyclic loading to make inferences on the likely behaviour of the *in situ* sediment mass.

REFERENCES

Briggs K.B. and Logan M. (1996) "Eel River Study 1996" Cruise Reports for W9605A, Leg 2, Preliminary Cruise Report, Naval Research Laboratories, Stennis Space Center, Mississippi *unpublished report*

Bryan G.M. and Stoll R.D. (1988) "The dynamic shear modulus of marine sediments" Journal of the Acoustic Society of America, volume 83, pp. 2159 - 2164.

Davis A.M., Bennell J.D., Huws D.G. and Thomas D. (1989) "Development of a seafloor geophysical sledge" Marine Geotechnology vol. 8, pp. 99-109.

Hardin B.O. and Black W.L. (1968) "Vibration modulus of normally consolidated clay" Journal Soil Mech. Found. Div., ASCE, vol. 94, pp. 353-399.

Hardin B.O. and Richart F.E. (1963) "Elastic velocities in granular soils" Journal of the Soil Mechanics Foundation Division, ASCE, volume 89, pp. 33-65.

Hardin B.O. (1978) "The nature of stress-strain behaviour for soils" In Proceedings of the speciality conference on earthquake engineering and soil dynamics, ASCE, Pasadena, pp. 30-90.

Pyrah J.R. (1996) An integrated geotechnical - geophysical procedure for the prediction of liquefaction in uncemented sand University of Wales PhD Thesis, unpublished.

Richardson M.D., Muzi E., Miaschi B. and Turgutcan F. (1991) "Shear wave velocity gradients in near-surface marine sediments" In: Shear waves in marine sediments, eds. J.M. Hovem, M.D. Richardson and R.D. Stoll, Kluwer Academic Publications, Dordrecht, pp. 295-304.

Stoll R.D. (1989) Sediment Acoustics Lecture notes in earth sciences, no. 26, Springer Verlag, Berlin.

Woods R.D. (1991) "Soil properties for shear wave propagation" In: Shear waves in marine sediments, eds. J.M. Hovem, M.D. Richardson and R.D. Stoll, Kluwer Academic Publications, Dordrecht, pp. 29-39.

PUBLICATIONS ARISING FROM CBBL PROJECT 1996

Haynes R., Huws D.G., Davis A.M. and J.D. Bennell "Geophysical seafloor sensing in a carbonate sediment regime". Submitted to Geo-Marine Letters.

Richardson M.D., Briggs K.B. and A.M. Davis "Geoacoustic properties of carbonate sediments". EOS 76(3): OS172.

Shear Wave Measurement Points Along S-Line with Reference to S40-70

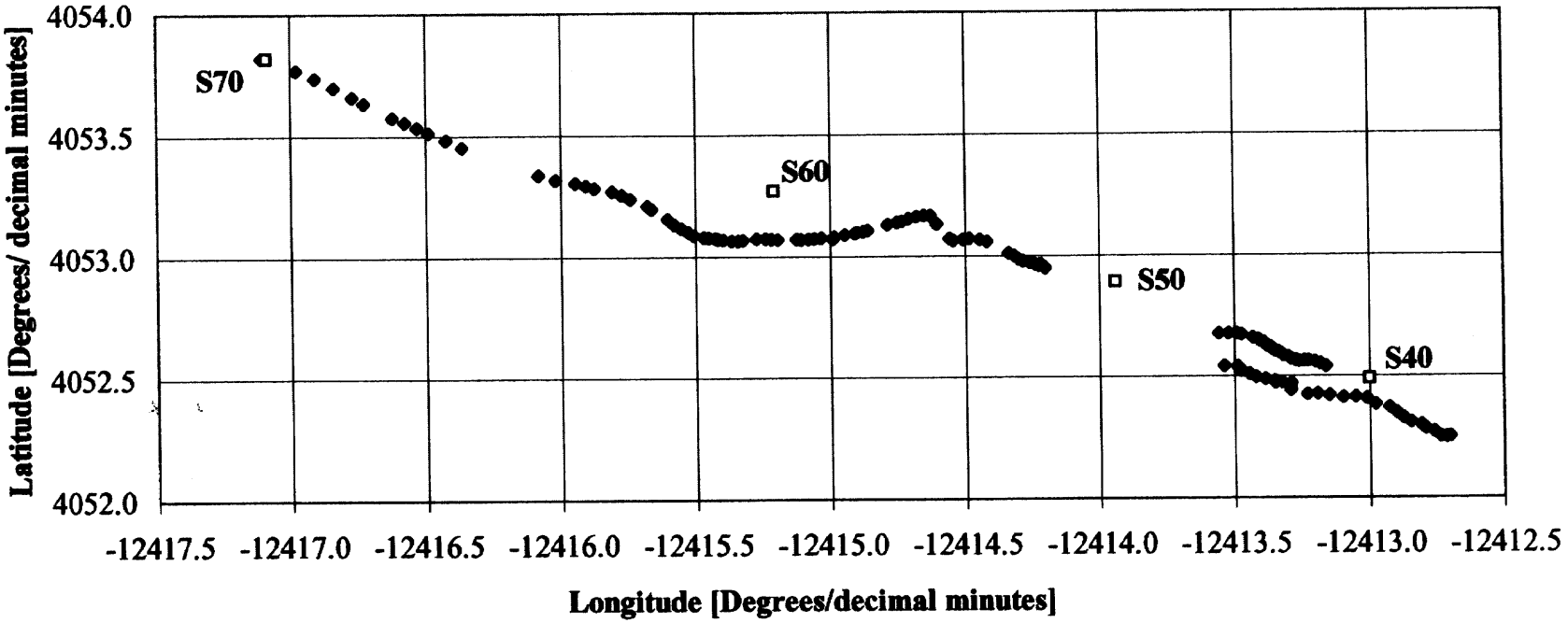

Variation of Apparent Shear Wave Velocity along S-Line with Reference to S40-70

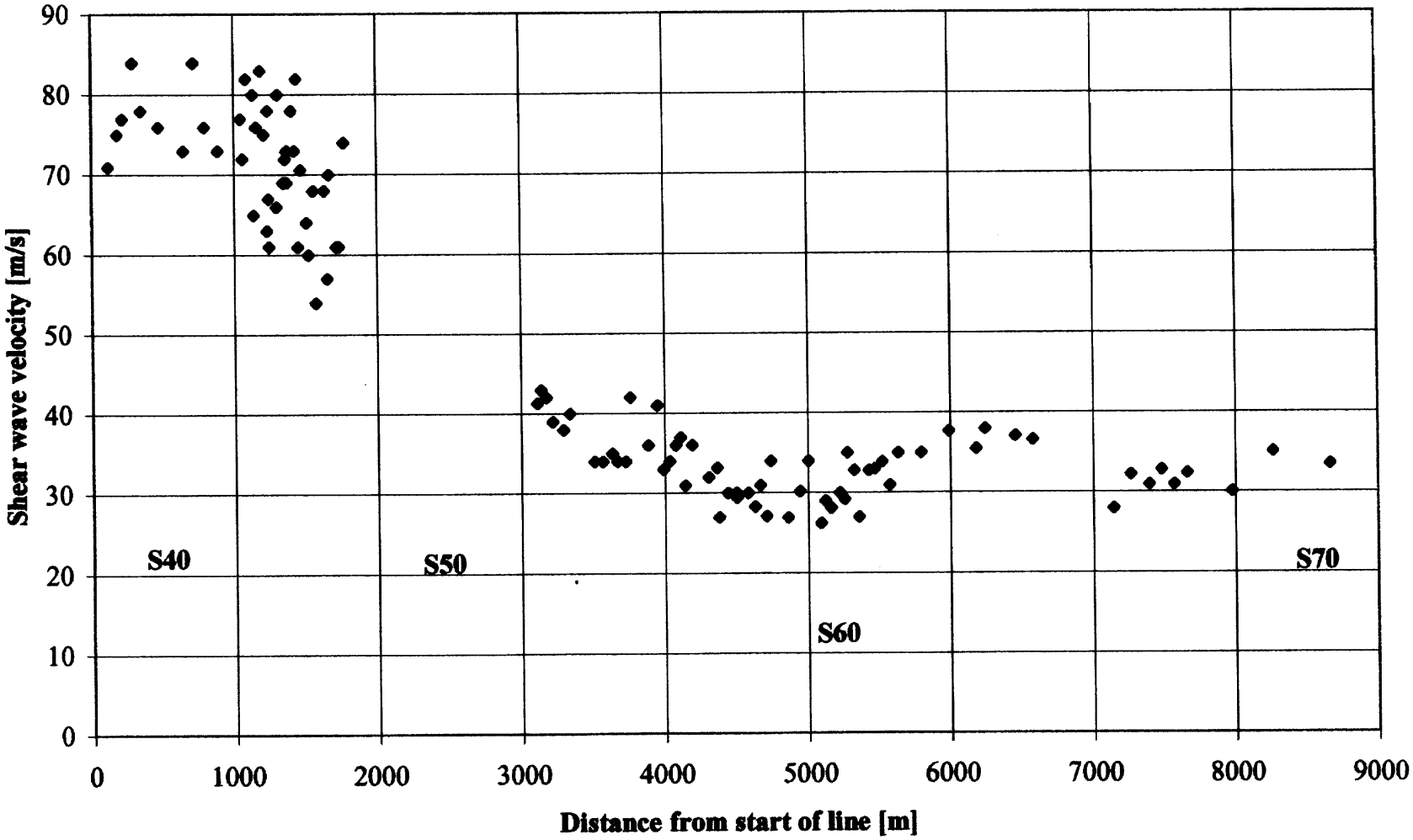

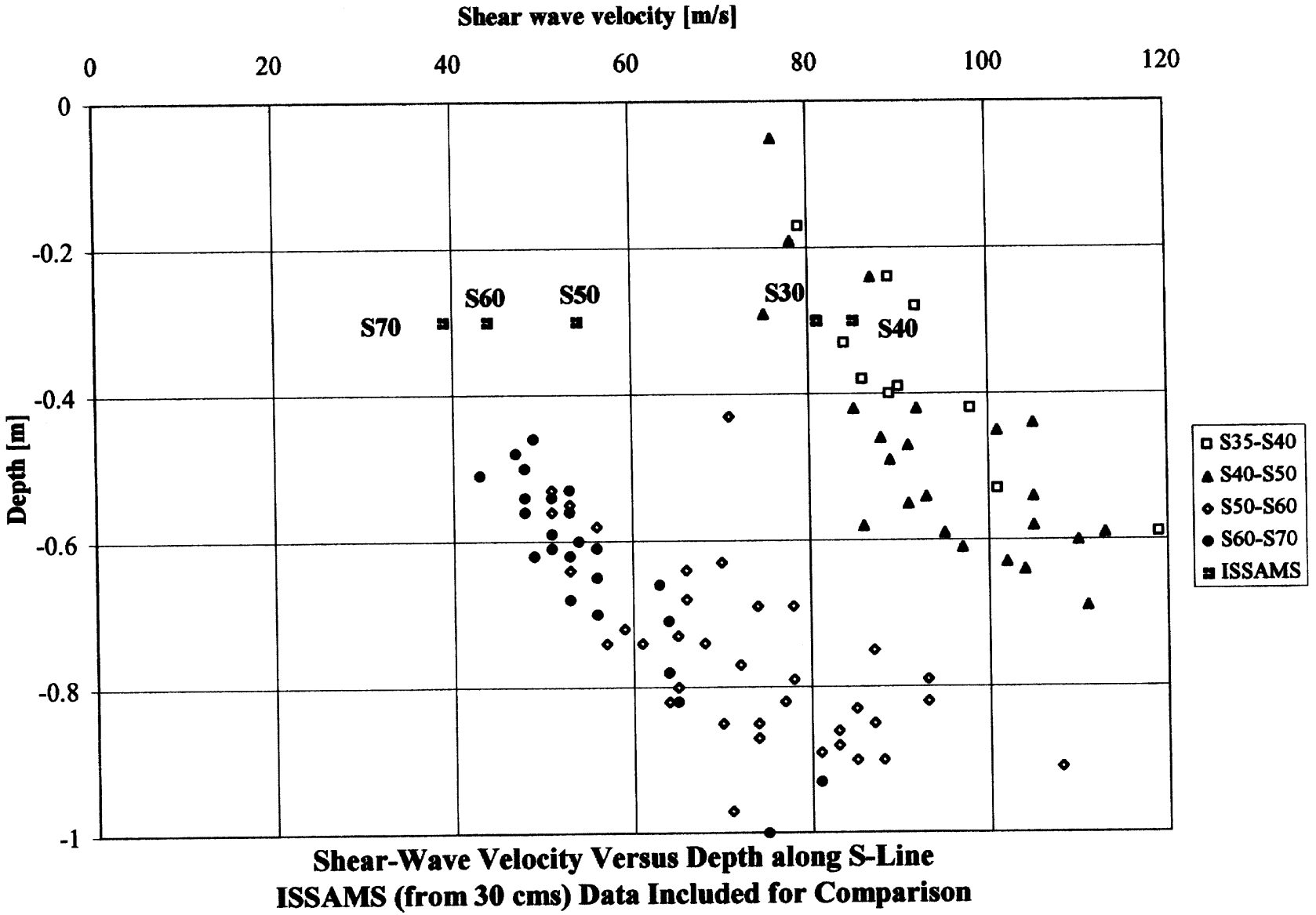

Shear-Wave Velocity Versus Depth along S-Line
ISSAMS (from 30 cms) Data Included for Comparison

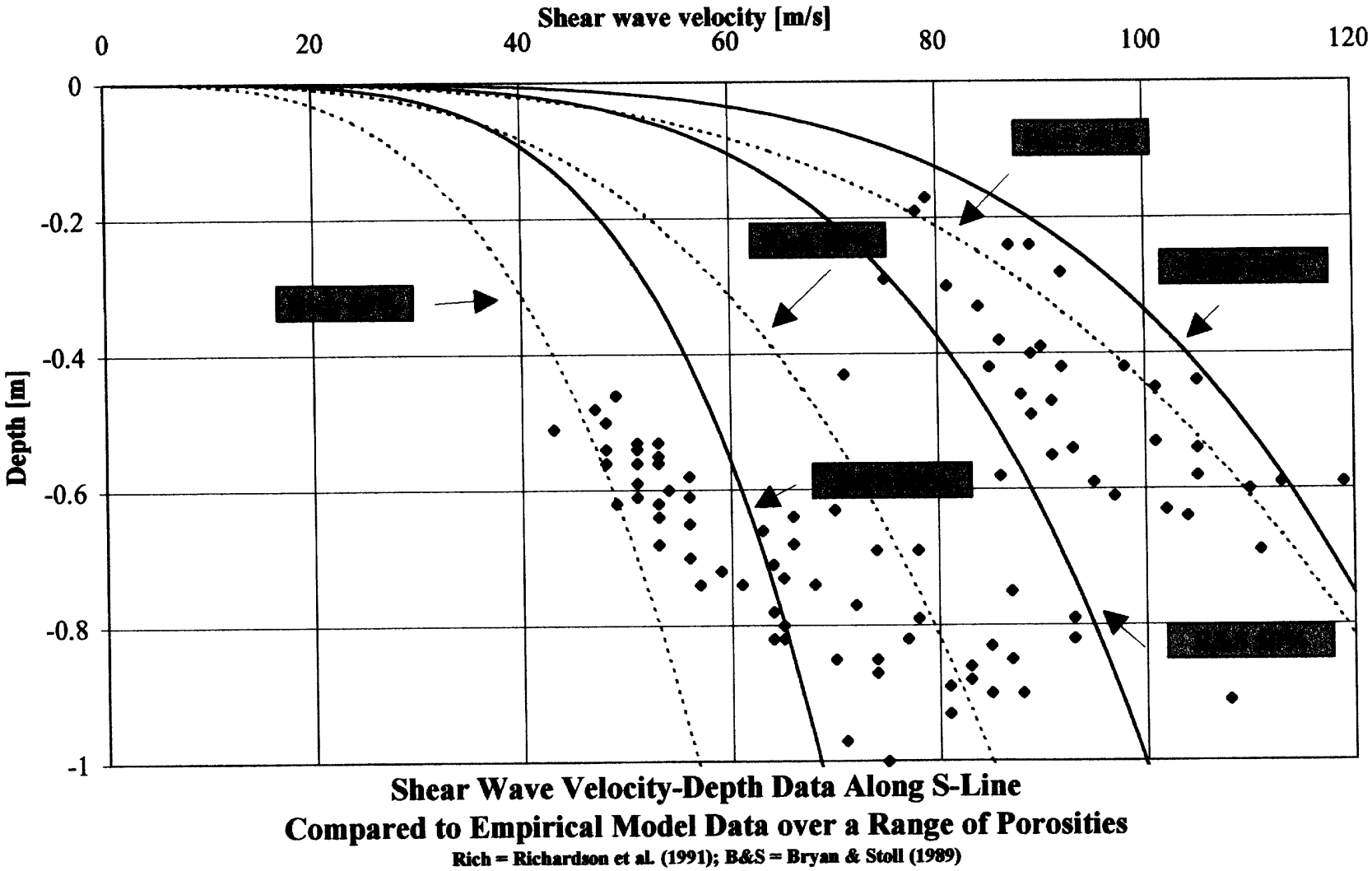
Shear wave velocity [m/s]
0
20
40
60
80
100
120
0
-0.2
-0.4
-0.6
-0.8
-1
Depth [m]
Shear Wave Velocity-Depth Data Along S-Line
Compared to Empirical Model Data over a Range of Porosities
Rich = Richardson et al. (1991); B&S = Bryan & Stoll (1989)

Figure 4.

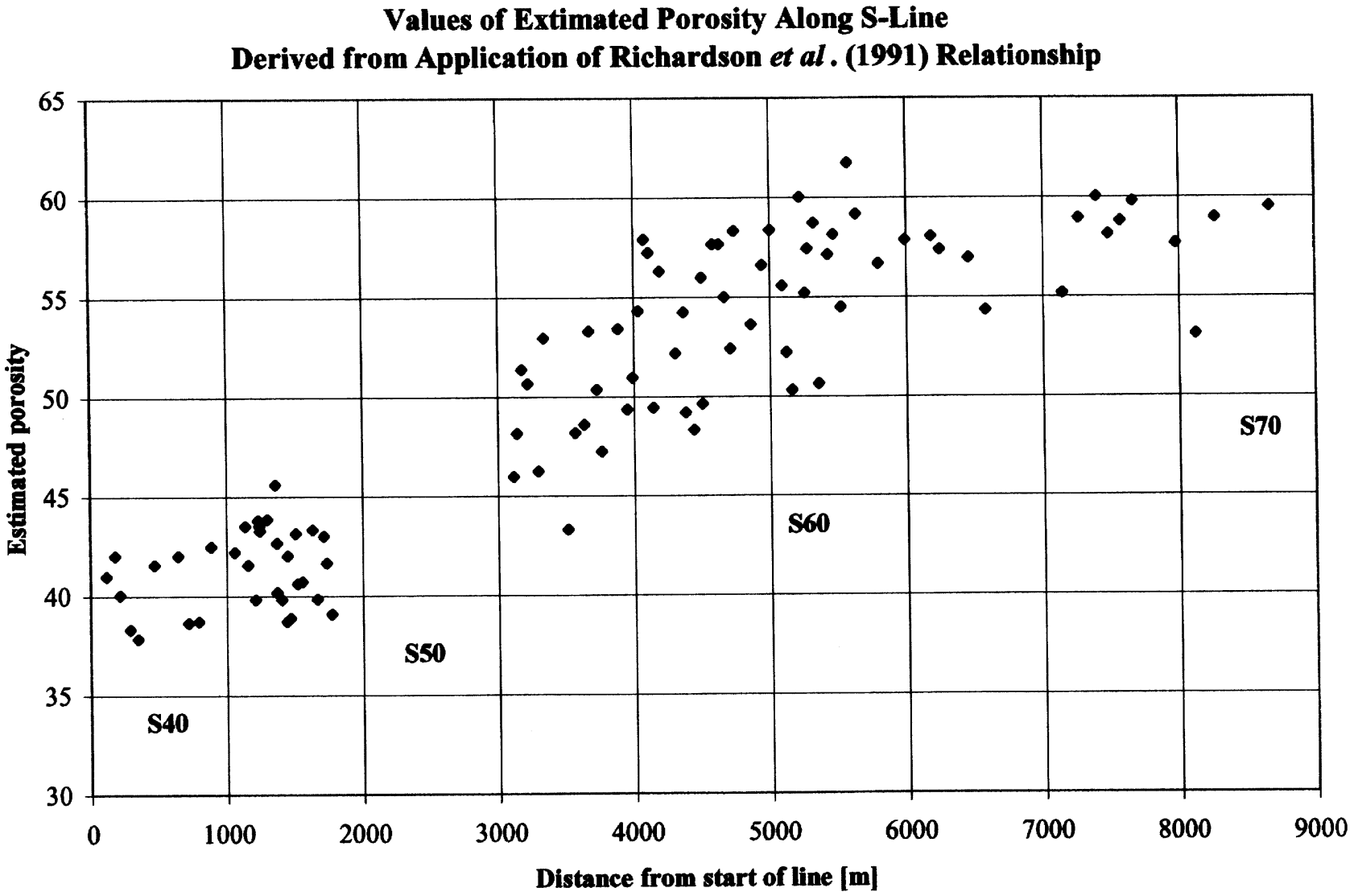
Values of Extimated Porosity Along S-Line
Derived from Application of Richardson et al. (1991) Relationship
Estimated porosity
65
60
55
50
45
40
35
30
0
1000
2000
3000
4000
5000
6000
7000
8000
9000
Distance from start of line [m]
S40
S50
S60
S70

Figure 5.

(a).

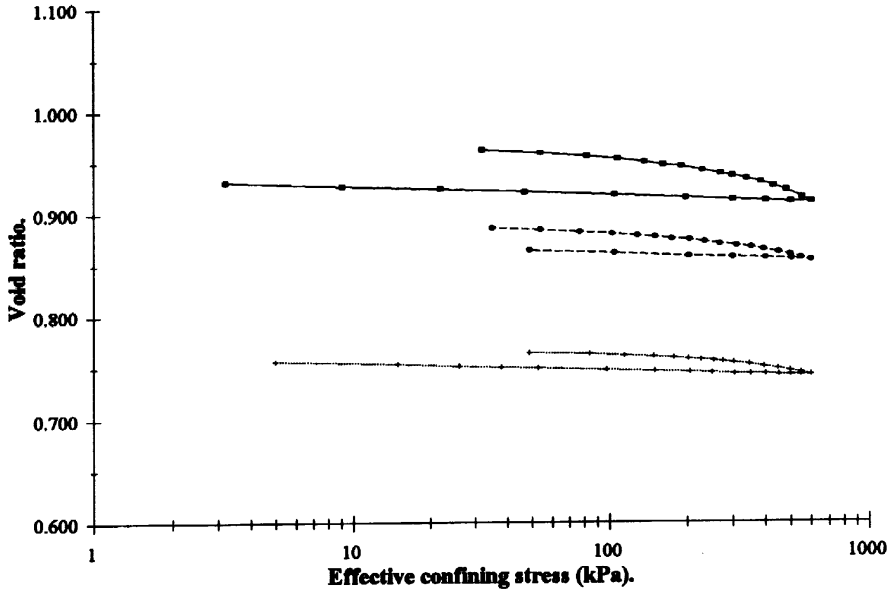

(b).

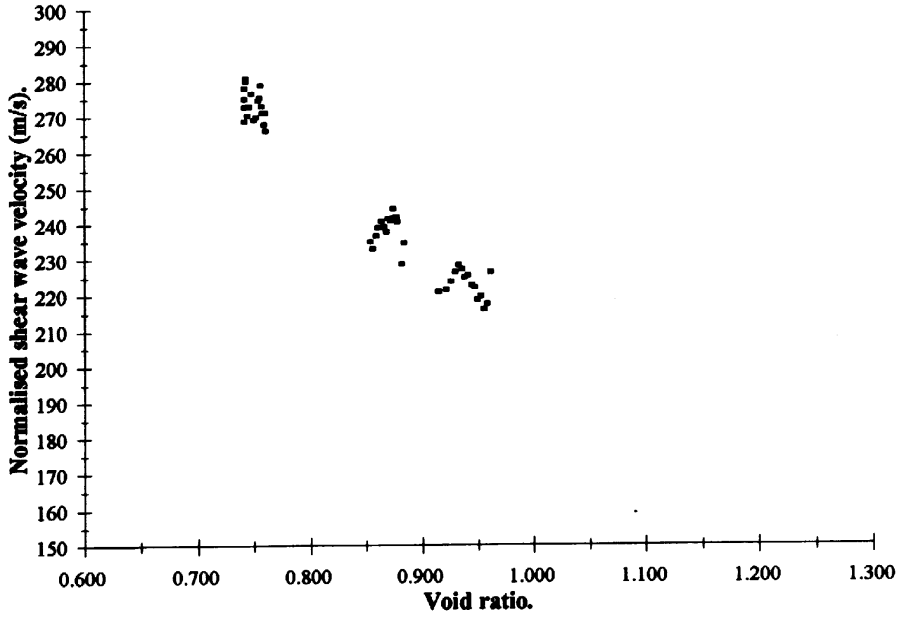

Figure 6. a. Typical isotropic compression curves for sands of differing initial density.
b. Initial relationship between normalised shear wave velocity and void ratio. (shear wave velocity normalised to 100kPa).

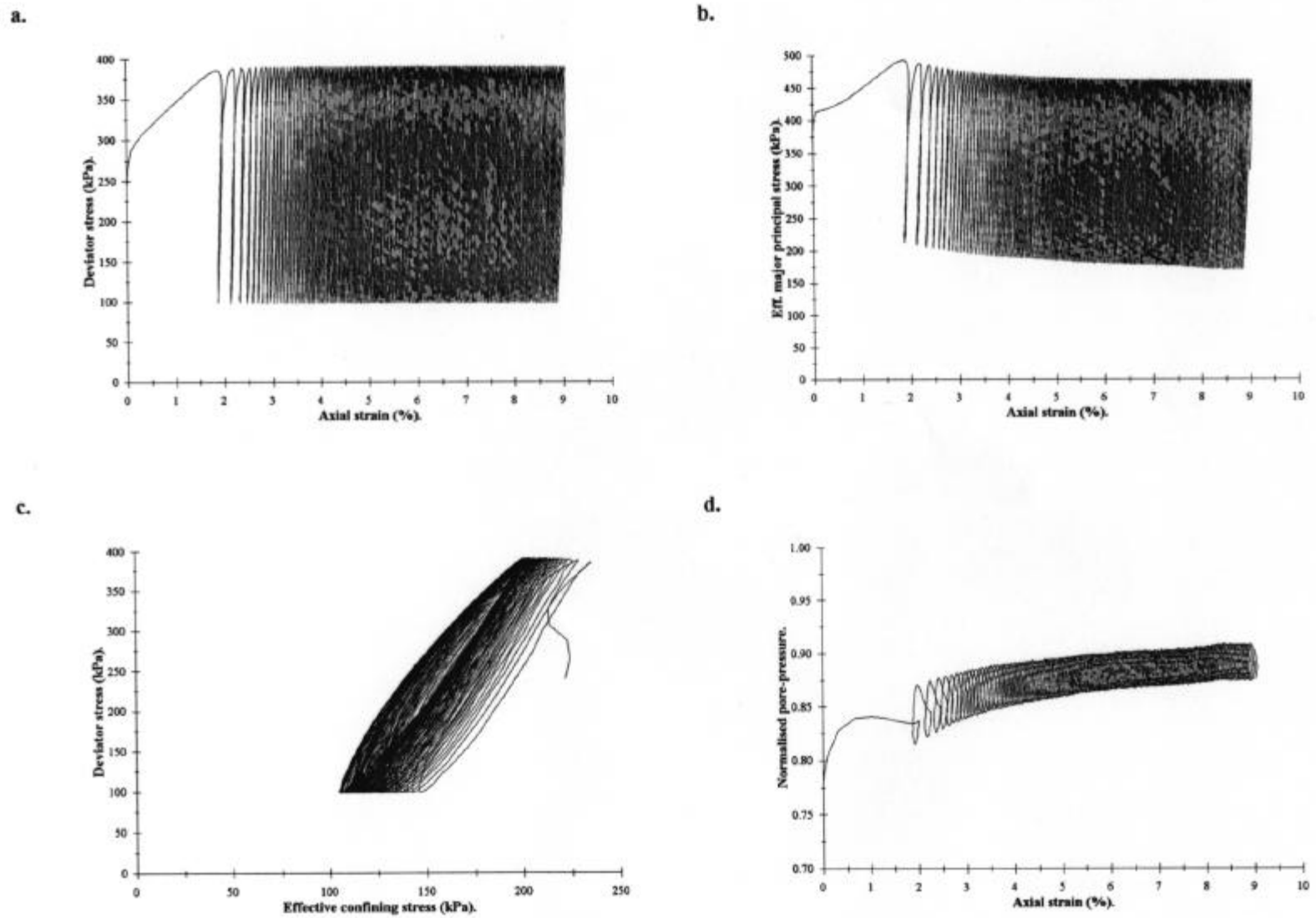

Figure 7. Typical undrained cyclic response of a medium dense sample of Key West Carbonate sand.

2.8 A Geochemical Investigation of Early Diagenetic Effects on Sediment Structures (Principal Investigators: Y. Furukawa and D. Wiesenburg)

Yoko Furukawa and Denis Wiesenburg
Institute of Marine Sciences
University of Southern Mississippi
Stennis Space Center, MS 39529

Introduction

Biogeochemical reactions during early diagenesis alter structures and physical properties of shallow marine sediments. The change in pore water chemistry causes production of gas phases, precipitation of authigenic minerals and dissolution of other solid phases. The change in sediment fabric due to the gas production, dissolution, and precipitation causes the sediment to behave differently in response to compaction, shearing, and the application of acoustic waves.

Quantitative correlation between biogeochemical reactions and fabric alteration is necessary for a comprehensive modeling of the effect of benthic boundary layer processes on sediment physical properties. However, quantifying such relationship has not been straightforward. Whereas our understanding of the thermodynamics of biogeochemical reactions is fairly comprehensive, we do not yet have a complete set of kinetic rate constants for diagenetic reactions. Moreover, our ability to quantify the effect of mixing due to such physical processes as storms, bioturbation, and bioirrigation is limited because of the spatial and temporal variability in the extent of such physical processes. Quantitative representation of sediment fabric also suffers from the variability caused by such processes.

One of the latest tools to quantify the effect of diagenetic biogeochemical reactions is the reactive transport modeling. Whereas currently available codes require input variables that include kinetic rate constants, bioturbation coefficients, and bioirrigation coefficients, such input variables can be refined by comparing the model output to the measured values of sediment chemistry and adjusting the input values accordingly for the further iterations. Moreover, the extent of dissolution of solid phases, production of gas phases and precipitation of authigenic minerals can be calculated and compared to the actual observation of fabric. The reactive transport modeling allows us to calculate the solute and solid concentrations of sediments deeper than the depths where sampling and analyses are relatively easy. They also allow us to calculate the variables that are not easily measured.

During FY96, this study focused on the quantitative imaging of sediment fabric and evaluation of the currently available reactive transport codes for the modeling of early diagenesis. For FY97, we plan to expand the image data set for more statistically sound image analysis. Also, we plan to further refine the input variables and output results of the biogeochemical modeling using the expanded sediment chemistry data set that will be collected during the planned cruise in the Dry Tortugas area in February 1997.

Methods

The sediment samples taken near the Dry Tortugas, Florida were air-dried and impregnated in Spur's resin. After the resin was cured, the samples were prepared for petrographic microscopy (thin sections), scanning electron microscopy (SEM; polished stubs), and transmission electron microscopy (TEM; ultrathin sections) following the standard methods. The samples were then imaged using the microscopes, and the images were recorded using the standard photographic techniques. The TEM imaging was most emphasized during FY96. Some of the TEM images were recorded using a CTD camera for digital processing of the images.

Some of the digitized TEM images were processed and analyzed using ImageTool, an image processing and analysis package developed at University of Texas Health Sciences Center, in order to quantify the change in the particle morphology. As geochemical alterations were more pronounced among the matrix particles rather than in grains (Furukawa et al., in review), the image analysis was conducted on the matrix images. The TEM images of matrix were fist converted to binary images representing the particles as black and void space as white as shown in Figure 1. Consequently the black objects (i.e., matrix particles) were analyzed for their morphology related variables such as perimeters and areas.

Reactive transport codes specifically developed for the study of early diagenesis, CANDI1.2 (Boudreau, 1996) and STEADYSED1 (Wang and Van Cappellen, 1996) were evaluated for the sediment chemistry characterization. Physical and geochemical variables measured by the authors and other participants of CBBLSRP (Shiller, 1996; Briggs et al., 1996; Bentley, personal communication) were used as the boundary conditions for the modeling.

Results and Discussions

The TEM images of the Dry Tortugas samples are shown in Figure 2. They indicate that the mechanical and chemical breakdown of grains results in the formation of matrix particles. This process is identical to the 'micritization' processes reported by Reid et al. (1992) in samples from Belize Lagoon.

Elongation, (i.e., the ratio of major axis length to minor axis length) was measured for each particle in the matrix images. The average values are plotted in Figure 3. Major axis length is the length of the longest line that can be drawn through the object, and minor axis length is the length of the longest line that can be drawn though the object perpendicular to the major axis. A needle-shaped particle results in the elongation much larger than 1 whereas a rounded or equi-dimensional particle has the elongation near unity. The depth profile of the average elongation (Figure 3) shows that needle shaped matrix particles alter to more rounded particles as the diagenesis progresses and the particles are buried deeper. The elongation depth profile coincides with the depth profiles of mineralogy and grain size (Furukawa et al., in review) in which dissolution of aragonite needles within grains and precipitation of high-Mg calcite occur as the diagenesis proceeds. More image acquisitions and image analyses are planned in order to assure the results to be statistically sound.

The depth profiles of pore water chemistry did not match between the measured values and calculated values using STEADYSED1 and CANDI1.2. Further refinement in the input variables such as sedimentation rates and the amount of reactive organic matter will be necessary in order to accurately hindcast and predict the sediments' response to early diagenesis in the study area.

Plans for FY97

(1) Another cruise to the Dry Tortugas area
Sediment chemistry data will be collected so that the boundary conditions can be defined more rigorously for the reactive transport modeling of biogeochemical processes. The variables to be measured include bottom water and pore water chemistry (e.g., dissolved O_2, pH, alkalinity, major cations, SO_4^{2-}) and solid phase chemistry (e.g., total organic carbon, total Fe(III), total Mn(IV)). All variables will be measured for the whole length of gravity cores (~2 m). With more confidence in the boundary conditions, the modeling will yield more confident kinetic rate constants and rates and magnitudes of dissolution and precipitation reactions. The magnitudes of dissolution and precipitation reactions will be used to predict the change in sediment fabric.

(2) More imaging of sediment fabric
The predicted changes in sediment fabric will be evaluated against the observed fabric. More imaging will be conducted to expand the data set for statistically sound image analyses.

(3) Data integration
The comparison will be put into a numerical format so that the extent of biogeochemical alteration can be used to model the alteration in sediment physical properties.

(4) Publication
Two more reviewed publications are planned. One is to present all the fabric results including images and image analysis results, and the other is to integrate the biogeochemical modeling and fabric results.

References

Boudreau, B. P. (1996) A method-of-lines code for carbon and nutrient diagenesis in aquatic sediments. *Computers & Geosciences*, **22**, 479-496.

Briggs, K. B., Lavoie, D. L., Stephens, K. P., Richardson, M. D., and Furukawa, Y. (1996) Physical and geoacoustic properties of sediments collected for the Key West Campaign, February 1995: A data report. Naval Research Laboratory.

Furukawa, Y., Lavoie, D and Stephens, K. (in review) The effect of geochemical diagenesis on sediment structure and mineralogy in shallow marine carbonate sediments near the Dry Tortugas, Florida. *Geo-Marine Letters*.

Reid RP, MacIntyre IG and Post JF (1992) Micritized skeletal grains in northern Belize Lagoon: A major source of Mg-calcite mud. *Journal of Sedimentary Petrology* **62**: 145-156.

Shiller, A. (1996) Effects of carbonate dissolution and precipitation on sediment physical properties and structure: pore water flux component. *In* Coastal Benthic Boundary layer Research Program: A Review of the Third Year (ed. M. Richardson) Naval Research laboratory.

Wang, Y. and Van Cappellen, P. (1996) A multicomponent reactive transport model of early diagenesis: Application to redox cycling in coastal marine sediments. *Geochimica et Cosmochimica Acta*, **60**, 2993-3014.

Publications supported by CBBLSRP

Peer-reviewed articles

Furukawa, Y., Lavoie, D and Stephens, K. (in review) The effect of geochemical diagenesis on sediment structure and mineralogy in shallow marine carbonate sediments near the Dry Tortugas, Florida. *Geo-Marine Letters*.

Lavoie, D., Furukawa, Y., Lavoie, D., Burkett, P. J., and Urmos, J. (in review) Apparent underconsolidation in Eckernforde Bay sediments: A model based on physical, geochemical and microfabric properties. *Journal of Continental Shelf Research*.

Abstracts and reports

Furukawa, Y. and Lavoie, D. (1995) The use of mineralogy and microfabric as the indicators of early diagenesis in shallow-water carbonate sediments from western Florida Keys. *Geological Society of America Abstracts with Program*, **27**.

Furukawa, Y., Lavoie, D. and Wiesenburg, D. (1995) Oxidation of aqueous sulfide in porewater as the possible cause for carbonate dissolution during early diagenesis. *The 1st SEPM Congress on Sedimentary Geology Congress Program and Abstracts*, **1**.

Furukawa, Y. and Lavoie, D. (1996) Mineralogy and microfabric of early diagenesis in shallow-water carbonate sediments from western Florida keys. *1996 Annual Meeting of the Mississippi Academy of Sciences*.

Furukawa, Y. and Lavoie, D. (1996) The impact of early diagenesis on sediment 3-D structure on shelf carbonate sediments near the Dry Tortugas, Florida. *American Geophysical Union 1996 Spring Meeting*.

Furukawa, Y. Lavoie, D. and Stephens, K. (1996) Carbonate sediment fabric as a tool to quantify early diagenesis. *American Geophysical Union 1996 Fall Meeting*.

Briggs, K. B., Lavoie, D. L., Stephens, K., Richardson, M. S. and Furukawa, Y. (1996) Physical and geoacoustic properties of sediments collected from the Key West Campaign, February 1995: A data report. Naval Research Laboratory, Stennis Space Center, MS. NRL/MR/7431--96--8002.

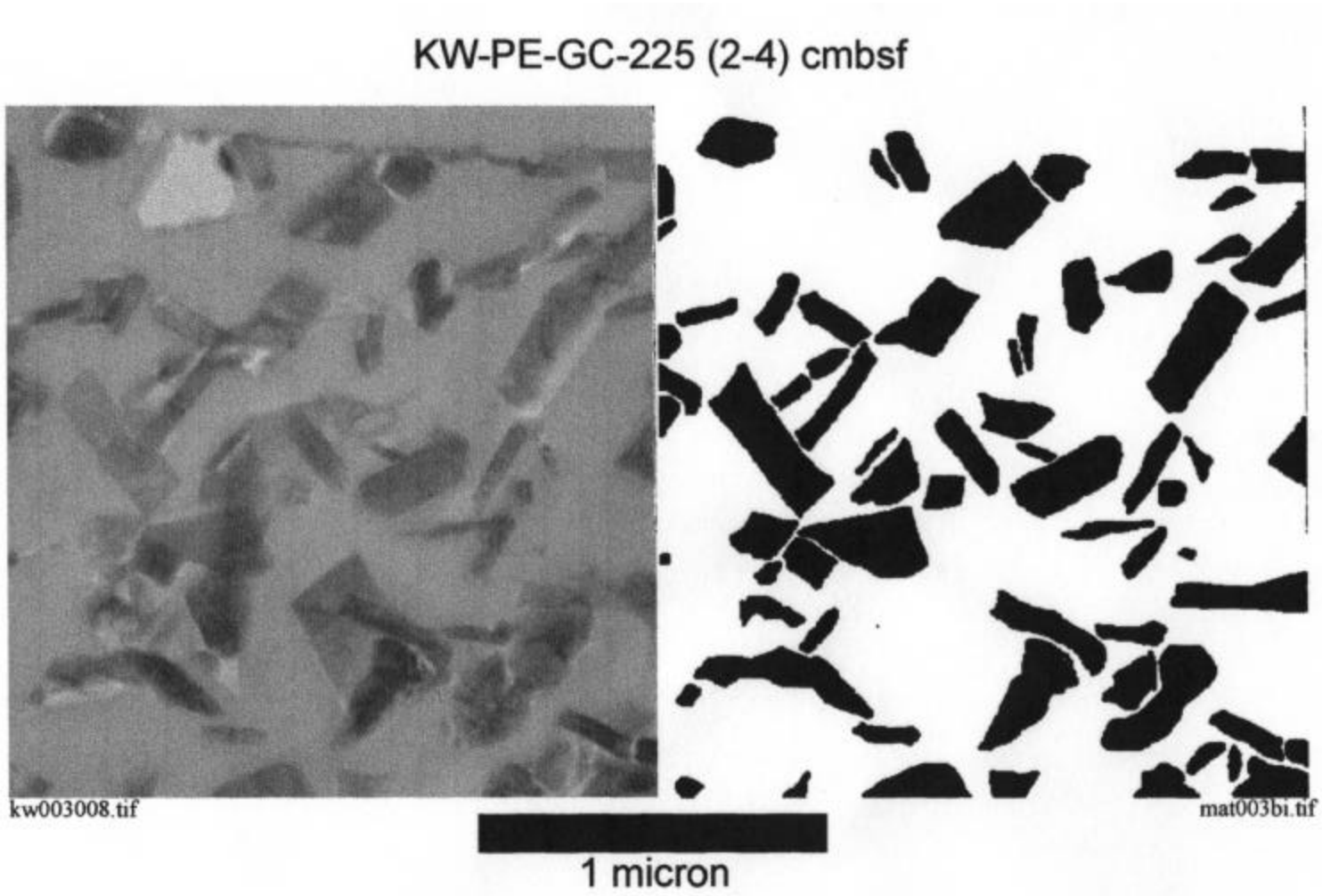

Figure 1. The TEM image of matrix within the sample from a gravity core (KW-PE-GC-225 (2-4) cmbsf) (left), and the binary image converted from the TEM image showing particles in black and void space in white (right). The image analysis was conducted on binary images such as above, right, to quantify the particle morphology.

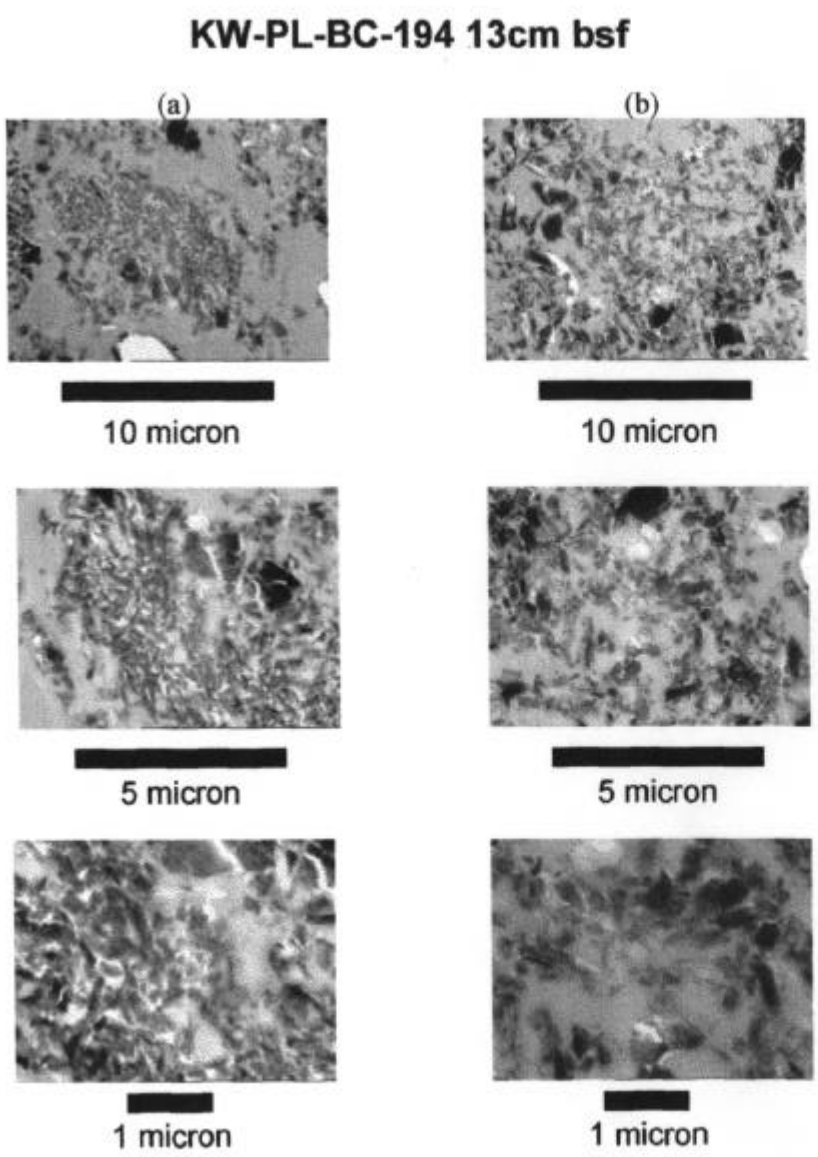

Figure 2. The representative TEM images of Dry Tortugas fabric samples. The samples are from a box core, 13 cm below sediment-water interface (KW-PL-BC-194 13 cmbsf). The first series of the images (a) indicates a grain that has been slightly altered in the lower left part. The unaltered part consists of tightly packed aragonite needles of similar morphology, whereas the altered part is characterized by the loose aggregates of particles with more varied morphology. The second set of images (b) shows an aggregate that has been extensively altered ('micritized') through mechanical and chemical processes. The loose aggregate is consist of particles with variety of morphology.

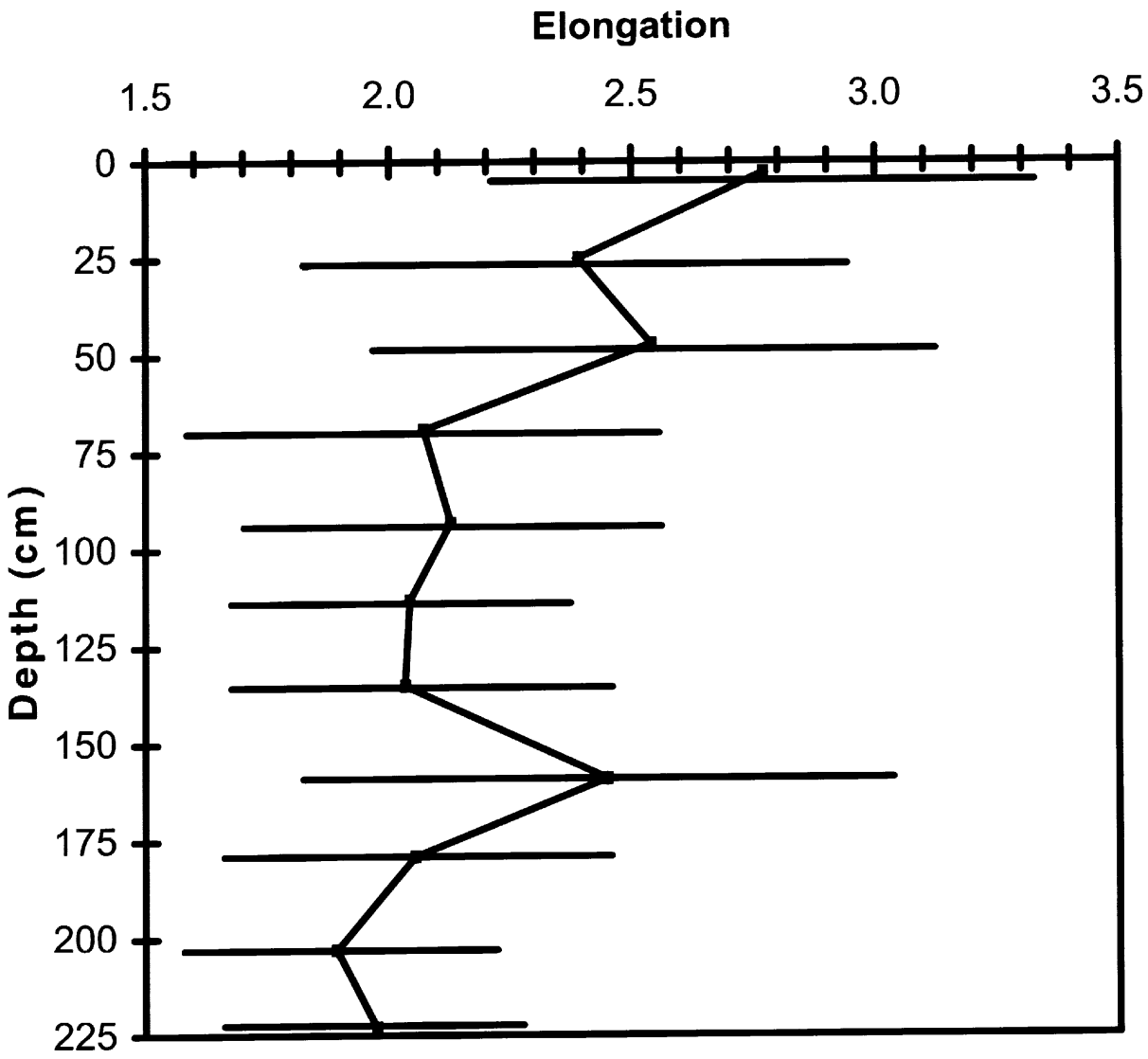

Figure 3. The average elongation (ratio of major axis length to minor axis length) of matrix particles is plotted against the sample depths. The matrix particles are more needle-like near surface and more rounded as buried deeper.

2.9 Image Analysis of Sediment Texture (Principal Investigators: R.J. Holyer, D.K. Young, and J.C. Sandidge)

CBBL FY96 Year-End Report for Image Textural Analysis Project

Ronald J. Holyer, David K. Young, and Juanita C. Sandidge

Naval Research Laboratory
Stennis Space Center
Mississippi 39529 USA

The long-term goal of our investigations is to derive new sediment textural classification methodologies based on image analysis and to use resulting variables directly as predictive model inputs or as proxy measures of and predictors for acoustic and physical properties of marine sediments. These image-based textural parameters could be particularly useful in quantifying inhomogeneities of sediment fabric patterns, including sediment contrast boundaries, gradients, interfaces, and anisotropy of component features (Young, et al., 1994). Previous work has focused on analysis of X-radiographs of marine sediments from Eckernförde Bay. Relationships between image-based values and bulk measurements of density have been demonstrated (Holyer, et al., 995). Scales, orientation, and isotropy of density fluctuations imaged in X-radiographs of marine sediments have been analyzed by image-based methods (Holyer, et al., 1996).

Activities in FY96 have focused in three areas: (1) multi-scale analysis of Eckernförde sediments, (2) correlation of density and electrical resistivity in Eckernförde sediments, and (3) analysis of sand particle size distributions by image analysis. These areas are summarized below.

Multi-scale Analysis of Eckernförde Bay Sediments: Several cores from Eckernförde Bay were sampled and photographed at different scales using different imaging techniques. X-radiographs capture density structure at centimeter (cm) scales, conventional photographs of thin sections capture structure at millimeter (mm) scales, and TEM imagery of ultra-thin sections capture structure at micron scales. This unique data set allows comparison of structure as a function of scale. The multi-scale sampling was repeated at depths of approximately 2 and 17 cm below the water/sediment interface so that interscale relationships can be investigated as a function of depth. Figures 1 through 3 show typical X-radiograph, thin section photograph, and thin section TEM images, respectively, from one of the shallow (~2 cm) samples of Eckernförde sediment.

Eckernförde bay sediments exhibit patches of significant layering resulting from deposition associated with major storm events (Orsi, et al., 1996). Other patches give evidence of reworking of the sediments by benthic invertebrates (Bentley, et al., 1996). Undisturbed storm deposits could be expected to consist of horizontal stratification leading to structure that is elongated in the horizontal direction relative to the vertical direction (anisotropic structure).

Reworked sediments, on the other hand, could be expected to consist of structures that are randomly oriented leading to isotropic structures. The questions addressed here are (1) can image analysis techniques measure anisotropy of sediment structures, (2) are areas of significantly different anisotropy found in Eckernförde sediments, and (3) is anisotropy present at all scales?

Images like Figures 1 through 3 have been processed and analyzed using procedures described in Holyer, et al., (1995). At one step in the processing, the images are reduced from gray-scale to black-and-white form. Darker areas in the images are converted to black, lighter areas to white. These images (which we call binary images) are then analyzed for the average "run lengths" in black and white pixels. Runs are rows of consecutive pixels of the same color (black or white). Average run lengths of black and white pixels are calculated in both the vertical and horizontal directions. A ratio of these average vertical and horizontal run lengths is a quantitative measure of the anisotropy of the structure represented in the black-and-white images. Table I gives the run length anisotropy for shallow and deep samples at each of the aforementioned scales.

TABLE I. Anisotropy Observations for Eckernförde Bay Sediments

	X-radiograph	thin section photo	thin section TEM
shallow sample (~2 cm)	1.30	1.04	1.06
deep sample (~17 cm)	1.12	1.12	1.05

Note in Table I that TEM images and thin section photographs (particle and pellet scales) show less anisotropy than the cm scale features in the X-radiographs. Within the X-radiograph there is more anisotropy near the surface than at depth. Our hypothesis is that anisotropy in this sediment results from depositional laminations resulting from storm events (Bentley, et al., 1996). This hypothesis explains the anisotropy increase at larger scales because storm laminae are scaled at a centimeter thick or more. The decrease in anisotropy with depth is explained because the deeper sample was from a preserved bioturbated layer unaffected by storm events.

Correlation of Density and Electrical Resistivity in Eckernförde Sediments: Electrical resistivity was measured by Peter Jackson of the British Geological Survey on some of the same Eckernförde sediment cores that were X-rayed by Kevin Briggs of NRL. The result is a data set offering a unique opportunity to examine relationships between bulk density and electrical resistivity. Methods for measuring electrical resistivity and producing microresistivity images are given by Jackson et al., (1996). Our contribution to this effort was to perform the image processing required to bring the two data sets in positional registration as closely as possible. The electrical resistivity was measured at 5 mm spacings. The X-radiograph represented spatial sampling at much higher density. Electrical resistivity was resampled to a finer grid and X-radiographs were resampled to a coarser grid. Images were shifted and aligned (a somewhat subjective procedure) so that the result was electrical resistivity and X-radiographs (representing bulk density) spatially coregistered as 1 mm per pixel images. We have analyzed spatial scales of variability in both density and resistivity and have calculated anisotropy values for both data types. The coregistered image pairs are being analyzed by Briggs and Jackson for density,

porosity, resistivity relationships. The combination of resistivity and X-ray data has enabled zonation in terms of both microstructure and sediment tortuosity. In addition, this approach offers the potential to provide a sensitive remote indicator of biogenic gas. A publication is in preparation.

Sand Particle Size Distributions by Image Analysis: The major activity in FY96 has been development of image analysis tools for measuring particle size, particularly for sand-sized particles. The automated measurement of particle size distributions based on image analysis consists of two parts. The first is called image segmentation, which is identifying particle pixels vs. non-particle pixels in an image. The second is measuring the size of the particles. We have addressed the second part of the problem in FY96 and have had reasonable success.

However, the image segmentation part of the problem has proven to be more difficult. The best way discovered to date to perform the image segmentation is to photograph the particles in silhouette. That is, opaque particles are placed on a white, backlight, translucent surface and photographed from the front. In this case, the particle silhouettes are black, and the interparticle space in white. A simple threshold operation gives a straightforward method for making the particle/no particle decision for each pixel. Figure 5 is an example of a backlight photograph of opaque sand grains which has been converted to black-and-white using a simple threshold. If particles are translucent, the above method of photography does not work. A more sophisticated segmentation, perhaps segmentation based on image texture, is required. An improved particle segmenter will be the objective of next year's investigation.

Given this type of segmented image, the run length computation mentioned previously in connection with anisotropy calculations can be applied to the size distribution of the black particle. If we model the particles as black dots, the average black run length in the image could be related to dot size. The average run length is, however, not identical to the dot diameter because many of the possible transects through the dot do not pass through its center. Those transects that pass off center result in black run lengths that are shorter than the diameter of the dot so that average run length will be smaller than particle diameter. This effect has been modeled mathematically and it was determined that the average run length must be scaled by 1.273 to yield particle diameter.

Another confounding factor in run length determination of particle size is the fact that particles overlap or touch so that in silhouette form, they look like a single larger particle and produce run lengths longer than particle size. This effect biases run length statistics to the high side. There are, therefore, two counteracting errors sources, (1) off-diameter transects of the particle producing small run length, and (2) overlapping particles producing large run lengths. If particles are sparsely spaced, the first effect dominates, if they are densely spaced, the second effect dominates. For some particle density, the two effects should balance and the average black run length will be equal to particle diameter. These effects have been modeled for circular dots randomly positioned in the image. The result of this simulation is shown in Fig. 5 where a correction factor to convert average run length to particle diameter is given as a function of percentage of the image covered by particles. The figure shows that the effects are in balance when approximately 42% of the image is particles.

Consider, as an example, the binary image of sand particles shown as Fig. 4. The particles photographed in this case range in diameter from 1.7 to 2.0 mm. Average horizontal and vertical run length of black pixels in this case is 1.82 mm. The image is 74% black which according to Fig. 5 results in an average run length that is too large by a factor of 1.54. When correction for this effect is applied to the average run length the resulting estimate of particle size is 1.19 mm. In this case the average run length gave the correct particle size without the correction factor from Fig. 5. The reason that the corrected value was less accurate than the uncorrected value is that the correction is intended to account for particle touching or overlap which occurs when particles are randomly positioned as they are in the mathematical model. In Fig. 4 there appears to be no overlap of particles and only minimal touching. Therefore, the experimental data did not match the model and the modeled correction was not necessary. This example illustrates the difficulties associated with developing a simple mathematical model of a complex physical problem. Other observed disagreement between particle size and run lengths is attributed to the particle segmentation problem previously mentioned. Sand particles are translucent in many cases so the backlight particle is not black, but rather some shade of gray which leads to an incorrect particle/background segmentation. Improved modeling and segmentation techniques developed in FY97 will produce more accurate particle sizes for these cases in the future.

In addition to relating average run length to average particle size, it is possible to apply this method to an aggregation of particles of varying sizes and to infer the particle size distribution from the distribution of run lengths. This has not been demonstrated yet on sediment particle images, but we have produced a simulated image with particles of 10, 17, 30 and 43 pixel diameters as shown in Fig. 6. The run length distribution for this image is shown in Fig. 7. Note the peaks in the run length distribution at lengths corresponding to the known particle diameters. An approximation to the particle size distribution is indeed present in the run length distribution in this case.

Future Plans: No participation in field experiments in planned during FY97. X-radiographs from the Strataform cruise to the Eel River during 1996 will afford us the opportunity to examine and quantify relationships among imaged textural structure and properties of these sediments. These X-radiographs collected collaboratively by Kevin Briggs will be calibrated with aluminum wedge permitting better quantification of imaged density structure.

We now have a rich database with which to develop unifying hypotheses for tests of image-base quantification and classification of sediment structure. These tests which form the culmination of our CBBL work will be the primary focus of our work in FY97. Comparisons of image-based statistical estimates of sediment texture with measured sediment properties from each experimental site will provide a rigorous test of the robustness of the image textural approach. We plan to analyze imagery of sediments over a wide range of size scales in differing sedimentary environments to obtain statistical estimates of measured sediment properties and geoacoustic parameters. We will add fractal geometry to our analyses which may contribute to unifying theories. Use of these image-based textural parameters in integrated benthic boundary layer models will be investigated.

Specific activities during FY97 include: (1) continued multiscale analysis of Eckernförde sediments with inclusions of Key West Expedition sediments, (2) demonstration and validation

of image-based analysis of sediment particle size, and (3) demonstration and calibration of determination of sediment bulk density using X-radiography. Publication will be prepared of interpretations and summarizations of results from these activities.

Presentations:

Holyer, R.J., D.K. Young, J.C. Sandidge and K.B. Briggs (1994) Sediment density structure inferred by textural analysis of cross-sectional x-radiograph and electron microscopy images. EOS, Transactions American Geophysical Union, 75(3):202.

Young, D.K, R.J. Holyer and J.C. Sandidge (1995) Texture of sediments from Eckernförde Bay: An image analysis approach. Gassy Mud Workshop, FWG, 11-12 July.

Holyer, R.J., D.K. Young and J.C. Sandidge (1995) Density structure of Eckernförde Bay sediments derived from image analysis: Relationships with sediment properties. Workshop on Modeling Methane Rich Sediments of Eckernförde Bay, Eckernförde, Germany, 26-30 Jun.

Holyer, R.J. (1995) Image analysis of sediment texture. Workshop on Sediment Geoacoustical and Geotechnical Constituitive Modeling, University of Rhode Island, Narragansett RI, 13-14 November.

Publications:

Holyer, R.J., D.K. Young, J.C. Sandidge and K.B. Briggs (1996) Sediment density structure derived from textural analysis of cross-sectional X-radiographs, *Geo-Marine Letters*, **16**, 204-211.

Briggs, K.B., R.J. Holyer, P.D. Jackson, and J.C. Sandidge (1996) Two-dimensional variability in sediment porosity, density and electrical resistivity in Eckernförde Bay sediment. In preparation.

References:

Bentley, S.J., C.A Nittrouer and C.K. Sommerfield (1996) Development of sedimentary strata in Eckernförde Bay, southwestern Baltic Sea. *Geo-Marine Letters*, **16**, 148-154.

Holyer, R.J., D.K. Young, and J.C. Sandidge (1995) Density structure of Eckernförde Bay sediments derived from image analysis: Relationships with sediment properties. In Wever, T.F. (Ed.), *Proceedings of the Workshop on Modeling Methane Rich Sediments of Eckernförde Bay*, Eckernförde, Germany, 26-30 June, FWG Report 22, pp. 225-232.

Holyer, R.J., D.K. Young, J.C. Sandidge, and K.B. Briggs (1996) Sediment density structure derived from textural analysis of cross-sectional X-radiographs. *Geo-Marine Letters*, **16**, 204-211.

Jackson, P.D., K.B. Briggs and R.C. Flint (1996) Evaluation of sediment heterogeneity using microresistivity imaging and X-radiography. *Geo-Marine Letters*, **16**, 219-225.

Orsi, T.H., F. Werner, D. Milkert, A.L. Anderson, and W.R. Bryant (1996) Environmental overview of Eckernförde Bay, Northern Germany. *Geo-Marine Letters*, **16**, 140-147.

Young, D.K., R.J. Holyer and J.C. Sandidge (1994) Texture of sediments from Eckernförde Bucht: An image analysis approach. In Wever, T.F. (Ed.), Proceedings of Gassy Mud Workshop, Kiel, Germany, 11-12 July, FWG Report 14, pp. 76-83.

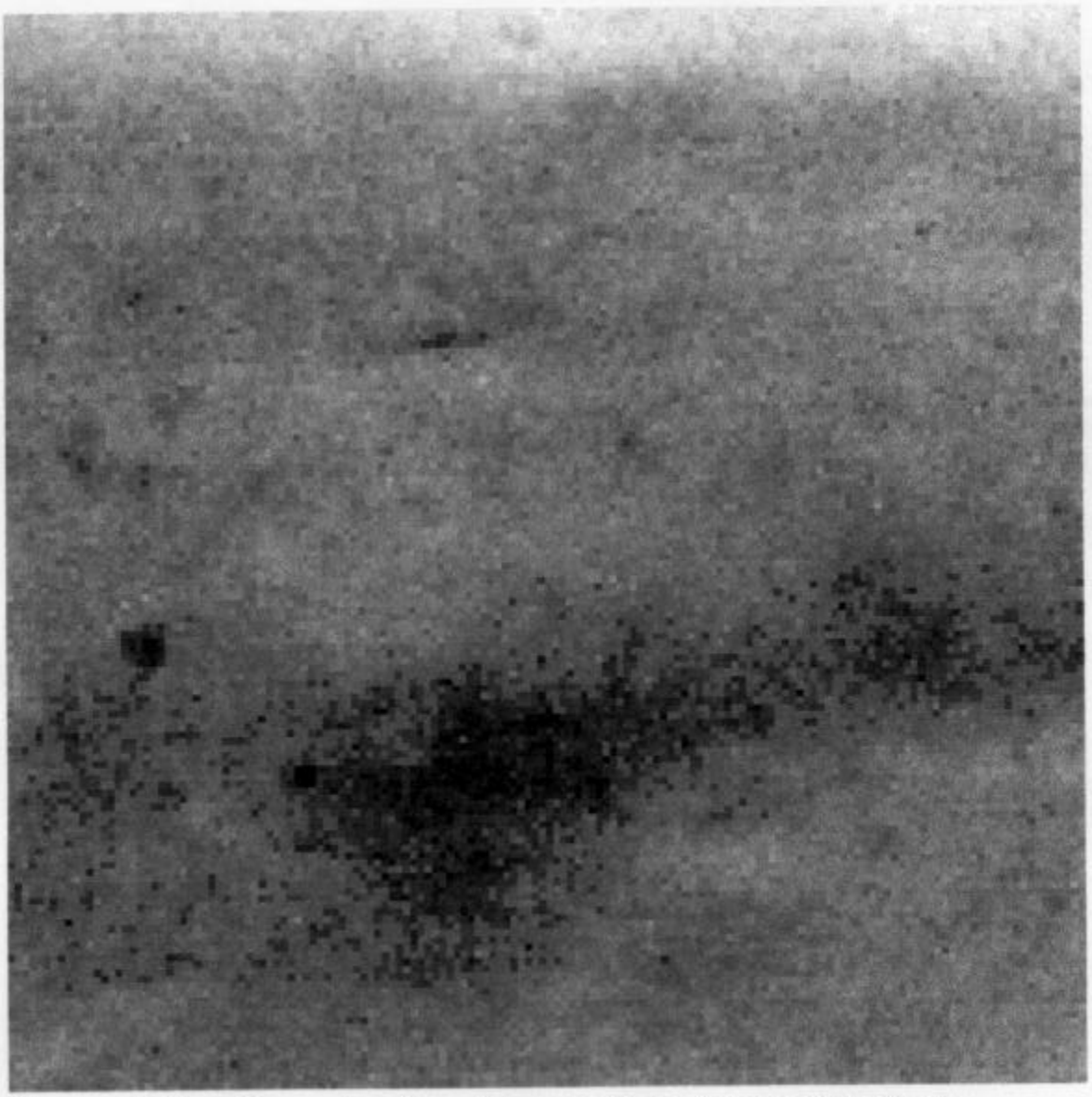

Figure 1 X-radiograph of 4 x 4 cm portion of core 634 where samples for Figs. 2 and 3 were taken

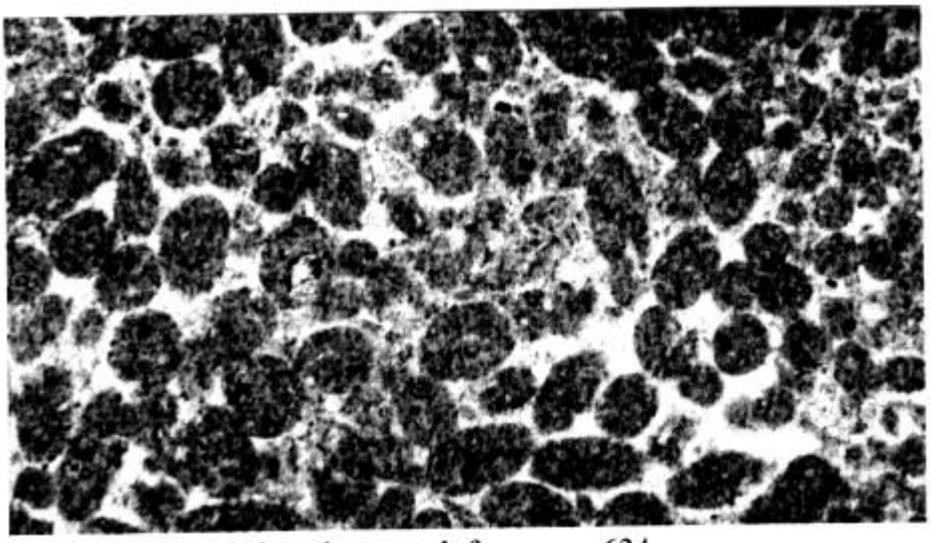

Figure 2 Thin-section photograph from core 634

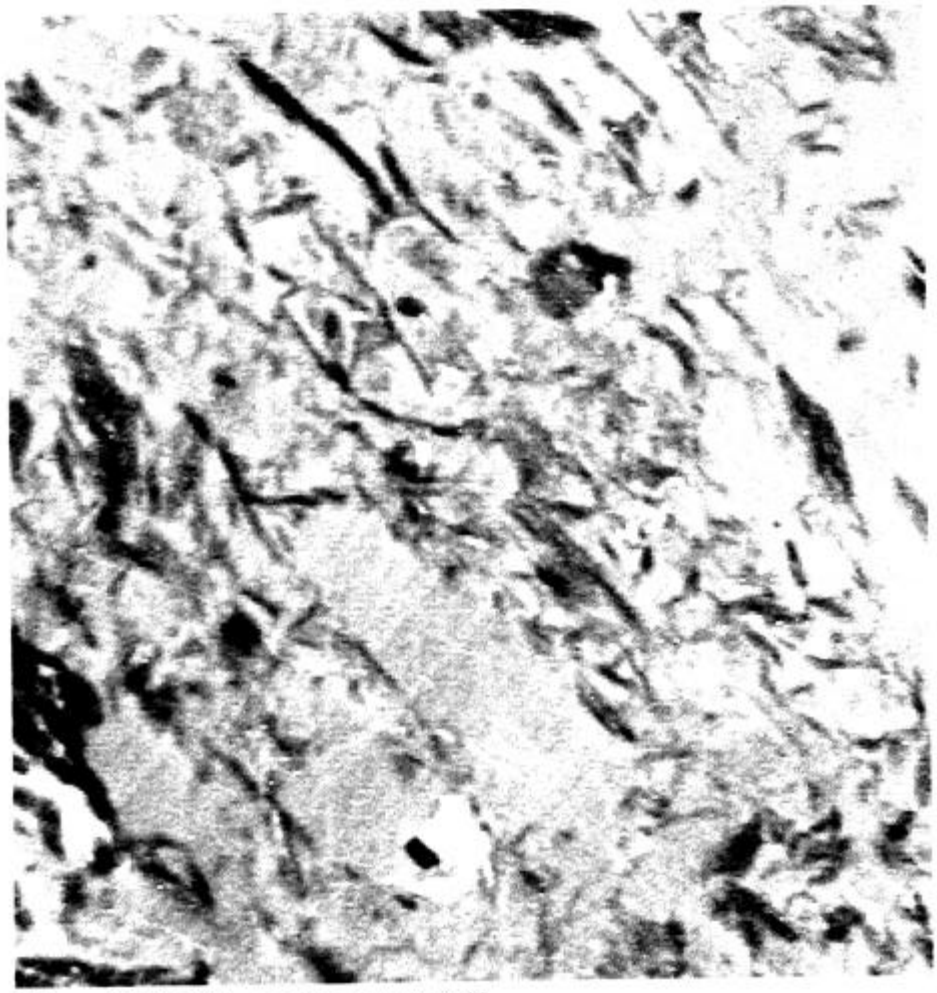

Figure 3 TEM image from core 643

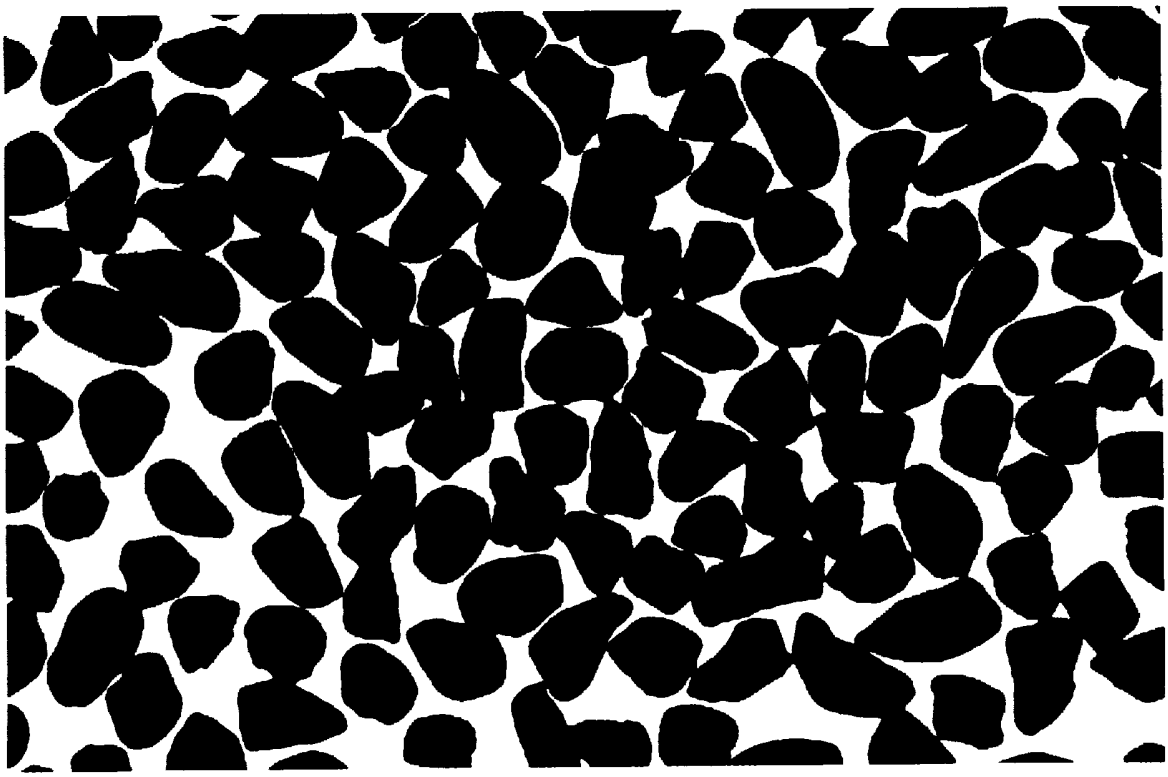

Figure 4 Binary image of sand grains

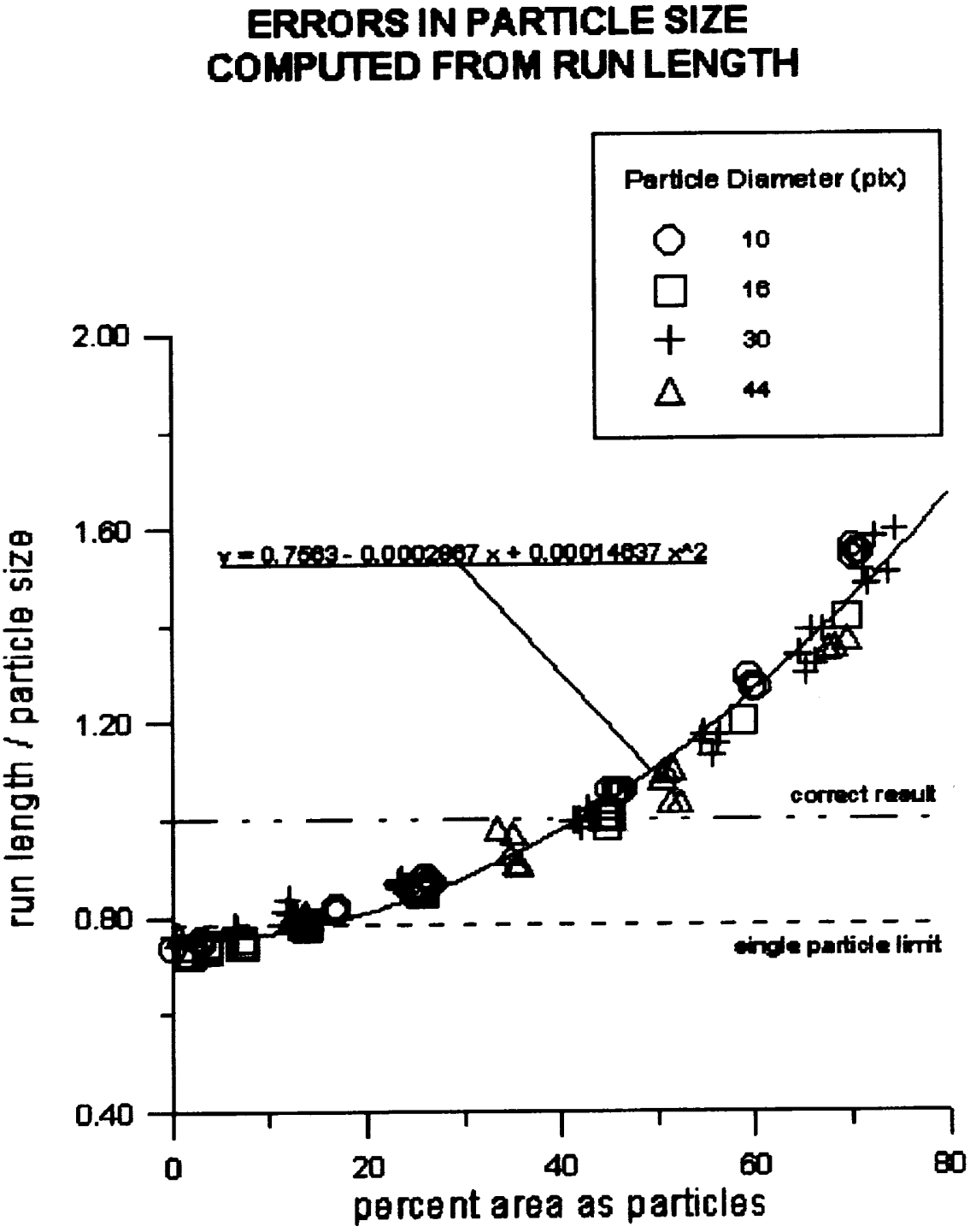

Figure 5 Correction factors for conversion of average run length to average particle diameter

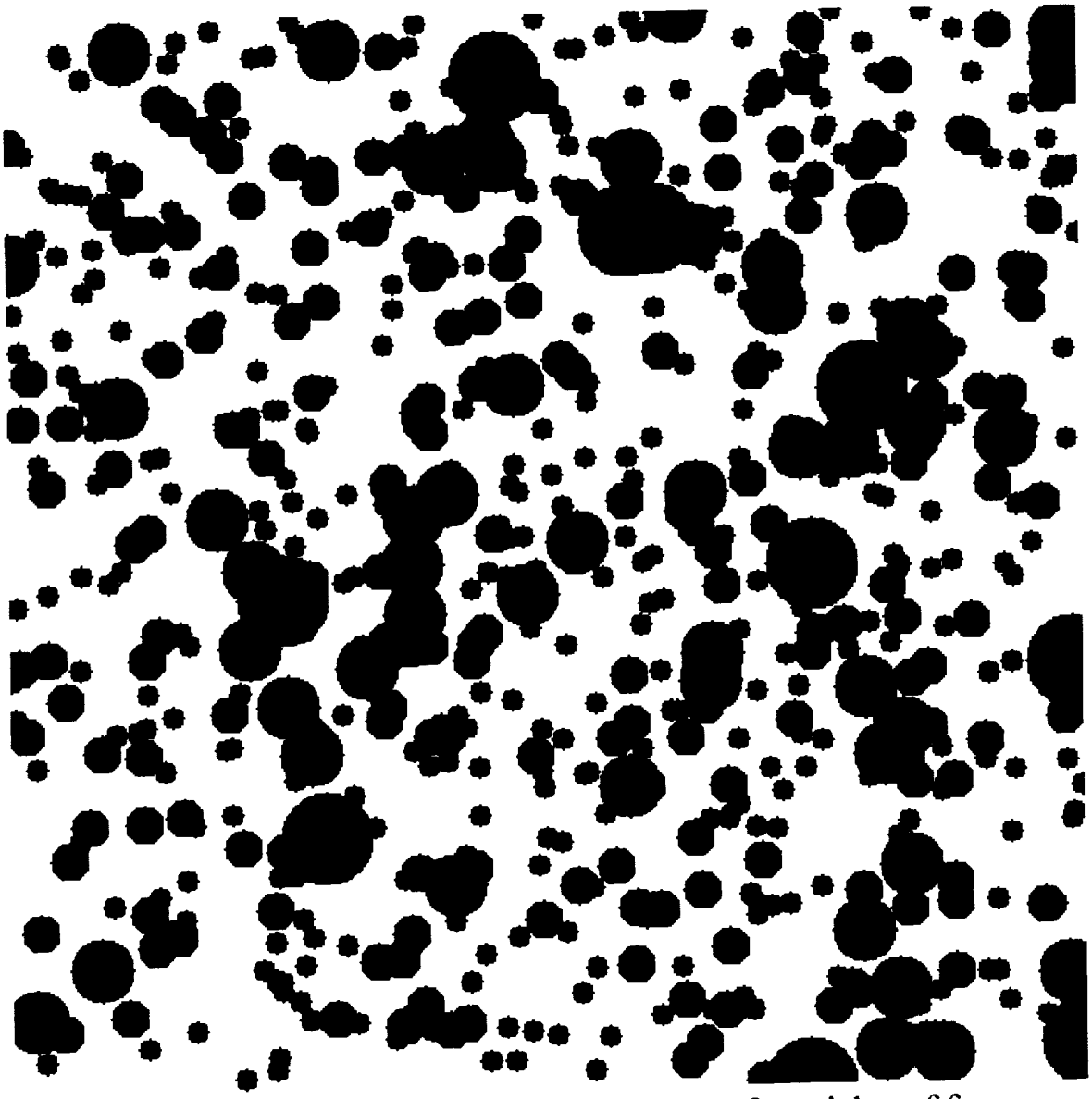

Figure 6 Simulated binary image of a mixture of particles of four sizes

DISTRIBUTIONS OF PARTICLE DIAMETERS AND IMAGE RUN LENGTHS

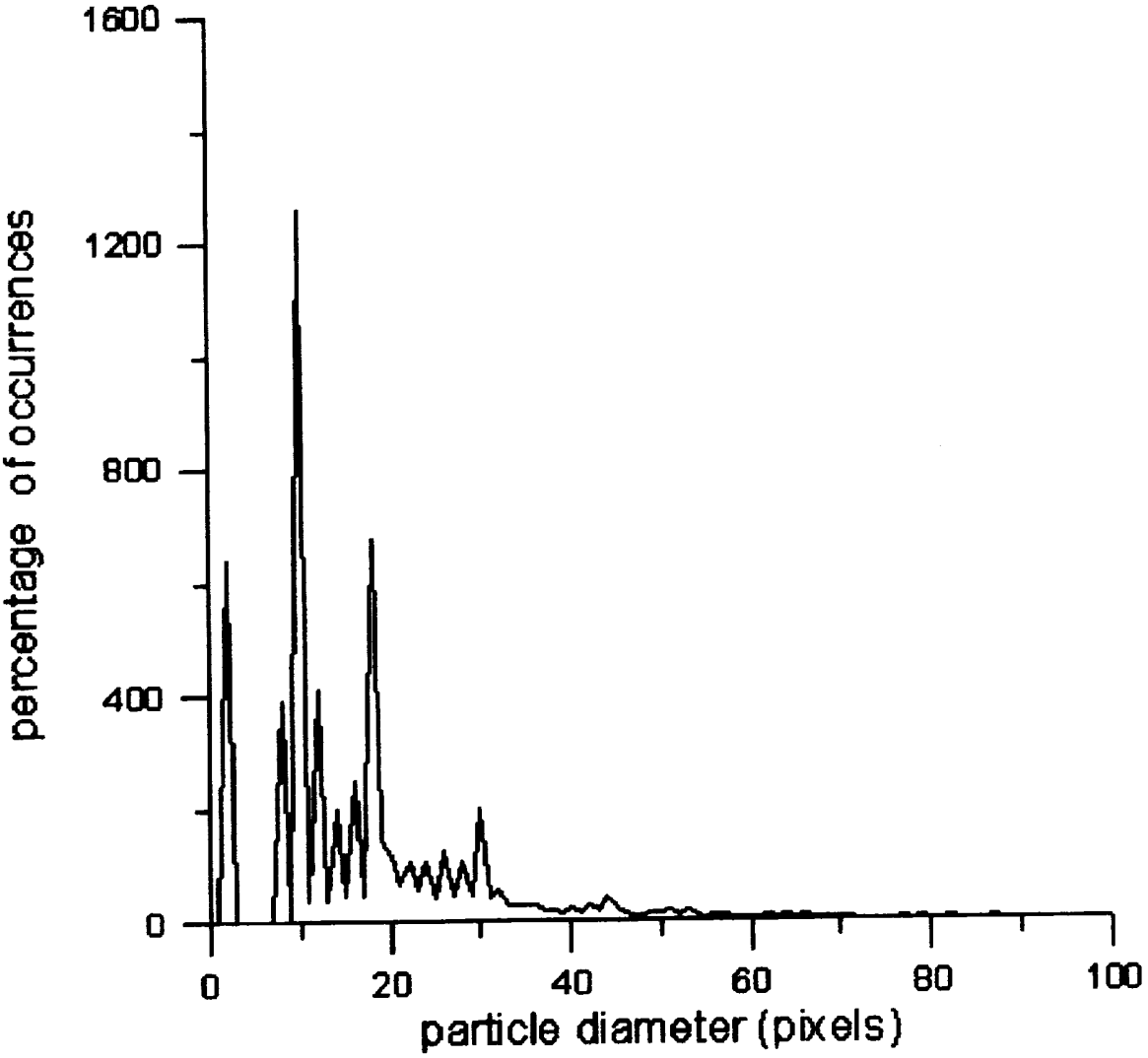

Figure 7 Black run length distribution in Fig.6

2.10 Measurement of High-Frequency Acoustic Scattering From Coastal Sediments (Principal Investigators: D.R. Jackson and K.L. Williams) Measurement of High-Frequency

Acoustic Scattering From Coastal Sediments

Darrell R. Jackson
Kevin L. Williams
Applied Physics Laboratory, College of Ocean and Fishery Sciences,
University of Washington, Seattle, Washington 98195

Introduction

The focus of this work is measurement of monostatic and bistatic scattering from shallow water sediments. One objective is to use the scattering data to clarify mechanisms responsible for scattering. Another is to use the backscatter data to acoustically monitor physical and biological processes that affect the seafloor. During FY96, processing and interpretation of the Key West bistatic data was the major effort. In addition, backscatter model-data comparisons for all three CBBL sites were completed, and the sonar events seen at Eckernförde were studied in detail.

Results - FY96

Bistatic Scattering - Key West

Performance of the bistatic scattering experiments from a vessel in a four point moor allowed better control over experimental geometry and collection of a much larger data set, over a larger range of angles, than in previous bistatic scattering experiments. Of particular note is that there is data encompassing bistatic scattering angles from 0 to 180 degrees (forward scattering to backscattering) and that enough data were acquired to allow better estimation of mean bistatic scattering strength as a function of bistatic scattering angle.

The data are compared in Figures 1 and 2 with the model of Jackson 1993. The model inputs used in Figure 1 were obtained from NRL data as explained in Jackson, Williams, Briggs, and Richardson 1996. The figure has four individual panels. In each panel, all the bistatic scattering strengths with associated incident and scattered grazing angles within a specified range (given in the figure) are plotted as a function of bistatic angle (phi). There are two model curves shown in each panel; one calculated using the incident and scattered grazing angles set to the lowest value of the panel and one with them set to the highest value, e.g., in the top left panel one model curve is for (thetai = thetas = 5 degrees) and the other is for (thetai = thetas = 15 degrees). The overall fit to the data is good throughout most of the bistatic angle range from backscattering to forward scattering. However, there are two characteristics of the data/model comparisons that warrant further comment.

Examination of the top right panel (with thetai and thetas between 10 and 20 degrees) indicates a phi region around 50 degrees where the data fall below the model. Examination of the relative surface and volume scattering in this region indicates that both contribute significantly. Figure 2 shows the same data but with the ratio of compressibility to density fluctuations for the volume

scattering changed from the -1.31 given in Jackson, Williams, Briggs, and Richardson 1996 to a value of -0.66. There is better agreement in the phi range near 50 degrees and little effect outside this range.

Examination of the bottom two panels in Figure 1 or 2 indicate that for the higher incident and scattered grazing angles of these figures the data in the phi region from backscattering (180 degrees) to 90 degrees lies above the model. This effect is also seen in the backscattering data for this site. The reason is unknown but one possibility, as noted below, is the need to account for gradients in sound speed and porosity.

Backscattering - All Sites

Figures 3-5 compare the 40 kHz backscattering data from all three sites with various backscattering models. The model inputs were obtained from NRL data as explained in Jackson, Williams, Briggs, and Richardson 1996. These comparisons indicate that roughness scattering was dominant at the Panama City and Key West sites, while volume scattering due to bubbles was dominant at the Eckernförde site (Tang et al. 1994). Generally, first-order perturbation theory gave a good fit to the roughness scattering data, although strong gradients in the sound speed and porosity at Key West suggest that a model allowing for such gradients should be used (Ivakin 1994, Moe and Jackson 1994). Although the composite roughness model is generally considered to be a refinement of the perturbation approximation, it resulted in similar or poorer fits.

Eckernförde Acoustic Events

As noted in last year's report, short-lag correlation images show impulsive events localized at a few patches within the sonar field of view. The correlation of these events with sea floor pressure suggests that they are due to ebullition of methane, but the possibility that the events are nothing more than scattering by fish is suggested by their approximately diurnal period. To clarify the nature of these events, we have performed processing to locate the events in three-dimensional space. Matched filtering was used to improve range resolution, and interferometry was used to determine scatterer altitude. Figure 6 shows images of events occurring in one particularly active period. Study of images such as this supports the ebullition hypothesis, as the scatterers tend to form plumes extending from the bottom and have dimensions considerably smaller than expected for fish schools.

Significance of Results to CBBL objectives

The results obtained to date address CBBL objectives at two levels. First, the acoustic data have provided a means of monitoring biological and physical processes over relatively large regions and time spans (as compared to point sampling). Interesting acoustic phenomena that are environmentally driven have been observed, notably, extremely rapid acoustic change at the Panama City site and impulsive events at Eckernförde Bay. Second, the data have been used to test physical models for acoustic scattering. In particular, models for scattering by interface roughness and by gas bubbles have been found to provide reasonable fits to the data with no free parameters.

Plans for FY97

We plan to test the bistatic model, as applied to Key West sediment, against forward scattering horizontal coherence data. A journal article will be written documenting the Key West data/ model comparisons. Also, long-term correlation results from the CBBL experiments will be examined further and used in fitting the parameters of a sediment reworking model under development.

References

D. R. Jackson, A Model for Bistatic Bottom Scattering in the Frequency Range 10-100 kHz, APL-UW TR 9305, Applied Physics Laboratory, University of Washington, August 1993.

A.N.Ivakin, "Sound scattering by rough interfaces of layered media," Proceedings of the Third International Congress on Air- and Structural-Borne Sound and Vibration, pp. 1563-1570, June 1994.

J.E. Moe and D.R. Jackson, "First-order perturbation solution for rough surface scattering cross section including the effects of gradients," J. Acoust. Soc. Am. vol. 96, pp. 1748-1754, Sept. 1994.

D.R. Jackson, K.L. Williams, and K.B. Briggs, "High-Frequency Observations of Benthic Spatial and Temporal Variability," Geo-Marine Letters Vol. 16 212-218 (1996).

D.R. Jackson, K.B. Briggs, K.L. Williams, and M.D. Richardson, "Tests of models for high-frequency seafloor backscatter," IEEE J. Oceanic Engr. Vol. 21 (October 1996).

D. Chu, K.L Williams, D. Tang, and D.R. Jackson, "High-frequency bistatic scattering by sub-bottom gas bubbles," J. Acoust. Soc. Am. (In press).

D.R. Jackson, K.L. Williams, T.F. Wever, C.T. Friedrichs, and L.D. Wright, "Sonar observation of events in Eckernförde Bay," Continental Shelf Res. (Submitted)

Tang, D., Jin, G., Jackson, D.R., and Williams, K., "Analysis of high-frequency bottom and sub-bottom backscattering for two distinct shallow water sites," J. Acoust. Soc. Am. Vol. 96, 2930-2936 (1994).

Accomplishments Over Past 4 Years

Acquired large, high-quality bistatic and monostatic acoustic scattering data sets from well-characterized sites.

Verified bistatic and monostatic scattering models for Panama City and Key West sites.

In collaboration with Tang and colleagues, tested their bubble scattering model and identified multiple scattering effects.

Measured rate of benthic acoustic change at three sites and found time scales varying by two orders of magnitude

Demonstrated that scattering at Panama City site is a surficial process. Measured spatial and temporal frequency of pressure driven changes in gaseous methane at Eckernförde.

Developed strong evidence that acoustic events in Eckernförde data are due to methane ebullition.

Publications resulting from this work

Tang, D., Jin, G., Jackson, D.R., and Williams, K. (1994) Analysis of high-frequency bottom and sub-bottom backscattering for two distinct shallow water sites. Journal of the Acoustical Society of America, Vol. 96, 2930-2936.

D.R. Jackson, K.L. Williams, and K.B. Briggs, "High-Frequency Observations of Benthic Spatial and Temporal Variability," Geo-Marine Letters Vol. 16 212-218 (1996).

D.R. Jackson, K.B. Briggs, K.L. Williams, and M.D. Richardson, "Tests of models for high-frequency seafloor backscatter," IEEE J. Oceanic Engr. Vol. 21 (October 1996).

D. Chu, K.L Williams, D. Tang, and D.R. Jackson, "High-frequency bistatic scattering by sub-bottom gas bubbles," J. Acoust. Soc. Am. (In press).

D.R. Jackson, K.L. Williams, T.F. Wever, C.T. Friedrichs, and L.D. Wright, "Sonar observation of events in Eckernförde Bay," Continental Shelf Res. (Submitted).

K. L. Williams, D. R. Jackson, "Bistatic Bottom Scattering: Model, Experiments, and Model/Data Comparison," APL TR 9602, J. Acoust. Soc. Am. (Submitted)

D. R. Jackson, K. L. Williams, "High Frequency sea-bed scattering measurements in shallow water," Proceedings of 3rd European Conference on Underwater Acoustics.

K. L. Williams, D.R. Jackson, "Monostatic and bistatic bottom scattering: Recent experiments and modeling," Proceedings of Oceans '94, September 1994

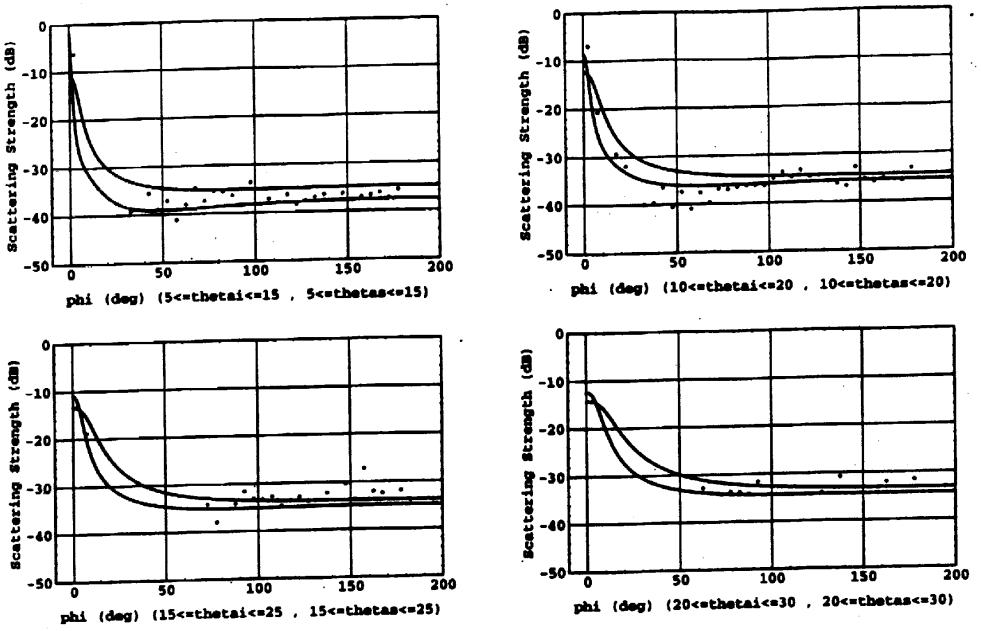

Fig. 1 Bistatic scattering data and model results for Key West. In each panel, all the bistatic scattering strengths with associated incident and scattered grazing angles within a specified range are plotted as a function of bistatic angle (phi). There are two model curves shown in each panel; one calculated using the incident and scattered grazing angles set to the lowest value of the panel and one with them set to the highest value, e.g., in the top left panel one model curve is for (thetai = thetas = 5 degrees) and the other is for (thetai = thetas = 15 degrees).

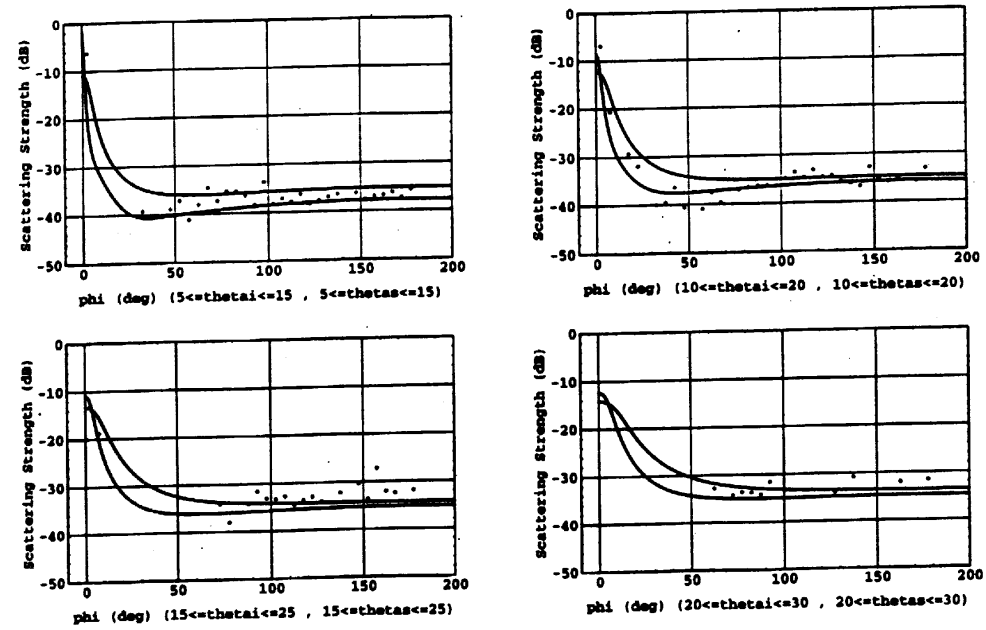

Fig. 2 Same as Figure 1 but with the ratio of compressibility to density fluctuations for the volume scattering changed from the -1.31 given in Jackson, Williams, Briggs, and Richardson 1996 to a value of -0.66. There is better agreement in the phi range near 50 degrees in the top right panel and little effect outside this range.

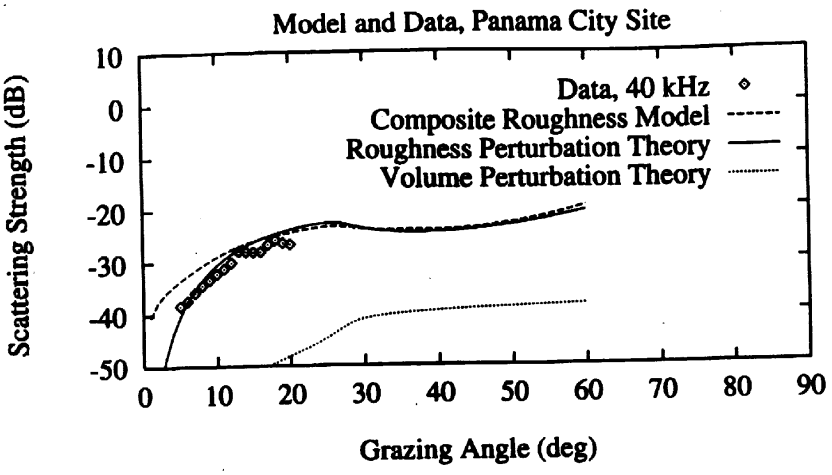

Fig. 3 Backscattering strength data and model predictions for the Panama City site.

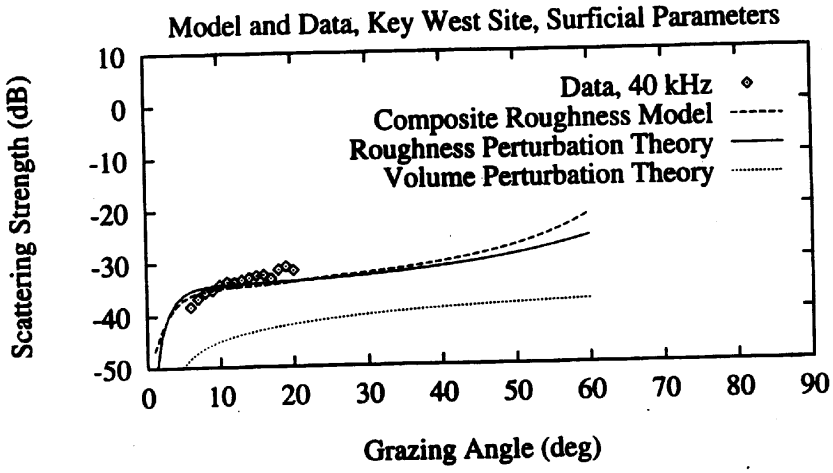

Fig. 4 Backscattering strength data and model predictions for the Key West site using surficial parameters

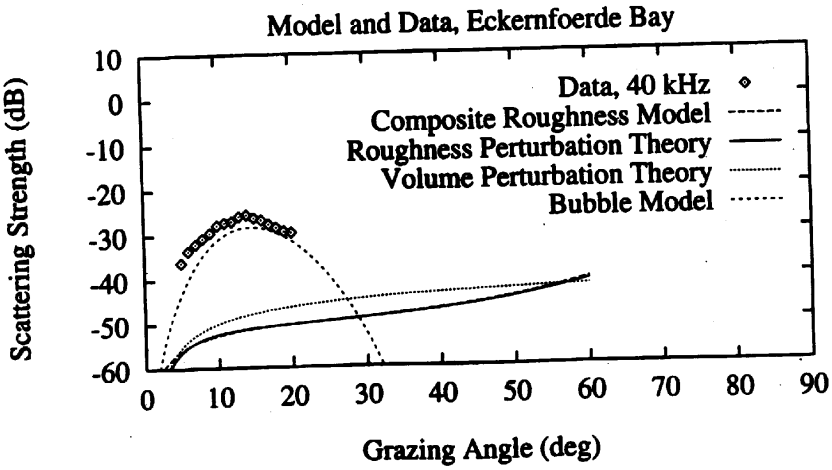

Fig. 5 Backscattering strength data and model predictions for the Eckernfoerde site using parameters averaged over core depth.

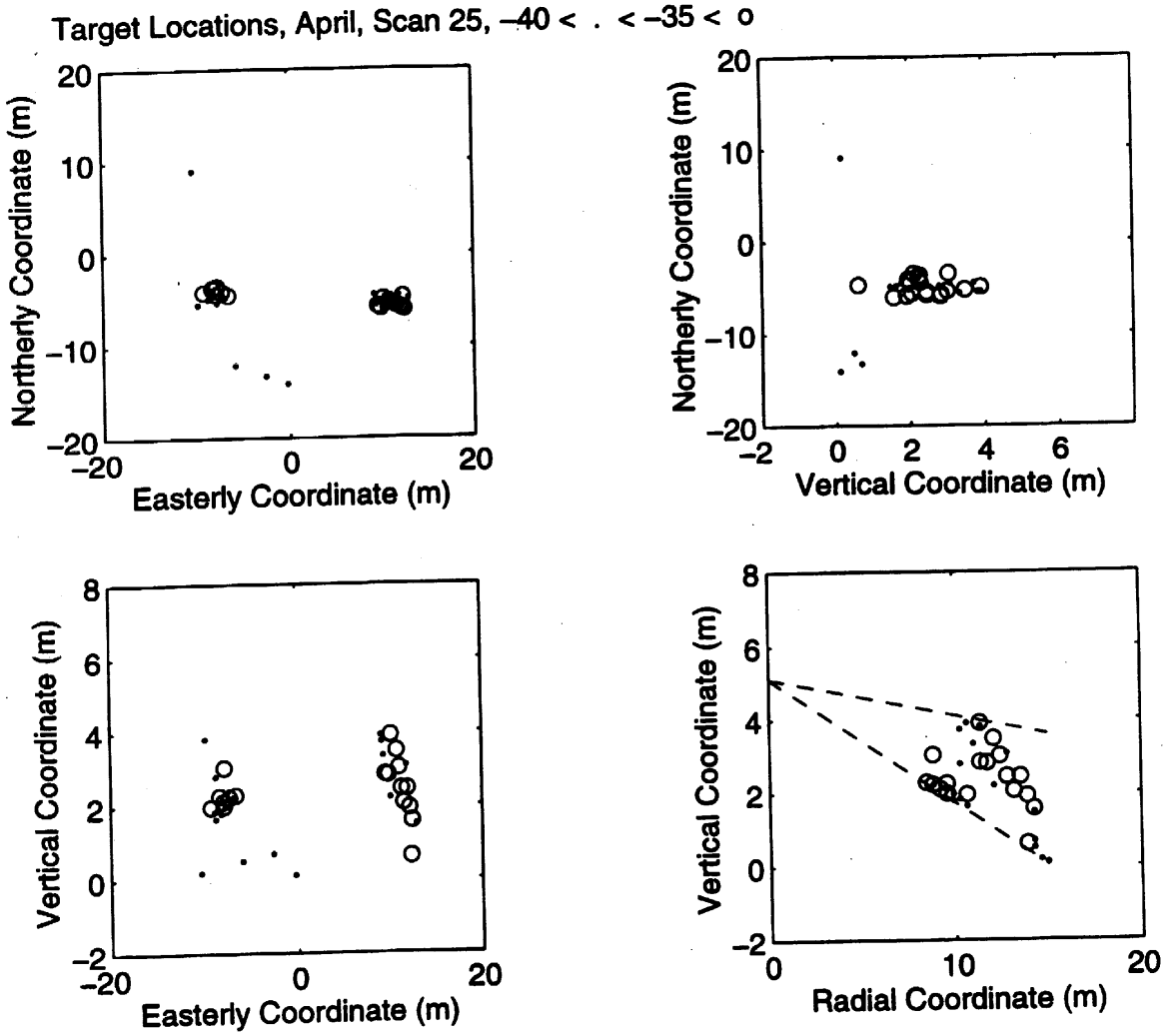

Fig. 6 High resolution images showing targets within 15 m of the sonar transducer. Strong targets having strengths greater than -35 dB are shown as open circles. Weaker targets with strengths between -40 and -35 dB are shown as dots. The limits set by the transducer directivity are shown as dashed lines.

2.11 Quantification of High Frequency Acoustic Response to Seafloor Micromorphology in Shallow Water (Principal Investigators: D.N. Lambert and D.J. Walter)

D.N. Lambert and D.J. Walter
Naval Research Laboratory, Code 7431
Stennis Space Center, MS 39529

Project Objectives

The overall objectives of this project are (1) to investigate new methods of quantifying the effect of sediment micromorphologic structure on high frequency acoustic response in shallow water and its relationship to in situ acoustic and geotechnical properties and (2) to provide a 3-D digital high resolution micromorphologic characterization of the various CBBL program experimental sites.

Introduction:

During FY96, a significant amount of the high resolution ASCS data previously collected during FY94 and FY95 off Key West, Florida was analyzed and compared to ground truth core and in situ probe data. Results of these efforts have been presented at several conferences and Don Walter is using these data sets as the basis for a Masters Thesis. ASCS data from this area has also been distributed to a number of other CBBL investigators for specific modeling studies. The objective of developing an improved, more accurate method for predicting sediment acoustic impedance and thus, sediment geotechnical properties, was continued with promising results. These results led to a new linear least square inversion method being developed which appears to make accurate, real time predictions of sediment properties. This technique will be implemented in the ASCS software during FY97. In addition, the ASCS team spent several weeks collecting ASCS data in the STRATAFORM program study area off the Eel River, in northern California. This fieldwork, unfortunately, consumed much of the available CBBL funding, thus, some other planned objectives were not accomplished.

Current Status and Progress

Personnel from the ASCS group (Lambert, Walter, Griffin, and Mang) participated in two legs of a research cruise aboard the R/V WECOMA in the ONR sponsored STRATAFORM Program study area off Eureka, California in late May and early June 1996. A major objective of this effort was to obtain a data set that would serve as a precursor to the FY97 new start 6.2 Mine Burial Processes Project. The majority of the data was acquired while underway using the standard, single frequency, short pulse length ASCS technique. A color-coded map of surficial sediment impedance along the ship track is provided in Figure 1. As indicated, the diagonal track transited along the 70 meter isobath, while the tracks perpindicular to it transit along the designated lines. A detailed summary of ASCS data collected during the survey phases of the Eel River Study is provided in "Cruise Reports for W9605A, Leg 2", compiled by Kevin B. Briggs and Matthew Logan 1996.

Additional data was collected using an FM sweep transmit pulse technique. The increased bandwidth of the FM sweep tends to improve vertical resolution for determining microscale features in the stratigraphic record. A second objective of this field work was to characterize the seafloor in the vicinity of Line S at the 70 meter isobath. To accomplish this a survey grid was planned and run that covered approximately a 2.0 x 2.5 nautical mile area bordered by lines S and U and running between the 55 and 75 m isobaths. Figure 2 is another surficial sediment impedance map generated by the ASCS during this survey. As indicated in the caption some of the ASCS settings were incorrect during portions of this survey and will need to be re-processed. Sample acoustic imagery along lines 4, 6, and 7 are provided in Figure 3 which show a transition from coastal sands to a silty sand further offshore. This transition occurs approximately between the 55 and 60 meter contours along these tracks.

A further objective was to obtain correlative ASCS data over areas which have varying degrees of backscatter intensity as indicated on swath bathymetry/imagery charts provided by the University of New Brunswick, Canada. ASCS/FM sweep data was collected over several of the sites, in water depths less than 70 meters, by suspending the transducer in the water column while the ship occupied bottom sampling and in situ measurement stations. Specifically, this sweep data was obtained along the "S" line at 35, 40, 45, 50, 55, 60, and 70 meter depths and also at the 70 meter isobath on lines V, O, L, I, and C.

Prior to this field effort, a tank calibration of the ELAC narrow beam transducer was conducted at Stennis Space Center/Marine Fisheries Tank Facility. Various FM sweep wavelets were generated using the ASCS configured with both the new OMNI Tech power amplifier and an Instruments Inc. power amplifier. The transducer was deployed in an inverted ("upward looking") mode on the bottom of the test tank to achieve a theoretically near-perfect high impedance return from the water/air interface.

A candidate wavelet was selected to deconvolve the ASCS/FM sweep (1 - 50-kHz, 3 ms pulse) during the Eel River field work. A deconvolution scheme is required to both improve the real-time ASCP/FM sweep display during acquisition and enhance the sampling resolution. Although the deconvolution routine was written into the ASCS software just prior to the field trip, it was not utilized because it had not been tested during real-time data acquisition. However, as indicated above, ASCS/FM sweep data was obtained at selected locations in the Eel River Study Area. Data from the above sites are presently being analyzed by Warren Wood under the auspices the Mine Burial Processes Project.

Publications

Slowey, N.C., W.R. Bryant, and D.N. **Lambert**, 1996. Comparison of High-Resolution Seismic Profiles and the Geoacoustic Properties of Eckernfoerder Bay Sediments. Geo-Marine Letters, vol. 16, no. 3, pp. 240-248.

Stanic, S., M.D. Richardson, D.N. **Lambert**, K. Briggs, J.A. Hawkins, A. Anderson, E. Kennedy, and J.C. Cranford, 1996. Scattering and Attenuation of High-Frequency Acoustic Normal Incident Energy in Gassy Muds, Geo-Marine Letters, submitted.

Hawkins, J.A., M.E. Duncan, A.L. Anderson, A.P. Lyons, D.N. **Lambert**, and D.J. Walter, 1996. Spectral Ratios from Bubbly Sediment Acoustic Returns. Jour. of the Acous. Soc. of Amer., submitted.

Walter, D.J., D.N. **Lambert**, and D.C. Young, 1996. Mine Burial Prediction Using Acoustic Techniques in a Shallow-Water Carbonate Environment. Proceedings of The Technical Cooperative Program (TTCP), Subgroup G-Wide Symposium on Shallow Water UnderSea Warfare, Oct. 21-25, 1996, Halifax, Nova Scotia, Canada. Poster and Abstract.

Tooma, S., D. Lott, D.N. **Lambert**, J. Preston, G. Hearld, K. Murphy, R. Hurst, 1996. TTCP Sediment Classification Sea Trials Off Key west, FL., 1-16 February 1995. Proceedings of The Technical Cooperative Program (TTCP), Subgroup G-Wide Symposium on Shallow Water UnderSea Warfare, Oct. 21-25, 1996, Halifax, Nova Scotia, Canada.

Hurst, R.B., J.F.F. Pope, R.H. Poeckert, D.N. **Lambert**, 1996. A Small Seabed Penetrometer for Measuring Sediment Bearing Strength. Proceedings of The Technical Cooperative Program (TTCP), Subgroup G-Wide Symposium on Shallow Water UnderSea Warfare, Oct. 21-25, 1996, Halifax, Nova Scotia, Canada.

Walter DJ Lambert DN Young DC (1995) A 3-D acoustic View of the Seafloor Near Garden Key, Dry Tortugas FL. 1st SEPM Congress on Sedimentary Geology "Linked Earth Systems", St. Petersburg Beach FL.

Walter, D.J., D.N. **Lambert**, D.C. Young, P. Vogt, J. Halka, H. Herrmann, 1996. Acoustic Classification of Surficial Sediments at Seven Sites in the Chesapeake Bay. EOS,. AGU Spring Meeting, May 20-24, Baltimore, MD. Abstract and Poster.

Patents

Lambert, D.N., F.S. Carnaggio, and D.C. Young, 1996. Sediment Classification System, Patent Application and Invention Award, Navy Case No. 75,520. Patent Issued September 24, 1996, Patent Number 5,559,754.

Lambert, D.N.**,** J.C. Cranford, and M. Crowe, 1996. Data Acquisition System and Method, Patent Application and Invention Award, Navy Case No. 75,521. Patent issued. Patent Number 5,606,533.

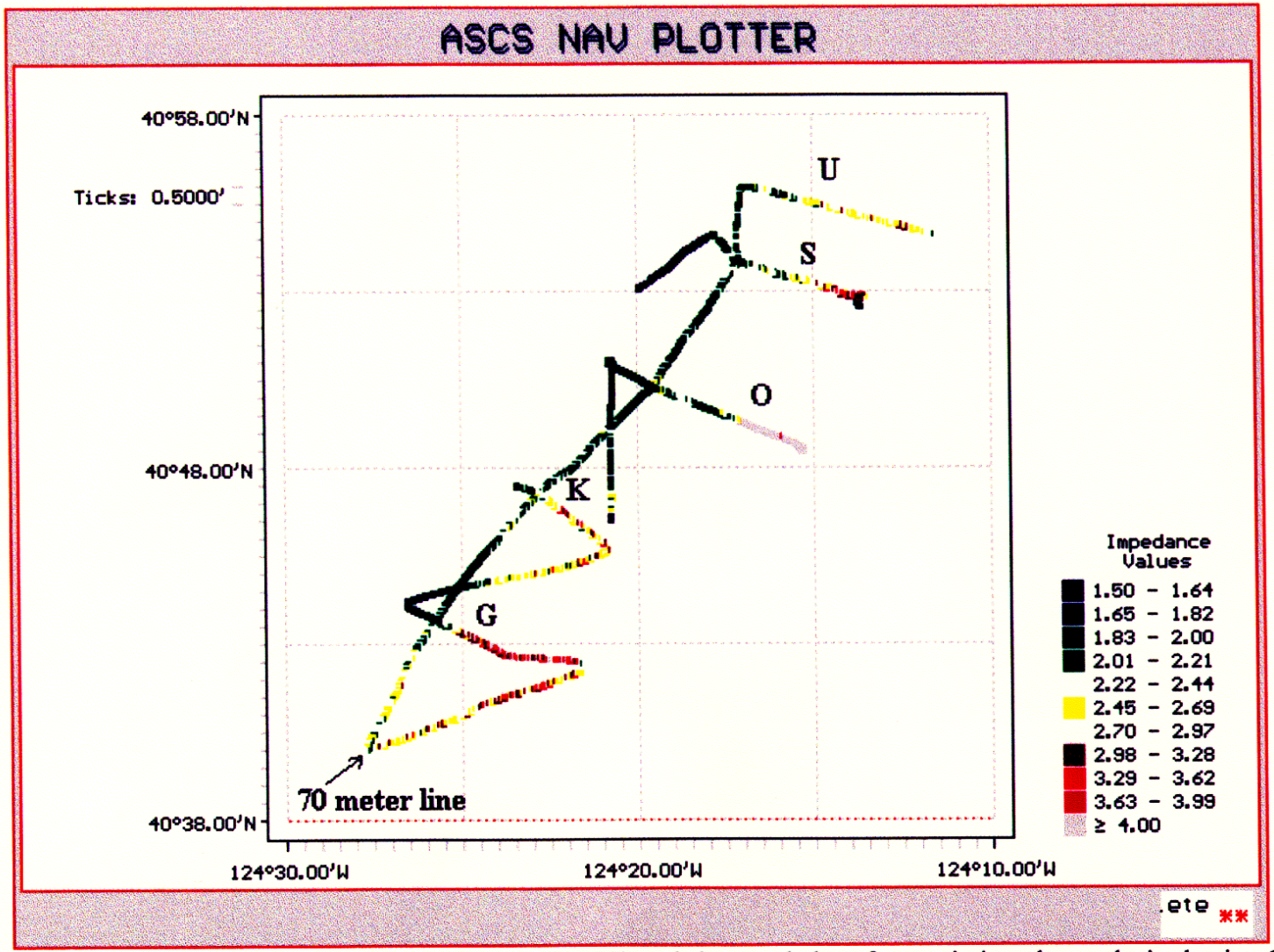

Figure 1. NRL/Acoustic Seafloor Classification System (ASCS) real time trackplot of acoustic impedance obtained using 15 kHz during Leg 1 of R/V WECOMA Cruise W9605B (Eel River). Grays are off scale and result from improper settings and should actually be in red color zone. Reds are coastal sands. Yellow and green colors indicate areas which transition from softer muddy sands to muds (or silts), respectively. Blues are indicative of very soft silts or muds.

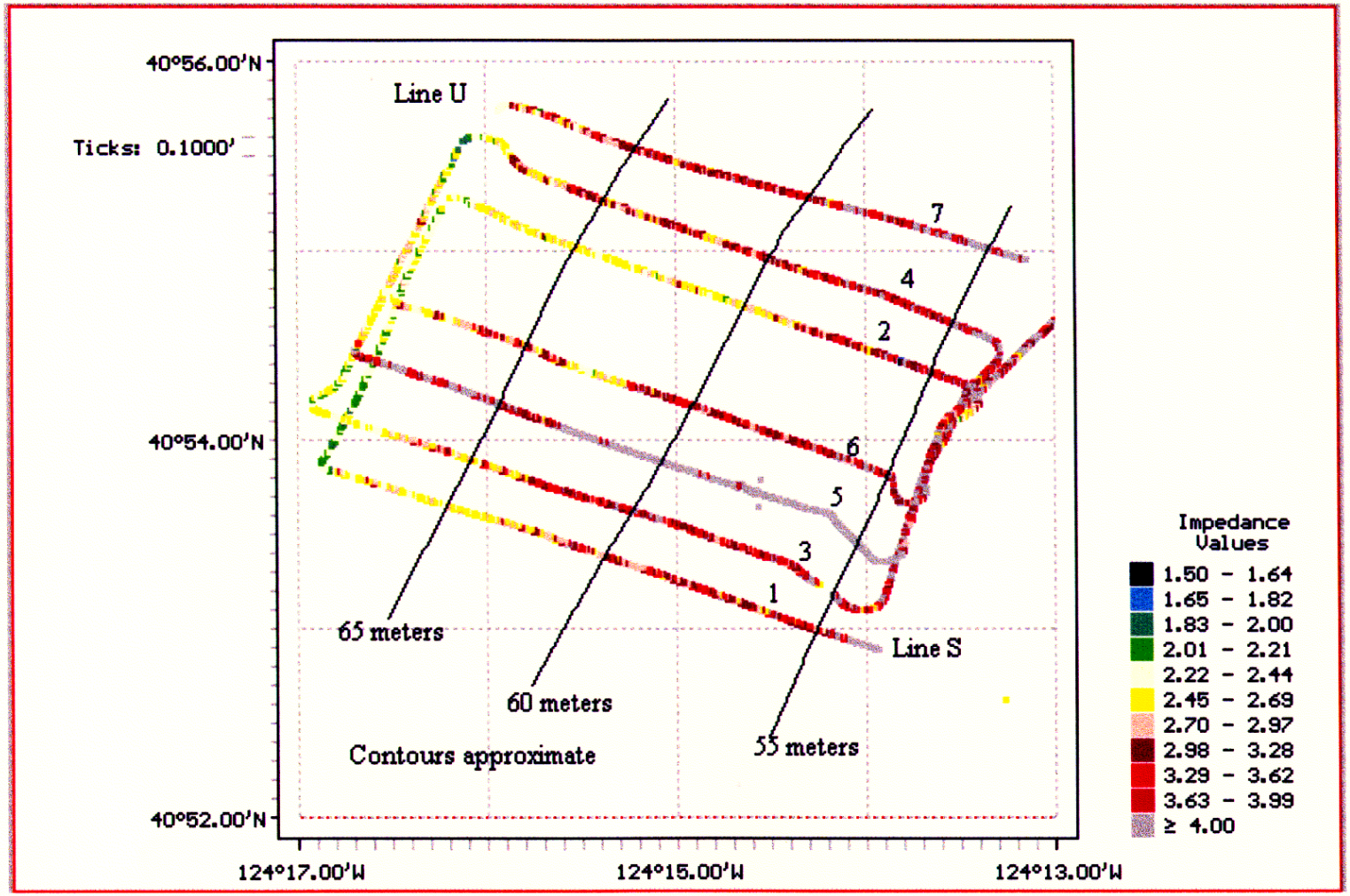

Figure 2. 30 kHz ASCS survey grid run between Lines S and U. Contours shown are approximate and transcribed from backscatter chart (not taken directly from acoustic data). Settings used to calculate the impedance during some of the runs (i. e lines 3 and 5) were incorrect. All of this data will be re-run, post cruise, to construct a map which more accurately represents the impedance of the upper 20 cm of the sediment column. Bottom transitions occur along tracks 4, 6, and 7. Images of these events are provided on the next page in Figure 3.

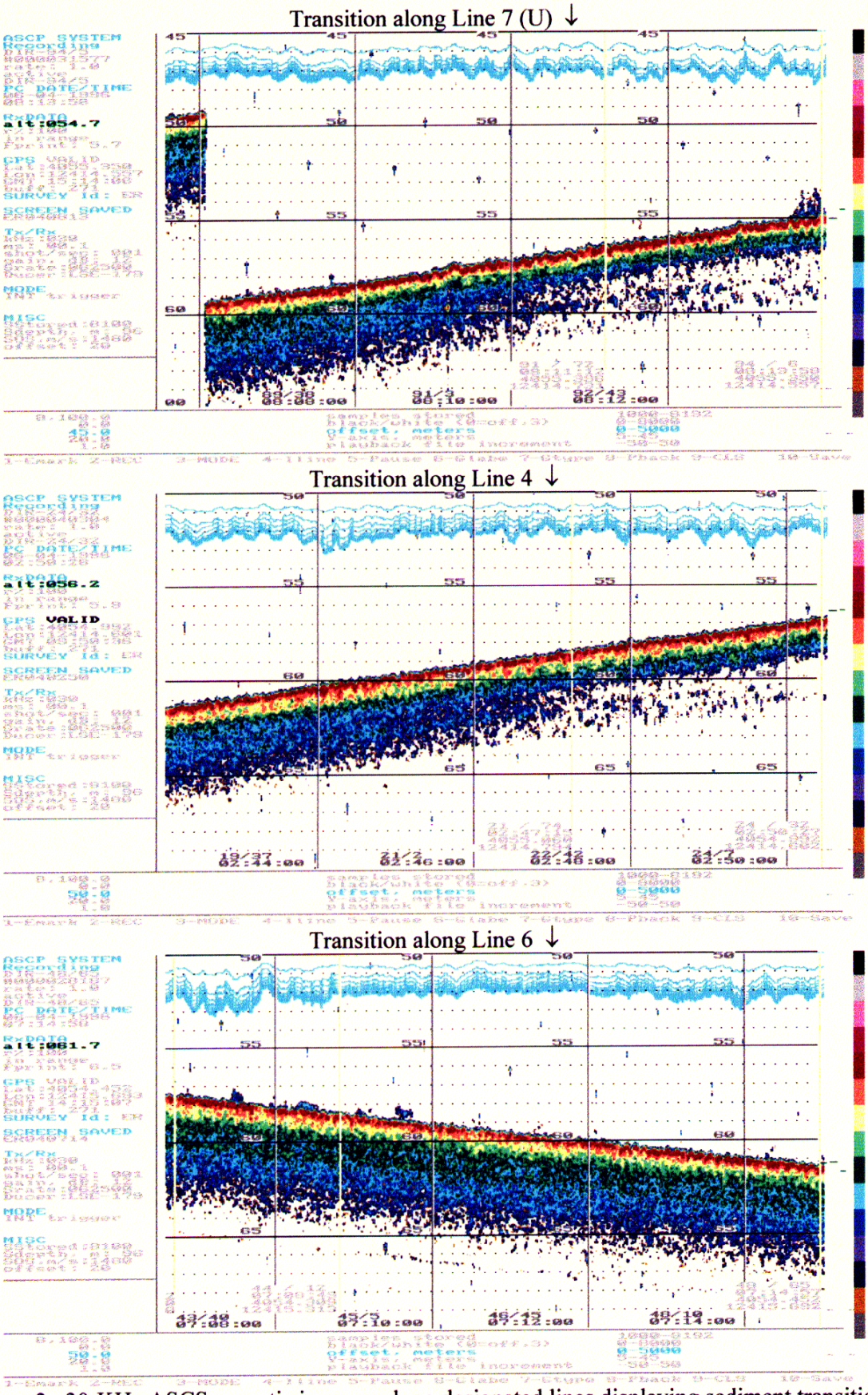

Figure 3. 30-KHz ASCS acoustic imagery along designated lines displaying sediment transitions.

2.12 Sediment Properties from Grain and Microfabric Measurement (Principal Investigators: D.M. Lavoie and Patti Jo Burkett)

SEDIMENT PROPERTIES FROM GRAIN AND MICROFABRIC MEASUREMENTS

Dennis M. Lavoie and Patti Jo Burkett

INTRODUCTION

The term microstructure encompasses both the physical arrangement of particulate constituents (the microfabric) and the physico-chemical forces among the constituents. The **overall hypothesis** of this study is that sediment microstructure provides the fundamental control on sediment macro-scale mechanical properties and behavior. A specific prediction of this hypothesis is that measurements derived from the study of microfabric can be related to bulk properties of sediment. Experimental support for this hypothesis would justify development of microfabric parameters for constitutive models of sediment structure and, subsequently, development of continuum models that deal with sediment macro-scale dynamic response to environmental processes and stresses.

The **scientific objective** of the project is to examine qualitative and quantitative descriptions of microfabric of selected sediments and relate them to the bulk physical properties of those sediments.

The **general approach** is to use current methods for the qualitative study microfabric and extend them to produce quantitative data in both 2D and 3D. Quantification will rely on computerized image analysis, stereology, and volume reconstruction techniques. The work will be done in close coordination with other CBBL investigators so that coincident samples are collected for both microfabric and physical properties measurements.

PROGRESS AND CURRENT STATUS

Focus of this year's work has been to support other CBBL data requirements (notably Dave Young and Ron Holyer/Nita Sandidge); to initiate cooperative work with Dr. Rajah Anandarajah of Johns Hopkins University on micromechanical modeling of siliciclastic microfabric; to complete publication of the previous year's work; and to develop the necessary techniques for serial sectioning of siliciclastic and carbonate sediment samples in order to produce 3-D reconstructions of sediment microfabric.

Accomplishments for FY96 include:

• Two peer-reviewed articles and one short technical article were published in FY96; one peer-reviewed article is still in review.

• Coordination of data analysis and micromechanical modeling was initiated with Rajah Anandarajah of JHU. Through the efforts of Dawn Lavoie, Dr. Anandarajah will work at NRL-SSC for a short time this coming summer, and one of his students will be here most of the summer.

• Image porosity analysis of Key West samples has been completed on gravity cores 72, 147, and 203, and x-ray cores 172, 191, and 197, and diver core 160-2. Image porosities of cores 147 and 203 were compared to Dawn Lavoie's analyses of physical properties. Core 72 was analyzed before and after consolidation tests conducted by Dawn Lavoie and compared with her data. Core 160-2 was analyzed at 0.5 cm intervals from 4 to 14 cm for comparison with Laura Pyrak-Nolte's (JHU) acoustic imaging analysis of the same section.

• Separate analyses of interparticle void space and interparticle porosity (the latter weighted by differential areas of *Halimeda* fragments and matrix) show that all the porosity measured by bulk techniques can be accounted for in an analysis of 2-D images. This finding validates the hypothesis that 2-D imagery can by used to make measurements of microfabric that can be related to bulk measurements and that may by used in micromechanical models of sediment behavior.

Plans for FY97. We are completing analysis of the Key West samples in preparation for a journal article. Coordination with Dr. Anandarajah has been transferred to Dr. Lavoie for the completion of the project, although we will still be providing imagery. Daunting technical problems have been encountered in producing serial sections of clay-dominated Eckernförde sediment for TEM analysis, and we have abandoned this approach for others, including imaging of pore spaces with confocal microscopy. In terms of Key West carbonate sediments, serial imaging using backscatter electron signal of SEM is more tractable problem, and we believe that 3-D reconstruction of this sediment is possible. We are also extending analyses of Key West sediments to include fraction distributions of *Halimeda* fragments and matrix with depth, grain contact frequencies and areas, and tortuosity of pore space.

CUMULATIVE PUBLICATIONS LIST

Journal Articles

_ Lavoie DM, Lavoie DL, Pittenger HA, and Bennett RH. Bulk sediment properties interpreted in light of qualitative and quantitative microfabric analysis. Geo-Marine Letters 16:226-231

_ Lavoie DM, Baerwald RJ, Hulbert MH, and Bennett RH. A drinking straw mini-corer for sediments. Journal of Sedimentary Research, Section A: Sedimentary petrology and Processes 66:

_ Bennett, R.H., M.H. Hulbert, M. Meyer, D. Lavoie, K.B. Briggs, D. Lavoie, R.J. Baerwald and W.-A. Chiou. Fundamental response of pore water pressure to microfabric and permeability characteristics: Eckernförde Bay. Geo-Marine Letters 16:182-188

Workshops

_ Bennett, R.H., M.M. Meyer, D.M. Lavoie, M.H. Hulbert, S. Stewart and E. Littman. 1994. Sediment pore pressure and permeability in Eckernförde Bay, Germany, (pps 65-69). In: Wever, T.F. (ed.), Proceedings of the Gassy Mud Workshop held at the FWG, Kiel, Germany, 11-12 July 1994. FWG Report 14.

_ Lavoie, D.L., D.M. Lavoie, A. Pittenger and R. Bennett. 1994. Microfabric predictors of sediment properties, (pps 70-75). In: Wever, T.F. (ed.), Proceedings of the Gassy Mud Workshop held at the FWG, Kiel, Germany, 11-12 July 1994. FWG Report 14.

_ Lavoie, D.L., D.M. Lavoie and Y. Furukawa. 1995. A comparison of sediment properties along the Schock line and at the NRL test site, Eckernförde Bay, Germany, (pps 58-64). In: Wever, T.F. (ed), Proceedings of Modelling Methane-Rich Sediments at Eckernförde Bay, held at Eckernf_rde, Germany, 26-30 June 1995.

Lavoie, D.M. 1997. Microfabric of Dry Tortugas and Marquesas carbonate sediments. Key West Workshop

Published Abstracts

_ Bennett, R.H., D. Lavoie, M. Meyer, E. Litman, and S. Stewart. 1994. Pore pressure field in Eckernförde Bay, Germany. EOS, 75(3):201.

_ Lavoie, Dennis, R.H. Bennett, W. Chiou, R.J. Baerwald, and M.H. Hulbert. 1994. Sediment microfabric of gassy sediments in Eckernförde Bay. EOS, 75(3):201.

_ Lavoie, D.L, M.D. Richardson, Lavoie D.M. and Y. Furukawa. 1996. Geoacoustic properties of Dry Tortugas carbonate sediments from a microfabric perspective. Mississippi Academy of Sciences, 22-23 February 1996, Jackson MS. 0601153N32 (ISSAMS)

2.13 Quantification of Biogeochemical Processes Controlling Early Diagenesis and Biogenic Gases in Marine Sediments (Principal Investigators: C.S. Martens and D.B. Albert)

CBBLSRP FY96 YEAR-END REPORT

Christopher S. Martens
Daniel B. Albert

Marine Sciences Curriculum
CB#3300 12-7 Venable Hall
University of North Carolina
Chapel Hill, NC 27599-3300

OVERVIEW OF RESEARCH EFFORTS DURING 1996

One of the primary goals of the Coastal Benthic Boundary Layer Special Research Program (CBBLSRP) is the production of comprehensive models of sedimentary biological, physical, and geochemical processes coupled to acoustic properties. This is an optimistic goal within the time-frame of the SRP, but one towards which considerable progress has been and can be made. During FY1996, almost all of our own effort has focused on numerical modeling of biogeochemical processes controlling dissolved gases and gas bubbles in organic-rich sediments in general, and in Eckernförde Bay sediments in particular. This work took a standard biogeochemical model (Berner, 1980) as its starting point, but to deal realistically with the issues involved in methane gas formation in sediments it was necessary to develop a coupled model of sulfate and methane depth distributions driven by realistically parameterized biogeochemical processes. The model we have now developed, with the indispensable aid of Marc Alperin, represents the new state-of-the-art for modeling dissolved and gaseous methane distributions. From this work two manuscripts have been prepared and submitted for the special issue of Continental Shelf Research that will be forthcoming on the Eckernförde Bay work. One of these manuscripts (Martens et al., 1997) presents the general model in detail with examples of its use in different environments, while the other (Albert et al., 1997) presents specific applications in Eckernförde Bay sediments with varying acoustic properties. This report will present some results from this effort.

Modeling of sulfate and methane concentrations in sediments

In coastal sediment it is quite common for organic carbon input to be high enough for some metabolizable carbon to survive burial through the sulfate reduction zone and thus fuel methanogenesis. Methane concentrations therefore rise in the methanogenic zone leading to a concentration gradient that drives a diffusive flux into the overlying sulfate reducing sediments where it is oxidized. Given enough metabolizable carbon within the methanogenic sediments, concentrations can rise to exceed methane solubility and thus form gas bubbles.

Bubbles of biogenic methane gas within the sediments of Eckernförde Bay lead to widespread "acoustic turbidity" in acoustic surveys of the Bay, masking the sedimentary structure below the gassy horizon. Acoustic windows, where the gas does not appear to be present, occur in several locations in the Bay, often surrounded by acoustically turbid sediments. Pockmarks, shallow depressions in the sediment, are also found in Bay sediments and may show acoustic turbidity at even shallower depths below the interface than surrounding sediments. To understand the origin of the methane distributions in these sediments, three sites in Eckernförde Bay were sampled in May 1994 to determine concentrations of methane, sulfate and chloride in the sediment porewaters.

The NRL site, chosen because it is representative of much of bay below the 20 m depth, revealed methane saturated conditions by about 75 cm depth below the interface confirming inferences from acoustic scattering data that gas was present in the sediment. Above this, the methane concentration profile was concave-upward, indicative of methane oxidation in the overlying sulfate-reducing sediments. These porewaters showed a slightly decreasing chlorinity with depth. At an acoustic window site, methane concentrations rose to a maximum at about 125 cm depth, but did not reach saturation. Below this depth they decreased in a concave-down pattern. Chloride profiles at this site showed a strong freshening with depth, indicative of vertical freshwater flow from below. The third site was a pockmark exhibiting very shallow acoustic turbidity at about 25 cm depth. Here methane concentrations rose to exceed saturation within 25 cm depth below the interface and the porewaters became almost fresh by 1.5 m depth, indicative of a stronger flow of freshwater from below.

These groundwater flows have competing effects on the methane inventory. They help exclude sulfate from the sediment, allowing the earlier/shallower onset of methanogenesis, but they also aid loss of methane through advection. Because of the complication of these competing effects it is impossible to quantify what will happen to the methane profiles without the use of a diagenetic model. The model we developed couples the biogeochemistry of sulfate and methane to explain the presence or absence of methane gas in these sediments in relation to the flow rate of fresh groundwater from below.

The model:

For sulfate (S) the steady-state diagenetic equation has a diffusive transport term for its input from the overlying seawater, an advective transport term to cover burial and the effect of the upward percolation of sulfate-free groundwater, and a reaction term to describe consumption of sulfate through bacterial sulfate reduction:

$$D_S \frac{d^2S}{dz^2} - \vartheta \frac{dS}{dz} - f_1 \left[\frac{1}{2} k_G G + k_M M_{diss} \right] = 0 ,$$

where D_S is the sediment diffusion coefficient for sulfate at the *in situ* temperature and salinity, ϑ is the sum of downward advection due to sedimentation and upward advection associated with groundwater flow (υ), k_M is the rate constant for methane oxidation and M_{diss} is the dissolved methane concentration. Sulfate reduction is represented by the term in brackets. Note that it has components for the oxidation of organic matter and dissolved methane. The coefficient (f_1) for the rate term is the error function (integrated Gaussian) which is used to simulate a smooth

transition from sulfate reduction to methane production when the sulfate concentration falls below a threshold value.

The steady-state diagenetic equation for methane concentrations (M) is similar, but contains both a production term proportional to the overall carbon degradation rate at any depth and a consumption term to represent anaerobic methane oxidation via sulfate reduction:

$$D_M \frac{d^2 M_{diss}}{dz^2} - \vartheta \frac{dM_{diss}}{dz} + f_2 f_3 \left[\frac{1}{2} k_G G\right] - f_1 \left[k_M M_{diss}\right] + f_3 \left[k_D M_{gas}\right] = 0$$

where D_M is the sediment diffusion coefficient for methane at in situ temperature and salinity, k_D is the rate constant for dissolution of methane gas, and M_{gas} is the concentration of gaseous methane. Methane is the product of organic matter decomposition only when sulfate concentrations are below a threshold value (S^*, Table 1) and dissolved methane is only produced when methane concentrations are below *in situ* solubility (M^*). This is controlled by the coefficients f_2 and f_3 on the first rate term which are error function toggles allowing the smooth transitions required for numerical stability of the model. The coefficient f_1 is the error function toggle that allows methane oxidation (via sulfate reduction) only when sulfate concentrations are above S^*.

Gaseous methane concentration is described by a steady-state diagenetic equation balancing sedimentation and methane production with gas bubble ebullition and dissolution:

$$-\omega \frac{dM_{gas}}{dz} + f_2 f_4 \left[\frac{1}{2} k_G G\right] - \left[k_B M_{gas}\right] - f_3 \left[k_D M_{gas}\right] = 0$$

where k_B is a rate constant for ebullition (i.e. ebullition is assumed to be a first order with respect to gas volume) and f_3 is the error function toggle that "turns on" gaseous methane production when dissolved methane concentrations exceed saturation (M^*).

The model results fit the dissolved sulfate and methane data for the NRL site very well (Figure 1.). The sulfate data is fit almost exactly. The upward concavity in the methane data due to methane oxidation and the peak concentrations between 1 and 1.5 m are also reproduced very closely. Methane gas bubbles are predicted between 80 and 120 cm by this run, with a peak gas concentration of only 0.3% by volume at 120 cm. A low percentage in gas volume was a targeted result because computer aided tomography (CAT) scans of cores retrieved and maintained under *in situ* pressure and temperature at this site have shown that this seems to be the condition present *in situ* (Abegg et al., 1995).

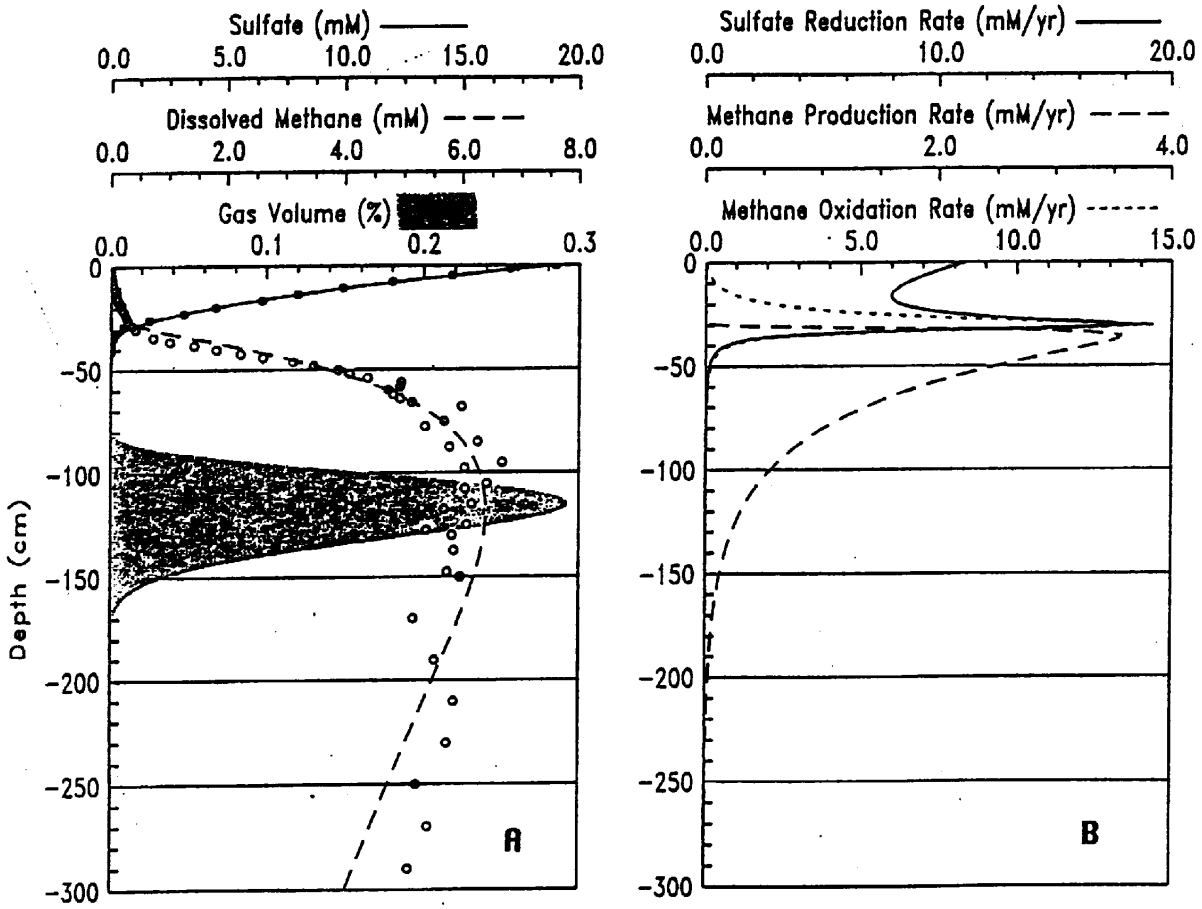

Figure 1. NRL Site model results compared to data

Figure 1. NRL Site model results compared to data

The same model parameters were also used to model the acoustic window site with the exception that the groundwater advection rate changed to 3.5 $cm \cdot y^{-1}$. The justification for holding all other parameters constant is that the acoustic window areas along the north side of Eckernförde Bay are not distinguished by topographic variation from the surrounding areas of methane saturated, acoustically turbid sediments (Fiedler and Stender, 1995; Lambert et al., 1995). It seems unlikely that they receive significantly different inputs of reactive organic carbon or have different bulk sedimentation rates. Model results for the acoustic window site are shown in Figure 2.

The increased advection of methane and sulfate-free groundwater from below the organic-rich, methanogenic sediments does indeed lead to a loss of methane-saturated conditions and hence the gassy layer. This disappearance of methane saturation is accomplished in spite of the fact that the sulfate depletion depth has moved upward from 32 cm to 25 cm increasing the depth-integrated methane production from 0.44 to 0.54 $mol \cdot m^{-2} \cdot y^{-1}$. Thus the advective loss of methane exceeds the higher production rate.

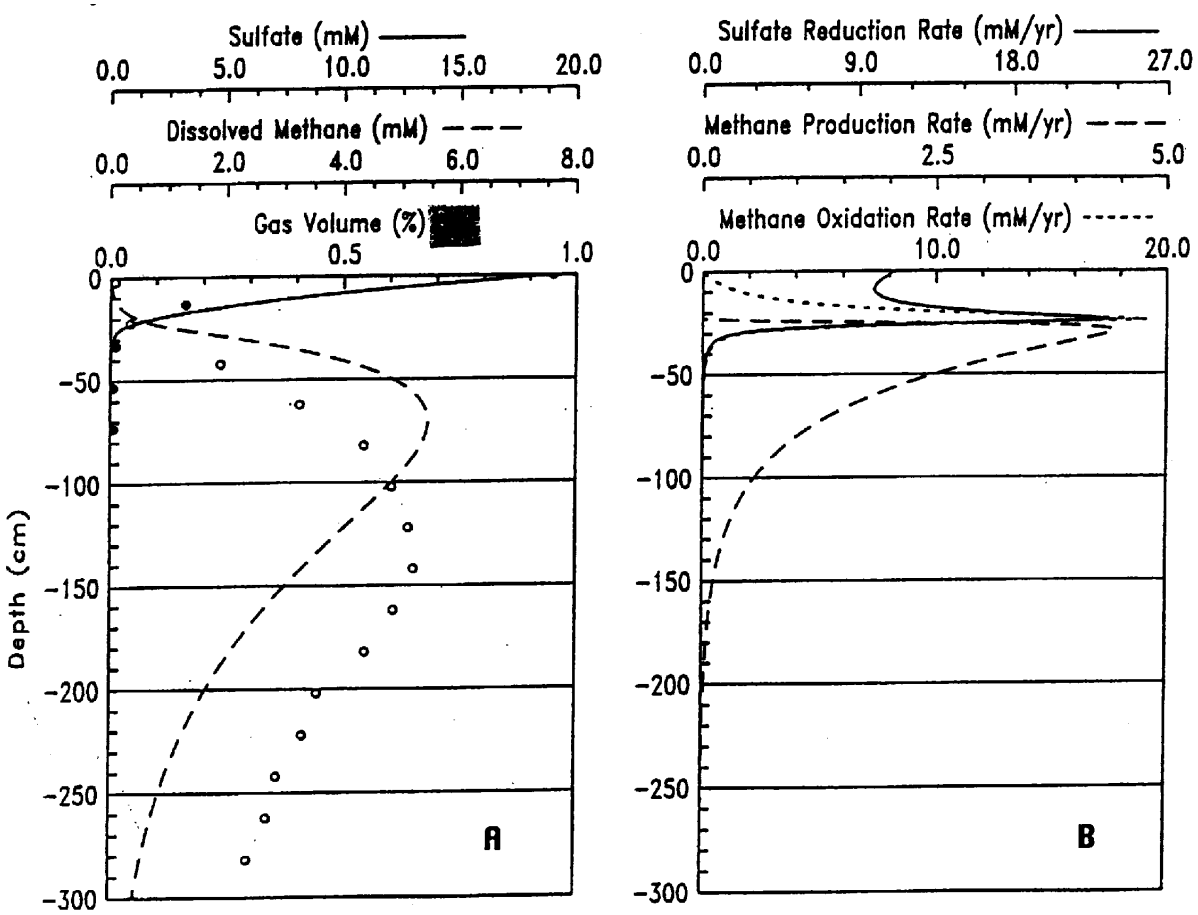

Figure 2. Acoustic Window Site model results compared to data

Figure 2. Acoustic Window Site model results compared to data

Using the same input parameters to model the pockmark site with only the advection rate changed to 10 $cm \cdot y^{-1}$ yields the profiles shown in Figure 3. Methane concentrations peak at about 4 mM at 40 cm and no gas is produced (saturation at the sediment water interface is 6.26 mM). Again it is apparent from the fit of the model methane profile to the actual data that there is more production of methane at depth in the sediments than the model predicts. This is very apparent at this site, as at the window because of the higher advection rates. The original hypothesis we wanted to test was whether the gradient in advective flow rates from 1 cm at the NRL site to 10 at the pockmark would lead first to undersaturation, as in the window case, and then resaturation at the pockmark due to greater sulfate exclusion from the sediments and hence higher methane production. It proves easy to move from the gassy NRL site model to an acoustic window, but it is not possible to return to methane saturated conditions by simply further increasing the flow rate. The advective loss of methane cannot be made up for by the increased production. With the 10 $cm \cdot y^{-1}$ flow rate sulfate is depleted by 18 cm depth and 58 percent of organic carbon remineralization is through methanogenesis, but it occurs too near the sediment surface to be retained in the sediment methane inventory long enough to reach saturation.

Unlike the acoustic window areas, the pockmarks, as the name implies, are actual topographic depressions of about 1 meter vertical scale. This makes it likely that the pockmark site experiences enhanced accumulation of fine-grained sediment and, hence, a higher reactive organic carbon flux (F_G). Pockmarks might act as traps for suspended sediment carried in near-bottom currents. Increasing the reactive organic carbon input (F_G) to the model by about 50% results in the production of some methane gas bubbles. Doubling (F_G) results in a gassy layer between 25 and 65 cm with up to 8.5% gas (Figure 4). CAT scans of pressurized cores from this pockmark have revealed gas concentrations that exceed 5% (Abegg et al., 1995).

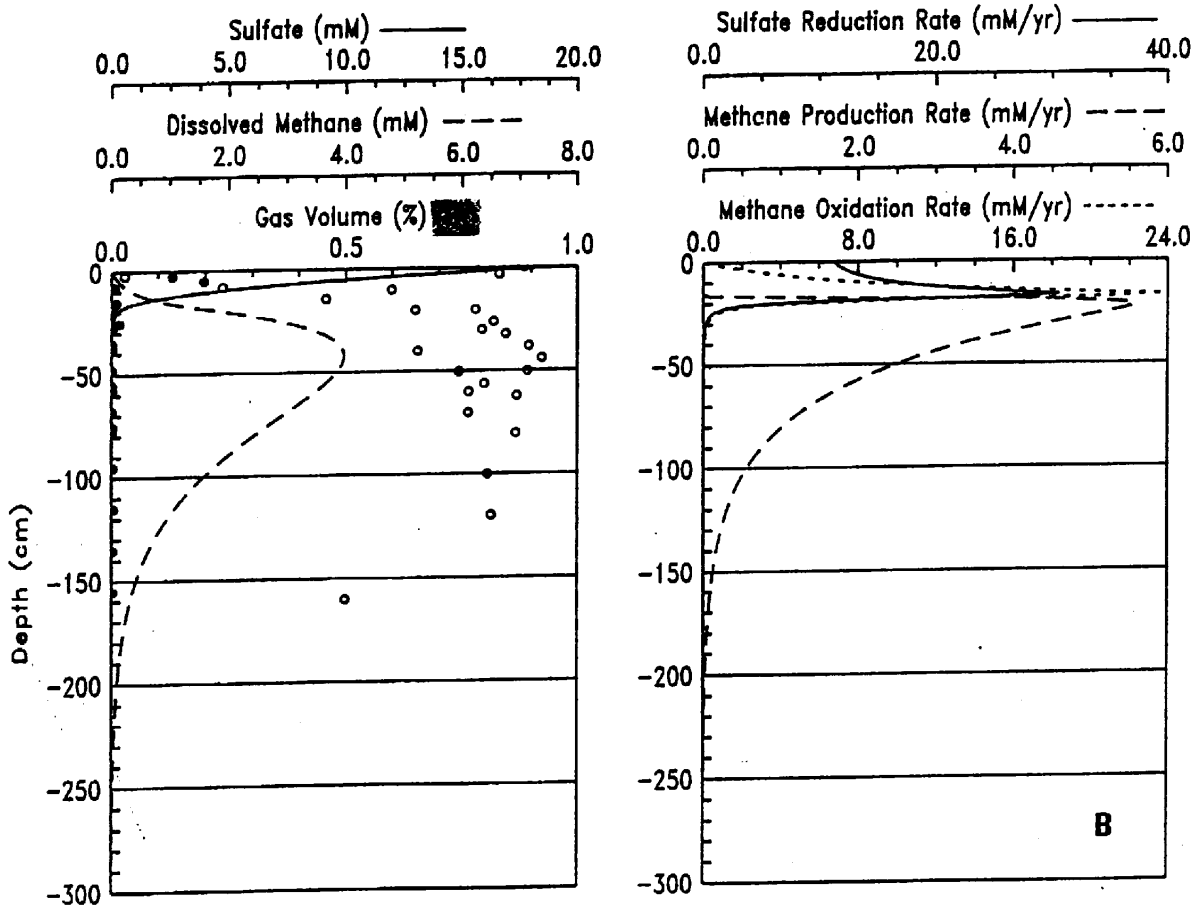

Figure 3. Pockmark Site model results compared to data

igure 3. Pockmark Site model results compared to data

The rapid transitions from acoustically turbid conditions to acoustic windows and back again that occur along transects throughout Eckernförde Bay are likely due to minor variations in the flow rate of fresh groundwater through the organic-rich Holocene sediments. The observed freshening of porewater with depth at the acoustic window site sampled in this study is indicative

of a vertical advection rate of about 3.5 $cm \cdot y^{-1}$. It would be impossible to quantitatively predict the net effect of such flows without modeling because there are competing processes at work. This advection constantly carries away some of the methane produced, but it also helps exclude sulfate from the sediment, thus allowing earlier (shallower) onset of methanogenesis. A coupled model

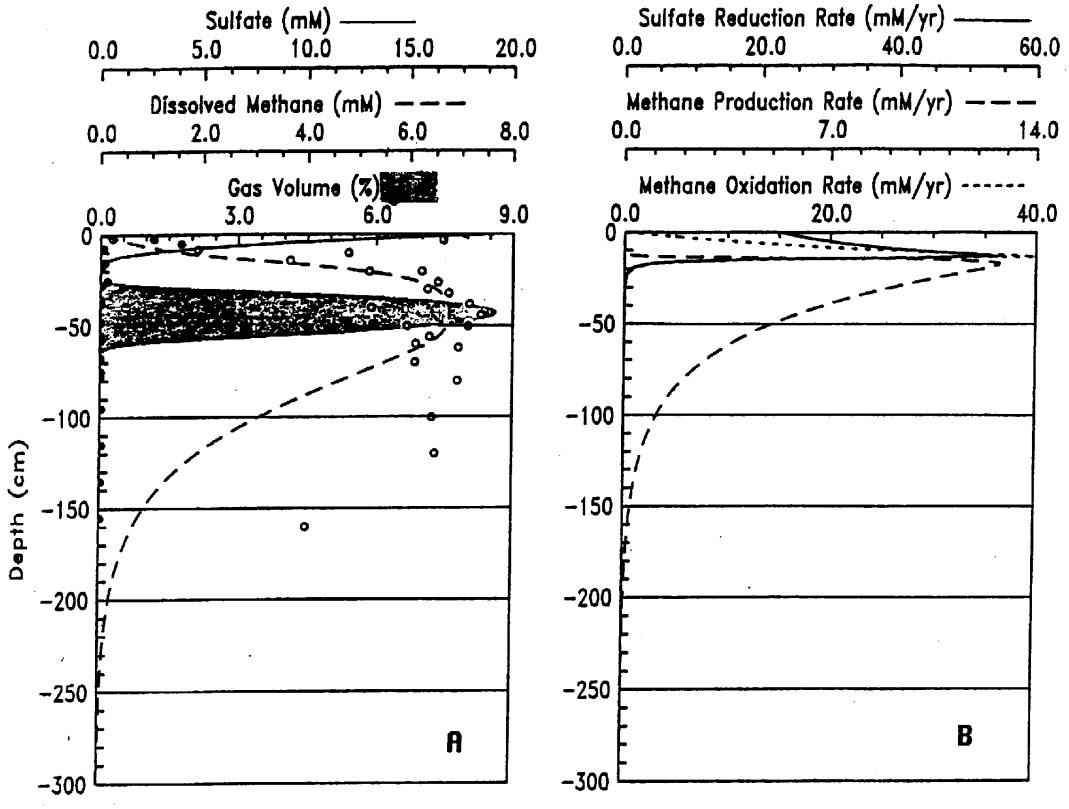

Figure 4. Pockmark Site model results (with increased carbon input) compared to data

Figure 4. Pockmark Site model results (with increased carbon input) compared to data

of the type used here allows us to say with confidence that the window areas can indeed be produced by merely varying the flow rate through the sediment. Thus part of our original hypothesis is correct. We cannot, however, mimic the production of a gassy pockmark by merely increasing the flow rate more. The model results imply that additional carbon input is required to achieve the levels of gas production necessary. Hopefully, additional work in Eckernförde Bay will allow us to further refine the model and accurately determine input parameters to test these ideas.

Manuscripts and Presentations: 1996-97

Martens, C. S., D. B. Albert and M. J. Alperin. 1997. Biogeochemical processes controlling methane in gassy coastal sediments 1. A model for predicting the distribution of gaseous methane. Submitted to Continental Shelf Research.

Albert, D. B., C. S. Martens and M. J. Alperin. 1997. Biogeochemical processes controlling methane in gassy coastal sediments 2. Groundwater flow control of acoustic turbidity in Eckernförde Bay sediments. Submitted to Continental Shelf Research.

Alperin, M. J., C. S. Martens and D. B. Albert. 1997. Biogeochemical processes controlling methane in gassy coastal sediments: A model for predicting the distribution of gaseous methane. Abstracts. American Society of Limnology and Oceanography Aquatic Sciences Meeting, Santa Fe, NM Feb.10-14, 1997 p. 82.

Albert, D. B., C. S. Martens and M. J. Alperin. 1997. Groundwater flow control over methane-induced acoustic turbidity in Eckernförde Bay sediments. Abstracts. American Society of Limnology and Oceanography Aquatic Sciences Meeting, Santa Fe, NM Feb.10-14, 1997 p. 80.

Work to be completed in 1997

We have an exceptional set of methane and carbon dioxide stable carbon and hydrogen isotope data as well as radiotracer methane oxidation and sulfate reduction rates from Eckernförde Bay in 1994. During the remainder of this year we will be interpreting, modeling and preparing manuscripts from this dataset. We anticipate two more manuscripts from our work there.

References Cited

Abegg F. and A. L. Anderson (in press 1996) The acoustic layer in muddy sediments of Eckernfoerde Bay, Western Baltic: methane concentration, saturation and bubble characteristics. (Unpublished draft of accepted manuscript, *Marine Geology*)

Berner, R.A. (1980) *Early Diagenesis*. Princeton University Press. Princeton, NJ

Fiedler, H., and I. H. Stender. (1995) The acoustic turbidity horizon in Eckernförde Bay sediments - an update. in *Proceedings of the Workshop Modeling Methane-Rich Sediments of Eckernförde Bay, Eckernförde, 26-30 June, 1995.* T. F. Wever (ed.) Forschungsanstalt der Bundeswehr für Wasserschall- und Geophysik.

Lambert, D. N., D. J. Walter and J. A. Hawkins. (1995) Delineation of shallow, subbottom gas concentrations using a narrow beam, high frequency acoustic system. in *Proceedings of the Workshop Modeling Methane-Rich Sediments of Eckernförde Bay, Eckernförde, 26-30 June,*

1995. T. F. Wever (ed.) Forschungsanstalt der Bundeswehr für Wasserschall- und Geophysik.

2.14 Physical and Biological Mechanisms Influencing the Development and Evolution of Sedimentary Structure (Principal Investigators: C.A. Nittrouer and G. R. Lopez)

Physical and Biological Mechanisms Influencing the Development and Evolution of Sedimentary Structure

Charles A. Nittrouer
Glenn R. Lopez

Marine Sciences Research Center
State University of New York
Stony Brook, NY 11794-5000

INTRODUCTION

Research completed during this year included: production of final papers regarding Eckernförde Bay, and continued laboratory analysis of Key West samples and data. Two new papers were submitted for publication, covering sedimentology/radiochemistry (Bentley and Nittrouer, in press b) and benthic biology of Eckernförde Bay (D'Andrea and Lopez, in press b). In addition, a summary paper (Nittrouer et al., in press) was produced, integrating our studies with the physical oceanography and sediment transport studies of the VIMS group. For the Key West study areas, analytical work was the focus of our efforts, although two papers were generated for the *Geo-Marine Letters* special issue (Bentley and Nittrouer, in press a; D'Andrea and Lopez, in press a).

SEDIMENTOLOGY AND RADIOCHEMISTRY

This report presents recent results from modeling of strata formation in Eckernförde Bay, and an initial interpretation of the Dry Tortugas study area.

Eckernförde Bay

Sedimentological and radiochemical investigations of sediments in Eckernförde Bay were coordinated with observations of benthic biology and benthic-boundary-layer dynamics to identify processes influencing the formation of preserved sedimentary fabric. The bay is a trap for fine sediments because of its fjord-like basin geometry and hydrodynamic regime (Friedrichs and Wright, 1995). Sediments are derived from both local sources (eroded and transported by winter storms) and sources in adjacent Kiel Bight (fair-weather transport of suspended sediment by internal waves) (Milkert, 1994). In the central basin of the bay, strata consist of pelletized, clay-rich beds and silty laminations (Fig. 1), and reflect the interaction of bioturbation with alternating fair-weather and storm-associated sediment transport and deposition (Fig. 2).

Sediment-accumulation rates in the central basin of the bay are ~0.44 cm/yr (from ^{210}Pb geochronology). Results from a numerical model, as well as study of x-radiographs and accumulation rates, indicate that fair-weather processes contribute about half of the time-

averaged sediment accumulation, and the remaining half is contributed by storm-generated deposition.

A pioneer benthic community of juvenile deposit-feeding polychaetes and bivalves is maintained by seasonal oxygen depletion (D'Andrea et al., 1996). Excess ^{234}Th analyses indicate that bioturbation is restricted to the upper 1 cm of the seabed. Macrofaunal feeding activity produces abundant ovoid fecal pellets (200-500 μm long), creating pervasive biogenic microfabric in beds deposited under fair-weather conditions. In contrast, primary depositional fabric is preserved as laminations when storm deposits thicker than the depth of bioturbation overwhelm the macrofauna and disrupt bioturbation (Fig. 2).

Florida Keys

Sedimentological studies were undertaken in the Dry Tortugas to examine biological and physical influences on the formation of sedimentary fabric. ^{234}Th, ^{210}Pb, grain-size, porosity, and fabric analyses reveal the presence of a soft, fine-grained, well mixed surface layer underlain by compact, shelly, intensely bioturbated carbonate muds (Fig. 3). Vertical zonation of biogenic structures indicates that sediment mixing deep in the seabed is advective and results in transport of fine material to the seabed surface. Potential for preservation of this layering in the rock record is low, however, due to differences in rates.

Vertical partitioning of the benthic community (see next section) into a surface community (characterized by diffusional mixing) and a deep community (characterized by advective mixing) results in tiering of two distinctive dominantly biogenic sedimentary fabrics. Preservation potential is poor for the thin, high-porosity surface layer, but high for the deep, anisotropic fabric produced by the *Callianassa/Notomastus* community. Model results indicate that only the most extreme sediment-transport events (e.g., hurricanes) are capable of overwhelming this intense mixing and imparting physical stratification to preserved sedimentary fabric.

BENTHIC BIOLOGY

This report presents the most recent results from modeling fecal-pellet production, breakdown, and transport in Eckernförde Bay, Germany, and a summary of our faunal analyses of the Florida Keys samples to date.

Eckernförde Bay

Benthic studies of functional group composition and particle mixing rates were conducted in 1993, and augmented by repeated sampling in 1994 and the addition of a shallow transect to investigate fecal-pellet dynamics in Eckernförde Bay. The functional group composition and particle mixing rates were published this year (D'Andrea et al. 1996), and have been presented in previous reports. This report will emphasize the recent modeling of fecal-pellet dynamics.

The primary fecal-pellet producers identified in this system were the tellinid bivalve *Abra alba*, capitellid polychaetes (*Capitella* sp. and *Heteromastus filiformis*), and tubificid oligochaetes. Fecal-pellet abundances increased significantly with depth, and the greatest abundances are

found at the base of the margin slope. Pellet size was significantly greater at depths greater than 20 m than along the shallower flanks of the bay. However, high abundances of fecal pellet producers were found at the shallowest transect stations.

We hypothesized that pellets would be transported from the shallower portion of Eckernförde Bay toward the base of the slope, with pellet dynamics in the central basin controlled by the annual resident pellet-producer populations. The major factors controlling the amount of fecal pellets in surface sediments include pellet production, destruction, and deposition or erosion (Kraeuter, 1976; Levinton and Lopez, 1977; Risk and Moffat, 1977; Jumars et al., 1981). In systems lacking strong physical conditions, the rate of fecal-pellet formation relative to the rate of disintegration determines the steady-state availability of particles. We developed a simple model of pellet formation and breakdown to test our hypothesis. Our model takes into account daily pellet egestion rate and population densities of pellet producers, time, and pellet breakdown.

Figure 4 illustrates a five-year simulation of steady-state pellet production for three important transition depths: the shallowest transect station (14 m), the base of the margin slope (25 m), and the central basin (26 m). The pellet-producer community at the 14-m station is capable of producing two orders of magnitude greater number of fecal pellets than observed (Fig. 4A). At the base of the margin slope, the measured pellet abundances are two orders of magnitude greater than the resident benthic community could produce (Fig. 4B). The steady-state pellet production and measured pellet abundances are almost identical in the central basin (Fig 4C). Figure 5 shows the transition in pellet production from the shallow flanks to the central basin. Pellets at 14 m depth are primarily transported towards deeper water. This transport signal is noted as shallow as 17 m (Fig. 5B). The disparity increases with depth to the base of the margin slope (25 m). This seems to be the maximum depth of pellet transport. Modeled and measured pellet abundances were the same in the central basin.

The distribution of fecal pellets follows the pattern of sediment transport and tempestite deposition in Eckernförde Bay, and supports the hypothesis that the central basin is a sink for fine particles. Our results also support models of storm sediment transport (Milkert 1994, Milkert et al. 1995) and organism-sediment interaction (Jumars et al. 1981). In addition, this study indicates that the spatial distribution of robust fecal pellets may be a good biogenic indicator of sedimentary processes in shallow coastal systems.

Florida Keys

Benthic faunal samples were collected in three study areas of the lower Florida Keys for macrofauna abundance, functional-group composition, and bioturbation potential. The study areas included the Dry Tortugas, Marquesas, and stations between them. This report presents results from the Dry Tortugas and surrounding stations.

The benthic assemblage in the Dry Tortugas can be divided into two parts. The first is primarily a surface deposit feeding community dominated by the spionid polychaete *Prionospio cristata* and the oweniid polychaete *Myriochele oculata* (Table 1A). This community, dominated by surface deposit feeders and suspension feeders, is capable of mixing the top 1-4 cm of the

sediment on short time scales (days to weeks) based on functional group and animal size. The second community is a deep-dwelling community dominated by large (>6 cm) *Notomastus* and *Callianassa* sp., a deep burrowing thallasinid shrimp (Table 2A). This deep community is dominated by carnivores/scavengers, deep deposit feeders, and head-down deposit feeders (Fig. 6B).

The benthic community at the intermediate stations has similar fauna to the Dry Tortugas community, but the animals tended to be much smaller (<1 cm). The surface community was dominated by *M. oculata*, a surface deposit feeding polychaete (Table 1B) and abundances were an order of magnitude less than the Dry Tortugas (Fig 6A). Surface deposit feeders in the surface community were less important at the intermediate stations, and suspension feeders, shallow deposit feeders, and carnivores/scavengers were proportionally more important (Fig 3B). The deeper community at the intermediate stations were dominated by a small (<2 cm) sipunculan and capitellid polychaetes (Table 2B). The functional groups of the deep community at the intermediate stations were more evenly distributed in comparison to the Dry Tortugas with a noticeable absence of the large, deep deposit feeders common at depth in the Dry Tortugas.

The benthic assemblage at the Dry Tortugas includes a surface deposit-feeding community capable of mixing the top 2-4 cm on short time scales (days to weeks), and a deep community which can intensely bioturbate the deeper sediment layers. Both *Notomastus* and *Callianassa* have great potential for biogenic alterations of the deep layer. Fossil evidence indicates that this association may be geologically important. Benthic-boundary-layer processes suggest biological control of sediment structure in fair-weather conditions, and rapid removal of physical structure developed by storms. In contrast, the benthic community at the stations intermediate between the Dry Tortugas and Marquesas consists of a shallow (<10 cm) deposit-feeding community and should be important for shallow sediment structure on short time scales. However, the community may be dominated by physical processes, particularly during storm conditions, due to low abundances and small animal sizes at these stations.

REFERENCES

Generated by this grant

Bentley, S.J. and C.A. Nittrouer (in press a) Biogenic influences on the formation of sedimentary fabric in a fine-grained carbonate-shelf environment: Dry Tortugas, Florida Keys. *Geo-Marine Letters.*

Bentley, S.J. and C.A. Nittrouer (in press b) Physical and biological influences on the formation of sedimentary fabric in a fjord-like depositional environment; Eckernförde Bay, southwestern Baltic Sea. *Palaios.*

Bentley, S.J., C.A. Nittrouer and C.K. Sommerfield (1996) Development of sedimentary strata in Eckernförde Bay, southwestern Baltic Sea. *Geo-Marine Letters*, 16, 148-154.

D'Andrea, A.F. and G.R. Lopez, (in press a) Benthic macrofauna in a shallow water carbonate sediment: Major bioturbators at the Dry Tortugas. *Geo-Marine Letters*.

D'Andrea, A.F. and G.R. Lopez, (in press b) Deposit feeder fecal pellets as tracers of sedimentary movement in Eckernförde Bay, Germany. *Journal of Marine Research*.

D'Andrea, A.F., N.I. Craig and G.R. Lopez (1996) Benthic macrofauna and bioturbation in Eckernförde Bay, southwestern Baltic Sea. *Geo-Marine Letters*, 16, 155-159.

Nittrouer, C.A., G.R. Lopez, L.D. Wright, S.J. Bentley, A.F. D'Andrea and C.T. Friedrichs (in press) Oceanic processes and the preservation of sedimentary structure in Eckernförde Bay, Baltic Sea. *Continental Shelf Research*.

General

Friedrichs, C.T. and L.D. Wright (1995) Resonant internal waves and their role in transport and accumulation of fine sediment in Eckernförde Bay, Baltic Sea. *Continental Shelf Research*, 15, 1697-1721.

Jumars, P.A., A.R.M. Nowell, and R.F.L. Self (1981) A simple model of flow-sediment-organism interaction. *Marine Geology*, 42, 155-172.

Kraeuter, J.N. (1976) Biodeposition by salt-marsh invertebrates. *Marine Biology*, 35, 215-233.

Levinton, J.S. and G.R. Lopez (1977) A model of renewable resources and limitation of deposit-feeding benthic populations. *Oecologia*, 31, 177-190.

Milkert, D. (1994) Auswirkungen von Stürmen auf Schlicksedimente der westlichen Ostsee. Berichte-Report Geologisch-Paläontologisches Institut Universitat-Kiel 66, 153 pp

Milkert, D., U. Hentschke, F. Werner (1995) Influence of storms on sediments in Eckernförde Bay. *In* Proceedings of the Workshop Modeling Methane-Rich Sediments of Eckernförde Bay, T.F. Wever (ed.), FWG, Kiel, FWG-Report 22, 149-158.

Risk, M.J. and J.S. Moffat (1977) Sedimentological significance of fecal pellets of *Macoma balthica* in the Minas Basin, Bay of Fundy. Journal of Sedimentary Petrology, *47*, 1425-1436.

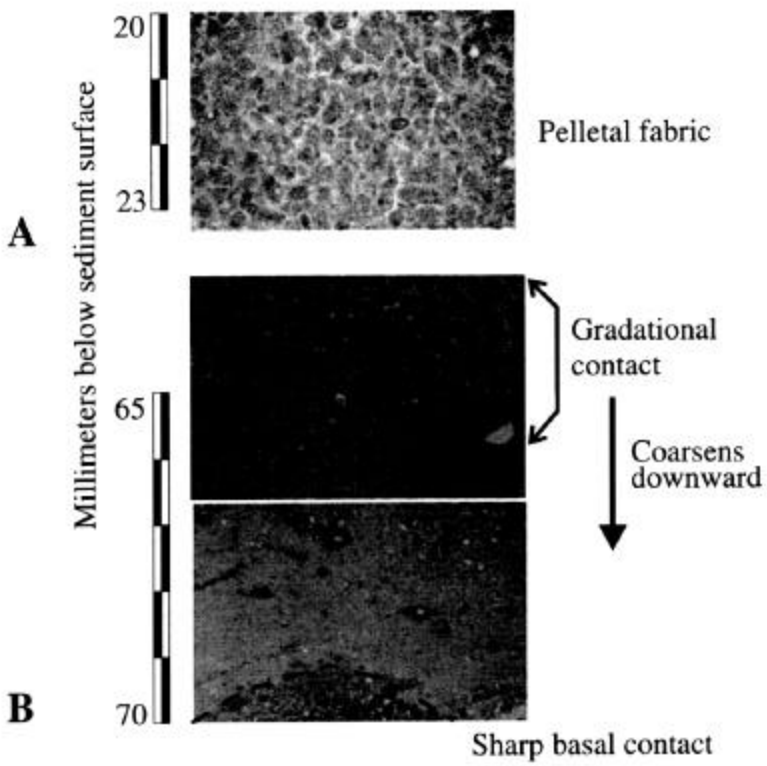

Figure 1 - Photomicrographs from deep basin in Eckernfoerde Bay (field of view is 5.0 mm wide, and all images are to same scale). A) 2.0-2.3 cm depth, plane light: pelletal microfabric characteristic of thick beds visible in x-radiographs; fecal pellets produced by the *Abra/Capitella* community of D'Andrea and Lopez (in press b). B) 6.3-7.0 cm depth, polarizers crossed 45°: upper and lower contacts of storm-deposited lamination. The upper contact is gradational between pelletal and underlying non-pelletal fabric. The basal contact (between the lamination and underlying pelletized sediment) is sharp. Fine-scale stratification is evident in the lower portion of the lamination.

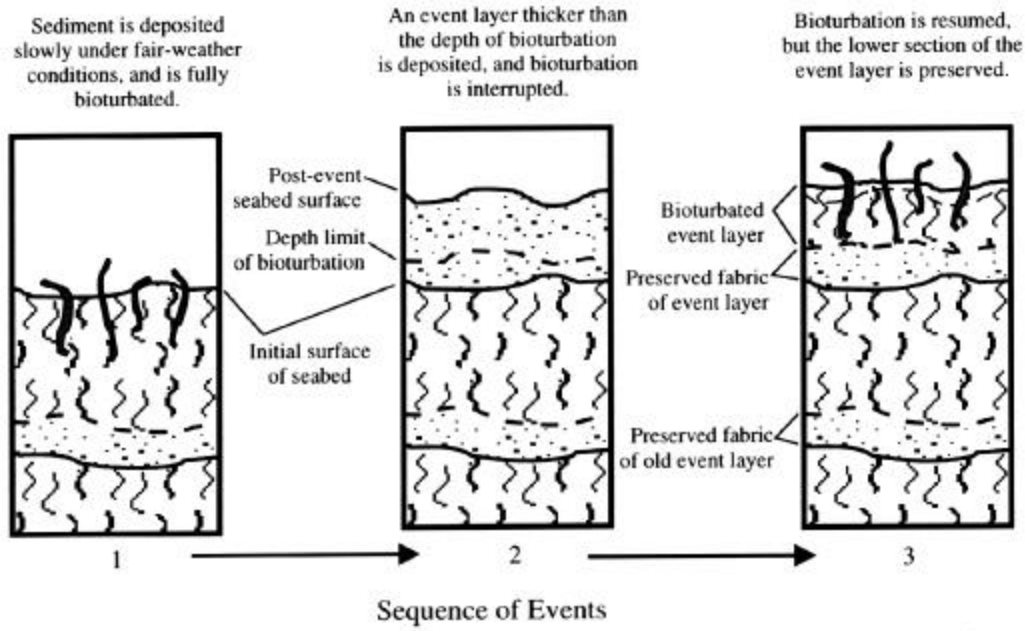

Figure 2 - Relationships between event-layer thickness and bioturbation depth, and resulting preservation potential for lower portions of the event layer. This is a graphic illustration of the approach to event-layer bioturbation used in constructing our model for Eckernfoerde Bay.

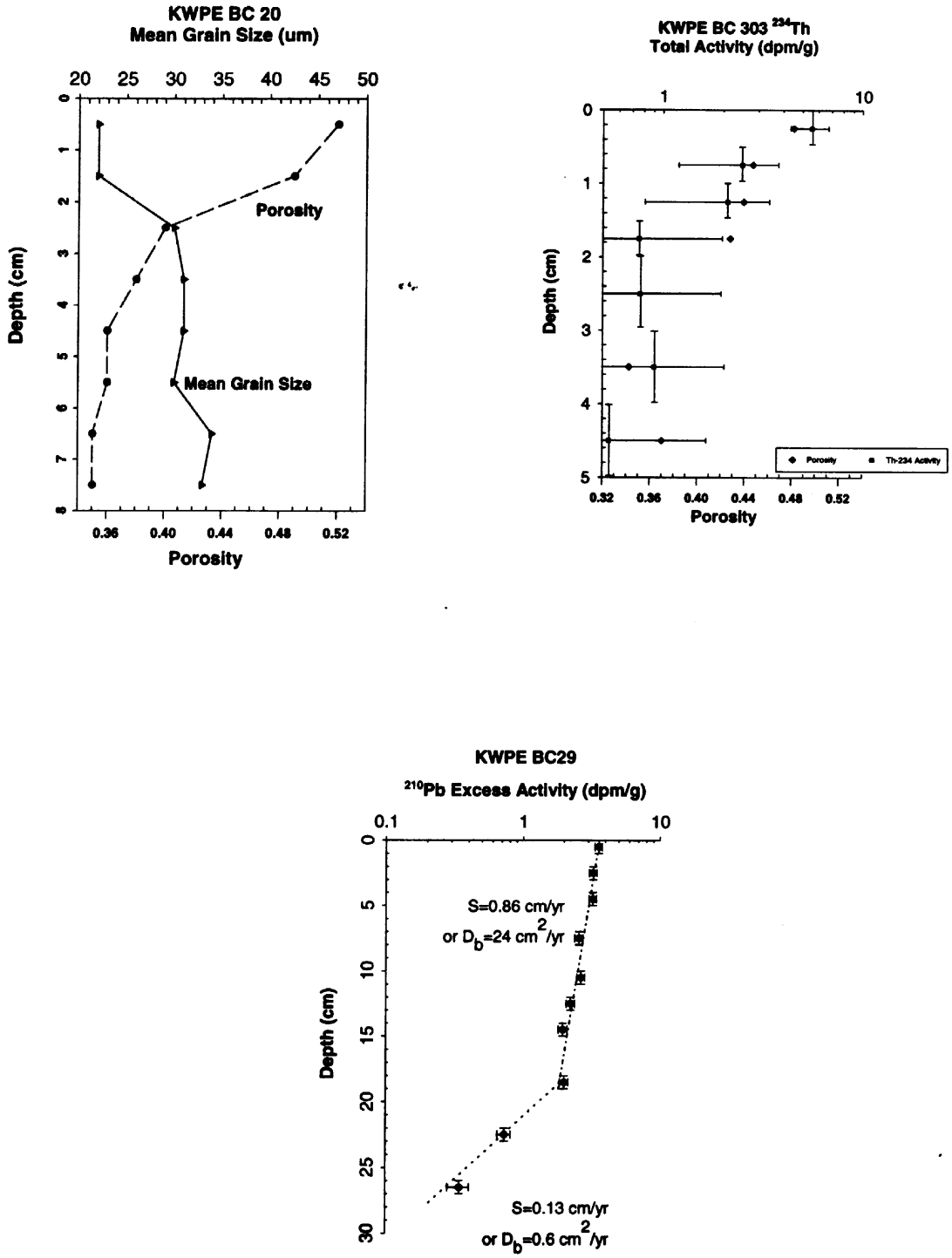

Figure 3 - A) Profiles of mean grain size and porosity for the Tortuga study area, close to the tetrapod site. Low porosity and finer grain size delineate the surface layer. B) ^{234}Th activity and porosity profiles for the same area. Excess activity is restricted to the upper 2 cm, and the activity gradient is tracked by the porosity trend. C) ^{210}Pb profile showing end-member estimates for accumulation rate (S) and mixing coefficient (D_b) along two distinct gradients in the profile. Calculations for S assume negligible mixing effects, and calculations for D_b assume insignificant accumulation.

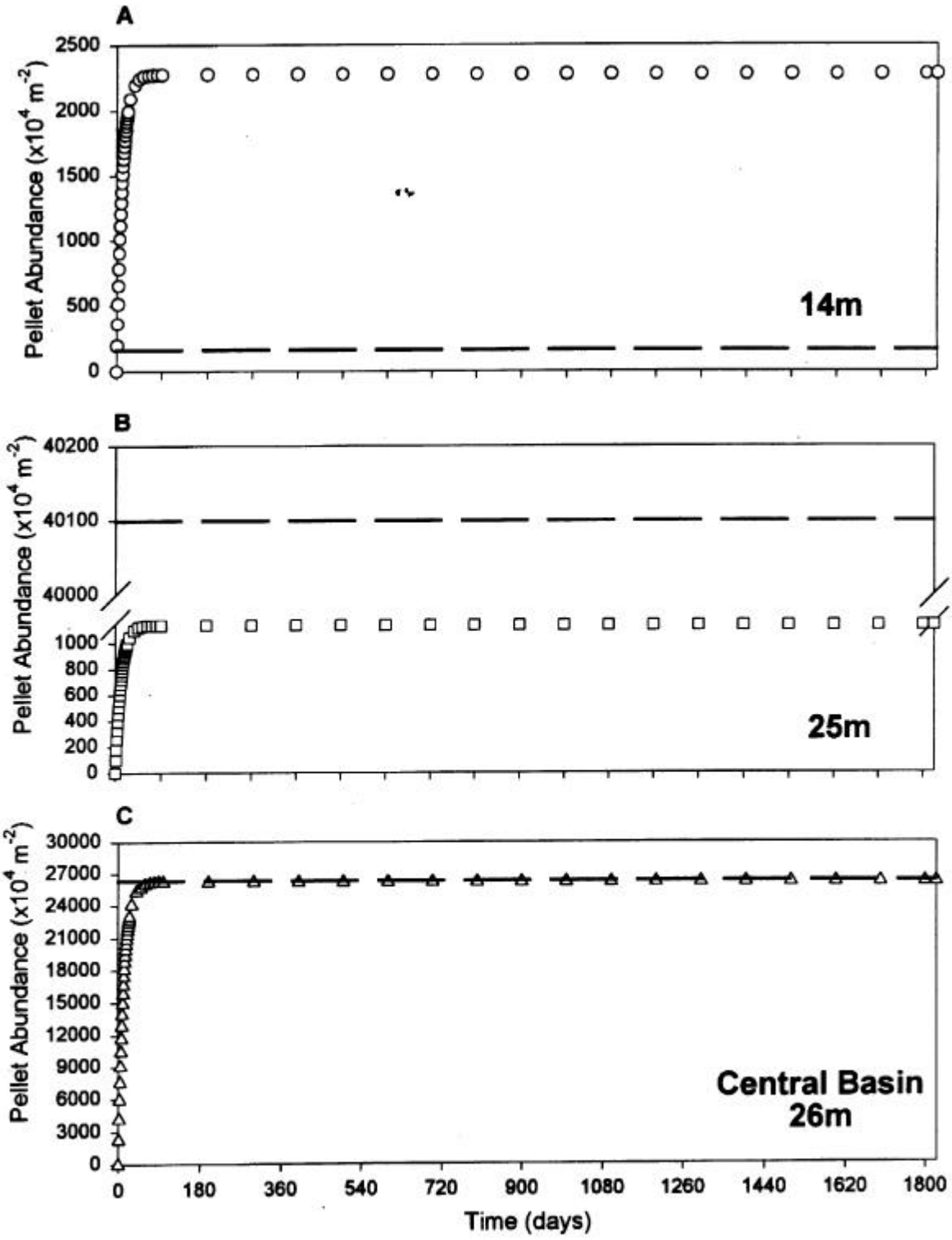

Figure 4 - Results of steady-state pellet production model for Transect Stations D (Fig. 4A) and A (Fig. 4B), and the Tower Stations in the central basin (Fig. 4C). The long, dashed lines represent measured pellet densities at each station. Note the differences in scale among the stations and the break in the axis of Fig. 4B.

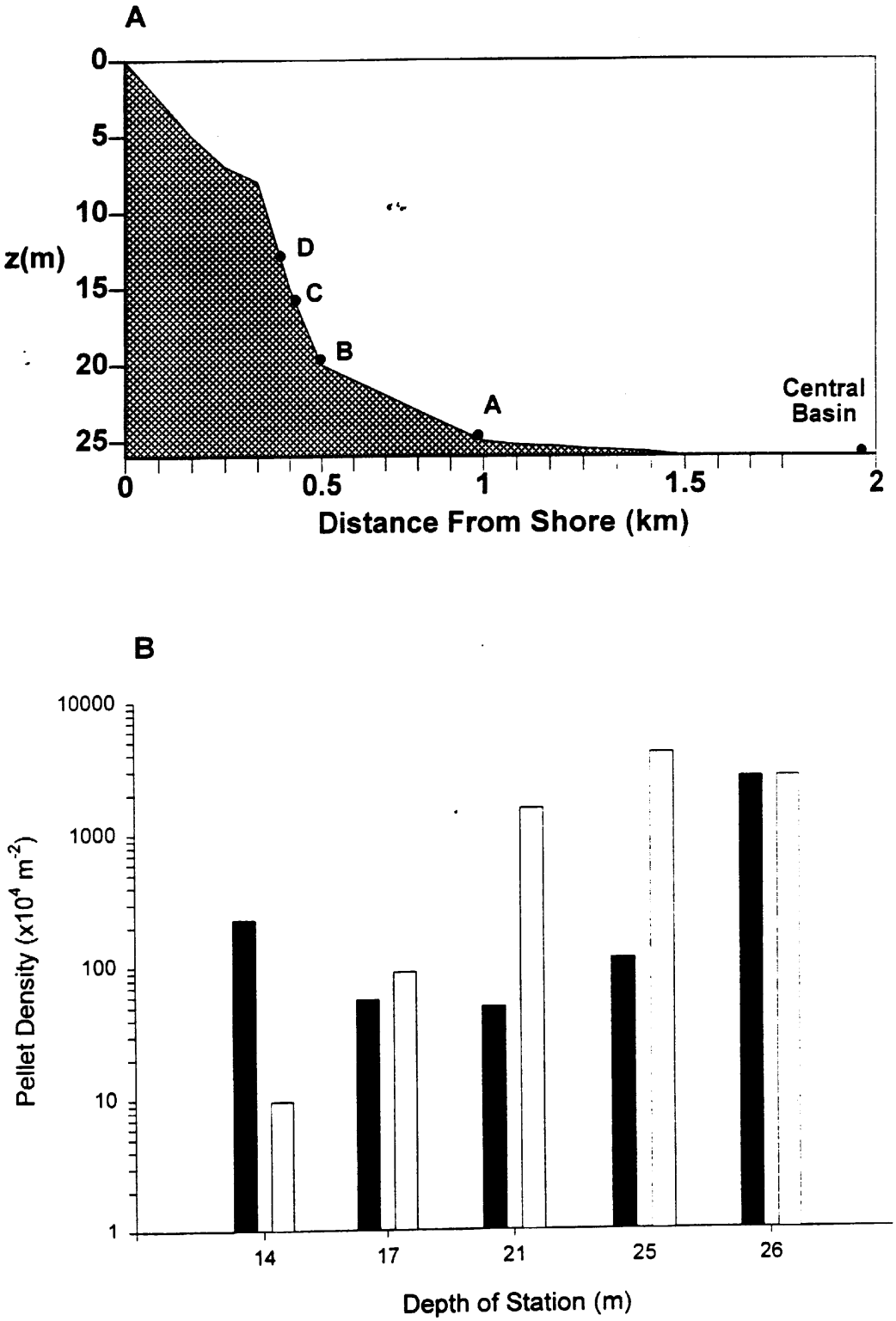

Figure 5 - Profile of bathymetry from the northern shoreline to the central basin indicating the distances and depths of stations used in our analyses (A), and pellet density (x 10^4 m^{-2}) with depth of stations (B). The modeled steady-state pellet densities are indicated by solid bars, and measured pellet densities by the white bars.

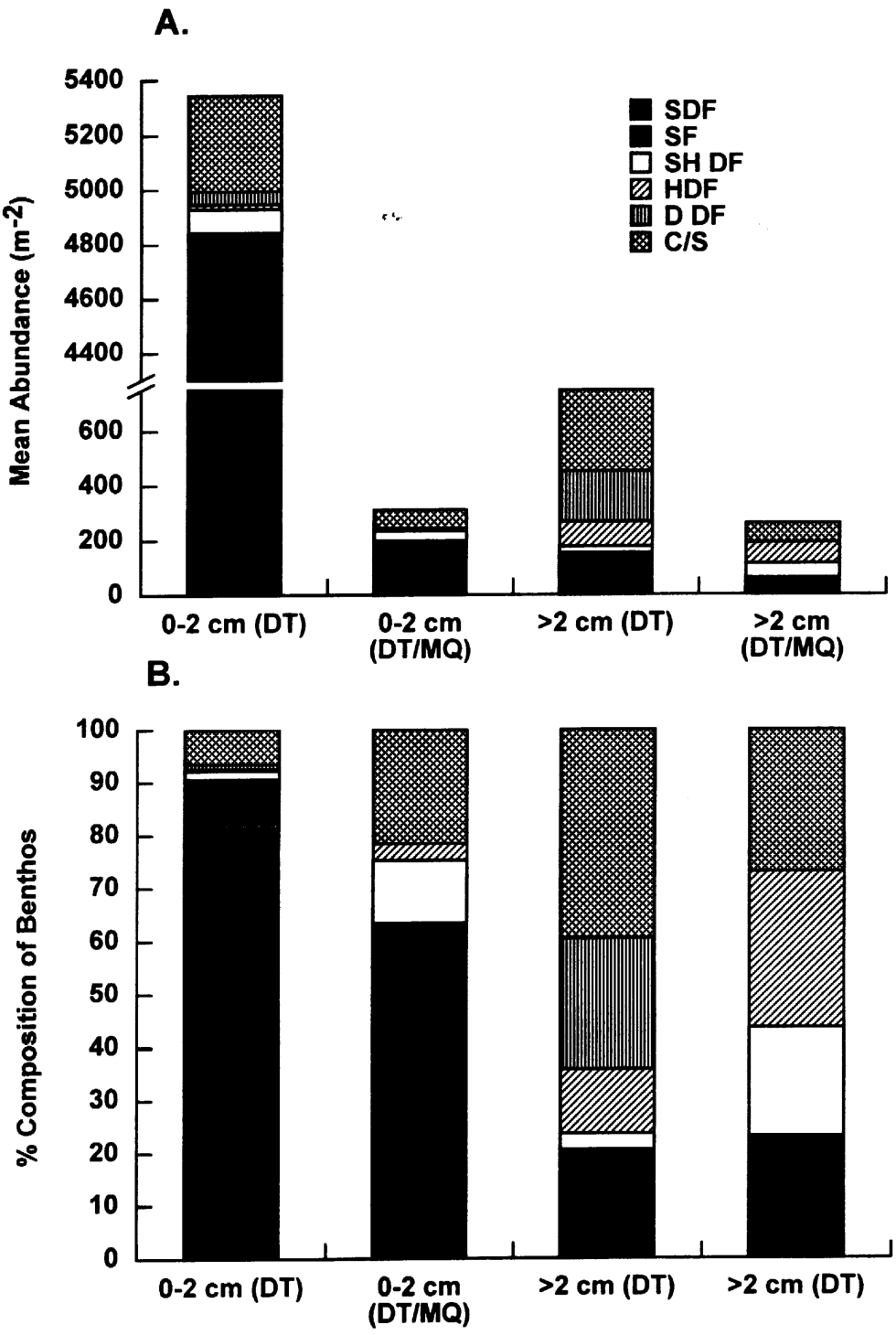

Figure 6 - Mean abundances (A) and % composition (B) of functional groups at the Dry Tortugas tetrapod station (DT) and stations between the Dry Tortugas and Marquesas (DT/MQ). The results are divided into 0-2 cm and > 2 cm depth intervals. SDF = surface deposit feeders; SF = suspension feeders; SH DF = shallow deposit feeders; HDF = tubicolous head-down deposit feeders; D DF = deep-burrowing deposit feeders; C/S = carnivores, omnivores, and scavengers.

Table 1. Rank order, functional group, and mean abundances of major benthic fauna in the top 2 cm at the Dry Tortugas tetrapod site (A) and at stations intermediate between the Dry Tortugas and Marquesas. (B). SDF = surface deposit feeders; SF = suspension feeders; SH DF = shallow deposit feeders; HDF = tubicolous head-down deposit feeders; D DF = deep-burrowing deposit feeders; C/S = carnivores, omnivores, and scavengers.

A. Dry Tortugas

Species	Functional Group	Mean Abundance (m^{-2})
Prionospio cristata	SDF	3052.5
Myriochele oculata	SDF	539.0
Pseudocyrena sp.	SDF	466.5
Leptochelia sp.	SDF	389.5
Tellinid Bivalves (4 spp.)	SDF	217.4
Diplodonta sp.	SF	203.8
Lucina nassula	SF	176.6
Gammarid amphipods (3 spp.)	SDF	126.8
Penaeid shrimp (2 spp.)	S/C	117.8
Cyclaspis sp.	SDF	90.6
Caprellid amphipod	S/C	81.5
Sabellid sp.	SF	63.4
Corbula sp.	SF	54.4
Syllid sp.	S/C	54.4
Armandia maculata	Sh DF	54.4
	OVERALL ABUNDANCE:	**5344.2**

B. Intermediate Stations

Species	Functional Group	Mean Abundance (m^{-2})
Myriochele oculata	SDF	46.9
Holothurian	SH DF	26.8
Mulinia lateralis	SF	26.8
Corophiid amphipod	SDF	26.8
Polynoid sp.	C/S	23.5
Caprellid amphipod	C/S	16.8
Lima sp.	SF	13.4
Leptochelia sp.	SDF	13.4
Macoma tenta	SDF	13.4
Lucina nassula	SF	10.1
Amphiurid Brittlestar	SDF	10.1
Sipunculan	SH DF	6.7
Glycera sp.	C/S	6.7
Ampelisca sp.	SDF	6.7
Prionospio cristata	SDF	6.7
	OVERALL ABUNDANCE:	**312.1**

Table 2. Rank order, functional group, and mean abundances of major benthic fauna at depths > 2 cm at the Dry Tortugas tetrapod site (A) and at stations intermediate between the Dry Tortugas and Marquesas. (B). SDF = surface deposit feeders; SF = suspension feeders; SH DF = shallow deposit feeders; HDF = tubicolous head-down deposit feeders; D DF = deep-burrowing deposit feeders; C/S = carnivores, omnivores, and scavengers.

A. Dry Tortugas

Species	Functional Group	Mean Abundance (m^{-2})
Notomastus sp.	D DF	113.2
Caprellid amphipod	S/C	95.1
Lumbrineris verilli	S/C	72.5
Penaeid shrimp (2 spp.)	S/C	72.5
Prionospio cristata	SDF	58.9
Tellinid bivalves (4 spp.)	SDF	49.8
Callianassa sp.	D DF	40.8
Maldanid sp.	HDF	40.8
Capitellid sp.	HDF	31.7
Sipunculan worm (2 spp.)	D DF	31.7
	OVERALL ABUNDANCE:	**747.3**

B. Intermediate Stations

Species	Functional Group	Mean Abundance (m^{-2})
Sipunculan	SH DF	33.6
Capitellid sp.	HDF	30.2
Tubificid sp.	HDF	23.5
Corophiid amphipod	SDF	20.1
Syllid sp.	C/S	20.1
Prionospio cristata	SDF	13.4
Glycera sp.	C/S	13.4
Phyllodoce sp.	C/S	13.4
Capitella capitata	HDF	10.1
Mediomastus californiensis	HDF	10.1
	OVERALL ABUNDANCE:	**261.7**

2.15 Contact Micromechanics for Constitutive Acoustic Modeling of Marine Sediments (Principal Investigators: M.H. Sadd and J. Dvorkin)

Contact Micromechanics for Constitutive Acoustic Modeling of Marine Sediments

Martin H. Sadd
Mechanical Engineering & Applied Mechanics Department
University of Rhode Island
Kingston, RI 02881

Jack Dvorkin
Geophysics Department
Stanford University
Stanford, CA 94305-2215

Introduction

The overall objective of the research program is to create new geoacoustic constitutive models of coarse-grained particulate and cemented particulate seafloor sediments as found in the CBBL sites at Panama City and Key West. The models include two important phenomena that strongly affect the acoustic properties of such sediments. One phenomenon is energy transfer through interparticle contact cement. Such cementation may be elastic (e.g., calcite), or viscoelastic (e.g., clay, silt). The other phenomenon is squirt flow (fluid squirting from the contacts during wave propagation).

Both contact mechanisms are explicitly considered at the particulate scale through the analytical development of new contact laws, and the resulting solutions are incorporated into a numerical discrete element modeling scheme. Numerical simulations are conducted for a variety of sediment models with various fabric in order to explore the effect of microstructure as well as macroscopic inclusions (cemented patches and layers) on acoustic wave velocities and attenuation. In addition, we are working on consistently incorporating our micromechanical models into the general framework of the macroscopic Biot theory.

Since starting in April 1996, two contact models have been developed. The first new model is for the cemented case including the effect of elastic cementation between elastic spherical particles. A rigorous theory of elasticity solution for this problem has been obtained earlier. In this effort we reduced the complicated functional form of this solution (an ordinary integral equation) to simple algebraic formulas that can be easily programmed for use in a numerical DEM scheme. The second analytical model considers the case of a linearly viscous fluid at contacts between spherical particles (viscous cement). Both models have been incorporated into our existing discrete element computer code, and several preliminary simulations have been run for each case.

Micromechanical Modeling

The *elastic cement* model is based on a rigorous theory of elasticity solution (obtained earlier) to the problem of normal and tangential deformation of two elastic spheres with elastic cement at their contact (Figure 1a). We reduced the complicated form of this solution to the following algebraic equations that can be directly plugged into a numerical DEM scheme:

$$
\begin{aligned}
&S_n = 2pR(K_c + \frac{4}{3}G_c)[A_n(\Lambda_n)a^2 + B_n(\Lambda_n)a + C_n(\Lambda_n)],\\
&A_n(\Lambda_n) = -0.024153 \cdot \Lambda_n^{-1.3646},\ B_n(\Lambda_n) = 0.20405 \cdot \Lambda_n^{-0.89008},\\
&C_n(\Lambda_n) = 0.00024649 \cdot \Lambda_n^{-1.9864};\\
&S_t = 2pRG_c[A_t(\Lambda_t, n)a^2 + B_t(\Lambda_t, n)a + C_t(\Lambda_t, n)],\\
&A_t(\Lambda_t, n) = -10^{-2} \cdot (2.26n^2 + 2.07n + 2.3) \cdot \Lambda_t^{0.079n^2 + 0.1754n - 1.342},\\
&B_t(\Lambda_t, n) = (0.0573n^2 + 0.0937n + 0.202) \cdot \Lambda_t^{0.0274n^2 + 0.0529n - 0.8765},\\
&C_t(\Lambda_t, n) = 10^{-4} \cdot (9.654n^2 + 4.945n + 3.1) \cdot \Lambda_t^{0.01867n^2 + 0.4011n - 1.8186};\\
&\Lambda_n = \frac{2G_c}{pG}\frac{(1-n)(1-n_c)}{1-2n_c},\ \Lambda_t = \frac{G_c}{pG},\ a = \frac{a}{R};
\end{aligned}
\qquad (1)
$$

where S_n and S_t are the normal and tangential stiffnesses of a two-grain combination, respectively; G and n are the shear modulus and the Poisson's ratio of the grains, respectively; G_c, K_c, and n_c are the shear modulus, bulk modulus, and the Poisson's ratio of the cement, respectively; a is the radius of the contact cement layer (Figure 1a); and R is the grain radius. These formulas are statistical approximations of the rigorous cementation theory solutions (Dvorkin et al., 1994). The error does not exceed one percent. The validity of these formulas have been confirmed by applying them to calculate P-wave velocity in high-porosity cemented reservoir rocks from North Sea (Figure 2).

The *viscous cement* model is based on a combination of the Hertz contact theory and approximate Navier-Stokes equations of viscous radial flow (Figure 1b). It is assumed that fluid pressure does not affect the geometry of elastic contact between two grains. If the fluid is modeled as incompressible, and the inertia term in the equations is neglected, the contact force F_C due to the normal displacement of the grain center $d(t)$ is:

$$
F_C = \frac{8G\sqrt{R}}{3(1-n)}d\sqrt{d} + \frac{3}{2}pmR^2\frac{\dot{d}}{d}, \qquad (2)
$$

where m is fluid viscosity, and the other symbols are the same as in the previous equations.

Currently, we have developed this equation only for the normal deformation (presumably, the dominant factor) and for the case where the grains are not separated. We will continue by including into consideration the compressibility and inertia of the fluid, and fluid's effect on the contact geometry.

Discrete Element Modeling

The developed interparticle contact laws for cementation and pore fluid modeling as described above were incorporated into our basic discrete element computer code. To date, several DEM simulations have been carried out, and examples of these preliminary results follow.

Cemented Particulate Sediment Models

With regard to the cementation model, relations (1) have been incorporated into the discrete element code. Several simulations have been conducted on both one and two-dimensional arrays of spherical particulate sediment models. Presented results include the case of identical particles of 2 mm diameter and 2200 kg/m^3 density . The elastic moduli parameters for the grains and cement were chosen as: G = 26.2 GPa, n = 0.277, G_c = 1.2 GPa, and n_c = 0.377, and these values correspond to the case of glass particles cemented by epoxy. Acoustic input was modeled as an applied particle loading of triangular time dependence with amplitude 2 N and duration 5 μs to simulate a wave front acoustic pressure on the order of 1Mpa. Our preliminary DEM simulations focused primarily on the effect of variations of the cementation parameter a .

An example shown in Figure 3, consists of a hexagonal close packing (HCP) of cemented spherical particles. A localized acoustic input is applied to the center of the assembly, as shown, and propagation and attenuation behavior is studied along the line defined as the Primary Chain. The sediment model has been constructed with a two-layer cemented system with the cementation parameter a having two different values (a_1, a_2) in each of the layers. Discrete element simulations were then conducted on this model for several different cementation cases. The results include two homogeneous cases with a_1 = a_2 = 0 and 0.6, and a non-homogeneous two-layer model where a_1 = 0 and a_2 = 0.6. For the homogeneous models the wave speeds for the a = 0 case (no cementation) was approximately 600m/s, while the heavily cemented case of a = 0.6 gave a speed of 4440m/s. Therefore, as expected, cementation acts to increase the wave speed. Wave attenuation results (as measured by the interparticle load transfer) along the primary chain are shown in Figure 4. It can be seen for the homogeneous cases that increased cementation acts to decrease attenuation. For the layered model, wave amplitude undergoes a sudden local increase when moving from uncemented to cemented material. This occurs due to the mismatch in material impedance between the two layers.

Additional DEM simulations were conducted on HCP models which included preferential anisotropic cementation such that the cementation factor was chosen as a_h for horizontal contacts and a_o for all other vertically oriented contacts. For this case the acoustic loading was changed to a planar input loading along the top of the entire assembly shown in Figure 3. Results of this case are given in Table 1. The transmission ratio here is a measure of attenuation and represents the ratio of the averaged output signal (interparticle forces) to the averaged input. It is apparent that the oriented cementation produced very dramatic wave propagation differences in the HCP material model, and this is certainly related to the model's special fabric in which the vertically oriented contacts essentially conduct all of the wave motion. Large differences in wave speed and attenuation exist between horizontally and vertically distributed cementation.

Random sediment models were also constructed and one example is shown in Figure 5. Particle and cement parameters were chosen identical to the previous cases, and the acoustic input was a planar loading applied vertically to the top of the model system. In order to quantify the

fabric of such a material model the distributions of *branch vectors* (drawn between adjacent contacting particles) are commonly used. For the assembly under study, the branch vector distribution plot is shown in Figure 5, and this indicates a near-vertical, preferential direction for energy transfer. The cementation for this material model has been distributed by the following relations:

$$\textit{Vertical Distribution: } a = \begin{cases} 0.4, & |q_v| \le 50^o \\ 0.0, & \textit{otherwise} \end{cases}$$

$$\textit{Horizontal Distribution: } a = \begin{cases} 0.4, & |q_h| \le 50^o \\ 0.0, & \textit{otherwise} \end{cases} \qquad (3)$$

where q_v and q_h are the angles measured from the vertical and horizontal. Using this type of biased cementation, a *cementation branch vector* can be defined as the product $\boldsymbol{ab}$. Distribution plots of this new fabric variable for vertical and horizontal cementation distributions are shown in Figure 6. DEM simulation results for this random assembly are shown in Table 2. Results again indicate that preferred directional cementation will produce significant differences in wave propagational characteristics.

Sediment Models with Squirt Flow

The approximate model of particulate sediment with viscous fluid flow (viscous cement) has also been incorporated into the discrete element code. In order to use the contact law given by equation (2), the model particulate systems must have some small initial compression to avoid having a zero local strain value in the denominator. This was achieved by subjecting models to initial compressive loadings. To date, preliminary computer runs have been conducted for one-dimensional models under different initial compression.

Plan for Future Work

Future plans include the development of a more accurate and rigorous model for the squirt-flow mechanism and incorporation it into the macroscopic Biot formulation. We will construct realistic particulate models based on the experimental descriptions of ocean sediments obtained within the CBBL program, and special cooperation with Dr. Armand Silva at the Marine Geomechanics Laboratory (MGL) is planned. The microscopic contact laws will be incorporated into a DEM scheme and wave propagation parameters will be obtained on realistic particulate systems. Comparisons with acoustic data being collected at MGL and numerical results from a Biot wave propagation model will be made. In this regard preliminary work has already begun with a one-dimensional Biot code originally developed by Bob Stoll.

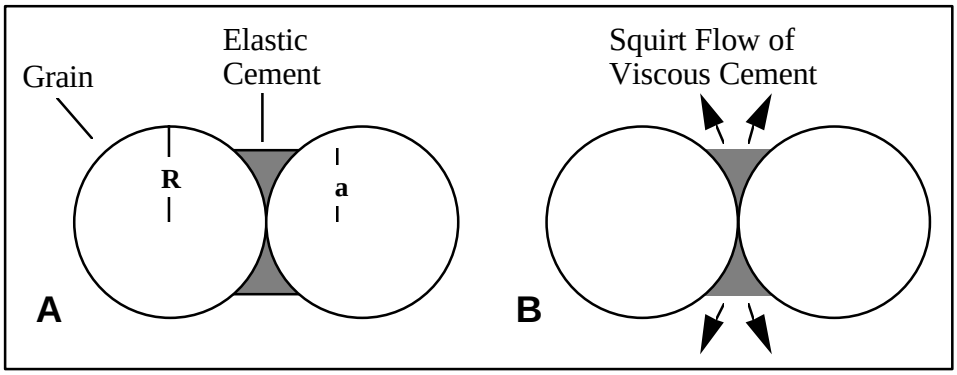

Figure 1. Contact geometry for two grains with (a) elastic and (b) viscous cement.

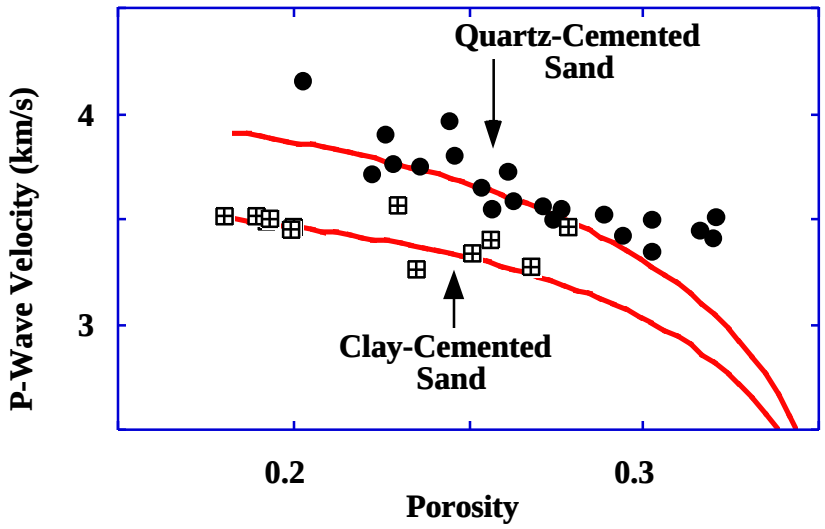

Figure 2. P-wave velocity in reservoir sand cemented with quartz and clay. Symbols are laboratory data, solid lines are theoretical predictions.

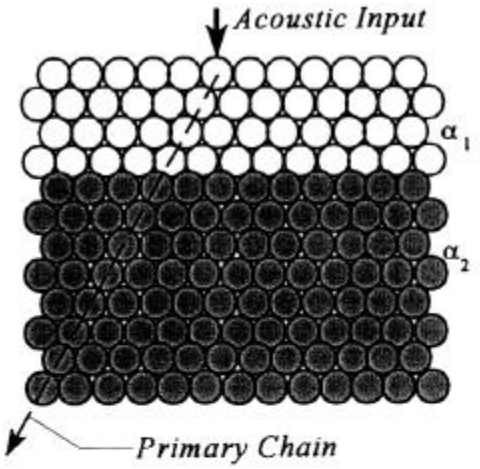

Figure 3. Layered Particulate Sediment Model

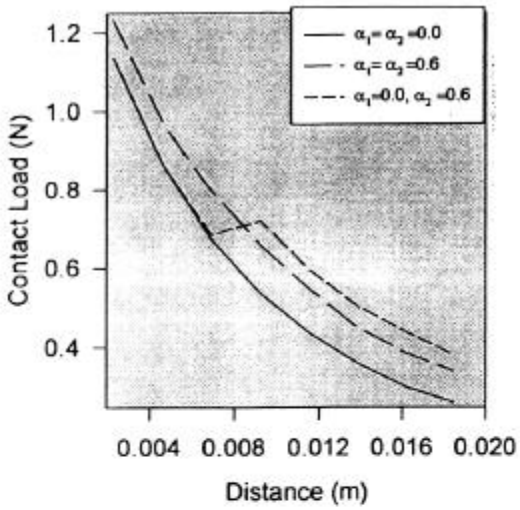

Figure 4. Attenuation Results for Layered HCP Model

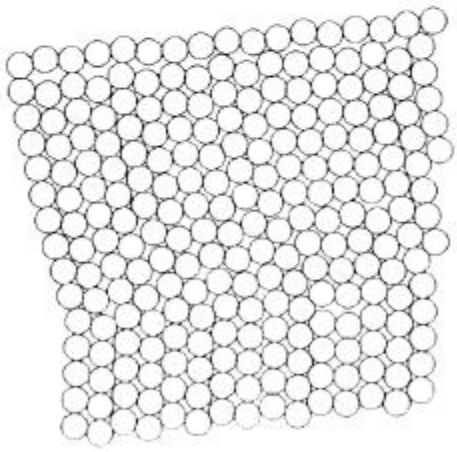

Model Assembly

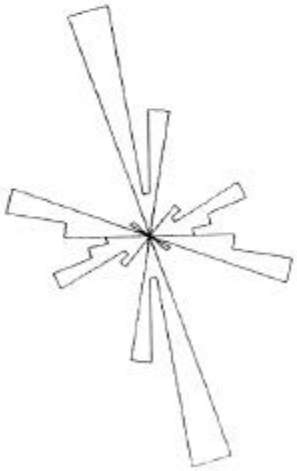

Branch Vector Distribution

Figure 5. Random Particulate Model and Branch Vector Fabric Distribution

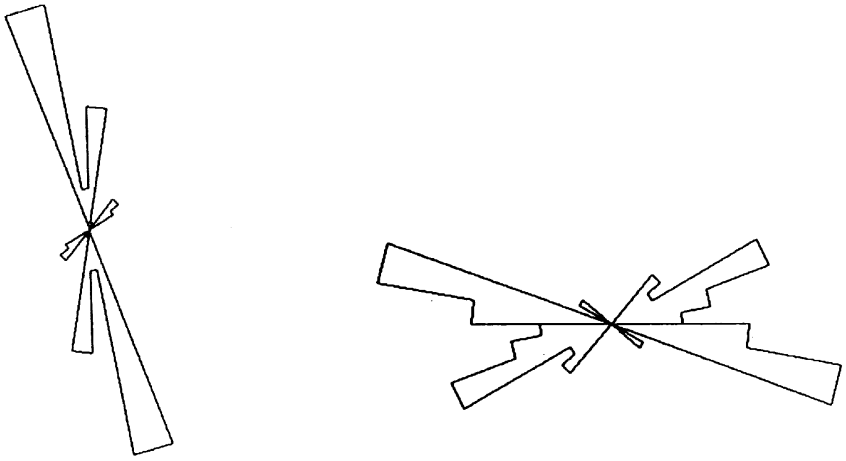

Vertical Cementation Distribution Horizontal Cementation Distribution

Figure 6. Cementation Branch Vector Distributions

Table 1. Plane Wave Propagation Results HCP-Model for Anisotropic Cementation

α_h	α_o	Transmission Ratio (TR)	Wave Speed (m/s)
0.6	0.0	0.426	1376
0.0	0.6	0.285	7938
0.0	0.0	0.426	1376
0.05	0.05	0.472	2268
0.2	0.2	0.405	4142
0.6	0.6	0.285	7938

Table 2. Wave Speed and Transmission Ratio Results Random Assembly Model

Cementation Case	Wave Speed (m/s)	Transmission Ratio
Vertical	3114	0.048
Horizontal	1004	0.0548
Uniform (α=0.0)	1015	0.0527
Uniform (α=0.4)	3044	0.0513
Uniform (α=0.8)	3520	0.044

2.16 Detection of Continuous Impedance Structures Using a Full Spectrum Sonar (Principal Investigator: S. Schock)

Detection of Continuous Impedance Structures Using a Full Spectrum Sonar

Steven G. Schock

Dept of Ocean Engineering
Florida Atlantic University
777 Glades Road
Boca Raton, FL 33431

INTRODUCTION

This research project focuses on developing techniques for remotely predicting the acoustic and physical properties of sediments using chirp sonar data. The objectives of this project are:

1) To develop an acoustic model that predicts the frequency response of the seabed from vertical impedance profiles estimated from sediment cores.
2) To utilize the predicted frequency response of the seabed to develop techniques for measuring the vertical impedance of the top 10 meters of the seabed.
3) To acquire normal incidence FM data over the frequency range of 1 to 15 kHz for imaging the subsurface features of the seabed and for estimating sediment properties at CBBL experiment sites.
4) To test algortihms for sediment property prediction developed for the Office of Naval Research and to compare those properties with in situ measurements made by other investigators.

1995-1996 ACCOMPLISHMENTS

1. The analysis of impedance data provided by NRL was completed showing the effect of the continously varying impedance structure on the spectrum backscattered acoustic data at normal incidence. The study showed that predicting subsurface impedance contrasts using subsurface reflector amplitudes measured with a reflecion profiler can have large errors due to transition zones between adjacent subsurface layers. In general, since interlayer transitions are usually greater than 5 cm, frequencies greater than 10 kHz cause reflection amplitude measurement errors greater then 10 percent due to the destructive interference caused by the sequence of transition zone reflections. To ensure that the measurement error is less than 10% ensure the acoustic wavelength is greater than 3 times the transition zone thickness. (ref 1)

2. A technique was developed and tested to generate an absolute calibration for ASCS data sets (provided by Doug Lambert, NRL) so that core samples were not required to calibrate the ASCS data sets. Em, the energy of the water multiple and the Es, the energy of the sediment water interface reflection were used to obtain the reflection coefficient of the seabed and the system

calibration constant. The system calibration constant can be used to calibrate the entire ASCS data set as long as transmmission power and receiver amplifier gain did not change. Figure 1 shows subbottom profiles generated by ASCS and chirp sonar along the 'Schock' line in Kiel Bay. The pressure reflection coefficient and the system gain constant are calculated using

$$R = \sqrt{\frac{E_M}{E_S}}$$

$$K_{SYS} = \sqrt{\frac{E_M}{E_S^2}}$$

The running average of R and the system constant are shown in Figure 2. If the calibration is performed properly, the system constant should not change with sediment type or water depth. Note that the reflection coefficient increases by a factor of 3 as the grain size increases toward the Middle Ground while the system constant fluctuates by 20% about the mean value.

To test the accuracy of this procedure, ASCS and Chirp data collected along the 'Schock' line, were compared. This line was selected because of the gradual increase in grain size from deeper to shallower water depths. Since the X-Star system was calibrated at the pier by transmitting at the air-water interface, the sonar data had an absolute calibration. If water multiple method is accurate for providing an absolute calibration, the ASCS reflection coefficient should agree with the reflection coefficient measured with the chirp sonar. The reflection coefficients generated by the Chirp sonar and the ASCS system along the 'Schock' line are shown in Figure 3. Along most of the line the reflection coefficient measurements generated by the two systems are in good agreement. Differences in the reflection coefficient could be due to across track offsets and due to the frequency dependence of the response of the sediment-water interface.

3. A method of predicting compressional wave attenuation was developed using ACSC data. The frequency spectrum of 2-10 kHz chirp and 10-35 kHz ASCS data are shown in Figure 4. The chirp spectrum was measured during the pier calibration. The ASCS spectrum was derived from averaging the spectrums of the sediment-water interface reflections. The combination of the two systems provides about a bandwidth of 1 decade with good SNR. Because most of the core data was collected in the top meter, it is desirable to estimate the attenuation of the top 1-2 meters of sediment. Due to the short two-way travel paths, absorption is too small to estimate attenuation using frequencies below 10 kHz. ASCS data, which has frequency components at 13 and 30 kHz is ideal for measuring attenuation using the spectral ratio method. The backscattered 30 kHz signal is very sensitive to sediment type. Figure 5 shows the variation of the attenuation coefficient and the pressure reflection coefficient along the 'Schock' line. The attenuation coefficient was calculated from the sediment transfer function. A least squares fit of a line through the sediment transfer function (dB vs f) provides the slope. The slope divided by the two way travel distance is the attenuation coefficient.

PLANS FOR 1997

The primary objective for 1997 is to use the Chirp and ASCS data sets to provide acoustic property predictions using the decade of frequencies that is generated by the combination of the two systems. The acoustic predictions and the core data will be compared to establish the accuracy of the remote sensing measurements. In 1996 a method was derived and tested for

calibrating ASCS data. Given two calibrated data sets in two non-overlapping frequency bands two independent estimates of sediment properties can be made without aprior knowledge of the sediments. When the predictions of the two sonars agree, the confidence in the predicted properties is high and should agree well with insitu and core measurements.

Volume scattering coefficients, attenuation coefficients and impedance profiles will be estimated from the normal incidence data from the two systems. The scattering model requires the transmitted acoustic waveform, the beam pattern function of the transducers and calibrated data sets. The rms noise measured between sediment layers is converted to a volume scattering coefficient after accounting for the beam pattern and transmission losses. The attenuation is estimated from the spectral shift of the backscattered data. Impedance profiles are calculated by estimating the phase and amplitude of the subsurface reflections and recursively predicting the impedance of each sediment layer starting at the sediment-water interface.

PUBLICATIONS

Schock, S.G. and L.R. LeBlanc.1994. "Analysis of Wideband FM Subbottom Data from Kiel Bay, Germany," EOS Abstract,Jan 18, 1994 Suppl., Ocean Sciences 94, San Diego.

Schock, S.G. 1994. “High resolution volume backscattering and attenuation measurements in marine sediments," Abstract, Meeting of the Acoust. Soc of Amer., June 94

Schock, S.G. and L.R. LeBlanc. 1994. "FM sonar characteristics for normal-incidence sediment classification," JASA 96(5)Pt. 2, Nov 1994, p.3222.

DeBruin, D.L.. L.R. LeBLanc and S.G. Schock, "Correlation of acoustic impedance and volume scattering with sediment mean grain size and bulk density,” JASA 96(5), Pt. 2, Nov 1994,p.3223.

Schock, S.G., L. LeBlanc, D. DeBruin and L. Munro, 1995. "Normal incidence sediment classification using wideband FM pulses in Eckernforde Bay," Proceedings of the Workshop Modelling Methane-Rich Sediments of Eckernforde Bay, 26-30 June 1995, Eckernforde, FWG-Report 22.

Schock, S.G., L.R. LeBlanc and D. DeBruin. 1995. "Full Spectrum sediment property predictions near the Dry Tortugas and Marquesas,” Abstract. 1st SEPM Congress on Sedimentary Geology, St. Pete Beach, August 13-16, 1995.

Schock, S.G. 1996. "Predicting vertical profiles of sediment properties from seismograms" Oceanology International Conference Proceedings, Brighton, 5-8 March 1996, p.1-20.

DeBruin, D. 1995. “Classification of Marine Sediments Using a Fuzzy Logic Impedance Inversion Model” Ph.D. Dissertation. Florida Atlantic University, 1995.

Zhang, J.L. 1996. “The development and application of a numerical model for predicting the frequency response of the seabed from vertical profiles of sediment impedance,” Master’s of Science Thesis. Florida Atlantic University, 1996.

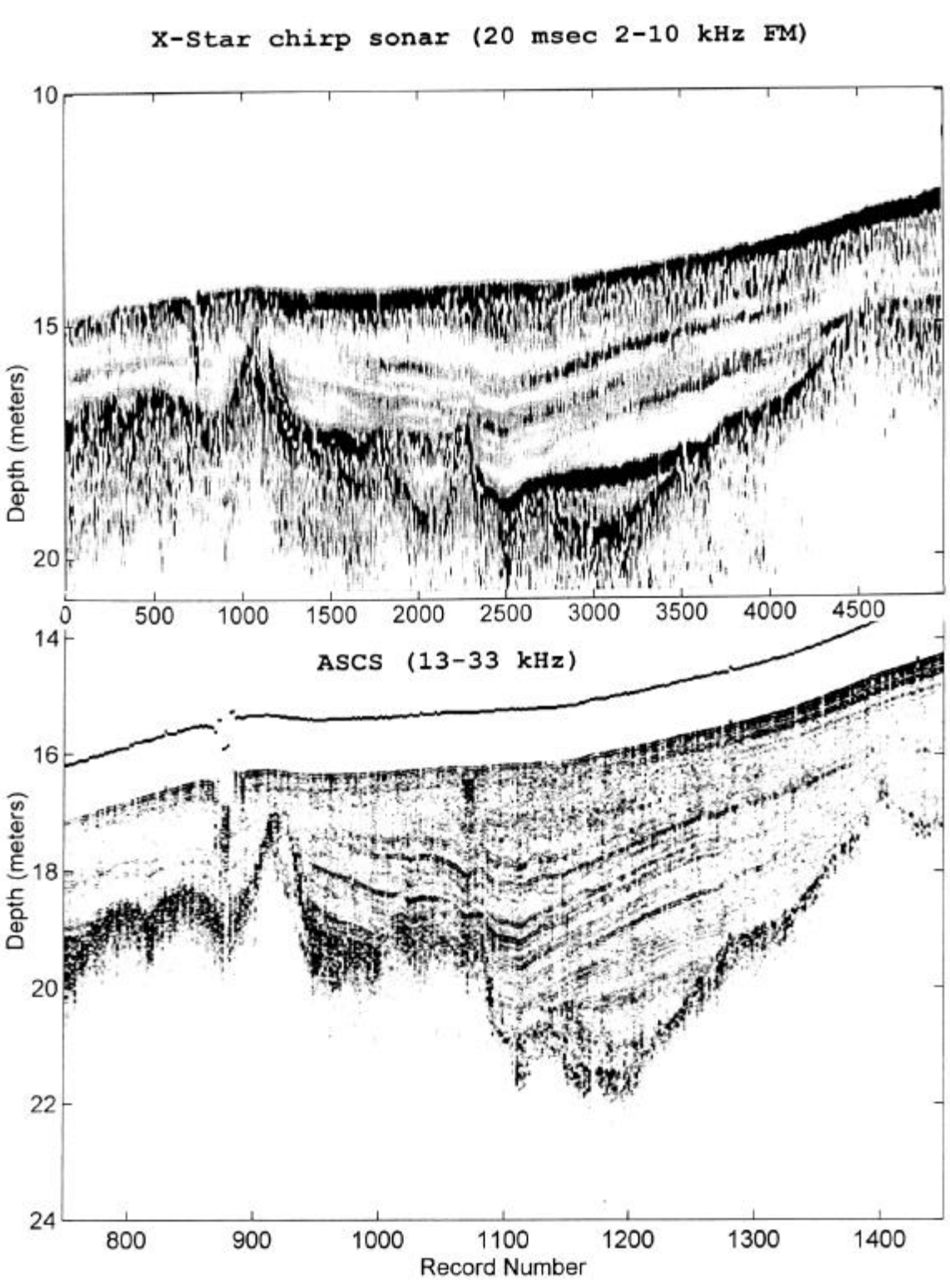

Figure 1. Images generated by the ASCS (13-33 kHz) and the X-Star chirp sonar (2-10 kHz) along the 'Schock' line in Kiel Bay.

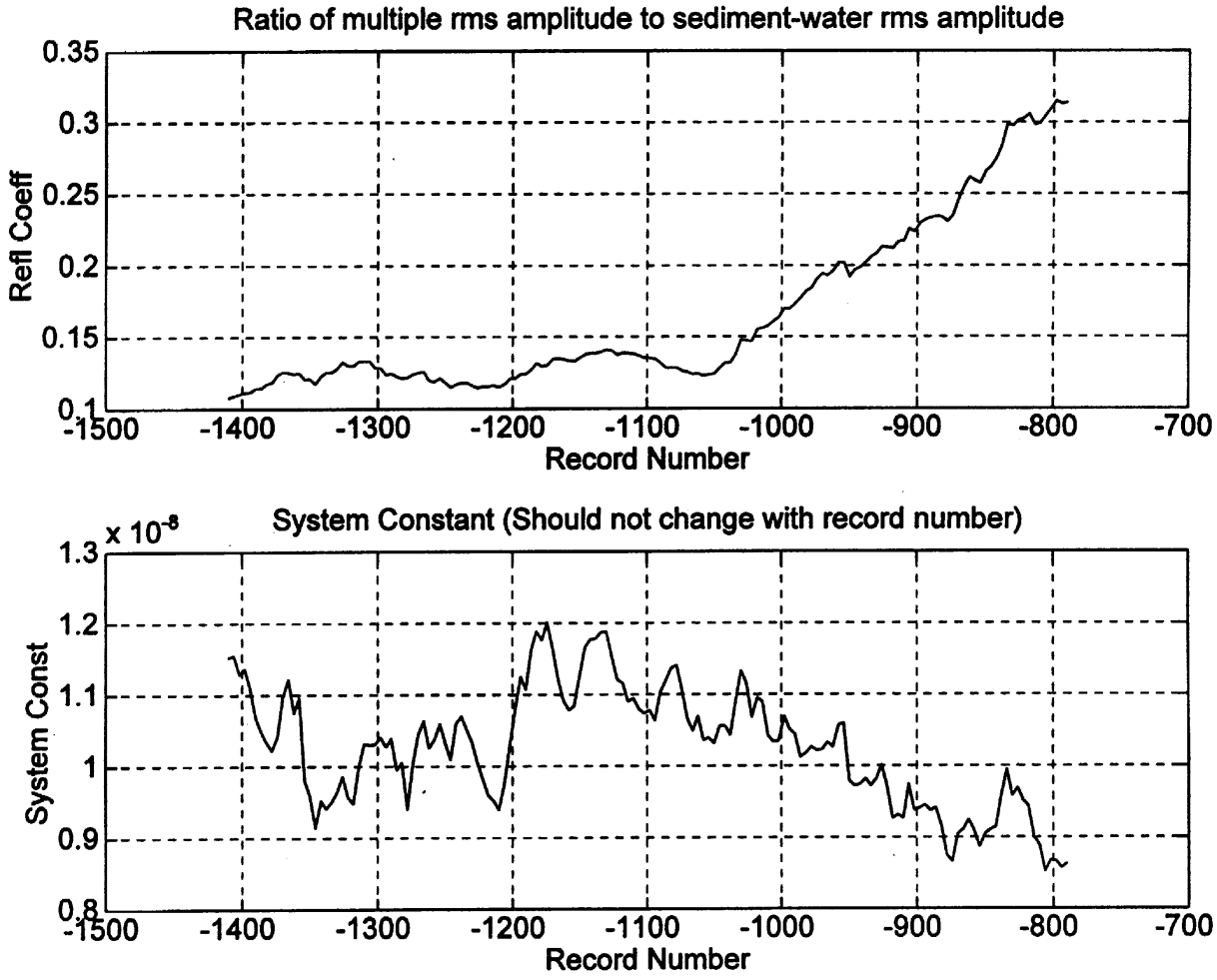

Figure 2. Reflection coefficient and system constant of ASCS derived from the energy of the water multiple and the the energy of the sediment-water interface reflection.

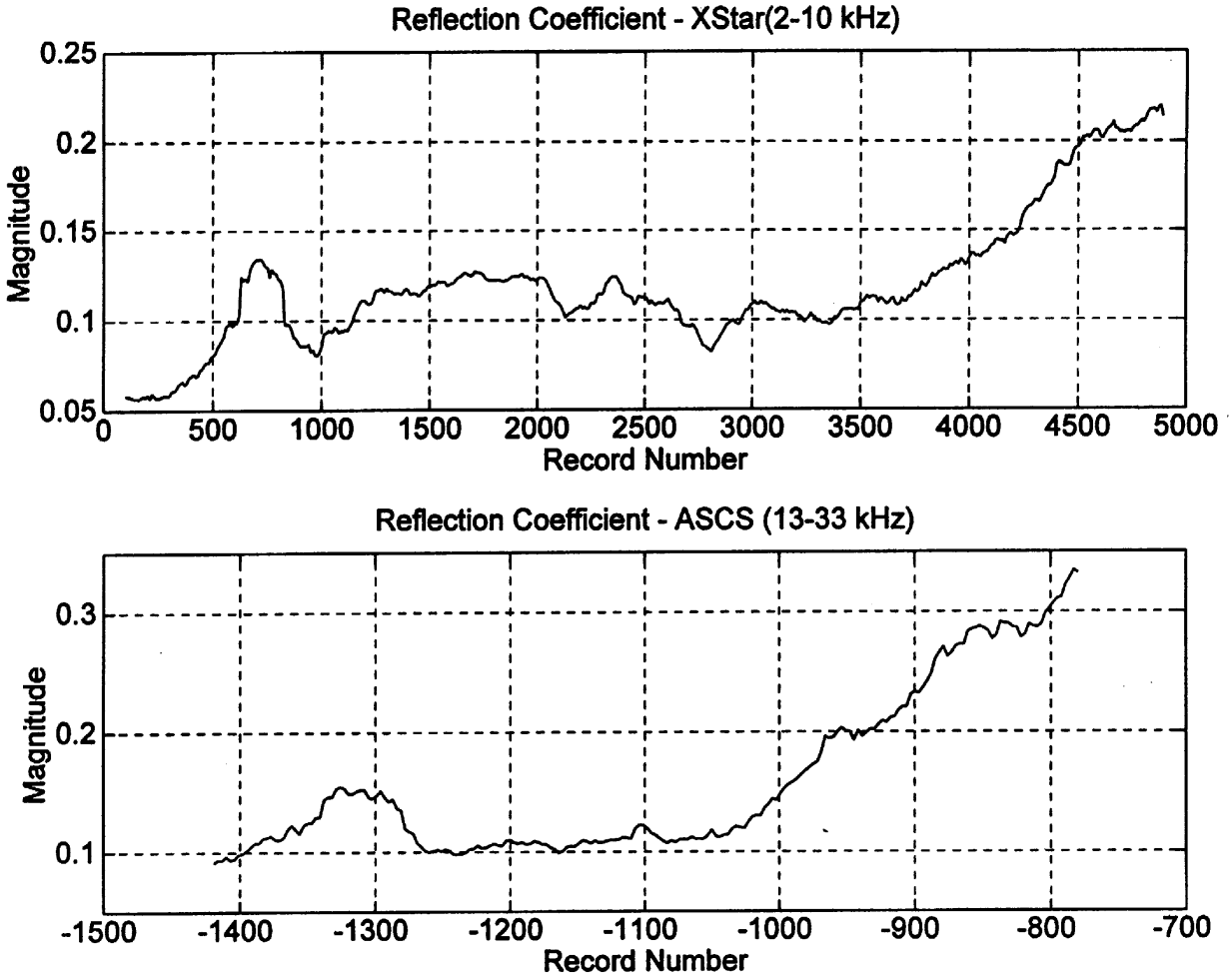

Figure 3. Reflection coefficient estimated using a water multiple calibration of ASCS data compared to the reflection coefficient measured by a calibrated chirp sonar transmitting 2-10 kHz FM pulses.

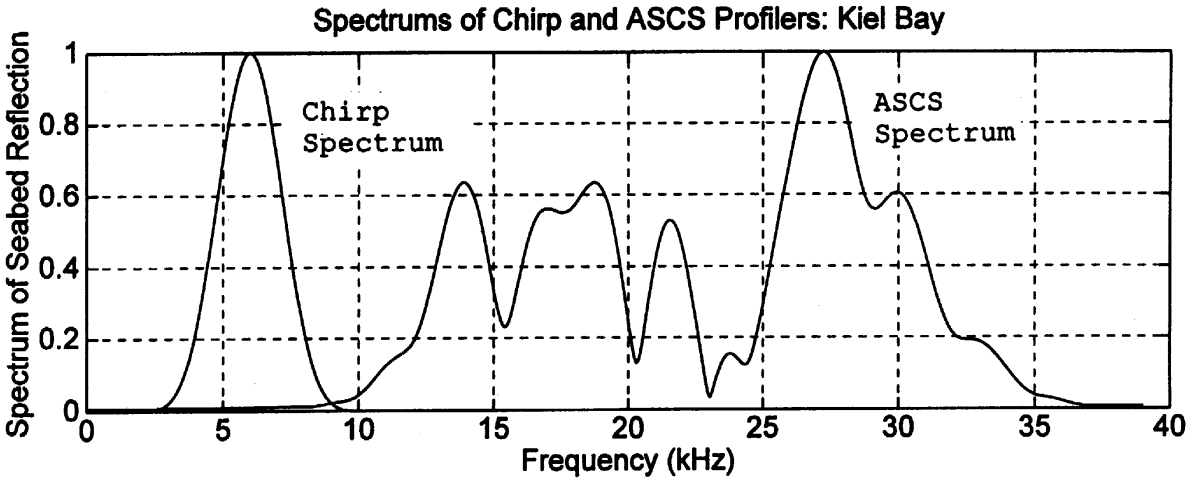

Figure 4. Frequency spectrum of subbottom profilers used to collect normal incidence reflection data in Kiel Bay, Germany.

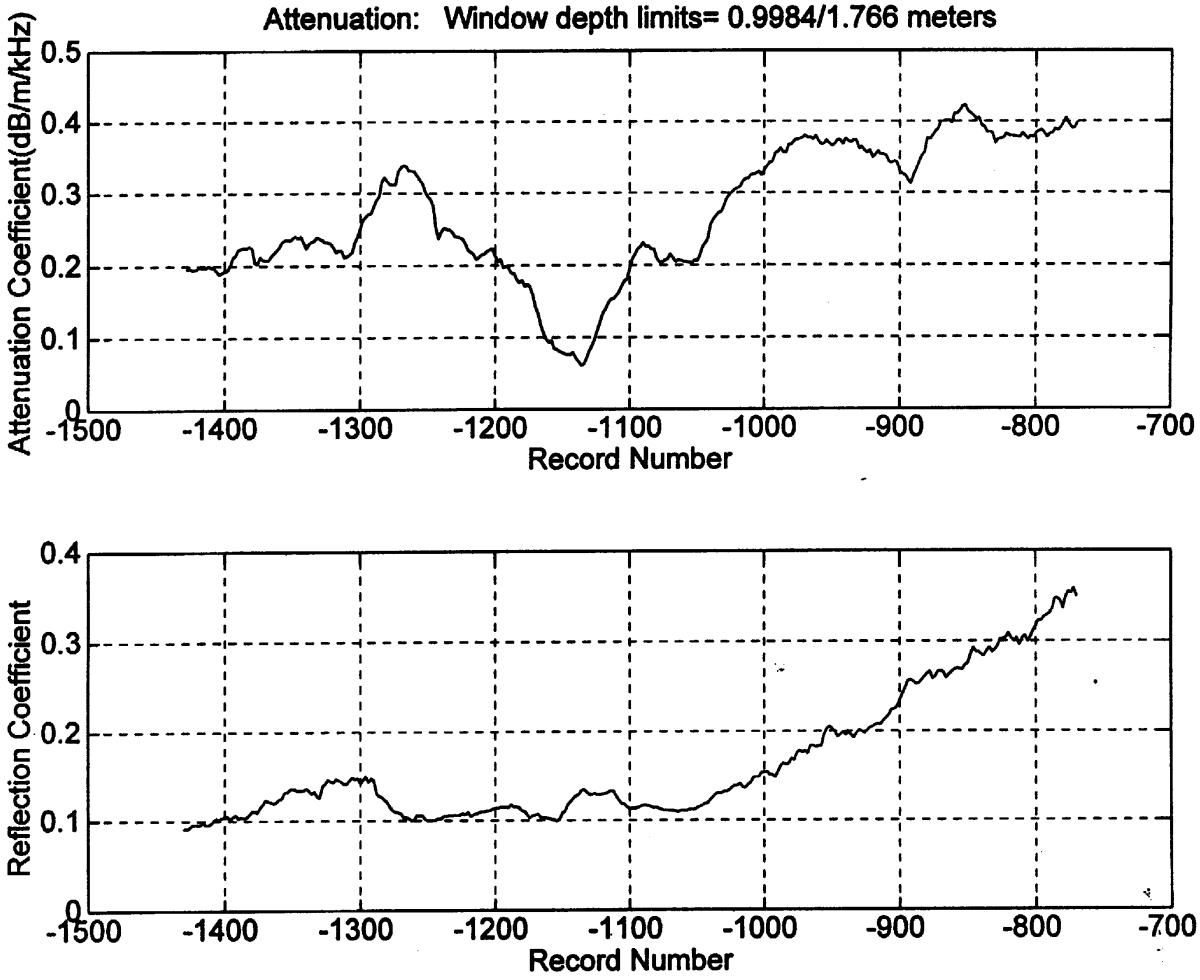

Figure 5. Comparison of attenuation coefficient and reflection coefficient measurements generated from ASCS data along 'Schock' line. As water depth decreases and grain size increases from left to right in the above graph, the reflection and attenuation coefficients increase. The attenuation coefficient was calculated using the transfer function of the sediments in the top 2 meters.

2.17 Effects of Carbonate Dissolution and Precipitation on Sediment Physical Properties and Structure: Pore Water Flux Component (Principal Investigator: A.M. Shiller)

Alan M. Shiller
Institute of Marine Sciences
University of Southern Mississippi
Stennis Space Center, MS 39529

INTRODUCTION

The objective of this project is to examine pore water chemistry in cores from carbonate sediments in the Dry Tortugas and Marquesas study area and to use this information in an effort to understand how degradation of organic matter within the sediments indirectly affects sediment physical properties and structure.

Degradation of organic matter in sediments proceeds via a sequence of thermodynamically-determined reactions (e.g., Froelich et al., 1979). Initially, the organic matter is consumed by normal oxic respiration. When oxygen is used up, certain bacteria can then mediate organic matter oxidation (and obtain energy in the process) using nitrate as the terminal electron acceptor rather than oxygen. As nitrate is used up, then manganese oxides, ferric oxides, and sulfate are all used in sequence. This diagenetic sequence is explained by thermodynamic calculations that show that the first oxidants in the sequence yield more energy per mole of oxidized organic matter than the later oxidants.

The above thermodynamic sequence of reactions is commonly observed in sediments and has implications for sediment physical properties and structure. There are a number of reasons for this. First, the various oxidative pathways can generate or consume protons, depending on the particular oxidant involved. For instance typical aerobic respiration generates protons whereas anaerobic respiration utilizing manganese oxides consumes protons. This consumption or production of protons also means that organic matter degradation can drive carbonate dissolution or precipitation in the sediments. In nearshore carbonate sediments (where productivity and hence sedimentary diagenesis rates are high) this could be an important factor in affecting sediment physical properties and structure.

A second way in which organic diagenesis can affect sediments in the study area relates to the production of dissolved Fe^{2+} and Mn^{2+} during the use of the metal oxides to oxidize organic matter. As carbonate phases are reprecipitated downcore, some of the pore water Fe and Mn may be incorporated into the carbonate, potentially affecting its properties.

An additional effect of organic diagenesis relates to the release of phosphate. Under certain conditions phosphate can precipitate to form phosphatic authigenic minerals such as apatite (a calcium fluor-phosphate mineral) and vivianite (ferrous phosphate). For instance, in the shallow, anoxic carbonate sediments of Florida Bay and Bermuda, Berner (1974) reported evidence for apatite formation.

RESULTS AND DISCUSSION

The accompanying figures show pore water profiles of dissolved phosphate, sulfate, fluoride, and manganese in some of our cores. Phosphate increases rapidly in the upper 5 cm of the cores and then level out somewhat, never reaching the much higher values seen in other highly productive environments. (Note that the scatter in the phosphate data is due to a faulty spectrophotometer lamp. These analyses will be repeated in the coming year.) Berner (1974) suggested that similarly low phosphate concentrations in Florida Bay and Bermuda carbonate sediments might result from phosphate uptake during apatite formation. For that reason we examined fluoride profiles, fluoride also being taken up during apatite formation. Our fluoride profiles show slight (~5-10%) but distinct depletion of this element. Diffusional modeling suggests a fluoride uptake rate of 2 μg F cm^{-2} yr^{-1}, though bioturbation should make this a minimum estimate. This is similar to the rate of fluoride uptake by apatite formation off western Mexico (Schuffert et al., 1994).

Apatite formation is generally thought to take place in a sub-oxic, but not sulfidic environments. Our sulfate data indicate that there is no appreciable difference between pore water sulfate and bottom water sulfate in these cores. Thus, the Dry Tortugas and Marquesas cores are not highly reducing, at least in the upper 30 cm. Manganese data indicate that this element is being reduced in the upper 5-10 cm of the cores. Dissolved manganese shows a maximum because of the uptake of manganese into reprecipitated carbonate phases below ~5 cm depth.

WORK PLAN

We intend to pursue the apatite formation question further. Dissolved phosphate profiles need to be reanalyzed. We will also coordinate with C. Brunner to look for phosphatic phases in the solids. Note that because of the high sedimentation rate in this region it is not clear if we can measure the change in solid phase P caused by apatite formation--this should be an increase of only ~0.003%. An interesting question is whether we are observing the formation of new apatite or the alteration of detrital apatite (possibly blown or washed in from recovery operations in Florida). We also hope to obtain further pore water data during a cruise back to the study area early next year.

REFERENCES

Berner, R.A., 1974. Kinetic models for the early diagenesis of nitrogen, sulfur, phosphorus, and silicon in anoxic marine sediments. In *The Sea*, Vol. 5 (E.D. Goldberg, ed.), Wiley, pp. 427-450.

Froelich, P.N. et al., 1979. Early oxidation of organic matter in pelagic sediments of the eastern equatorial Atlantic: suboxic diagenesis. *Geochim. Cosmochim. Acta 43*: 1075-1090.

Schuffert, J.D. et al., 1994. Rates of formation of modern phosphorite off western Mexico. *Geochim. Cosmochim. Acta 58*:5001-5010.

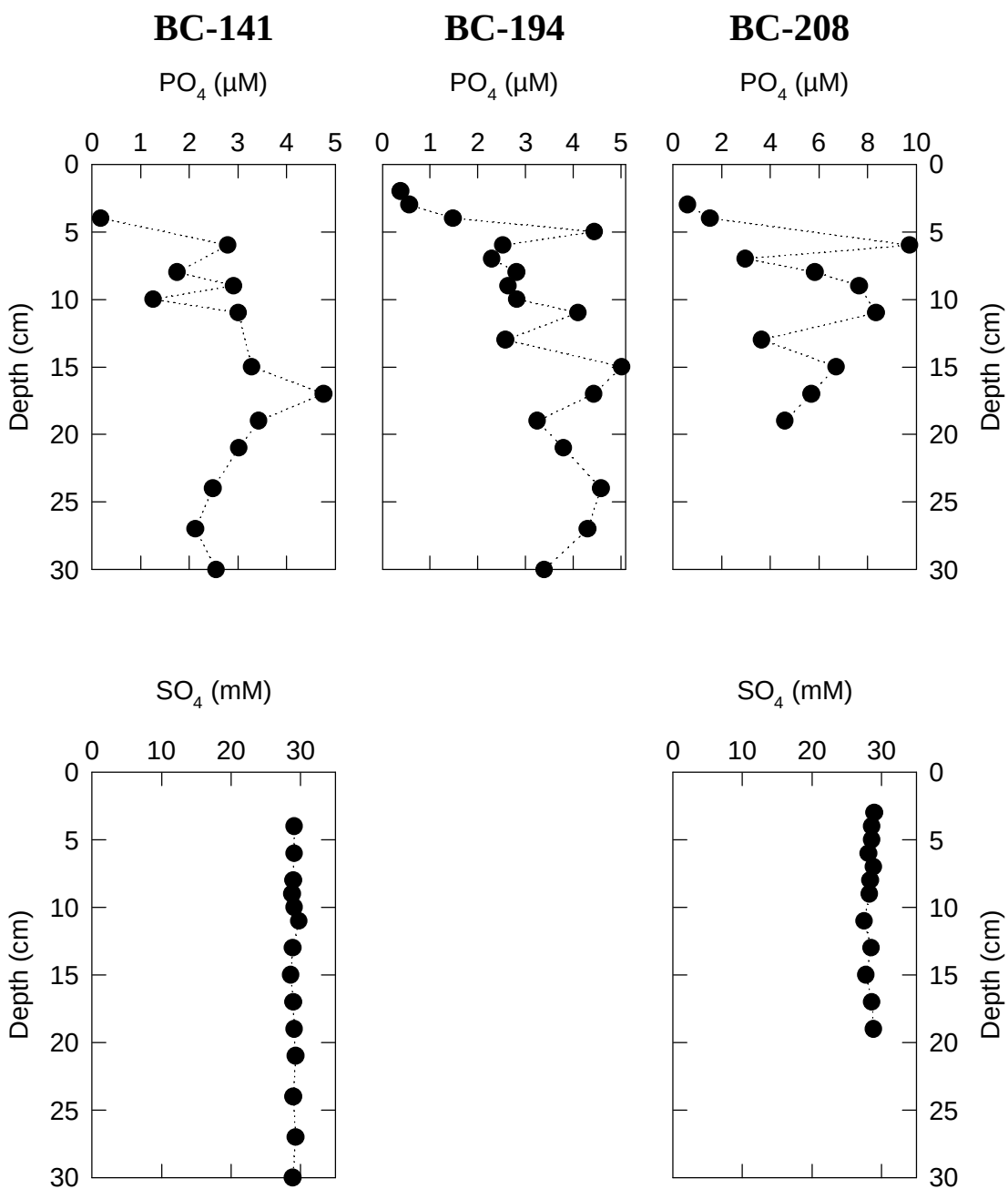
BC-141
BC-194
BC-208
PO4 (µM)
SO4 (mM)
Depth (cm)

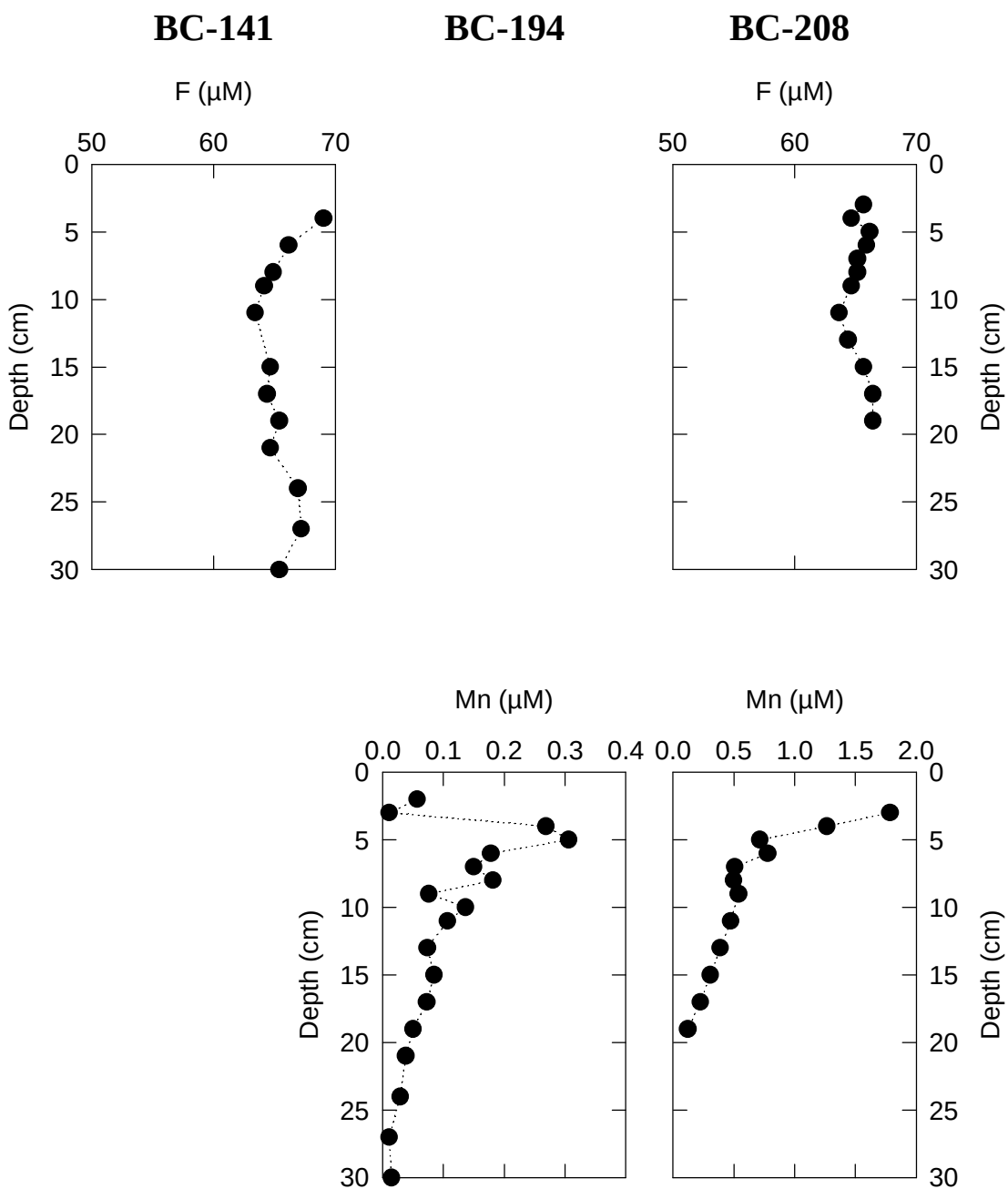

Figures: Dissolved phosphate, sulfate, fluoride and manganese in pore waters from the Dry Tortugas and Marquesas Keys.

2.18 Variability of Seabed Sediment Microstructure and Stress-Strain Behavior in Relation to Acoustic Characteristics (Principal Investigators: A.J. Silva, G.E. Veyera, M.H. Sadd and H.G. Brandes)

Variability of Seabed Sediment Microstructure and Stress-Strain Behavior in Relation to Acoustic Characteristics

Armand J. Silva, George E. Veyera and David R. Brogan

Marine Geomechanics Laboratory
University of Rhode Island
Narragansett, RI 02882

INTRODUCTION

This is the fourth annual report, covering activities during FY96 of the University of Rhode Island, Marine Geomechanics Laboratory (URI/MGL) research program as part of the Coastal Benthic Boundary Layer Special Research Program (CBBL SRP) sponsored by the Office of the Naval Research (ONR) and managed by the Naval Research Laboratory (NRL), Stennis Space Center, MS, with Michael D. Richardson as Chief Scientist. The focus of the URI/MGL program is on the variability of sediment geotechnical properties and microstructure with particular emphasis on stress-strain behavior and modeling in relation to geoacoustic characteristics.

During FY96, research activities at the MGL included: continued laboratory testing (triaxial compression; triaxial acoustic; geotechnical index properties) of calcareous sediments from the Key West sites; analysis and synthesis of laboratory and field data obtained to date (Baltic Sea; Panama City, FL; and Key West); and preparation of several manuscripts, theses, and reports. This report summarizes our activities for the period of October, 1995 through September, 1996.

FACILITIES

Equipment development and refinement has continued and various significant improvements have resulted in several state-of-the-art testing systems for studying the broad range of sediments collected from the three CBBL study sites. We are continuing our investigation of the geotechnical behavior and acoustic response of sediments from the different CBBL study sites which will be completed in FY97.

Triaxial Testing System:

A major technical accomplishment has been the refinement and improvement of our existing triaxial compression testing system for marine sediments. Specialized testing procedures have also been developed. The current system includes flow pumps for consolidation and permeability measurement and an electronic volume change device. Additional modifications and improvements are summarized below.

•*Submersible Internal Load Cell:* An important improvement to the triaxial testing system has been the incorporation of a submersible internal load cell for measuring axial load during testing. Two load cells have been purchased, with capacities of 44.5 N (10 lb) and 445 N (100 lb) to cover the range of strengths expected during testing. The internal load cells provide improved axial load measurement capabilities particularly for soft sediments.

•*Non-Contacting Radial Deformation Transducers:* A specially designed triaxial cell, fitted with non-contacting radial displacement transducers, has been incorporated into the triaxial testing system. The transducers provide radial deformation measurements at three locations (120^o apart in the same plane) on a sample. The system has been used in testing of sediments from the Key West site.

•*Geoacoustic Triaxial Testing System:* A digital storage oscilloscope was purchased to complete the geoacoustic triaxial system which is now fully operational and is being used to test carbonate sediments from the Key West site. This testing new system allows us to study sediment geoacoustic response(both compressional and shear wave loadings) under a variety of controlled laboratory conditions which simulate those found in situ. Specialized specimen preparation techniques and testing methodologies for acoustic testing of carbonate sediments have also been developed at the MGL.

PERSONNEL

During FY96, the MGL research personnel working on the project included: a) Principal Investigator and Project Director, A.J. Silva (Ocean and Civil Engineering); b) two Co-P.I.'s, G.E. Veyera (Civil and Environmental Engineering), and H.G. Brandes (Ocean Engineering); c) a laboratory manager, D. Brogan; d) three graduate students; A. Ag, P. Pizzimenti, and G. Sykora; e) two part-time undergraduate research assistants; f) a part-time administrative assistant; and g) various other technical support staff.

GEOTECHNICAL EXPERIMENTAL PROGRAM

Key West Sites

Core Processing and Physical Properties: Shelby tubes used to subsample box cores (BC) 284-BC and 324-BC recovered during the Key West campaign were processed. Additional consolidation and triaxial samples were obtained from these cores for laboratory testing. Vane shear measurements indicate undrained shear strengths ranging from 2 to 18 kPa in the upper 25 cm. Sensitivity measurements were made using undisturbed and remolded samples. Results showed sensitivities typically between 7 and 16 indicating the sediments are highly sensitive.

Physical property testing continued on several samples from gravity cores (GC) 178-GC, 199-GC, 211-GC, 213-GC, 214-GC, 232-GC, 257-GC, 269-GC, 285-GC, 301-GC, 313-GC, 321-GC and 326-GC (Table 1). Measured specific gravities range from 2.73 to 2.90 with most values near 2.80. Liquid limits (LL) range from 33 to 52 and plasticity indices (PI) from 4 to 25 (ASTM D-4318), excluding core 326-GC. Many of the samples were nonplastic and limits could

not be determined. Grain size analyses (sieve analysis (ASTM D 422) for the coarse fraction; the pipette method (Folk, 1974) for the fine fraction) were performed on several samples from various cores. The mean grain size of the Key West sediments ranges from 0.07 mm to 0.57 mm with an average mean grain size of about 0.14 mm.

Consolidation and Permeability: Constant rate of deformation (CRD) compressibility tests and permeability tests were performed on eighteen (18) samples from cores 178-GC, 313-GC and 326-GC at depths ranging from the upper 15 cm down to 230 cm. The compression data (Table 2) show that the sediments have very low compression indices (0.15 to 0.50) and recompression indices (0.01 to 0.05). The stress state ratio (preconsolidation stress normalized with effective overburden stress) for the samples ranges from about 1 to 63 reflecting the possibility of cementation and/or interparticle bonding. The permeabilities are relatively large for the very low void ratios of the samples and showed a linear relationship between void ratio and logarithm of permeability. In situ void ratios were determined from water content measurements on the samples and range from 1.0 to 1.8. Measured permeabilities range from 0.6×10^{-6}cm/s to 6.0×10^{-6}cm/s. A sample from core 313-GC at 147-151 cm depth was remolded to its original void ratio and retested. Remolding altered the sediment structure significantly as the compression index changed from 0.21 to 0.14 and the permeability changed from 4.6 to 0.6×10^{-6} cm/s (Figure 1).

Strength Testing: Seventeen (17) isotropically consolidated undrained (CIU) strength tests were performed on Key West sediments from cores 284-BC and 324-BC from the Dry Tortugas test site (Table 3). Eight (8) undisturbed samples were tested and nine (9) other samples were remolded prior to testing to study the influence of cementation, particle crushing and grain angularity. The strength behavior of these sediments is typical of uncemented calcareous sediments and loose sands. During shear, the strength response is stiff while large positive pore pressures are developed. The maximum effective stress ratio was used as the failure criteria which occurred at large axial strains of 11% to 12%. The resulting friction angles ranged from 37^{o} to 39^{o} for both undisturbed and remolded samples. For undisturbed samples (Figure 2), stress path characteristics during shear suggest initial cementation and restriction of particle movements (mobility), while for remolded samples (Figure 3), stress paths behavior indicates a degree of particle rearrangement due to a looser fabric. Grain size analyses were performed on undisturbed and remolded samples before and after shear. Results show that there was no significant particle degradation (crushing) due to remolding or during shear. Initial tangent moduli range from 130 to 18,873 kPa and are exponentially dependent upon the initial effective stress (Figure 4). It does appear that interlocking of the highly angular grains occurs with increasing effective stress. From elastic analysis, these moduli underpredict the compressional wave speed of the sediments.

Acoustic Testing: Preliminary isotropically consolidated undrained strength tests incorporating compressional and shear wave speed measurements were conducted on undisturbed samples from core 188-GC (Table 4). Compressional wave speeds (150 kHz) are on the order of 1,493 to 2,013 m/sec within an effective stress range of 0.3 to 17.5 kPa (Figure 5). It was not possible to obtain shear wave velocities in these samples which appears most likely due to the effects of large shells as well as the sample length. Additional measurements were made on sediment from core 188-GC at 98-112 cm depth which was reconstitued with all shells removed. Results gave slightly higher compressional wave speeds as compared with data from

the undisturbed samples. In addition, shear wave speed measurements were also made on the remolded samples, averaging 246 m/sec (at 10 kHz) and 129 m/sec (at 2.5 kHz) during consolidation and shear, respectively (Figure 6). This sample was then shortened 5 cm from its original length to 6.4 cm and consolidated. The average compressional and shear wave speeds are 1,492 m/sec and 82 m/sec, respectively. All results show a general increase in wave speed with an increase in effective stress. Improvements to shear wave signal quality have been made by shortening the sample, using a frequency of 2.5 kHz and embedding the transducers in a thin layer of Ottawa sand to improve acoustic coupling.

Modeling

Geoacoustic Micromechanical Modeling: Micromechanical modeling has been conducted in order to provide an understanding of how particular sediment microstructure or fabric effects the propagation of acoustic signals. Using discrete element simulations, specific propagational characteristics including wave speed and attenuation have been related to particular fabric configurations for granular sediments. The research has direct implications to acoustic characteristics.

This part of our program received separate funding for FY96. Details of the work performed can be found in the FY96 year end report by Sadd and Dvorkin (1996).

Macrostructural Finite Element Modeling: The objective of this portion of the program has been to develop a numerical capability for predicting the macrostructural, mechanical behavior of sediments that are of interest to the CBBL SRP. The results of our work indicate that the soft, fine-grained Baltic sediments are best treated using time-dependent plasticity-based critical state models, whereas for the coarse grained sands from the Panama City, FL site, a time-independent elastic model is probably more appropriate. Test results for Key West sediments have shown these materials to be very stiff possessing some degree of cementation and/or high interparticle bonding. The behavior of the Key West sediments would support the use of an elasto-plastic constitutive model which will be further investigated as testing is completed in FY97.

SUMMARY AND CONCLUSIONS

The fourth year (FY96) of our research has been extremely busy and productive for the URI/MGL portion of the CBBL program. The Key West carbonate sediments have been the primary focus of the geotechnical/acoustic work during FY96. Highlights of our recent work are summarized in this report and in publications listed below.

The Key West sediments are approximately 90% carbonate. The triaxial compression strength behavior of these sediments is typical of uncemented calcareous sediments and loose sands. These sediments have high friction angles (37^o to 39^o) for both undisturbed and remolded samples which may be caused by cementation and/or very high interparticle bonding. Strength testing results indicate that the sediment stress-strain behavior is strongly influenced by grain compressibility, grain mobility and the unique characteristics of the carbonate materials themselves. Triaxial testing is being continued in conjunction with acoustic wave speed measurements to further investigate these sediments.

Preliminary data from the acoustic triaxial system indicate that the wave propagation characteristics of the Key West sediments are affected by the applied effective stress, grain compressibility, bulk density and grain density. Also, the presence of shells and shell fragments was seen to influence the results. Further geoacoustic testing is currently underway to examine the relationship between sediment characteristics, sediment behavior and acoustic response and answer some of the questions which arose during initial testing.

Development of physical and acoustic properties profiles for the Dry Tortugas and Marquesas sites has been continued and will be completed in FY97. The results will be useful in correlating vertical variability with subbottom acoustic characteristics.

The micromechanical modeling aspect of our work was funded separately during FY96 and is being conducted by Sadd and Dvorkin (1996).

Constitutive model development for the Baltic, Panama City, FL and Key West sediments is continuing and related laboratory testing to determine the appropriate model parameters is ongoing.

PUBLICATIONS

Manuscripts and Abstracts

Brandes, H.G. and Silva, A.J. (1998) “Geotechnical Investigations of Calcareous Sediments from Two Shallow-Water Sites in the Florida Keys,” 2nd Int’l Conf. on Engrg. Properties of Calcareous Sediments, Bahrain, March (Abstract Submitted 8/96).

Silva, A.J. and Brandes, H.G. (1997) “Geotechnical Properties of High-Porosity Organic Sediments from Eckernförde Bay, Germany,” XIVth Int’l Conf. on Soil Mech. and Fndtn. Engrg., Hamburg, Germany, May (In Press).

Silva, A.J., Brandes, H.G. and Veyera, G.E. (1996) "Geotechnical Characterization of Surficial High Porosity Sediments in Eckernförde Bay", Geo-Marine Letters, 16: 167-175.

Brandes, H.G., Silva, A.J., Ag, A. and Veyera, G.E. (1996) "Consolidation and Permeability Characteristics of Surficial High Porosity Sediments of Eckernförde Bay,” Geo-Marine Letters, 16: 175-181.

Brandes, H.G., Silva, A.J. (1996) “Research Progress Report, January, 1996,” Technical Report to NRL-SSC (M.D. Richardson and S. Tooma), January, 34 p.

Silva, A.J., Veyera, G.E., Sadd, M.H., and Brandes, H.G. (1995) “Variability of Sediment Microstructure and Stress-Strain Behavior in Relation to Acoustic Characteristics - NRL CBBLSRP.” *FY95 Year-End Report to NRL-SSC,* Grant No. N-000149316007, Dec., 10 p.

Theses and Dissertations

Pizzimenti, P.B. (1996) "Stress-Strain Behavior of Surficial Carbonate Sediments from Key West, Florida,” Thesis submitted in partial fulfillment of the requirements for the Master of Science degree, Dept. of Ocean Engrg., Univ. of RI, Dec., 175 p.

Table 1. Physical Properties of Sediments from the CBBLSRP Key West Test Sites

Sample Designation	Location	Number of Samples	Specific. Gravity	Liquid Limit (%)[a]	Plasticity Index	Mean Grain Size (mm)
166-GC	M	5	2.87 2.85-2.90	43 35-43	12 8-17	-
178-GC	M	6	2.80 2.76-2.83	44 39-53	18 12-25	0.08 0.07-0.11
182-GC	M	5	2.78 2.75-2.80	44 43-46	16 13-20	-
192-GC	M	7[b]	-	40 38-44	13 9-18	-
211-BC	M	2	-	49 45-52	14 11-16	-
213-GC	M	4	2.80 2.79-2.81	47 46-48	19 14-23	0.09
214-GC	D	5[c]	2.81	40 38-42	6 4-7	0.11
216-BC	D	4	2.80	41 39-45	6 4-8	-
232-GC	D	1	2.85	-	NP	0.23
257-GC	D	1	2.86	-	-	-
269-GC	D	1	2.77	-	-	-
285-GC	D	2	2.85 2.83-2.86	-	NP	-
301-GC	D	1	2.80	-	NP	-
313-GC	D	9[d]	2.79 2.73-2.82	36 33-39	12 9-15	0.25 0.17-0.57
321-GC	D	3	2.84	-	NP	-
326-GC	R	8	2.77 2.71-2.83	49 45-56	20 15-31	0.08 0.07-0.11

Note:

M-Marquesas
D-Dry Tortugas

BC-Box Core
GC-Gravity Core
R-Rebecca Shoals

ratios = average / (min-max)

a-Corrected for 35 ppt salinity
b-Limits of two samples could not be determined
c-Limits of three samples could not be determined
d-Limits of six samples could not be determined
NP-No plastic limits could be determined

Table 2. Summary of Consolidation and Permeability Test Results for Key West Sediments

Sample[a]	Depth (cm)	Water Content (%)[b]	Compression Index, C_c	Recompression Index, C_r	Preconsolidation Stress, σ'_c (kPa)	Overburden Stress, σ'_o (kPa)	SSR	Permeability, k ($\times 10^{-6}$ cm/s)[c]
178-GC	11-16	44	0.22	0.02	4.3	1.0	4.3	-
	26-31	-	0.34	-	7.0	2.1	3.3	1.3
	54-59	63	0.40	0.02	10.0	4.1	2.5	0.7
	82-87	59	0.50	0.04	9.5	5.9	1.6	1.3
	181-186	53	0.26	0.01	11.0	13.0	0.9	-
	208-213	46	0.25	0.02	12.0	15.0	0.8	0.7
313-GC	5-9	49	0.25	0.01	30.0	0.5	62.5	5.5
	17-21	43	0.15	0.05	9.0	1.3	6.8	2.5
	45-49	42	0.23	0.01	72.0	3.6	20.3	6.0
	81-85	36	0.17	0.01	165.0	6.6	25.2	-
	147-151	35	0.21	0.01	64.0	12.3	5.2	4.6
R	147-151	35	0.14	0.01	-	-	-	0.6
	181-185	38	0.17	0.01	8.5	15.2	0.6	-
326-GC	10-14	41	0.16	0.02	6.0	0.8	7.5	5.5
	45-53	44	0.25	0.01	3.6	2.4	1.5	-
	79-83	53	0.38	0.01	8.6	6.4	1.4	3.9
	174-178	66	0.46	0.02	9.5	11.6	0.8	1.2
	229-233	48	0.39	0.02	28.0	17.2	1.6	-

Note:
R - Remolded
a - 178-GC - Marquesas Site; 313-GC and 326-GC - Dry Tortugas Site
b - corrected for 35 ppt salt content
c - at in-situ void ratio from e-log k plots

Table 3. Summary of Box Core Triaxial Compression CIU Strength Tests of Key West Sediments, Dry Tortugas Site

Core No.	Sample Depth[a] (cm)	Void Ratio e	Consol Stress p'_o (kPa)	Failure Strain ε_f (%)	Failure Eff. Stress Ratio	Failure Deviator Stress (kPa)	Pore Pr. Parameter A_f	Initial Tangent Modulus[b] E_i (kPa)
284	2-13 U	1.2	31.7	11.6	3.9	51.4	0.27	-
284	2-15 R	1.0	34.0	11.8	4.3	58.0	0.33	18873
284	2-13 U	1.1	16.0	12.7	3.9	28.6	0.22	6077
284	2-17 R	1.3	13.9	11.6	4.0	13.9	0.50	6981
284	2-13 U	1.1	15.0	10.5	4.4	21.7	0.39	4444
284	2-13 R	1.1	16.5	11.4	4.4	32.3	0.23	-
284	3-14 U	1.2	2.4	6.9	5.9	9.2	0.05	2077
284	3-16 R	1.2	2.2	11.9	6.1	3.3	0.39	530
284	9-11 R	1.0	1.8	11.1	8.4	6.6	0.14	650
324	1-12 U	1.3	29.6	11.7	4.4	34.0	0.57	11125
324	1-14 R	1.2	28.2	13.0	3.9	25.5	0.75	12444
324	1-12 U	1.3	10.5	11.7	4.3	18.4	0.27	3988
324	0-15 R	1.2	10.0	11.0	4.8	20.0	0.24	3879
324	3-14 U	1.3	8.3	9.2	4.2	17.6	0.15	2397
324	3-17 R	1.2	6.2	17.2	4.1	11.7	0.21	-
324	2-13 U	1.4	1.5	14.0	5.8	3.7	0.19	130
324	0-13 R	1.4	1.2	20.5	40.0	2.7	0.44	166

Note:
a -"U" and "R" denote undisturbed and remolded samples, respectively
b - Initial tangent modulus using Konder's (1963) method

Table 4. Summary of Triaxial Compression CIU Strength Tests and Acoustic Wave Speeds of Key West Sediments from Core 188-GC

Sample[a]	Sample Depth (cm)	Consol Stress p'_o (kPa)	Failure Strain ε_f (%)	Failure Eff. Stress Ratio	Failure Deviator Stress (kPa)	Pore Pr. Parameter A_f	Avg. Compressional Wave Speed[b] (m/sec)	Avg. Shear Wave Speed[c] (m/sec)
U	98-112	14.9	2.0	13.6	28.0	0.33	1565/1829	-
	137-151	22.0	2.0	11.0	15.0	0.75	1518/1518	-
RC	98-112	28.0	11.0	4.2	12.0	-	1623/1633	246[d]/129
Short	102-108	29.0	-	-	-	-	1492	82

Note:
a - U=Undisturbed, RC=Reconstitued from original samples with shells removed, 6 cm sample not sheared
b - Run at 150 kHz, see Figure 6. Wave speed during consolidation / wave speed during shear
c - Run at 2.5 kHz, see Figure 7. Wave speed during consolidation / wave speed during shear
d - Run at 10 kHz

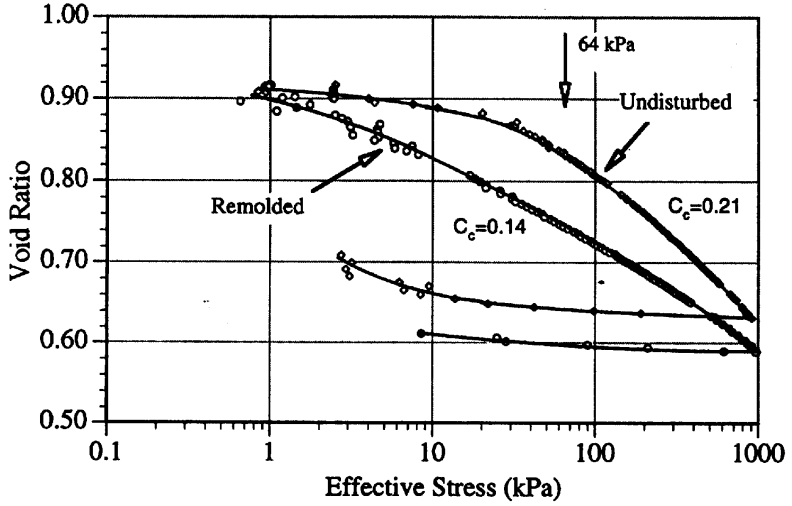

(a) Compression Curve

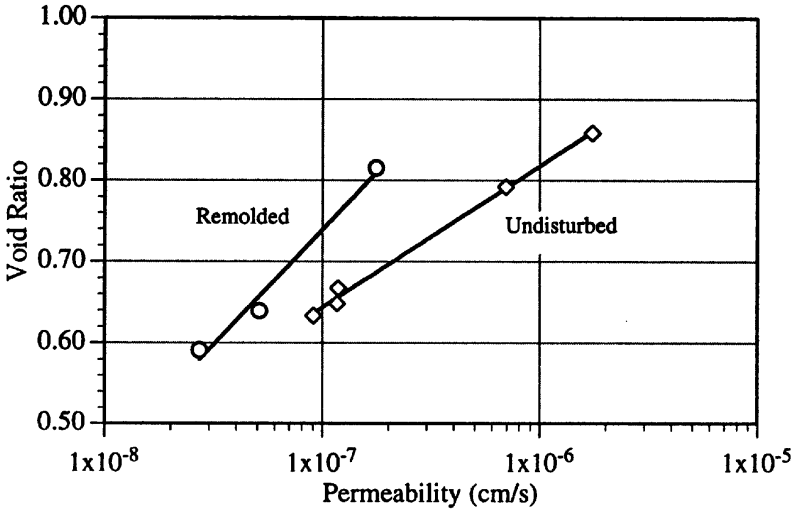

(b) Permeability Measurements

Figure 1. CRD Consolidation/Permeability Tests, Core 313-GC; 147-151 cm, Dry Tortugas Site

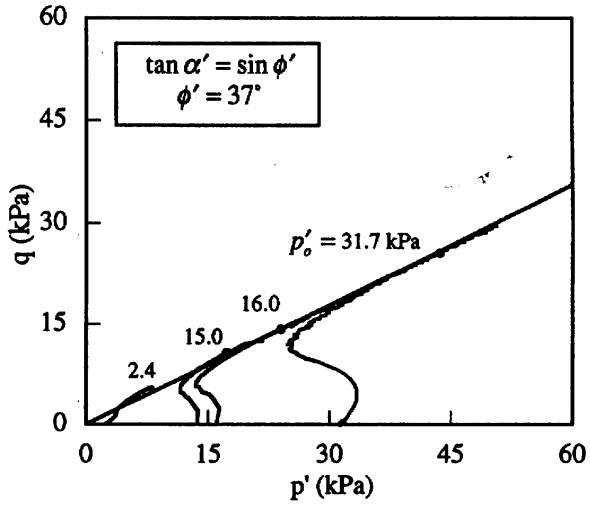

(a) Core 284-BC

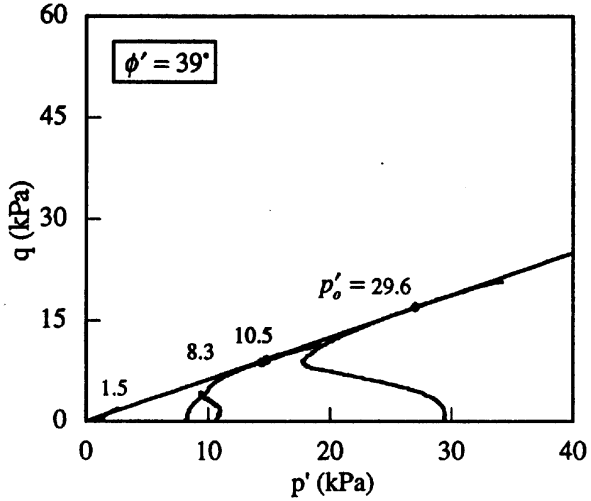

(b) Core 324-BC

Figure 2. Failure Envelopes of Undisturbed Sediment Samples from Dry Tortugas Site (CIU Triaxial Tests)

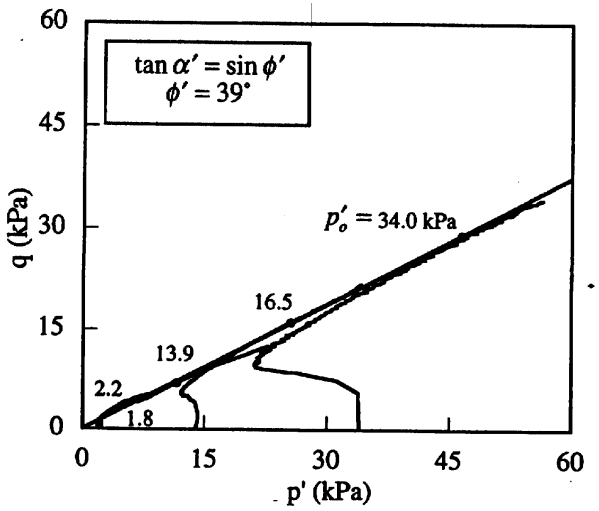

(a) Core 284-BC

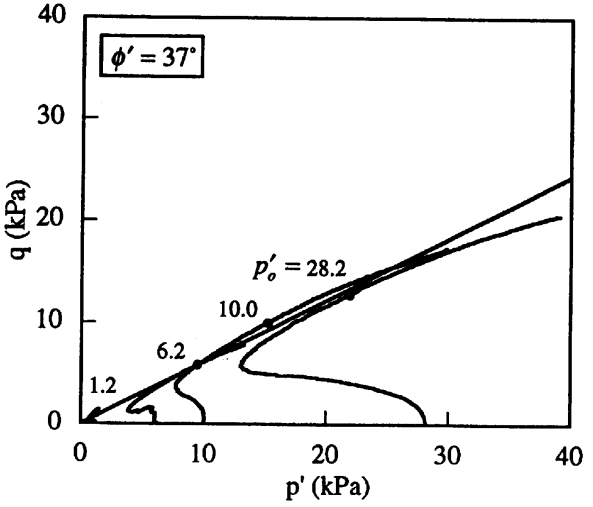

(b) Core 324-BC

Figure 3. Failure Envelopes of Remolded Sediment Samples from Dry Tortugas Site (CIU Triaxial Tests)

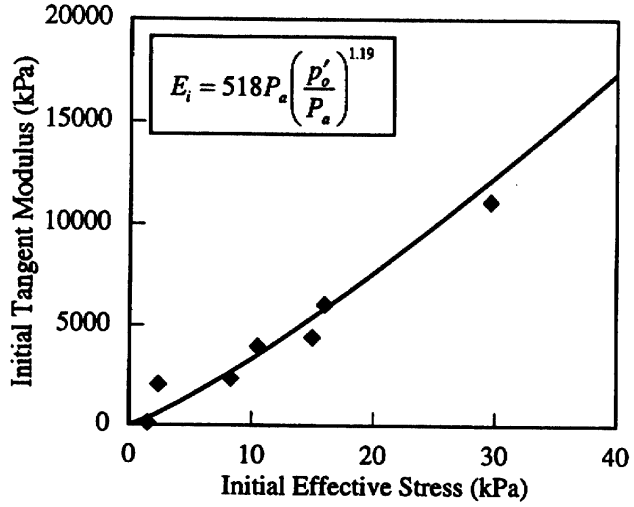

(a) Undisturbed Samples

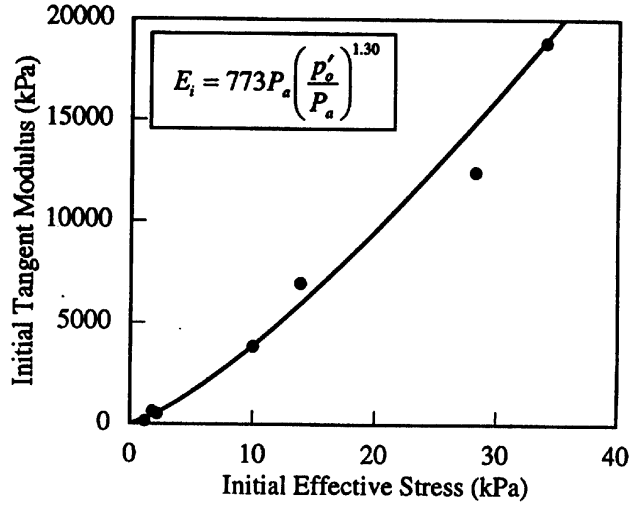

(b) Remolded Samples

Figure 4. Variation of the Initial Tangent Modulus with Initial Effective Stress in Sediments from the Dry Tortugas Site

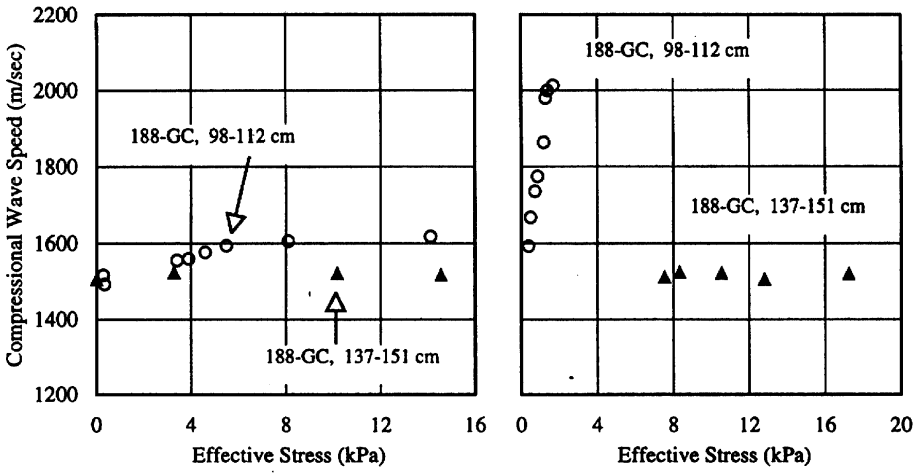

(5a) Undisturbed Samples During Consolidation (150 kHz)

(5b) Undisturbed Samples During Shear(150 kHz)

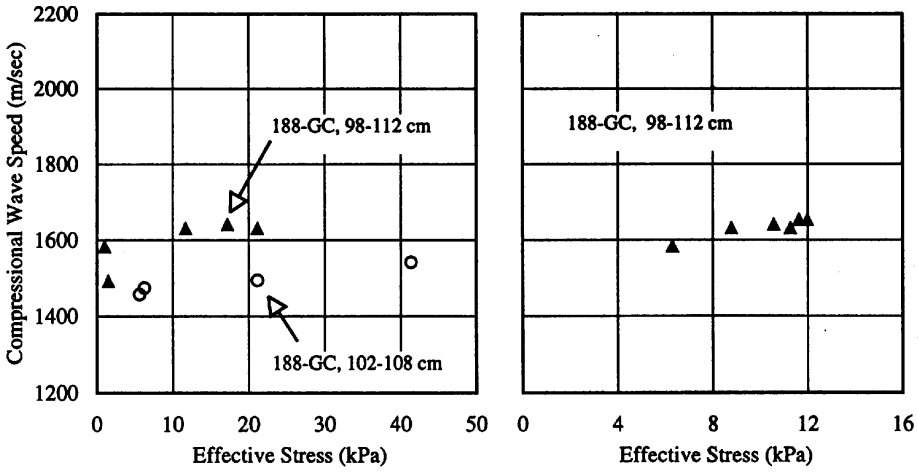

(5c) Reconstituted Samples During Consolidation (150 kHz)

(5d) Reconstituted Samples During Shear (150 kHz)

Figure 5. Laboratory Compressional Wave Speed Measurements for Sediments from Marquesas Site

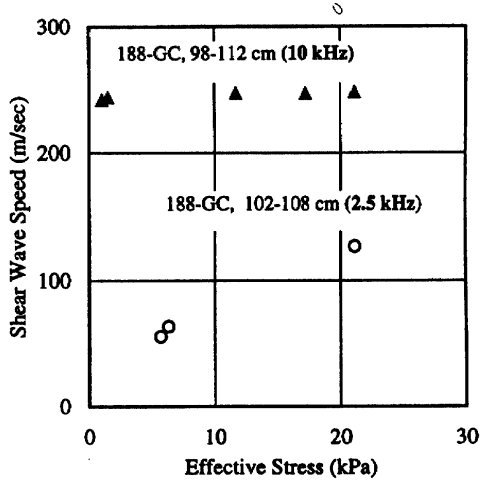

(6a) Reconstituted Samples During Consolidation

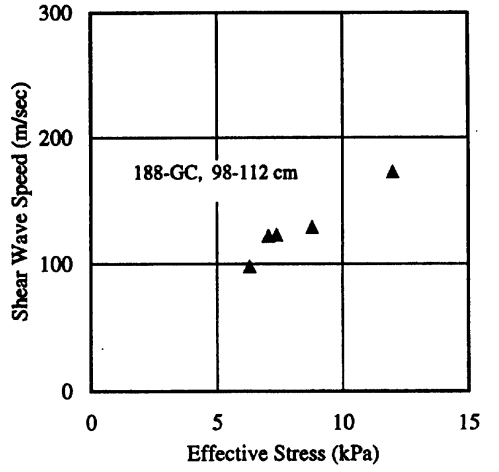

(6b) Reconstituted Sample During Shear (2.5 kHz)

Figure 6. Laboratory Shear Wave Speed Measurements for Sediments from Marquesas Site

2.19 Experimental and Theoretical Studies of Near-Bottom Sediments to Determine Geoacoustic and Geotechnical Properties (Principal Investigator: R.D. Stoll)

Experimental and Theoretical Studies of Near-Bottom Sediments to determine Geoacoustic and Geotechnical properties

Robert D. Stoll
Lamont-Doherty Earth Observatory
Palisades, New York 10964

INTRODUCTION

Our participation in the CBBL program during FY96 was limited to the preparation of a paper for submission to the journal Continental Shelf Research entitled "Using the Biot Theory to establish a Baseline Geoacoustic Model for Seafloor Sediments," by Robert D. Stoll and Edgar O. Bautista and continuing analysis of new field data obtained using the seafloor cone penetrometer developed early in the program.

CONTINENTAL SHELF RESEARCH PAPER

The main objective of this paper was to demonstrate how the Biot theory could be used to model soft, gassy sediments such as those found in Eckernförde Bay. In particular, we wished to establish a theoretical baseline model that would predict velocity and attenuation of the gas-free sediment which could then be perturbed in such a way that the effects of various distributions of gas bubbles could be studied. In the case of the Eckernförde sediments, preliminary calculations showed that global relative motion between pore fluid and sediment frame was relatively unimportant because of the sediment's low permeability. As a result, the sediment behaves essentially as a "closed system" (as in the Gassmann model) and so is controlled by a single complex modulus that reflects the combined effects of the bulk modulus of the fluid, the bulk and shear moduli of the skeletal frame in a water environment, and the bulk modulus of the individual grains, all of which are potentially complex and frequency dependent.

The input parameters for the Biot model were chosen on the basis of the extensive experimental data obtained during experiments carried out by a number of investigators under the CBBLSRP during the period from 1992 to 1995. Our contribution to the data base was the measurement of shear wave velocity and attenuation using Love waves generated by a new torsional source developed early in the program (details are given in Stoll et al (1994) and Bautista and Stoll(1995)). The low-frequency complex shear modulus in the upper meter or so of sediment was derived from an analysis of the velocity and attenuation of the Love waves generated by this source. Unfortunately there is no data on shear wave propagation available in the higher frequency ranges. In contrast, compressional wave velocity and attenuation was measured at 58 kHz and 400 kHz but no low frequency data is available. Thus our task was to fit

a model to an incomplete data set and so there is still considerable uncertainty about the "best" rheological model for this kind of high porosity medium over a wide frequency range.

The attenuation predicted by the model used as an example in the paper is shown in Fig. 1. At low frequencies the attenuation falls within the range of values measured by various investigators in fairly recent experiments. This range is significantly below the original "Hamilton band" which was used to justify the assumption of a linear dependence of attenuation on frequency or a constant "Q" for all types of sediment. As can be seen from Fig. 1, this assumption is clearly not justified if one wishes to build a model that will adequately bridge the gap from low to high frequencies. In our example we chose a viscoelastic model (a 4 parameter Cole-Cole model) for the bulk modulus of the skeletal frame which reflects the effects of local fluid motion in such a way that both low and high frequency predicted response of the overall model falls within the ranges of observed behavior.

NEW CONE PENETROMETER DATA

Since the initial development of our seafloor cone penetrometer at the beginning of the CBBL program, several new improved models have been built and this apparatus has become one of our most important tools for studying in-situ sediment properties. We have used the penetrometer to measure "ground truth" properties in many sediments ranging from soft mud to compact sands in the Mediterranean, Baltic, and Black seas, in the Gulf of Mexico and in the New York harbor area. In addition to using the cone penetrometer during the CBBL field work in Eckernförde and the Gulf of Mexico, we have deployed it many times during testing of an expendable seafloor penetrometer in a cooperative project with SACLANT Undersea Research Center. Our objective in all cases has been to establish "ground truth" regarding the in-situ shear strength of the sediment so that correlations could be made with other basic properties such as porosity and shear-wave velocity or maximum shear modulus. This is an ongoing project and much of our field data still needs to be analyzed.

Fig. 2a shows some preliminary results wherein maximum shear modulus derived from in-situ measurements of shear wave velocity are compared with cone penetration resistance. The solid line in this figure is the extension of a least squares fit to a large population of data points obtained by Mayne and Rix (1993) for 31 clay sites where both in-situ shear-wave velocity measurements and profiles of cone tip resistance have been measured. Fig. 2b is their plot of data from the 31 sites. As can be seen from Fig. 2a, most of our data was obtained for softer materials where the value of cone resistance, Q_c, is less than 100 kPa. Nevertheless, the extension of the regression curve derived by Mayne and Rix appears to fit our data quite well.

REFERENCES

Bautista, E. O. and Stoll, R. D. (1995) "Remote Determination of In-situ Sediment Parameters using Love Waves," J. Acoust. Soc. Am., 98, pp.1090-1098.

Mayne, P. W. and Rix, G. L. (1993) "G_{max}- q_c Relationships for Clays," Geotechnical Testing Journal, 16, No. 1, pp.54 - 60

Richardson, M. D. and Briggs, K. B. (1995) “The Effects of Methane Gas Bubbles on the Sediment Geoacoustic Properties in Eckernförde Bay,” Proc. Workshop Modelling Methane-Rich Sediments of Eckernförde Bay, Ed. T. Wever, pp.199-206.

Stoll, R. D., Bautista, E. O., and Flood, R. (1994) “New Tools for Studying Seafloor Getechnical and Geoacoustic Properties,” J. Acoust. Soc. Am.,96, 2937-2944.

Stoll, R. D. and Bautista, E. O. (1996)”Using the Biot Theory to Establish a Baseline Geoacoustic Model for Seafloor Sediments,” submitted to Continental Shelf Research.

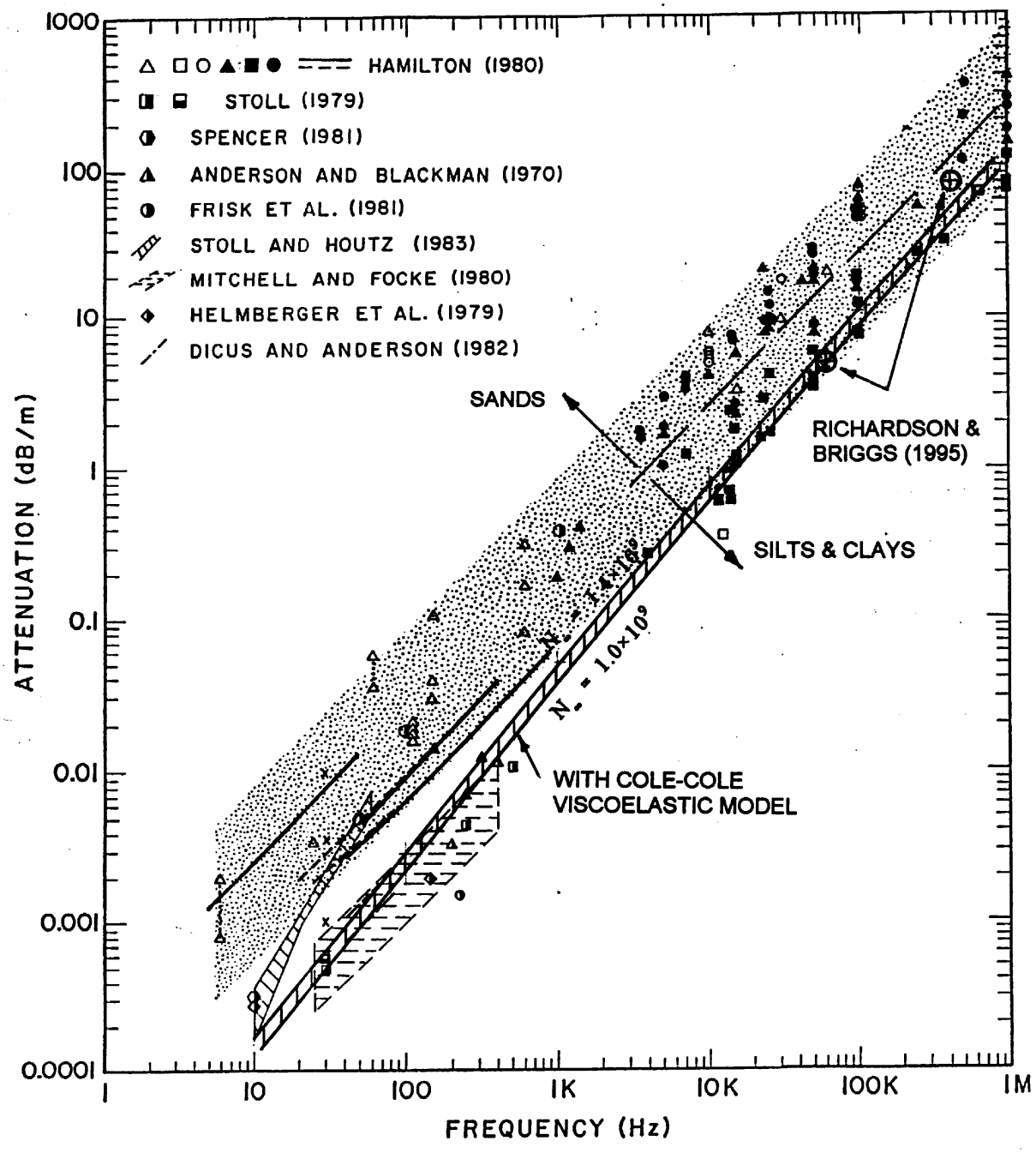

Fig. 1. Compressional-wave attenuation versus frequency. Historical data from Hamilton (1980) plus some newer data at low frequencies. Eckernfoerde data at 58 and 400 kHz from Richardson and Briggs (1995) is also shown. Cross-hatched band is example of model prediction with Cole-Cole viscoelastic modification included.

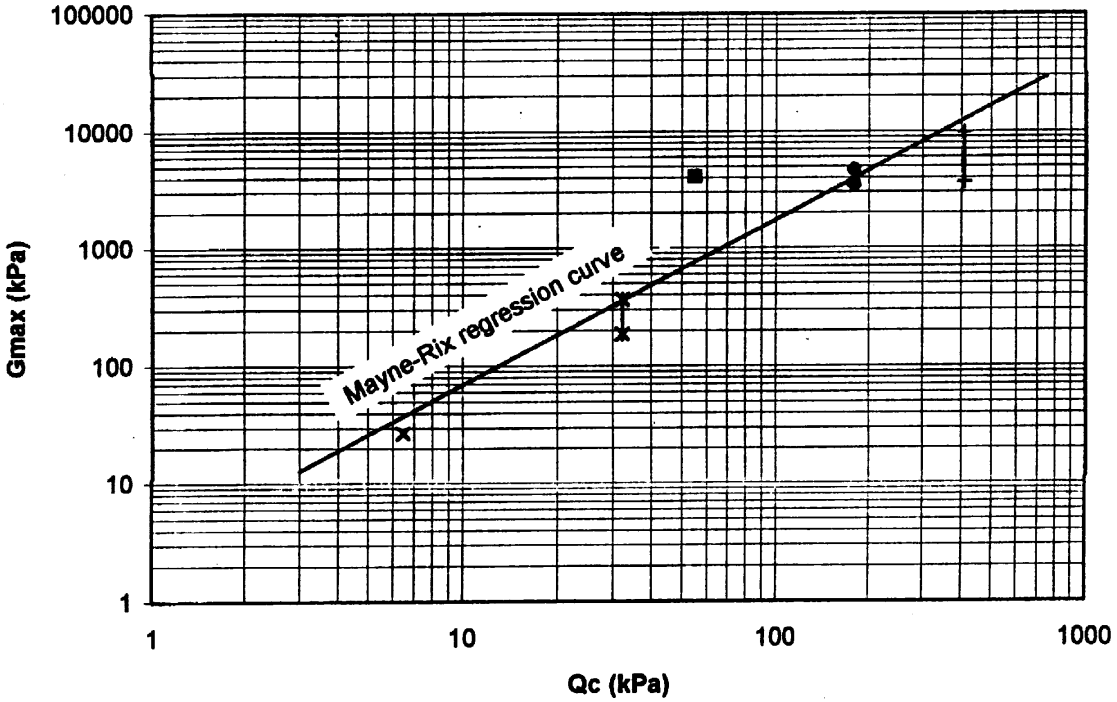

Fig. 2a. Maximum shear modulus, G_{max}, calculated from measurements of shear-wave velocity versus cone penetration resistance. Shear-wave velocities from Love wave measurements and from measurements using NRL ISSAMS apparatus (Richardson, M., personal communication).

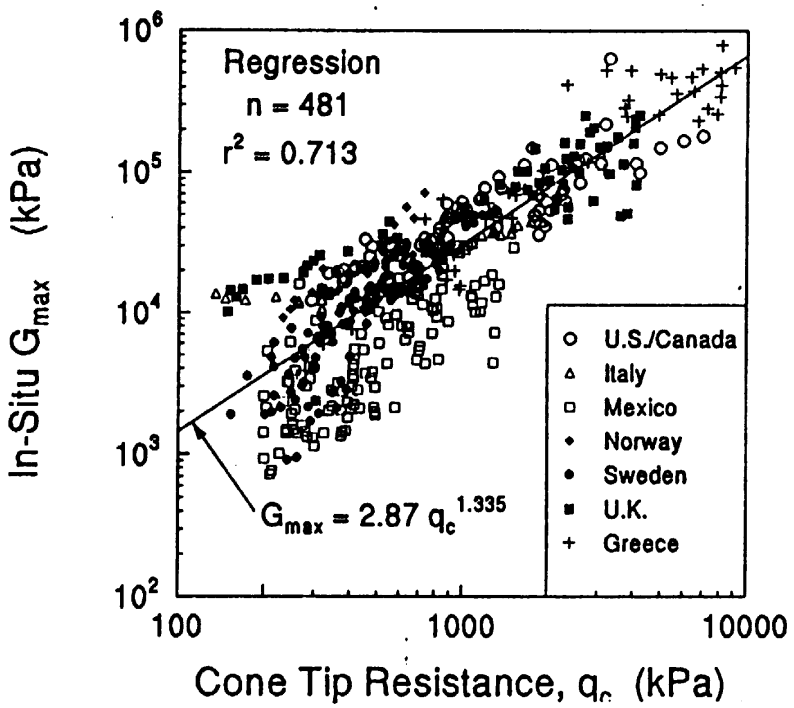

Fig. 2b. Apparent relation between initial tangent shear modulus (G_{max}) from in-situ measurements and cone tip resistance (q_c) for 31 clays located worldwide. (Mayne and Rix, 1993).

2.20 Characterization of Surficial Roughness and Sub-Bottom Inhomogeneities from Seismic Data Analysis (Principal Investigators: D.J. Tang and G.V. Frisk)

Dajun Tang* and George V. Frisk

Woods Hole Oceanographic Institution
Woods Hole, MA 02543

*Now at the Applied Physics Laboratory, University of Washington, Seattle, WA 98105

Objectives:

During the past year of the Coastal Benthic Boundary Layer Special Research program, we have continued our work on modeling scattering of sound waves by sediment bubbles. The data sets obtained in the experiment conducted at Eckernförde Bay, Germany, provided us the opportunity to study interactions of sediment bubbles and high-frequency acoustic scattering. Our objectives in this program are integrating various acoustic data with available environmental data, modeling the scattering processes in shallow water sediments. Our work completed in 1996 is a continuation of our efforts in the previous years. The emphasis is placed on the analysis and modeling of scattering by gassy sediments through multiple scattering.

Accomplishments:

During the past year, our primary work has been in the areas of developing a theory of high-frequency acoustic scattering from gassy sediments where multiple scattering is more than likely. The Eckernförde site features soft sediments where the sound speed in the top layer of sediment is slower than that in the water column near the bottom. In previous papers we found from analyzing high-frequency (40 kHz) scattered data from small grazing angle (5-20 degrees), a layer of scatterers are buried about a meter beneath the seafloor. These scatterers, treated as an equivalent surface scattering layer, have a relatively large backscattering strength of -10.8 dB. Coring and X-ray tomography analysis reveal methane gas voids of non-spherical shapes, which are clearly the dominant scatterers in this site. Usually, at small grazing angles, high-frequency acoustic waves are highly attenuated before reaching buried scatterers because the ray path traversed in the sediment is long. At the Eckernförde Bay, however, the combination of low attenuation and a slower bottom sound speed compared with that in the water column makes the scattering from the deeply buried gas voids measurable. It is interesting to notice that the estimated backscattering strength of -10.8dB is several decibels higher than that at a sandy site off Panama City, FL where bottom interface scattering is dominant. This is an indication that multiple scattering might be important. Based on a single scattering model we developed and used to interpret backscattered data, we extended the model to include bi-static scattering. The model was compared against bi-static scattering data obtained by Williams and Jackson of the Applied Physical Laboratory, University of Washington. While the simple model yielded very good comparison with data, energy conservation considerations pointed strongly to multiple scattering. In order to understand the multiple scattering phenomena, we used Foldy's general multiple scattering theory and conducted numerical simulations. Although this work is still on

going, it has shown that by including multiple scattering, the results so is promising. We tentatively conclude that by measuring in-sediment scattered field, we will be able to gain unambiguous information on multiple scattering and bubble resonance. Our multiple scattering work will continue in the next few years.

Publications:

D. Tang, G. Jin, D.R. Jackson and K.L. Williams, "Analyses of high-frequency bottom and sub-bottom backscattering for two distinct shallow water environments," J. Acoust. Soc. Am. Vol 65, 2930-2936 (1994).

D. Tang, C.J. Sellers, G.V. Frisk, and S.G. Schock, "Acoustic backscattering from methane gas voids buried in sediments," Proceedings of the Workshop, Modeling Methane-Rich Sediments of Eckernförde Bay, June 26-30 (1995).

D. Tang, "Modeling high-frequency acoustic backscattering from gas voids buried in sediments," Geo-Marine Letters, Vol. 16t, 261-265 (1996)

G. Jin and D. Tang, "Uncertainties of differential phase estimation associated with interferometric sonars," IEEE J. Ocean Engineering, Vol. 21, 53-63 (1996).

D. Tang, "A note on scattering by a stack of rough interfaces," J. Acoust. Soc. Am., Vol. 99, 1414-1418, (1996).

D. Chu, K.L. Williams, D. Tang and D.R. Jackson, "Modeling of bi-static scattering from sediment bubbles," J. Acoust. Soc. Am. (In press).

2.21 Observation of Bottom Boundary Layer Hydrodynamics and Sediment Dynamics in Eckernförde Bucht and the Gulf of Mexico off Panama City, Florida (Principal Investigators: L.D.Wright and C.T. Friedrichs)

L.D. Wright and C.T. Friedrichs

Virginia Institute of Marine Science
School of Marine Science
College of William and Mary
Gloucester Point, Virginia 23062

Summary of Work During the Period:

Effort in FY 1996 was focused on: (1) analysis and interpretation of field data collected off Key West in 1995, (2) submittal for publication of initial results from the Key West campaign, (3) further analysis and publication of results collected in Eckernförde Bay.

Objectives:

The overall objective of this ongoing study continues to be elucidation of temporal and spatial variability of the processes that form, modify and preserve sedimentary strata in a variety of shelf settings. In the specific case of the VIMS component of the larger multi-institutional effort, we have been addressing questions related to: (1) hydrodynamic forcings (benthic physical oceanography); (2) bed stress measurement, including the impact of near-bottom density stratification; (3) bed micromorphodynamics and roughness variations; (4) sediment resuspension; and (5) sediment flux divergence and bed level changes.

Eckernförde Bay:

Accomplishments:

Our efforts in Eckernförde Bay came to fruition in 1996 in the form of contributions to several peer reviewed journal articles. This year a paper on the sensitivity of bottom stress estimates to near-bed density stratification in Eckernförde Bay was accepted for publication by the Journal of Geophysical Research and will appear in early 1997. Over the past year we also collaborated with C. Nittrouer and D. Jackson on two papers submitted to the upcoming special issue of Continental Shelf Research on Modelling Methane-Rich Sediments. These papers address (i) oceanic processes and the preservation of sedimentary structure in Eckernförde Bay, and (ii) sonar observations of events in Eckernförde Bay.

Major Conclusions to date:

Friedrichs and Wright (CSR paper, 1995):

(1) The physical oceanography of Eckernförde Bay in April and May of 1993 appears to be dominated by a resonant internal seich forced, in turn, by a Baltic-wide barotropic seich.

(2) A simple two-layer analytic model explains the generation of these internal waves and accounts for velocities much larger than those otherwise predicted by barotropic processes.

(3) Turbidity events are associated this ~26-28 hour internal seich, but probably indicate advection of unconsolidated sediment flocs rather than local resuspension of the consolidated bed.

(4) Currents produced by the internal waves are sufficient to advect fine sediment into the bay, but internal wave breaking may limit stress levels to below that required for resuspension.

Friedrichs and Wright (JGR paper, in press):

(1) Eckernförde Bay also provides a natural laboratory for investigating the sensitivity of bottom stress and roughness measurements to density stratification.

(2) In central Eckernförde Bay, stratification causes overshooting of the classic logarithmic velocity profile, leading to a potential overestimate of bottom stress.

(3) Theoretical corrections successfully improve curve-fits and reduce estimates of stress and roughness to below the unreasonably high values predicted by simple log-profiles.

Jackson, Williams, Wever, Friedrichs and Wright (CSR paper, in review):

(1) Event-like changes in the acoustic signal are observed and shown to be caused by scatterers in the water column.

(2) The events do not correlate with seafloor current stress, temperature, or refraction due to stratification, but a strong correlation is seen with pressure at the seafloor.

(3) This indicates that gas ebullition due to pressure release may be the cause.

Nittrouer, Lopez, Wright, Bentley, D'Andrea and Friedrichs (CSR paper, in review):

(1) During fair-weather conditions import of sediment into central Eckernförde Bay is associated with internal waves; during storms, the erosion of shallow deposits provides sediment to deeper sites.

(2) Sediment is reworked to a limited depth (~1 cm) in the central basin of Eckernförde Bay by a pioneering community of benthic organisms which is maintained by seasonal hypoxia/anoxia.

(3) The very restricted thickness for the surface mixed layer and the substantial sediment accumulation rates give sediment a short exposure to modern oceanic processes before being buried.

Significance to CBBL objectives:

Our observations of velocity and sediment concentration from the center portion of Eckernförde Bay suggest that bottom stress levels are commonly sufficient to advect fine sediment into the bay, but are not normally sufficient to cause local resuspension. These conclusions, based on a study of the physical oceanography and structure of the bottom boundary layer, are highly consistent with complementary studies of stratigraphic development in the central bay performed by CBBL/SRP investigators from SUNY and elsewhere. Complementary studies led by C. Nittrouer, for example, found rapid rates of sediment accumulation and minimal physical mixing of surficial sediment. Generation of currents by internal wave resonance, in concert with the presumed gradient in near-bottom storm wave activity from shallow to deeper water, together provide a reasonable scenario for rapid, but quiescent accumulation of mud in the central bay. The rapid accumulation of mud with little physical mixing is, in turn, highly consistent with the ultimate generation of Methane-Rich sedimentary strata.

Key West

Accomplishments:

Preliminary analysis of velocity, temperature, suspended sediment records along with underwater video collected at the Dry Tortugas site in February 1995 was completed in 1996. Results were summarized in a manuscript submitted to the upcoming special issue of GeoMarine Letters.

Major Conclusions to date:

(1) Bottom roughness was dominated by shrimp burrows and worm mounds with rms roughness amplitudes ranging from 0.47 to 1.75 cm.

(2) Logarithmic velocity profiles show apparent total roughnesses ranging from 0.30 to 1.45 cm, values consistent with observed biological roughnesses.

(3) The bed sediments were weakly bound by an algal crust just below the sediment-water interface.

(4) Video imagery reveals that when this bound layer was scraped away by a mooring that was accidentally dragged, sharp-crested wave-induced ripples appeared within the resulting swath.

(5) The implications are that physically-induced roughness, if dominant, would be significantly higher than the biological roughness, but that physical roughness is biologically suppressed.

Significance to CBBL objectives:

A general goal of the Key West Campaign was to gain better understanding of the effects that biogeochemical processes have on the behavior of surficial sediments and associated geoacoustic properties in carbonate sedimentary environments. More specifically, the VIMS bottom boundary layer hydrodynamics and sediment transport experiments provided essential environmental information on the physical regime, hydraulic roughness, and the factors that affect sediment mobilization and mixing of the sediment column.

Publications and Presentations to Date:

Journal Articles:

Friedrichs, C.T., and L.D. Wright, 1995. Resonant internal waves and their role in transport and accumulation of fine sediment in Eckernförde Bay, Baltic Sea. Continental Shelf Research, 15: 1697-1721.

Friedrichs, C.T., and L.D. Wright, in press. Sensitivity of bottom stress and bottom roughness estimates to density stratification, Eckernförde Bay, Southern Baltic Sea. Journal of Geophysical Research.

Jackson, D.R., K.L. Williams, T.F. Wever, C.T. Friedrichs and L.D. Wright, in review. Sonar observations of events in Eckernförde Bay. Continental Shelf Research.

Nittrouer, C.A., G.R. Lopez, L.D. Wright, S.J. Bentley, A.F. D'Andrea and C.T. Friedrichs, in review. Oceanic processes and the preservation of sedimentary structure in Eckernförde Bay, Baltic Sea. Continental Shelf Research.

Wright, L.D., C.T. Friedrichs and D.A. Hepworth, in review. Effects of benthic biology on bottom boundary layer processes, Dry Tortugas Bank, Florida Keys. GeoMarine Letters.

Presentations:

Friedrichs, C.T., L.D. Wright, and B.-O. Kim, 1995. Sensitivity of bottom stress measurements to stratification, fluid acceleration and instrument settling, Eckernförde Bay, southern Baltic Sea. Proceedings of the Workshop Modelling Methane-Rich Sediments of Eckernförde Bay, Eckernförde, Germany, 26-30 June, 1995, pp. 140-144.

Nittrouer, C.A., S.J. Bentley, G.R. Lopez, and L.D. Wright, 1995. Observations of sedimentary character and their relationship to environmental processes in Eckernförde Bay. Proceedings of the Workshop Modelling Methane-Rich Sediments of Eckernförde Bay, Eckernförde, Germany, 26-30 June, pp. 145-148.

Richardson, M.D., K.B. Briggs, L.D. Wright and C.T. Friedrichs, accepted. The effects of biological and physical processes on near-surface sediment geoacoustic properties. American Geophysical Union Annual Fall Meeting, San Francisco, CA, 15-19 December, 1996.

Wright, L.D., 1994. Benthic transport phenomena in Eckernförde Bay (Baltic Sea). Proceedings of the 1994 Ocean Sciences Meeting, San Diego, CA, 21-25 February. Eos, Transactions of the American Geophysical Union, 75 (3, suppl.): 180.

Wright, L.D., and C.T. Friedrichs, 1995. Physical processes responsible for the transport and accumulation of fine-grained sediment in Eckernförde Bay, southern Baltic Sea. Proceedings of the Workshop Modelling Methane-Rich Sediments of Eckernförde Bay, Eckernförde, Germany, 26-30 June, 1995, pp. 135-139.